REACTIONS OF UNSATURATED HYDROCARBONS OVER SUPPORTED METAL CARBONYL CATALYSTS

T H E S I S

SUBMITTED FOR THE DEGREE OF

DOCTOR OF PHILOSOPHY

OF THE

UNIVERSITY OF GLASGOW

BY

GEOFFREY E. MORGAN B.Sc.

OCTOBER, 1977

ProQuest LLC.
789 East Eisenhower Parkway
P.O. Box 1346
Ann Arbor, MI 48106 – 1346

A C K N O W L E D G E M E N T S

I should like to express my sincere thanks to Dr. G. Webb for suggesting the present topic of research and for his help and encouragement throughout the course of this work.

I acknowledge the assistance of Dr. R. Cross for his useful advice concerning the practical detail of metal carbonyl preparation; Dr. T. Baird for the electron microscopic examination of the catalysts; and Mr. J. Connolly and his colleagues for their glass-blowing expertise.

I am also indebted to the Polymer Group for their co-operation in carrying out T.V.A. and T.G.A. of the supported complexes.

I should also like to record my gratitude to my Aunt Isobel for the typing of this thesis.

Finally, I gratefully acknowledge a Glasgow University Grant for the duration of this research.

Geoffrey Morgan.

SUMMARY

An investigation has been carried out on the effect of supporting metal carbonyl complexes in a highly dispersed state on an "inert" carrier. A study of the catalytic activity of these complexes in the heterogeneous phase has also been carried out. The metal carbonyls which have been examined are $Os_3(CO)_{12}$ and $Re_2(CO)_{10}$, both of which retain their molecular structure when supported on silica, and the tetranuclear mixed-metal carbonyl $Rh_2Co_2(CO)_{12}$ which has been found to be less stable when supported, undergoing the loss of bridging carbonyl groups. Whereas the former carbonyls are very stable on exposure to air, the latter complex shows a tendency to decompose to the metals after only a short time.

By the use of various techniques including T.V.A., T.G.A., infra-red analysis and electron microscopy it has been found possible to monitor the change in structure and loss of carbon monoxide which occurs when the supported complex is thermally activated in vacuo. Hence the supported complex may be characterised at various stages in the activation process.

From the studies which have been carried out using the three supported complexes it has been found that a prerequisite for catalytic activity as measured by the hydrogenation and isomerisation of the n-butenes, is the loss of at least some of the carbonyl ligands on the complex.

In the case of $Os_3(CO)_{12}$ supported on silica, the active forms of the catalyst examined are (a) $Os_3(CO)_9$ and (b) a very high dispersion of osmium atoms, obtained after the loss of all carbonyls from the complex, in which there may or may not be cluster retention.

Comparisons between this latter catalyst and a more conventional supported osmium catalyst prepared by impregnation of osmium chloride followed by reduction at 320°C have been studied.

The loss of carbon monoxide from $Re_2(CO)_{10}$ takes place in a one-step process. The catalyst obtained by activation in vacuo to 250°C is believed to consist of highly dispersed rhenium atoms in the zero valent state. The catalyst is found to be active for the isomerisation of the n-butenes although rather less active for hydrogenation.

Activation in vacuo at 100°C of supported $Rh_2Co_2(CO)_{12}$ results in the loss of carbonyl groups from the complex, and the resulting supported species is active for the hydrogenation and isomerisation of the n-butenes. This may be interpreted in terms of exposure of sites capable of co-ordinating olefin molecules in a reactive form.

From investigations of the kinetics and energetics of the reactions of but-1-ene with hydrogen and deuterium over the three supported carbonyls in a static system, and from the product distributions of these reactions, the following conclusions have been reached :-

(1) Hydrogenation and isomerisation proceed independently in the reaction carried out over supported $Os_3(CO)_{12}$ after the loss of three carbonyl groups. Whilst isomerisation proceeds via inter- or intramolecular hydrogen transfer with the formation of a 1-methyl-Π -allyl intermediate, hydrogenation and olefin exchange occur by a Langmuir-Hinshelwood reaction with different rate-determining steps. Similar mechanisms exist on the catalyst formed after the loss of all carbonyl groups, the only difference being in the comparative

rates of each process.

(2) The rate of hydrogenation is relatively slow compared with the rate of isomerisation over the supported rhenium catalyst formed from $Re_2(CO)_{10}$. These reactions are thought to proceed independently, although isomerisation may be explained equally satisfactorily by an alkyl reversal process or an inter- or intra-molecular hydrogen transfer mechanism. Olefin exchange may be rationalised in terms of a mechanism involving the dissociative adsorption of a vinylic species.

3) Hydrogenation, isomerisation and olefin exchange all proceed via the formation of a "half-hydrogenated" butyl radical when the reaction is carried out over the catalytic species formed from the thermal treatment of $Rh_2Co_2(CO)_{12}/SiO_2$.

CONTENTS

CHAPTER 5 (CONTINUED) PAGE NUMBER

CHAPTER 6 (CONTINUED)

CHAPTER 7 (CONTINUED)

DISCUSSION SECTION

CHAPTER 9 (CONTINUED)

CHAPTER 1

INTRODUCTION

1.1 General Introduction.

A catalyst is a substance which increases the rate of attainment of equilibrium of a system, with only a slight modification of the free energy of the process. Ideally, the catalyst should undergo no net change in the course of reaction, although in real systems this rarely occurs and the catalyst deactivates with time.

In heterogeneous catalysis, reaction takes place at the phase boundary between gases or liquids and solids, whereas in homogeneous catalysis the reactants and the catalytic species exist in the same phase.

1.2 Heterogeneously Catalysed Hydrogenation of Alkenes.

1.2.1 Introduction.

Of all the catalytic reactions, those undergone by unsaturated hydrocarbons are among the most frequently studied. Alkenes, dienes, alkynes, aromatics and alicyclic compounds are all extremely useful in providing information concerning the various processes which occur on catalyst surfaces. The mechanisms of these reactions are, however, still the subject of great controversy, despite the extensive studies which have already been carried out.

A study of the kinetics of a catalysed hydrogenation reaction is only of limited value for the elucidation of the mechanism. This may be of use in determining values for adsorption coefficients and hence the relative surface coverages of the reactants, but it gives us very little information about the actual processes which take

place between the adsorption of the reactants and the appearance of the products. Analysis of the products of reaction with hydrogen of the higher alkenes, together with mass spectrometric examination of the deuteration reaction show that the processes undergone by an unsaturated hydrocarbon when it reacts at the surface of a metal can be categorised as follows:-

(1) Hydrogenation of the double-bond.

(2) Cis/trans isomerisation.

(3) Double bond migration.

(4) Olefin exchange i.e. the replacement of H by D in the parent Olefin.

(5) Hydrogen exchange i.e. the formation of HD and D_2 in the gas phase.

An understanding of each of these processes is of prime importance in the specification of precise mechanisms for alkene hydrogenation.

1.2.2 Possible Reaction Mechanisms.

It is now generally accepted that in the hydrogenation of alkenes, direct addition of a hydrogen molecule across the double bond does not occur. This conclusion is based upon the observation that when reactions are carried out using unsaturated hydrocarbons and equilibrated and non-equilibrated hydrogen deuterium mixtures, the deuteroalkane distributions are identical (1, 2). A more likely mechanism is that first postulated by Horiuti and Polanyi (3, 4, 5), who suggested that the reaction proceeds by the formation of a "half-hydrogenated state" that is, an adsorbed alkyl radical, as a relatively stable intermediate. The further addition of a hydrogen atom to the adsorbed alkyl radical produces the alkane, which once

formed, is released into the gas phase. Thus the process of hydrogenation may be represented as in Figure 1.1. The only way in which the processes which occur concurrently with hydrogenation may be rationalised is to consider that the formation of the half-hydrogenated state is reversible. Therefore for olefin exchange, we can write

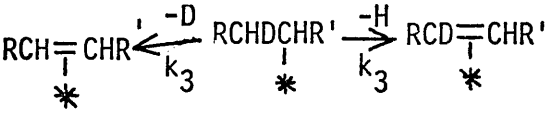

and for double bond migration

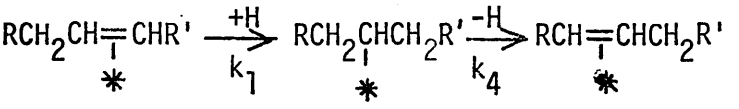

and cis/trans isomerisation

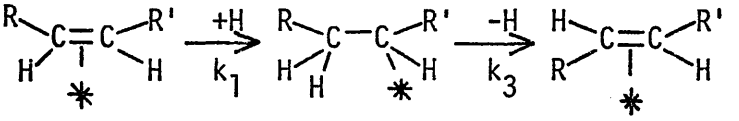

The proportion of products formed by exchange, isomerisation and hydrogenation will be totally dependent upon the relative values of k_1, k_3 and k_4, together with the rate constants k_2 for the addition of "hydrogen" to the half-hydrogenated state and k_d for desorption of the alkene.

An alternative mechanism, first postulated by Rooney and Webb (6) can be applied to C_3 and higher alkenes. This mechanism can account for isomerisation and exchange in alkenes, but it is unlikely that hydrogenation occurs via this mechanism. There is evidence for this theory from the work on supported rhodium catalysts by McNab and Webb (7). The proposal was that olefin exchange and isomerisation could occur through the formation of an

Figure 1.1

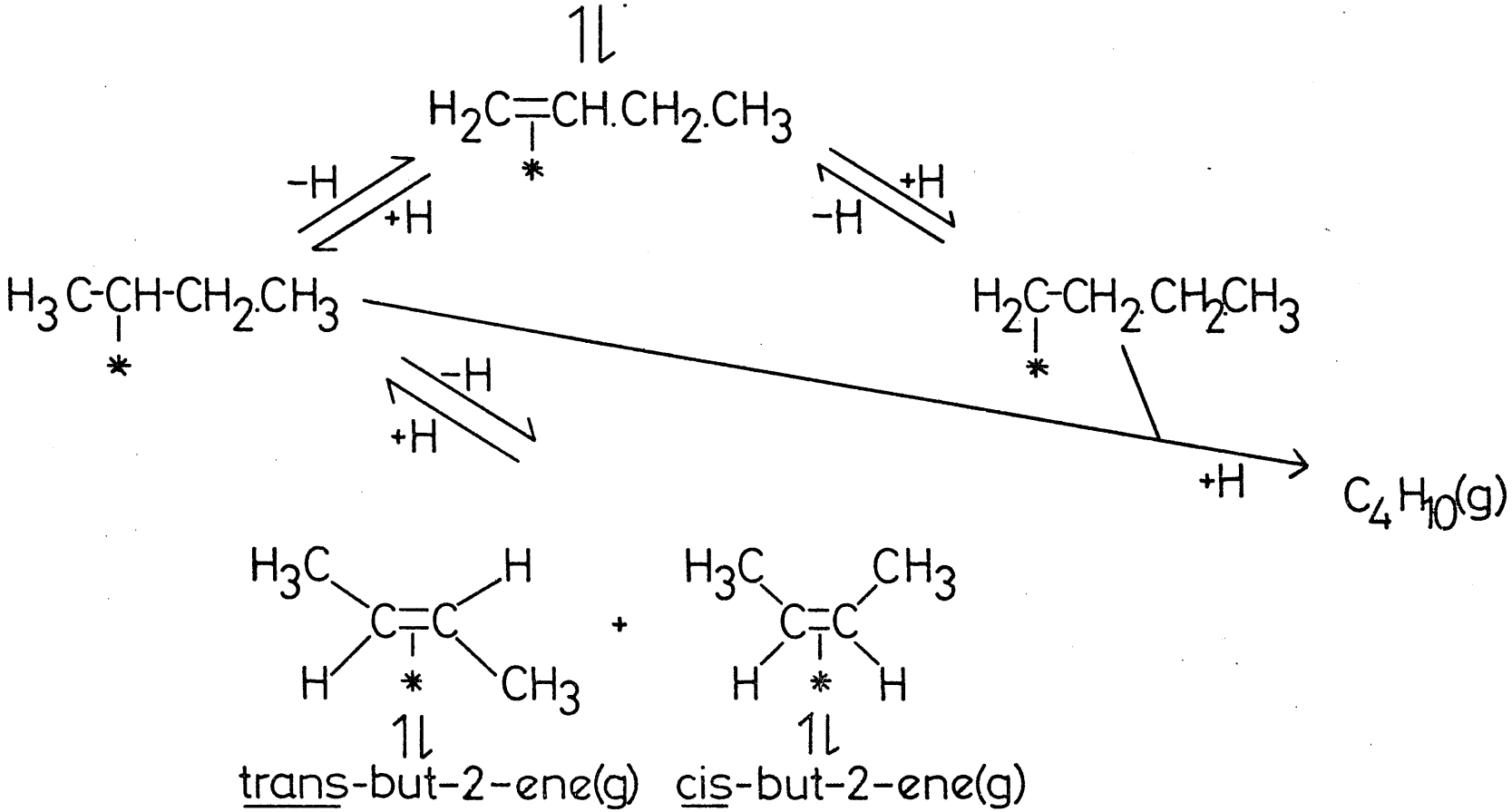
but-1-ene(g)
H2C=CH.CH2.CH3
-H
+H
+H
-H
H3C-CH-CH2.CH3
H2C-CH2.CH2CH3
-H
+H
+H
C4H10(g)
H3C
H
C=C
H
CH3
+
H3C
CH3
C=C
H
H
trans-but-2-ene(g)
cis-but-2-ene(g)

adsorbed π-allylic intermediate (Figure 1.2).

Two extremely important limitations arise as a consequence of this mechanism, which should make it possible to differentiate between it and the mechanism involving the half-hydrogenated state:-

(i) since in the π-allylic intermediate, free rotation is not possible, cis-trans isomerisation can only occur by this mechanism provided it is preceded by double bond migration (Figure 1.2).

(ii) complete exchange is not possible by the hydrogen abstraction-addition mechanism. This contrasts with the addition-abstraction mechanism where all the hydrogen atoms are exchangeable.

1.2.3 Hydrogenation of n-Butenes.

The reaction of the n-butenes with hydrogen is, mechanistically speaking, an extremely important system to observe as it allows a very deep insight into the surface processes taking place. The disadvantage in carrying out reactions of ethylene or propylene is that there is no method whereby the process of adsorbed alkene forming the half-hydrogenated state and then undergoing an alkyl reversal can be observed. This is feasible when the reaction of butene with hydrogen is observed, since there is the possibility that in undergoing an olefin - alkyl - olefin cycle the original alkene will re-appear as an isomerised product;

$$H_2C^{*}=CHCH_2CH_3 \underset{-H}{\overset{+H}{\rightleftharpoons}} C_4H_9(ads) \underset{+H}{\overset{-H}{\rightleftharpoons}} H_3CCH=CHCH_3^{*}$$

Figure 12

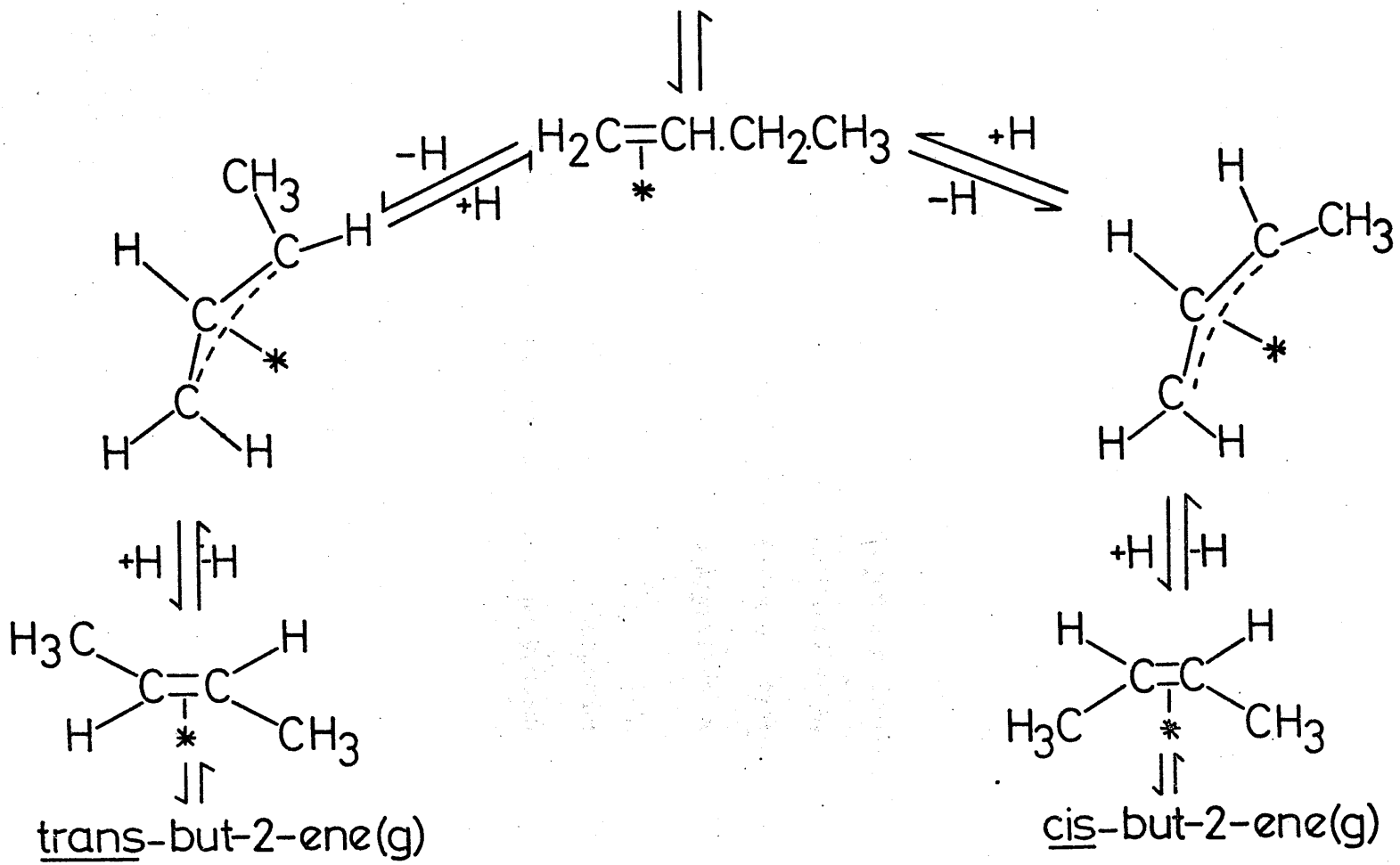
but-1-ene(g)
$H_2C{=}CH.CH_2CH_3$
-H
+H
+H
-H
+H
-H
+H
-H
trans-but-2-ene(g)
cis-but-2-ene(g)

Twigg (8) was one of the earliest pioneers in n-butene hydrogenation when he observed that for the reaction of but-1-ene over nickel wire in the temperature range 76 - 126°C hydrogenation and double bond migration occurred. Both reactions followed the same kinetics, namely,

$$\text{rate} \propto p_{H_2}^{0.5} \, p_{1\text{-B}}^{0.5}$$

whilst the activation energies were 10.5kJ mole^{-1} for hydrogenation and 24.7kJ mole^{-1} for double bond migration. Subsequent studies of the reaction of n-butenes with hydrogen and deuterium over a nickel wire catalyst (9) showed that the rates of hydrogenation were in the order but-1-ene > cis-but-2-ene > trans-but-2-ene. The kinetics for hydrogenation and double-bond migration were found to be similar to those calculated by Twigg when $p_{H_2} \sim p_{1\text{-B}} < 100$ torr, but with large excesses of hydrogen the rate was independent of hydrogen pressure and proportional to the but-1-ene pressure.

The reactions of the n-butenes with hydrogen and deuterium carried out over supported Group VIII metals have been extensively studied (10, 11, 12, 13, 14, 15). Typical results show that in the hydrogenation of butenes over palladium, ruthenium and rhodium catalysts, the butenes attain their thermodynamic proportions (16) in the course of the reaction. Platinum and iridium (10, 14), however, show little tendency to promote the isomerisation reactions. Osmium (11) exhibits behaviour intermediate between ruthenium and platinum. A series of hydroisomerisation activities may be drawn up for the reaction carried out at 100°C:-

$$\text{Ni} \sim \text{Rh} \gtrsim \text{Pd} > \text{Ru} > \text{Os} \gtrsim \text{Pt} \gtrsim \text{Ir}$$

In general, the kinetic studies carried out using the above mentioned metals show the rate of hydrogenation to be first order with respect to initial hydrogen pressure and zero order or slightly negative with respect to initial butene pressure. Data available for double-bond migration and cis-trans isomerisation tends to be more varied. Comparison of the activation energies for hydrogenation and double-bond migration shows that the values are quite different in many cases. This, however, does not necessarily point to a different overall mechanism for each process, but merely different rate determining steps (11).

The reactions of the n-butenes with deuterium have been studied over alumina supported platinum, iridium (10) and palladium (12). Examination of the deuterium distribution for palladium shows that alkene exchange is small, both in the reactant butene and the isomerised products. A hydrogen transfer process was proposed on this basis, together with the observation that the amount of hydrogen exchange is negligible.

It would appear from the similarities between reactions of ethylene, propylene and the n-butenes over Group VIII metals that there must be one basic unifying theory to explain the mechanisms of the three reactions. The isomerisation of the n-butenes cannot be explained in terms of the abstraction-addition mechanism (Figure 1.2) since this would involve the formation of a π-allylic intermediate which could not apply with ethylene and propylene. A more logical explanation would be that isomerisation occurs via an addition-abstraction mechanism.

Further studies of the isomerisation of n-butenes were carried

out over silica supported rhodium catalysts (7). By systematic mercury poisoning of the catalyst, it was concluded that hydrogenation and isomerisation occurred independently of each other. Hydrogenation and exchange were thought to occur on the metal surface, whilst isomerisation took place as a result of migration of adsorbed but-1-ene to the support.

Extensive studies have also been carried out on the reactions of n-butenes over various catalysts in the absence of hydrogen (17, 18, 19, 20, 21). Wells and co-workers (17, 18, 19) have shown that isomerisation occurs in the absence of hydrogen over cobalt wire and cobalt alumina catalysts and have suggested that the reaction occurs via an abstraction-addition mechanism. But-1-ene isomerisation in the absence of molecular hydrogen was also observed over alumina supported nickel, ruthenium, rhodium, osmium and platinum (19) iridium (17, 19) and palladium (19, 20). The observations were interpreted in terms of a hydrogen addition-abstraction process (Figure 1.1), where the alumina support was thought to be the source of hydrogen initially (17, 19). Unsupported osmium, iridium and platinum powders were found to be inactive for isomerisation, whilst platinum black was active (21).

The reactions of the n-butenes have also been extensively studied over evaporated iron (23) and nickel (24) films. Deuteration studies carried out over iron films revealed that the rate of exchange for but-2-ene to but-1-ene isomerisation ($\beta \rightarrow \alpha$ isomerisation) was twenty times faster than for but-1-ene to but-2-ene ($\alpha \rightarrow \beta$ isomerisation). Another observation was that the rate of exchange in the isomerisation of cis- to trans-but-2-ene and vice versa was negligible in comparison with exchange by $\beta \rightarrow \alpha$ isomerisation. In contrast, the rates of

isomerisation of cis-and trans-but-2-ene were similar to that for $\alpha \rightarrow \beta$ isomerisation. On the basis of these observations it was proposed that $\alpha \rightarrow \beta$ isomerisation, but-1-ene exchange and cis-trans isomerisation occurred by different mechanisms. But-1-ene exchange was suggested to occur via a dissociatively adsorbed vinylic species.

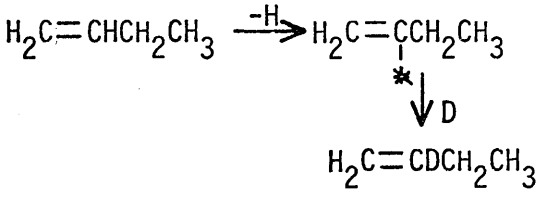

$\alpha \rightarrow \beta$ isomerisation was thought to involve an intramolecular hydrogen transfer mechanism, in which there was the formation of an intermediate, containing a bridged hydrogen atom between the α and γ carbon atoms, similar to that suggested by other workers (22) for the deuteration of cyclohexene. An addition-abstraction mechanism was postulated for cis-trans isomerisation. Also suggested was a direct process for cis-trans isomerisation, which was independent of C-H breaking and formation. Similar results were obtained with nickel films (24), where a microwave spectroscopic examination of the exchanged but-1-ene has confirmed the preferential formation of adsorbed but-2-enyl in the vinylic dissociation of but-1-ene.

In all of the foregoing theories regarding the mechanism whereby isomerisation and hydrogenation of the n-butenes occur, the basic assumption has been that the hydrocarbon, and usually the hydrogen as well, are adsorbed directly upon the metal. This has led to problems, in that the proposals put forward to explain the reaction, although large in number, have lacked a basic unifying theory.

Observations which have not been explained fully by the existing literature include the following;

1) Reproducible catalytic activity does not result from standard catalyst pretreatment.

2) Nature of metal surface has little effect on catalytic activity for ethylene hydrogenation, be it a film or a dispersed catalyst (25).

3) Hydrogenation is not a structure sensitive reaction e.g. the catalytic activity for cyclopropane hydrogenation is the same over a wide range of dispersions (26).

4) Self-hydrogenation of alkenes occurs on catalytically active metals, and results in the surface being covered with retained hydrogen deficient carbonaceous residues. (27, 28, 29, 30).

5) The lack of correlation between geometric and electronic features of metals and their catalytic activity.

These diverse features of alkene hydrogenation have recently been unified by a proposal of Thomson and Webb (31), who suggest that the metal is only of secondary importance in the hydrogenation reaction. On the basis of radiochemical evidence (133, 134, 135, 136) they suggest the initial formation of a permanently retained hydrogen deficient hydrocarbon species M - C_xH_y. on the catalyst surface. Hydrogenation then occurs by a hydrogen transfer between this adsorbed species and an adsorbed alkene, rather than the direct addition of hydrogen to an associatively adsorbed hydrocarbon. This new approach looks to be far more promising in solving the hitherto unexplained problems concerned with alkene hydrogenation and isomerisation.

1.3 Homogeneous Catalytic Reactions of Unsaturated Hydrocarbons.

1.3.1 Introduction.

Whereas homogeneous catalysis is a relatively recent field of study in comparison with heterogeneous systems, great advances have been made in the last twenty years and it is now better understood than heterogeneous catalysis is after a much longer time. This can be attributed to the relative ease of detection and isolation of intermediates and to the high reproducibility which is obtainable in the homogeneous system.

As a result of the progress which has been made in recent years, homogeneous catalysis has been the subject of extensive reviews (32, 33, 34, 35, 36, 37). Examples of reactions of interest include: the hydrogenation of alkenes catalysed by complexes of Rh (38), Ru (39), Co (40) and Pt (41, 42, 43); the isomerisation of alkenes catalysed by complexes of Rh (44, 45), Pt (41, 42, 43, 48), Co (47) and Pd (45, 46); the dimerisation of ethylene and polymerisation of dienes catalysed by complexes of Rh (49, 50); the hydration of acetylene catalysed by $RuCl_3$(51); the oxidation of alkenes by $PdCl_2$ (52).

Metal complexes which are active as homogeneous catalysts are generally those whose ligands are somewhat labile and readily replaced by substrate molecules. Also important are complexes whose central atoms have fewer electrons than the closed shell 8 or 18 electrons, for example the 16 valence electron square planar d^8 complexes, such as $Rh^{I}Cl(PPh_3)_3$, which, although it is stable, is capable of taking up additional ligand molecules.

The metal complex may have a number of properties which

increases its versatility in the catalysis of various reactions. These include:-

1) The ability to stabilise through co-ordination, a great variety of ligands e.g. hydrides (53) and alkyl groups (44) in the form of still reactive intermediate complexes.

2) The property of having more than one stable configuration differing in co-ordination or oxidation number, which means that it has the ability to promote re-arrangements e.g. in the isomerisation of alkenes, described in section 1.3.3

3) The ability to orientate the reactants in its co-ordination shell to make the reaction sterically favoured. An example of this type of network is in the cyclo-oligomerisation of buta-1:3-diene to cyclodecatriene (54).

1.3.2 Homogeneous Hydrogenation Reactions

Just as the group VIII metals may activate molecular hydrogen heterogeneously, so the essential feature in homogeneous hydrogenation is the activation of hydrogen (53). Although the precise manner in which molecular hydrogen is attacked by active catalyst species is not known, it is generally thought that a complex containing a hydride ligand is formed. Three types of hydrogen activation have been distinguished:-

$$M^n + H_2 \rightleftharpoons M^{n+2} H_2 \qquad \text{(a)}$$

$$2\,M^n + H_2 \rightleftharpoons 2\,M^{n+1} H \qquad \text{(b)}$$

$$M^n X + H_2 \rightleftharpoons M^n H + HX \qquad \text{(c)}$$

Type (a) is the most commonly encountered of the three and is termed an insertion process. In this case there is the oxidative addition of both hydrogen atoms to the same central metal atom. The outstanding example where this type of activation operates is in the hydrogenation of terminal alkenes in the presence of tristriphenylphosphine rhodium (I) chloride (38). In this reaction (Figure 1.3) initial loss of a Ph_3P ligand is followed by the insertion of hydrogen to form an isolable five co-ordinate dihydride species. Co-ordination of this species with the reactant alkene results in the formation of the alkane in addition to regenerating the catalyst. The possibility that the alkene complex is formed first is ruled out on the grounds that this complex, which may be isolated, does not react on treatment with hydrogen to form the alkane. Another interesting point is that ethylene does not undergo hydrogenation very readily, possibly due to it being very strongly co-ordinated in the complex. A similar mode of activation may occur with Ir (I) Cl $(CO)(PPh_3)_2$ (55).

Type (b) is known as activation by homolytic fission and involves the splitting of the hydrogen molecule into two neutral atoms which co-ordinate to different central metal atoms. Oxidation of the metal atom again occurs in the course of this type of addition. An illustration of this is the pentacyano cobalt (II) ion-catalysed hydrogenation of butadiene to butene (59), where it is proposed that the following equilibrium is established;

$$2Co\ (II)\ (CN)_5^{3-} + H_2 \rightleftharpoons 2Co\ (III)\ H(CN)_5^{3-}$$

Figure 1.3

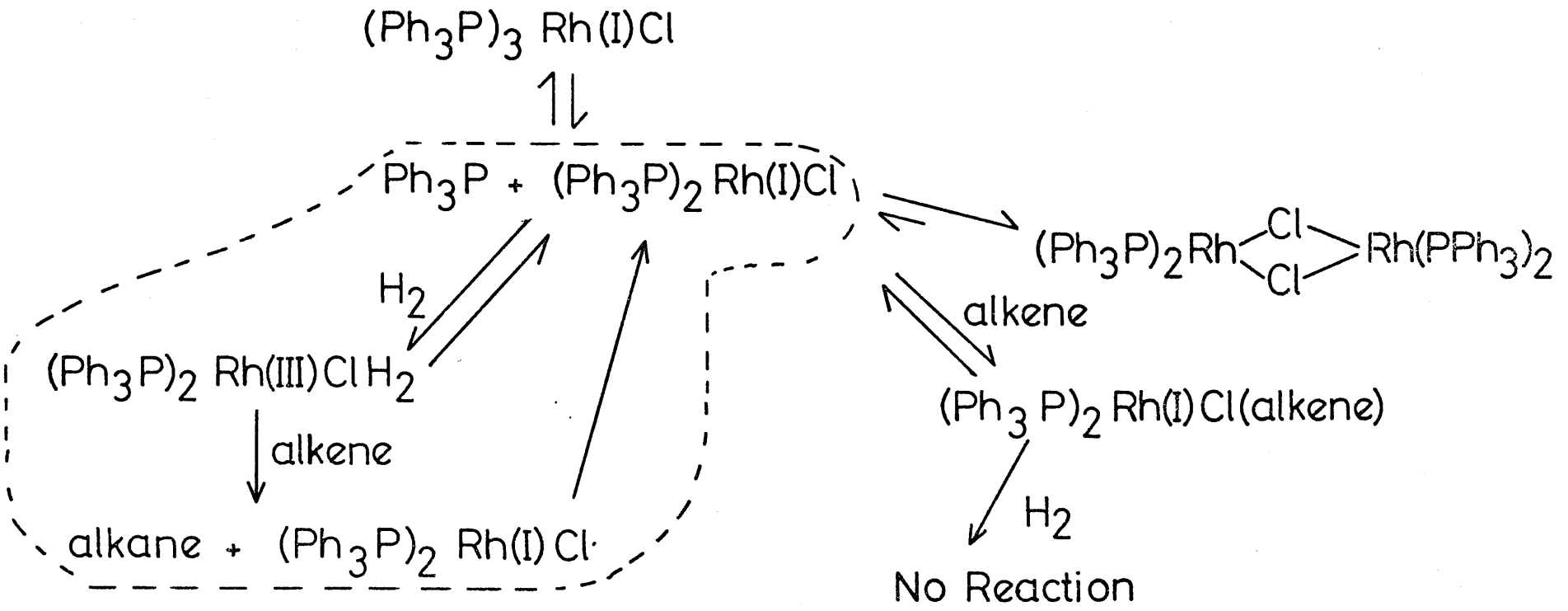

---- catalytic cycle

Mechanism for the Hydrogenation of Alkenes by Tristriphenylphosphine Rhodium(I) Chloride

Type (c) is the only non-oxidative addition of hydrogen to the complex and is termed heterolytic fission. This activation probably occurs in the presence of Ru(III) Cl_6^{3-} (56):-

$$Ru(III)\ Cl_6^{3-} + H_2 \rightleftharpoons Ru(III)\ HCl_5^{3-} + H^+ + Cl^-$$

Such a mechanism is postulated for the hydrogenation of fumaric acid catalysed by Ruthenium (II) chloride (39).

1.3.3 Homogeneous Isomerisation Reactions.

Two mechanisms have been proposed for the isomerisation of alkenes by transition metal complexes. First, the addition of a preformed metal hydride to a co-ordinated alkene with the formation of an alkyl intermediate has been suggested. This is followed by reformation of a metal hydride-alkene complex accompanied by double bond migration as shown below.

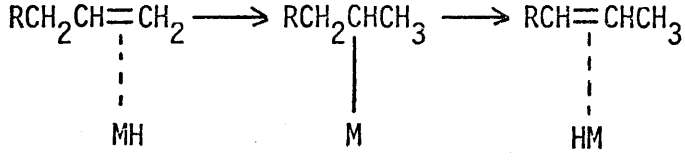

An alternative mechanism has been proposed in which isomerisation occurs via a π-allyl intermediate, followed by the addition of the hydride at a carbon atom different from its original location.

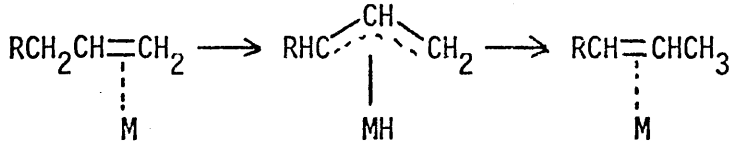

1.3.4 Comparison of Homogeneous and Heterogeneous Catalysis.

Comparisons between homogeneous and heterogeneous catalysis are well documented in the literature (58, 60, 61, 62, 63). There

are several close similarities which exist between the two systems. Thus, for example,

(i) the most active catalysts are confined, in both cases, largely to the Group VIII elements.

(ii) in general the same reactions can be catalysed both heterogeneously and homogeneously.

(iii) similar intermediates appear to exist, although in heterogeneous catalysis these have proved very difficult to isolate. Thus, for example, the following species, well known in homogeneous catalysis, are thought to have their counterparts in heterogeneous catalysis.

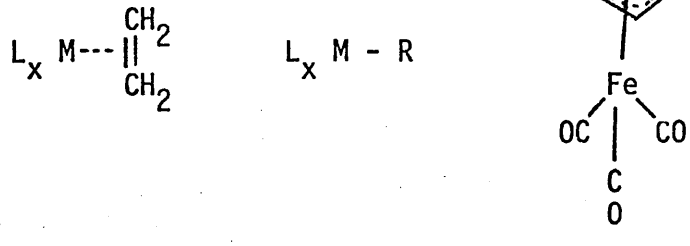

(iv) the bond involved in the intermediate complex formation for homogeneous catalysis is envisaged as being that suggested by Chatt (64) and confirmed by the X-ray crystallographic analysis of Zeise's salt $K^{+}(Pt\ Cl_3\ (C_2H_4))^{-} . H_2O$. Thus the metal alkene bond consists of two components: A metal alkene σ-bond by donation of electrons from a bonding π-orbital of the alkene to a suitable hybrid orbital (e.g. dsp^2) of the metal, followed by π-bond formation through back donation from the filled d orbitals of the metal to the empty antibonding π^* - orbitals of the alkene. A similar

bonding is postulated (6) for the chemisorption of alkenes in heterogeneous systems.

(v) similar types of hydrogen activation occur in both cases.

Contrasts which exist must also be considered. The most important of these factors are:-

(i) heterogeneous catalysts tend to be rather unspecific in nature, raising the question as to how many types of active sites exist on the catalyst surface. Homogeneous reactions, however, are usually restricted to one site and tend to be very specific.

(ii) whilst the steric and electronic nature of the catalyst is well understood in homogeneous systems, these features are still the subject of great controversy in the heterogeneous system.

Intermediate complexes such as

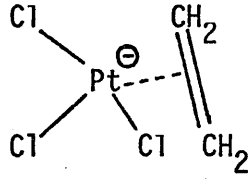

are well characterised and allow predictions to be made on how the catalytic activity may be altered by varying the complex ligands. Similar predictions are not possible in the heterogeneous system.

1.3.5 "Heterogenizing" Homogeneous Catalysts

On the industrial scale, heterogeneous catalysts are preferred to homogeneous catalysts for a number of reasons. These include

ease of separation of the catalyst from reaction products; use of flow methods, so that the system can be recycled if the yield of product is low; use of elevated temperatures. Ideally therefore the requirement must be to combine the above mentioned advantages of heterogeneous systems with the ability of homogeneous systems to be selective (65, 66). Attempts have been carried out at combining the convenience of a solid catalyst with the superior selectivity and efficiency in the use of metal atoms in homogeneous catalysts. Acres and Co-workers (67) have supported a solution of rhodium trichloride in ethylene glycol on silocel. The resulting supported solution was active in the isomerisation of pent-1-ene to cis and trans-pent-2-ene, but the salt was readily reduced to rhodium metal with use. The hydrogenation of ethylene to ethane was successfully carried out by Hayes (68) on alumina supported ethylene platinous chloride $(C_2H_4 . PtCl_2)_2$. Reduction of the salt to the metal did not occur, provided the ratio of ethylene to hydrogen in the reaction mixture was greater than unity, but exposure to hydrogen alone did result in the reduction. This was attributed to the hydrogenation of the π-adsorbed ethylene occurring in the absence of a σ-di-adsorbed intermediate.

The hydrogenation and isomerisation of the n-butenes over silica supported complexes have been studied (69, 70). Work carried out by Misono (69) showed a series of supported complexes of Pd(II), Pt(II), Ni(II) and Cu(II) with acetonylacetonate and dimethylglyoxime to be active in but-1-ene isomerisation. Catalytic activity was found to decrease in the order Pd(II) > Pt(II) > Ni(II) > Cu(II), irrespective of the chelating ligand. It was suggested that some co-ordinated intermediate was involved in the isomerisation reaction.

Robertson and Webb (70) have prepared a silica supported catalyst from $Ru_3(CO)_{12}$. The complex appeared to retain its structure on its support, and, on activation, underwent decomposition in a series of well defined stages. In the temperature range studied, the active catalyst for hydrogenation and hydroisomerisation was envisaged as being $Ru_3(CO)_5$. Tentative structures for the active surface were postulated as shown below.

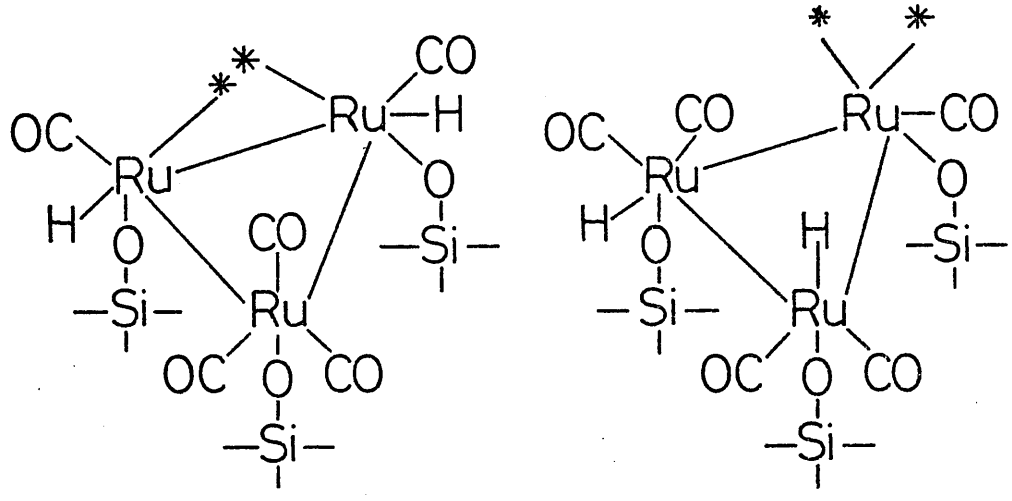

The experimental results were consistent with a mechanism in which hydrogenation occurred by the attack of molecular hydrogen on a π-butene-metal complex, whilst isomerisation involved a hydrogen abstraction-addition mechanism with the formation of a 1-methyl π-allyl intermediate. Thus a reaction scheme could be postulated (Figure 1.4) similar to that proposed for homogeneous reactions (46, 56). In this particular system the supported complex was extremely highly dispersed, allowing a close comparison with the homogeneous system to be made.

Disproportionation of propylene to butene and ethylene over a catalyst derived from alumina supported $Mo(CO)_6$ has been investigated by Kemball and co-workers (71). Infra-red analysis of the activated complex, along with mass spectrometric considerations, led them to

Figure 1.4

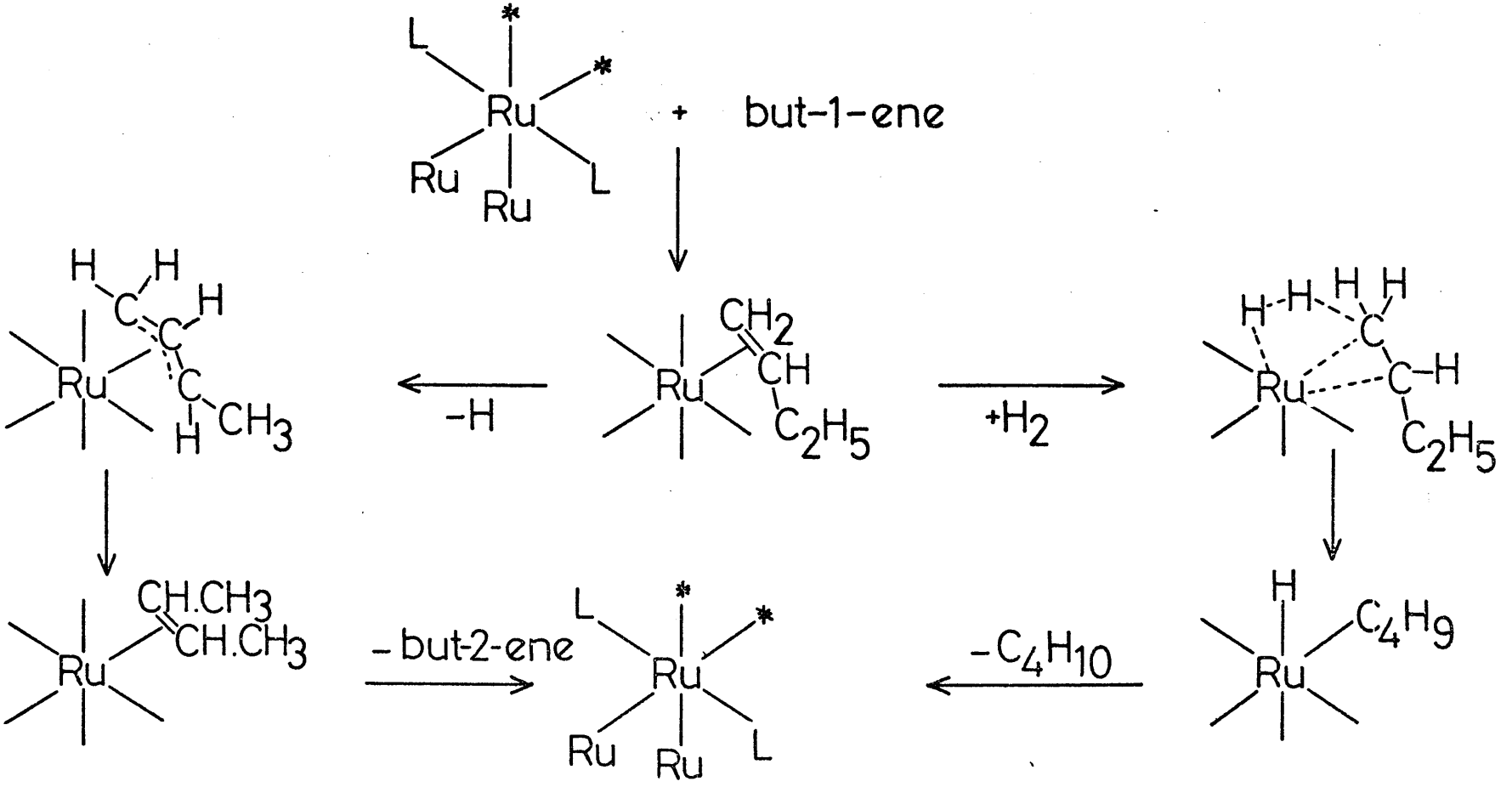

Possible Mechanism for the Hydrogenation and Isomerisation of But-1-ene over Catalyst derived from $Ru_3(CO)_{12}/SiO_2$

believe that the active species in disproportionation was $Mo(CO)_x(propylene)_{6-x}$ where x was suspected to be 3 or 4. Other workers (72) cited molybdenum in a higher oxidation state as being responsible for the catalysis.

1.4 Catalysis by Alloys and Bimetallic Clusters.

Historically, bimetallic catalysts have been of interest in the development of ideas related to an electronic factor in catalysis by metals (73, 74). Of all the metals, only those of Group VIII, which, according to Pauling's theory (75), are said to have incomplete d-bands, show appreciable activity in adsorption and catalysis. In contrast, a group 1B metal such as copper, having a filled d-band, is decidedly inactive. According to the original view of Mott and Jones (76) an alloy of a group VIII metal with a group 1B metal is characterised by a d-band which is filled to a greater extent than that of the pure group VIII metal. In the case of a nickel-copper alloy, the substitution of copper atoms for nickel atoms in the metal lattice adds extra electrons to the lattice. The extra electrons introduced with the copper enter the d-band until it is filled. By varying the composition of the alloy, one can alter the degree of filling of the d-band with electrons and observe the effect on catalytic activity. It was expected that abrupt changes in catalytic behaviour would be observed at an alloy composition corresponding to the complete filling of the d-band, the presence of d-band vacancies having been suggested as being a necessary prerequisite for catalytic activity (77). Consideration of a gold-palladium alloy, for example, would lead us to expect a change in

activity at a composition of 60 atom % gold, when the d-band of palladium would be filled. Couper and Eley (78) found in their studies of ortho-para hydrogen conversion on palladium-gold alloys that a plot of activation energy against percentage gold content showed very close agreement with the theoretical calculation. Other studies of formic acid decomposition (79), and the oxidation of carbon monoxide (80) over the same alloys show the expected sharp change in activation energy at approximately 60 atom percent gold. In general, however, there is little evidence to support the theory that a filled d-band can drastically affect the catalyst activity. The activation energy, for example, for acetylene hydrogenation over nickel-copper alloy powders (81) passes through a maximum at 80% copper, whilst for the hydrogenation of ethylene (82) and the hydrogenation of but- 2-yne over palladium-gold wires (83), the activation energy appears to be almost invariant with alloy composition.

Although progress in the use of alloys to elucidate the electronic factor in metal catalysis has been slow, interest in metal catalysis systems has not declined. In fact there has been a great revival of interest in the field in recent years, for reasons other than a renewed probing into the electronic factor alone (84, 85). These include (i) the realisation that bimetallic systems may exhibit major selectivity effects in catalysis, that is, markedly different behaviour towards different types of reactions (86, 87, 88, 89, 90) and (ii) the development of the idea of highly dispersed bimetallic systems known as "bimetallic cluster" catalysts (87).

The selectivity exerted by bimetallic catalysts is exemplified in recent studies using nickel-copper alloys, for the hydrogenolysis of ethane to methane and the dehydrogenation of cyclohexane to

benzene (86). In the case of ethane hydrogenolysis, the catalytic activity decreased markedly and continuously with the addition of copper to nickel over the whole range of alloy composition, although much of this decline in activity was observed on addition of the first few percent of copper. With cyclohexane dehydrogenation, however, the catalytic activity increased initially with addition of small amounts of copper and then remained insensitive to alloy composition over a wide range, finally decreasing sharply at compositions approaching pure copper. It seems that the effect of copper on the catalytic activity of nickel is strongly dependent on the nature of the reaction.

In an alloy of an inactive metal with a highly active metal, there is the possibility that the hydrogenolysis activity of the catalyst is dependent on the existence of sites comprising "multiplets" of active metal sites, as suggested by the work of Balandin (91). In the same context the term "ensemble" has been adopted by others (89, 92). In terms of a geometrical interpretation, a build up of concentration of the inactive metal may be instrumental in decreasing the activity of the catalyst manyfold. According to this view, the only function of the surface copper atoms in nickel-copper catalysts is to dilute the nickel atoms and thus limit the number of "multiplet" nickel atom sites. However, the possibility that electronic interactions between copper and nickel atoms may affect the catalysis cannot be ignored (93). In general the addition of a group 1B metal to a group VIII metal effects the decrease in hydrogenolysis activity markedly but has a much smaller effect on such reactions as dehydrogenation, hydrogenation and isomerisation of hydrocarbons (86, 87, 88, 89, 90).

"Bimetallic Cluster" catalysts are formed by the impregnation of a carrier with an aqueous solution of salts of the two metals of interest. This is then dried and treated with a stream of hydrogen at an elevated temperature to reduce the metal salts. Such methods lead to the question as to whether the clusters of the highly dispersed system contain atoms of both metals or each cluster contains exclusively one metal. On purely statistical grounds it would be expected that each individual cluster would contain atoms of both metals. This expectation is verified by experiments, even for cases in which components exhibit very low miscibility in the bulk (86). Verification of the existence of highly dispersed bimetallic clusters is complicated by the limitations involved in obtaining structural information, since the metal crystallites or clusters may be in the size range 10 to 20 Å where examination by techniques such as electron microscopy and X-ray line broadening are of limited applicability.

Direct experimental verification of bimetallic clusters in such highly dispersed systems is difficult but catalytic reaction can serve as a sensitive probe to obtain evidence of interaction between the atoms of the two metallic components. Experimentally, the hydrogenolysis of ethane is an interesting reaction in determining the effect of percentage composition on catalytic activity. Consideration of the bimetallic cluster containing copper and ruthenium for this reaction shows that incorporation of copper into the ruthenium metal decreases the hydrogenolysis activity by three orders of magnitude. The influence of dispersion upon the relationship between hydrogenolysis activity and catalyst composition is also very interesting (87). Comparison of the effect of copper increase in (i) 1% metal

dispersion and (ii) 50% metal dispersion shows that for (i) the addition of only 1 - 2% copper of the total ruthenium content decreases the activity 1000 fold whilst the same inhibiting factor in (ii) requires the presence of one atom of copper for every ruthenium atom. This indicates that the copper in the ruthenium-copper aggregate is confined to the surface, which is consistent with the very low miscibility of these two metals in the bulk state. Thus for a highly dispersed system, a bimetallic cluster may have a surface composition far outside the range of those possible in a bulk solid solution of the two metals.

1.5 Supported Rhenium Catalysts

The oxidation state of rhenium on various supports has been the subject of great controversy in recent years. It is now generally accepted that the method of impregnation and degree of dispersion has a profound influence on the oxidation state. Some workers have presented evidence that the rhenium is present as a highly dispersed oxide on an alumina surface at typical reforming conditions (94), whilst others have claimed that rhenium can be reduced to the metallic state (95). The data which supports reduction to the metallic state has been obtained on catalysts containing much higher rhenium concentrations then exist in the commercial catalyst, therefore it may well be that the rhenium concentration has an important bearing on its reducibility (96). Sinfelt and co-workers (97) found that a 10% rhenium on silica catalyst could be prepared by impregnation with perrhenic acid followed by reduction under a constant flow of Hydrogen at 500^{o}C.

For rhenium supported on γ-alumina Yao (98) suggested that rhenium existed on the surface in two forms:-

a) A two dimensional dispersed phase which interacted strongly with the alumina support and as a result could only be reduced to the zero valent state by hydrogen at > 500°C. Subsequent oxidation of the dispersed phase at 500°C only occurred to the non-volatile, tetravelent Re^{4+} instead of Re^{7+}. This stable Re^{4+} oxidation state may be responsible for the prevention of rhenium loss in the oxidative regeneration of rhenium containing, γ-alumina supported reforming catalysts or during other uses in an oxidising environment.

b) A three dimensional crystalline phase which could undergo oxidation or reduction between Re^{0} and Re^{7+} by treatment with hydrogen at 350°C. High temperature reducing conditions resulted in the slow aggregation of the zero valent dispersed phase into the three dimensional metallic crystallites.

It has been proposed by Boelhouwer (99), however, that in the catalyst prepared by impregnating alumina with Re_2O_7, a considerable amount of the Re^{7+} could be reduced to the metal at 500°C to form metal crystals. Subsequent oxidation by oxygen at 550°C resulted in the rhenium atoms being spread over the surface, reforming a monolayer of Re_2O_7.

Other workers (100) have proposed that for catalyst samples of 10 - 20% $Re_2O_7/\gamma\text{-}Al_2O_3$ rhenium does not exist in the form of Re_2O_7 particles on the support surface. Using differential thermal analysis, X-ray diffraction and Mossbauer spectroscopy, it has been concluded that a strong interaction between the rhenium and the support took place after impregnation and drying. They proposed that the rhenium was present as a tightly bonded surface compound

that was thermally stable in air up to 900°C.

The reactions of alkenes over supported rhenium catalysts are well documented in the literature and include disproportionation (100, 101, 102), isomerisation (102), metathesis (99) and hydrogenation (104), whilst $Re_2(CO)_{10}$ has been shown to be an initiator of free radical polymerisation and block copolymerisation (105). Examination of Re_2O_7/Al_2O_3 showed it to be active for but-1-ene disproportionation (102), where rhenium was found to be present in the +7 oxidation state. Reduction to the +4 state resulted in a loss of activity for olefin disproportionation and the appearance of activity for the isomerisation of but-1-ene to but-2-ene. The adsorption and disproportionation of ethylene (101) over Re_2O_7 was found to be dependent upon the oxidation state of rhenium, the support used and the rhenium oxide content of the catalyst.

The reaction of ethylene with hydrogen or deuterium has been studied in the temperature range 25 - 100°C over a 17% rhenium/silica catalyst (104). Complete reduction of the perrhenate to rhenium was adjudged to have been achieved by use of flowing hydrogen at 500°C for 12 hours, whilst the specific activity for the reaction was found to be lower by several orders of magnitude than for Group VIII metals. Mechanistically, the behaviour of rhenium closely resembled that of ruthenium and osmium, but differed significantly from the third row elements iridium and platinum.

The catalytic properties of supported rhenium for ethane hydrogenolysis has been investigated (97) for comparison with Group VIII metals. Consideration of the rhenium activity, together with the activities of the Group VIII metals of the same period revealed

a pattern for the variation of catalytic activity, which was similar to the variation in percentage d - character of the metallic bond, reaching a maximum at osmium

Probably the most important function of rhenium in catalysis nowadays is as an additive in platinum/alumina catalysts. The catalyst generally contains rhenium in an amount comparable to the amount of platinum present. The major advantage of rhenium in the catalyst is the improved maintenance of activity, which makes it possible to obtain longer reforming cycles or to operate at lower pressures to take advantage of higher formate yields. It has been shown (106), that the difficulty involved in the reduction of rhenium to the metal does not exist when the bimetallic cluster is coimpregnated on alumina. Platinum and rhenium are both reduced to the metallic state, the reduction of the rhenium compound being strongly catalysed by platinum. It has also been found (107) that, for such a bimetallic supported catalyst,

a) platinum and rhenium form alloys;

b) the percentage dispersion of the platinum plus rhenium metal phase is almost independent of the percentage platinum versus platinum plus rhenium composition for a large range of compositions, when the support is γ-alumina;

c) the surface composition of the (Pt + Re) alloy metal phase seems to differ by at most a little from the overall composition. The activity (107) of this supported bimetallic catalyst has been examined to ascertain whether its activity in various reactions is simply the sum of activities of platinum and rhenium, or whether more complicated features are observed.

It was found that the curves of activity as a function of the composition of the catalyst exhibited one or two maxima in benzene hydrogenation, benzene-deuterium exchange, cyclopentane and butane hydrogenolysis, whilst the rate of 1, 1, 3-trimethyl cyclohexane dehydrogenation decreased as the percentage of rhenium increased.

1.6 Metal Clusters

Whilst comparisons with homogeneous catalysis are having some degree of success in characterising species chemisorbed on metal surfaces, recent studies into the reactions involving metal clusters could prove to be extremely important in solving the mechanistic problems. The properties of this class of compounds are comparable in terms of structural, stereochemical and thermodynamic considerations, with those of a metal surface where there is extensive chemisorption of molecules, radicals or atoms (108).

Systematic evaluation of metal cluster chemistry is essential to the further development of the cluster-metal surface analogy. One of the most interesting of all metal clusters is $Os_3(CO)_{12}$. This cluster consists of an osmium triad, each osmium atom having four carbonyl ligands attached to it (109). This is a particularly stable complex as compared with its iron and ruthenium analogues. A feature of $Os_3(CO)_{12}$ less encountered with $Fe_3(CO)_{12}$ and $Ru_3(CO)_{12}$, is the tendency of certain electrophilic reagents, particularly halogens, to break exactly one of the three bonds in the metal triangle, so that a chain of three metal atoms linked by the necessary two metal bonds will be produced (110). Decomposition studies of $Ru_3(CO)_{12}$ and $Os_3(CO)_{12}$ (111) have shown that $Ru_3(CO)_{12}$ decomposes to ruthenium

metal and carbon monoxide, whilst $Os_3(CO)_{12}$ sublimes completely before decomposition, condensation of the vapour being observed on the quarz furnace tube.

The ability of the osmium cluster to break C-H and C-C bonds is an extremely striking property which enhances the feasibility of a comparison with metal surfaces. The reaction of $Os_3(CO)_{12}$ with ethylene (112, 113, 114) has resulted in the product of elementary composition $Os_3(CO)_9C_2H_4$. The two isomers which have been suggested are shown in Figure 1.5

Structure 1.5(b) was originally thought to be correct by analogy with the products of reaction of $Os_3(CO)_{12}$ with cyclic monoalkenes (115), but N.M.R. considerations (128) in addition to X-ray crystallographic analysis (114) have tended to favour structure 1.5(a). The M-H positions have not been unequivocally established but the hydrogen atoms are non-equivalent, although they become equivalent at high temperatures by an intramolecular exchange reaction (112, 116). The basic reaction of ethylene is effectively a dissociative "chemisorption" analogous to the well known dissociative ethylene adsorption on metal surfaces (117). This result, as noted by Deeming (112) raises the question as to whether the dissociative adsorption of ethylene on metal surfaces occurs by the loss of two hydrogen atoms from a single carbon atom equivalent to structure 1.5(a) or the loss of a one hydrogen from each carbon atom as has been universally assumed and which agrees with structure 1.5(b). Both types of species $\overset{*}{\underset{*}{>}}C{=}CH_2$ and $HC{=}CH$ may exist on metal surfaces.

Figure 1.5

Possible Isomers of $Os_3(CO)_9C_2H_4$

(a)

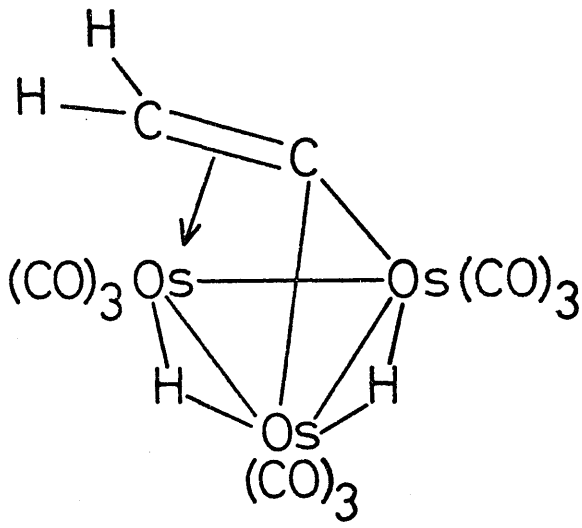

(b)

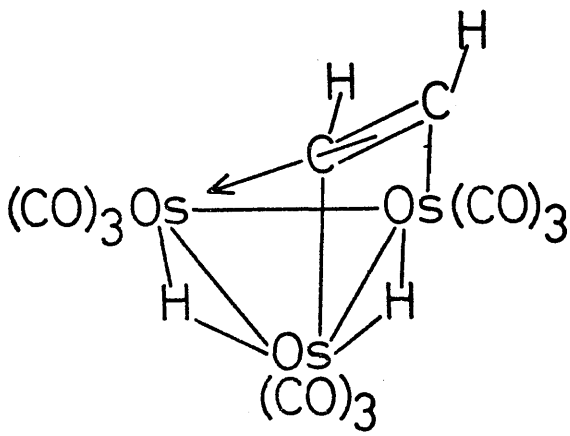

The hydrogenation of $Os_3(CO)_9C_2H_4$ in refluxing n-heptane has led to the formation of $H_3\ Os(CCH_3)(CO)_9$ (118), the structure of which has been established by nematic phase ^1H N.M.R. spectroscopy and X-ray powder analysis,

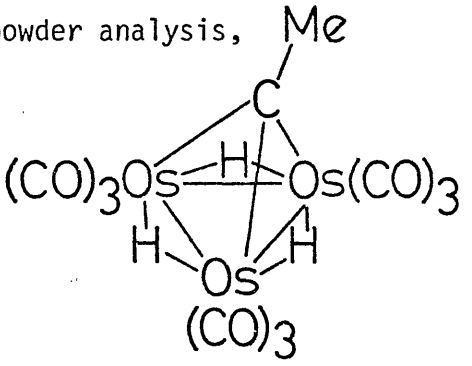

whilst the protonation of $Os_3(CO)_9C_2H_4$ by CF_3CO_2H in SO_2 yielded $Os_3(CO)_9H_3(C{=}CH_2)$ $^+$(112)

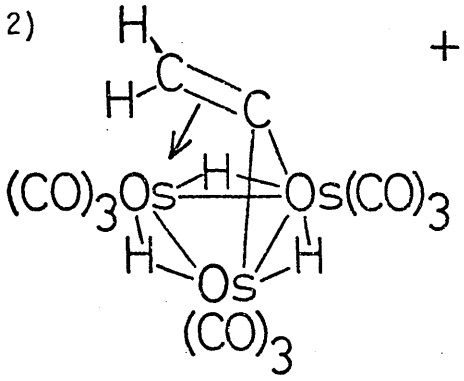

Similar triosmium cluster derivatives have been prepared from the reaction of unsaturated hydrocarbons with $H_2Os_3(CO)_{10}$. (119, 120, 121, 122, 123, 124). The reaction of acetylene and substituted acetylenes leads to the formation of $HOs_3(CH{=}CHR)(CO)_{10}$

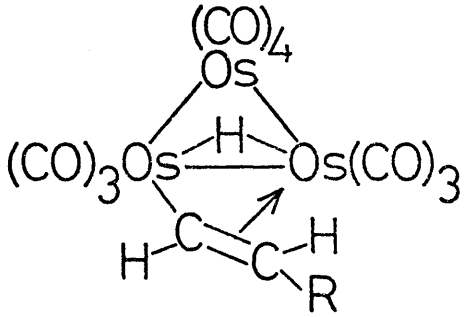

in which there has been a transfer of a bridging hydrogen atom to the organic molecule. Conversion of this structure to $Os_3(CO)_9C_2H_4$ can be achieved by heating with loss of CO and transfer of a hydrogen atom back to the metal. This hydrogen transfer process

from the bridging position to the organic molecule is a common feature in triosmium cluster chemistry, having been observed with alkynes (121), alkenes (122) and dienes (123, 124), and has recently been shown to promote the facile catalysis of alkene isomerisation (120).

Recent work has shown that metal clusters are active in the catalysis of many reactions. Examples of interest include: the cyclization of acetylene and buta-1:3-diene by $Ni_4(CNR)_7$ (125); the polymerisation of allene by $Ni(CNR)_7$ (125); Fischer-Tropsch synthesis by several clusters including $Ir_4(CO)_{12}$, $Rh_6(CO)_{16}$ and $Rh_4(CO)_{12}$ (126); the hydrogen reduction of carbon monoxide to alkanes by $Os_3(CO)_{12}$ and $Ir_4(CO)_{12}$(127). In these reactions there was no evidence to suggest that cluster fragmentation had occurred.

CHAPTER 2

THE AIMS OF THE PRESENT WORK

The object of the present studies was to investigate the feasibility of supporting metal carbonyls on a silica support, and of using such complexes or their derivatives as catalysts for alkene hydrogenation and isomerisation. The main reasons for undertaking such studies are:-

1) The potentiality of using supported metal and mixed metal carbonyls for the preparation of supported metal catalysts containing extremely small metal particles. Such methods also present the possibility of supporting Rhenium in the zero valent state using supported $Re_2(CO)_{10}$ as starting material.

2) The factors which determine the activity of heterogeneous catalysts are unclear. Discussion of the mechanisms of reactions of unsaturated hydrocarbons catalysed by metals is severely restricted by a lack of knowledge of the nature of the catalytically active form of the adsorbed species and the nature of the active site on the catalyst surface. Since the concept of homogeneous catalysis is better understood in terms of isolating reaction intermediates, reproducibility, selectivity and other factors, it is logical to support heterogeneously a group of compounds which have been known to be homogeneous catalysts and hence compare the catalytic behaviour of the two systems.

3) Currently, simple models of surfaces based upon metal clusters are being employed in the interpretation of chemisorption and catalytic processes. This makes the study of metal complexes such as $Os_3(CO)_{12}$ and $Rh_2Co_2(CO)_{12}$ of interest and importance.

The immediate aims of the research were as follows:-

a) To characterise the supported metal carbonyls before, during and after activation and to determine the conditions necessary for catalytic activity.

b) To study the kinetics of the hydrogenation and isomerisation reactions.

c) To determine the distribution of the reaction products in the reactions of n-butenes with both hydrogen and deuterium.

d) To examine the possibility of "support effects" in the systems under investigation.

e) To elucidate mechanisms for hydrogenation, isomerisation and olefin exchange in these catalytic systems.

CHAPTER 3

EXPERIMENTAL

3.1 Materials

3.1.1 Preparation of Mixed Metal Carbonyls.

Dirhodiumdicobalt dodecacarbonyl was prepared in a two stage reaction as follows:-

Pulverised rhodium trichloride trihydrate (Johnson Matthey Ltd.) was treated with a continuous flow of carbon monoxide over a period of several hours at a temperature of 100°C. Orange crystals were obtained, some of which sublimed onto the walls of the reaction tube, and the remainder of which was extracted from unreacted rhodium trichloride with n-hexane. Recrystallisation of the orange product resulted in pure $Rh_2(CO)_4Cl_2$ (129).

$$2\left(RhCl_3.\ 3H_2O\right) + 6CO \rightarrow\ Rh_2(CO)_4Cl_2 + 6H_2O + 2COCl_2$$

The infra-red and mass spectra of the recrystallised product agreed with those in the literature (129). Further reaction of $Rh_2(CO)_4Cl_2$ with $Co_2(CO)_8$ (Fluka Chemicals) under nitrogen at room temperature yielded dicobaltdirhodium dodecacarbonyl after three days (130). The solution was filtered and the solid product was extracted with n-hexane until the extract was colourless. Cooling of the combined washings to-70°C gave the brown crystalline product.

Infra-red analysis:-

Table 3.1

$\bar{\nu}$ (CO) (cm^{-1})

Table 3.1

ν (CO) (cm^{-1})

Literature	This Work
2074w	2073w
2064s	2064s
2059s	2059s
2038m	2040m
2030m	2030m
1920w	1920w
1910sh	1910sh
1885s	1885s
1871s	1870s
1855w	1855w

Elemental analysis showed:-

C = 22.8%; Co = 16.5% (required C = 21.8%; Co = 17.8%)

Mass spectrometric analysis proved very difficult owing to the instability of the mixed metal carbonyl. Introduction of the sample to the chamber resulted in a continuous evolution of carbon monoxide. The product was stored under nitrogen due to its instability in air.

Attempts were also made to prepare mixed iron-ruthenium carbonyls as carried out by Knight et al. (131) to ascertain their catalytic activity when supported on silica. Triruthenium dodecacarbonyl was refluxed with iron pentacarbonyl over a period of 20 hours. Subsequent separation of the products, namely $Ru_3(CO)_{12}$ (yellow), $FeRu_2(CO)_{12}$ (red) and $Fe_2Ru(CO)_{12}$ (purple) could be achieved by chromatrography using a silica column and 60/80 petroleum ether as eluant. This separation, however, could only be effected by a coarser grade silica than the "Aerosil" type which was desired as support.

As a result of the difficulty involved in eluting the products from the column and then supporting them on "Aerosil" silica, the preparation of catalysts of these mixed iron - ruthenium compounds proved unsuccessful.

3.1.2 Catalyst Preparation.

Silica Supported Triosmium Dodecacarbonyl ($Os_3(CO)_{12}$) and Dirhenium Decacarbonyl ($Re_2(CO)_{10}$).

2% W/W of triosmium dodecacarbonyl and 2% W/W dirhenium decacarbonyl on "Aerosil" silica were prepared in the following manner. 1g of "Aerosil" silica was pre-dried at 500°C *in vacuo* and then suspended in 25 ml of spectroscopic grade dichloromethane under a steady stream of dry nitrogen. 0.02g of $Os_3(CO)_{12}$ (Johnson, Matthey and Co. Ltd.) or of $Re_2(CO)_{10}$ (Fluka Chemicals) was dissolved in 10 ml of solvent and the resulting solution was added with constant stirring to the silica suspension, which was then stirred constantly and evaporated to dryness in the dry nitrogen stream. The residue, which was a free flowing powder, was stored under dry nitrogen until required.

Silica Supported Dicobaltdirhodium Dodecacarbonyl ($Rh_2Co_2(CO)_{12}$)

2% W/W of dicobaltdirhodium dodecacarbonyl supported on "Aerosil" silica was prepared as follows: 0.02g of $Rh_2Co_2(CO)_{12}$ was dissolved in 10 ml of spectroscopic grade *n*-hexane and the resulting solution was added, with constant stirring, to a silica suspension prepared in the same manner as described above for the rhenium carbonyl catalyst. The resulting suspension was evaporated to dryness under a steady flow of dry nitrogen to yield a free flowing powder.

The catalyst was then stored under dry nitrogen until required.

Silica Supported Osmium Metal Catalyst.

2% W/W osmium on "Aerosil" silica was prepared as follows:- an aqueous suspension of "Aerosil" silica (5g) was impregnated with an aqueous solution containing 0.155g of osmium chloride (approx. 64% osmium). The resulting suspension was evaporated to dryness on a steam bath and finally dried in an air oven at 120°C. The residue was a dark grey powder and this was stored in air.

3.1.3 Gases

Cylinder hydrogen (Air Products Ltd.) was used as supplied without further purification.

Deuterium (Norsk Hydro, Ltd.) was 99.95% isotopically pure and no further purification was carried out.

Chemically pure grade but-1-ene, trans - but-2-ene and cis - but-2-ene (Matheson Co. Inc.) were found to contain no impurities detectable by gas chromatography and were merely degassed before use.

Cylinder helium (Air Products, Ltd.) was used as the carrier in the chromatograph.

Oxygen free nitrogen (British Oxygen Company) was used to provide an inert atmosphere in which Thermogravimetric Analysis could be carried out, and also as an inert atmosphere for catalyst preparations.

3.2 Apparatus

3.2.1 The Vacuum System

The reactions were carried out in a static vacuum system (Figure 3.1), which was evacuated by a mercury diffusion pump P_2, backed by an oil filled rotary pump P_1 producing a vacuum of 10^{-4} torr or better. All taps and joints were lubricated with "Apiezon N" high vacuum grease. Storage vessels SV_1 and SV_2 for hydrogen and butene were connected to a further vessel MV, in which a mixture of the two reacting gases of the required composition was stored. A reaction vessel RV of capacity Ca. $100cm^3$ was used, which was connected to manometer M, allowing the measurement of the pressure change during the course of any reaction. Expansion vessel E was used for the collection of the products from the reaction, whilst condensation spiral F facilitated the separation of the hydrocarbon products from unreacted hydrogen. Sample tube G was the means whereby the products were transferred from the system for analysis.

3.2.2 Procedure.

For each series of reactions, 20mg of catalyst, in the case of the silica supported dicobaltdirhodium dodecacarbonyl, or 80mg of catalyst in all other cases were used.

Pretreatment of the catalyst varied depending on the catalyst and could be effected by surrounding the reaction vessel with an asbestos insulated electric furnace, the current to which was controlled by a "Variac" transformer. The temperature of the reaction vessel was measured using a "Comark" electronic thermometer fitted with a Cr/Al thermocouple.

To carry out a reaction, a suitable pressure of reaction mixture

The Vacuum System

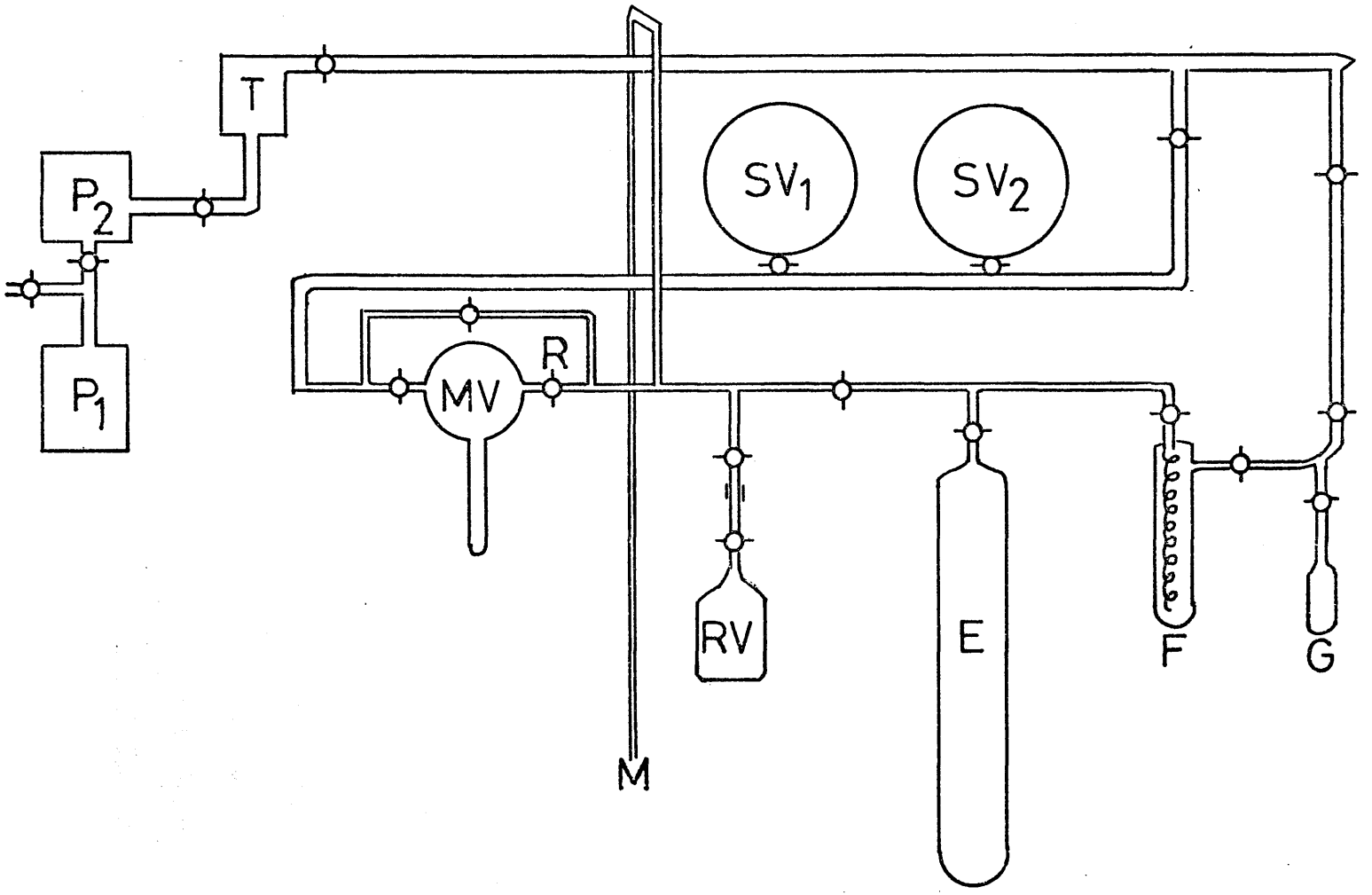

Figure 3.1

(200 torr) was admitted to the reaction vessel RV via tap R. The rate of the reaction was monitored by determining the observed pressure fall on the manometer at various time intervals, and the products were removed for analysis by expansion into vessel E which had previously been evacuated. Vessel F was now cooled by surrounding it with a Dewar flask containing liquid nitrogen. Evacuation of E resulted in all of the hydrocarbon products freezing out in vessel F, whilst all the unreacted hydrogen was pumped away. From the spiral trap the products were condensed into a sample vessel for transfer to the gas chromatograph. The whole system including the reaction vessel was then evacuated over a period of about 15 minutes between runs.

3.2.3 The Gas Chromatography System.

The system is shown as a block diagram in Figure 3.2.

The sample inlet system is designed to enable samples of reaction products to be introduced to the separating system and is shown in Figure 3.3

Procedure: The sample products from the reaction in the static system were introduced to the sampling system by attaching the vessel to the sample inlet and firstly evacuating that volume of the system which had been open to the atmosphere. By suitable manipulation of taps T_1 and T_2, the system could be arranged so that the carrier gas by-passed the U-tube, whilst at the same time the U-tube was being evacuated. After isolating the system from the pumps, the required pressure of sample was admitted and taps T_1 and T_2 were turned 120^{o} anti-clockwise simultaneously to allow the carrier gas to sweep the sample in the U-tube onto the column.

Figure 3.2

The Gas Chromatograpy System

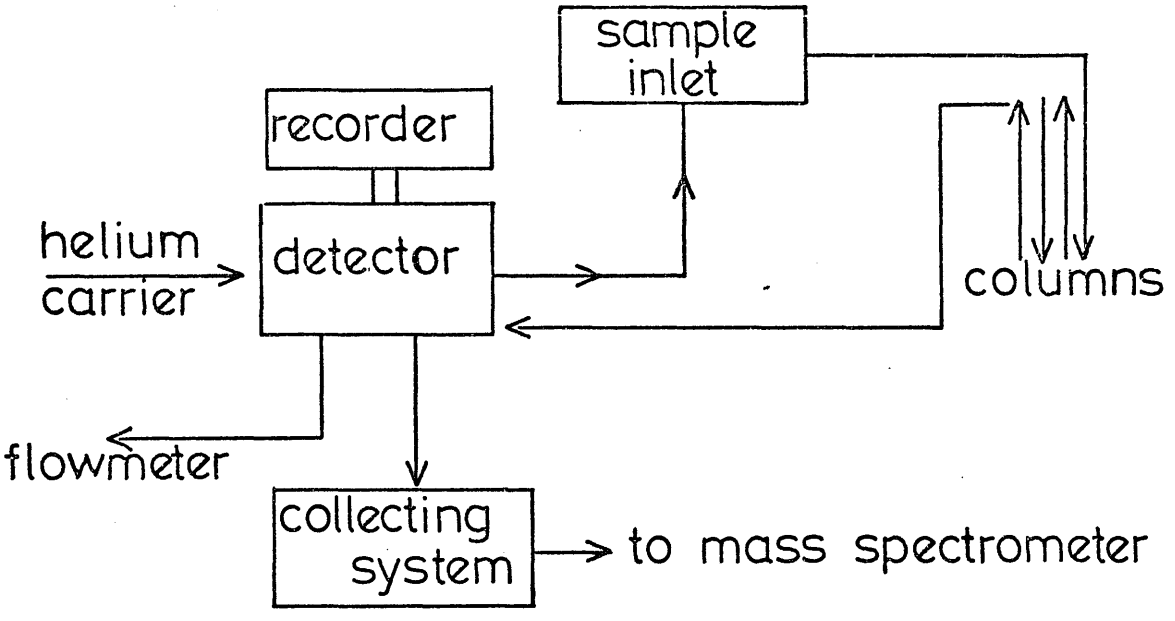

Figure 3.3

Sample Inlet System

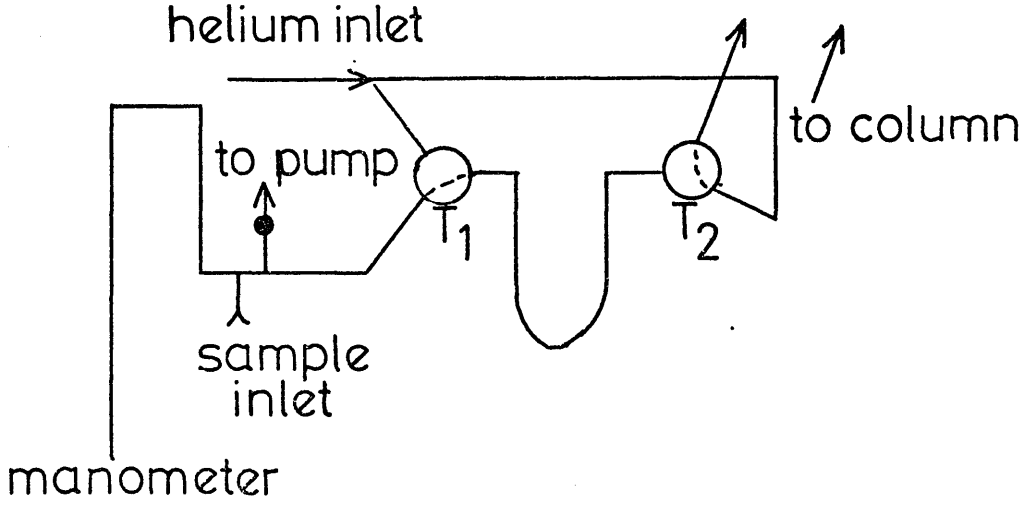

The column consisted of 12m of 6 mm O.D. glass tubing packed with 33% W/W dimethylsulpholane on 30-60 mesh firebrick. At an operating temperature of 20 $\pm$ 3^{o}C and a carrier gas flow rate of 40cm^{3} min^{-1}. the retention times were 26, 36, 44, 51 minutes for n-butane, but-1-ene, trans-but-2-ene and cis-but-2-ene respectively.

The detector was a Gow-Mac hot wire Katharometer operated at a filament current of 250mA. The output from the detector unit was fed into a Servoscribe potentiometric recorder operating at 10mV full scale deflection. A typical recorder trace for the products of reaction is shown in Figure 3.4.

At the start of each series of analyses, a sample of a "standard" mixture of the expected products of reaction was passed through the column. The mixture contained a known percentage of each of the constituents. Thus by measuring the area of each of the peaks in the trace obtained from this known sample using a fixed-arm planimeter, it was possible to derive a relationship between the partial pressure of each of the constituents in the standard and the area of each respective peak. The ratio of the two parameters was termed the sensitivity coefficient and this was used to calculate the partial pressure of each component in the unknown reaction product mixture.

3.2.4 Mass Spectrometry Analysis.

On elution from the chromatograph each hydrocarbon component of the reaction product mixture was collected and analysed by mass spectrometry. This was carried out for those reactions where deuterium was used.

Figure 3.4

A Typical Trace of Reaction Products

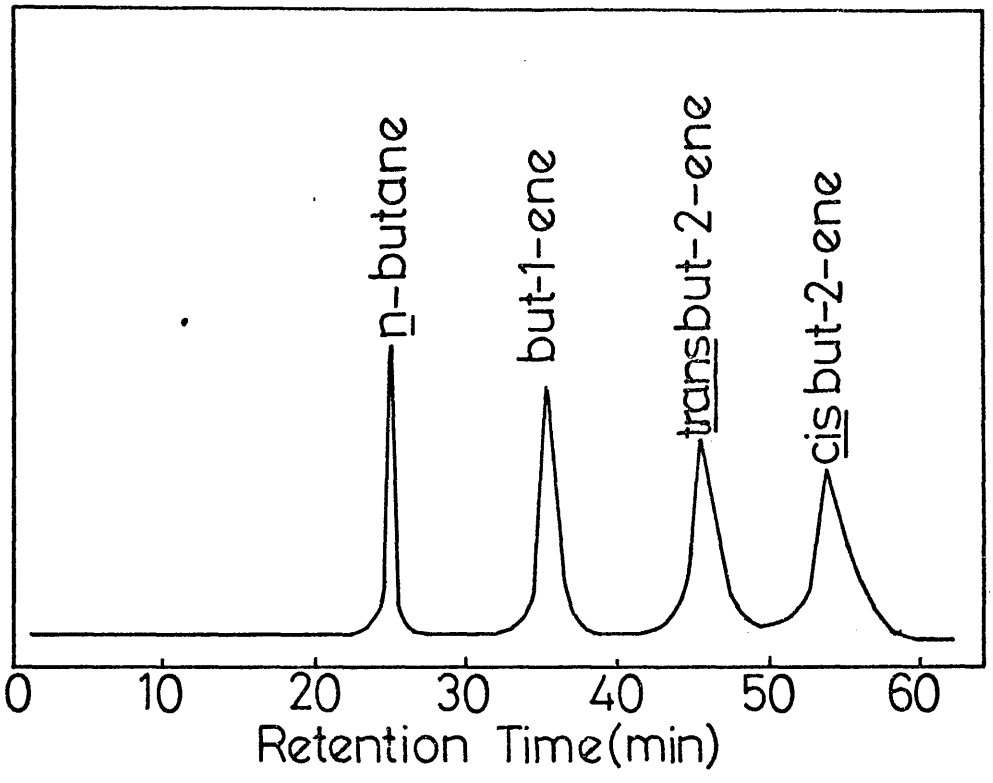

Figure 3.5

A Collector

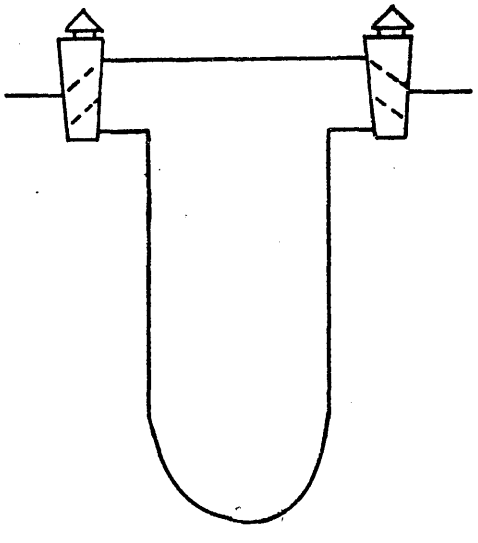

The method of collection involved the eluant gases being diverted so that they passed through a series of collecting traps similar to that shown in Figure 3.5.

The two-way taps in each collector could be arranged either to allow the gas flow to be directed through the U-tube or to direct the flow so that it by-passed the U-tube. Each U-tube was surrounded by a Dewar flask containing liquid nitrogen. As each gas was eluted from the column and passed through the detector, the response was registered on the recorder trace. At this instant the two way taps in each collector in turn were arranged to allow the gas to pass through the U-tube and condense out. Condensation was facilitated by the presence of glass wool in the trap.

After elution of the whole sample, the carrier gas was disconnected from the collecting series of cold traps. Each trap was, after evacuation to remove the carrier gas, allowed to warm to ambient temperature and the hydrocarbon sample was condensed into an evacuated sample vessel and transferred to the mass spectrometer for isotopic analysis.

Mass spectrometric analyses were carried out using an A.E.I. M.S.20 mass spectrometer under the following operating conditions.

Magnetic Strength	4.5 kG.
Electron Voltage	20 eV
Trap Current	50 V
Ion Repeller	- 2.8 V.

3.3 Analysis of Catalysts.

3.3.1 Infra-red Analysis of Catalyst.

Catalyst samples were examined by pressing 40 mg of a 2% carbonyl sample in a 16 mm stainless steel die at a pressure of 8 tons in^{-2} for five minutes and then transferring the disc immediately to a Unicam S.P. 200 G grating infra-red spectrophotometer, where a spectrum of the required region was taken.

3.3.2 Thermal Volatilisation Analysis (T.V.A.)

Basic Principles:- T.V.A. involves a continuous measurement of the pressure exerted by the volatile products as they are released from the heated catalyst. Degradation is carried out under high vacuum conditions and the volatile products are thus continuously pumped from the heated sample. The volatiles pass to a cold trap and the response of a pirani gauge placed between sample and trap is recorded continuously as a function of oven temperature.

Procedure.

150 mg of a 10% sample of the catalyst was heated on the base of a glass tube, 20 cm long and 4.5 cm diameter, constructed from a pyrex SRB 40 socket. The trap of the tube and the greased socket joint was cooled by a water jacket during the experiment. Heating was carried out by using a Perkin Elmer F11 oven equipped with a linear temperature programmer, by which the sample could be heated linearly from ambient temperature to $500^{o}C$ at a rate of $10^{o}C\ min^{-1}$. The oven temperature was recorded using a chromel-alumel thermocouple, fixed near the base of the tube.

The products of degradation could pass through four equivalent routes, each with a secondary cold trap, operating at four different temperatures, 0, - 45°, - 75°, - 100°C respectively. After each of these traps was placed a pirani gauge, which measures the pressure exerted by the volatile products which were not condensed by that particular trap, and a liquid nitrogen trap. A fifth pirani gauge was positioned after one of the liquid nitrogen traps. The outputs from the five pirani gauges were fed into a multipoint recorder via a multi-gauge head unit, where they were recorded in conjunction with the output from the oven thermocouple. Thus the volatiles from the heated sample were fractionated according to their condensability at each of the five temperatures and a differential condensation T.V.A. thermogram obtained. (See Figures 3.6 and 3.7).

3.3.3 Thermogravimetric Analysis (T.G.A.).

As the Du Pont 950 thermogravimetric analyser cannot be used under high vacuum conditions, all the T.G.A. experiments were carried out in an atmosphere of Nitrogen.

The boat shaped platinum sample holder measured 1 x 0.5 x 0.25 cm deep and the temperature measuring thermocouple was placed 0.1 cm from the sample holder. The rate of gas flow was 80cm^3 min^{-1} and the sample size was 5 mg. Due to low concentration of complex on the inert silica, the scale for weight loss on the y axis was adjusted such that full scale deflection was equivalent to only 20% weight loss. Degradation was carried out using a heating rate of 10°C min^{-1}, the sample being heated from ambient temperature to 500°C.

3.3.4 Electron Microscopy of the Catalyst.

To prepare the supported complex for examination, a small

Figure 3.6

T.V.A Apparatus

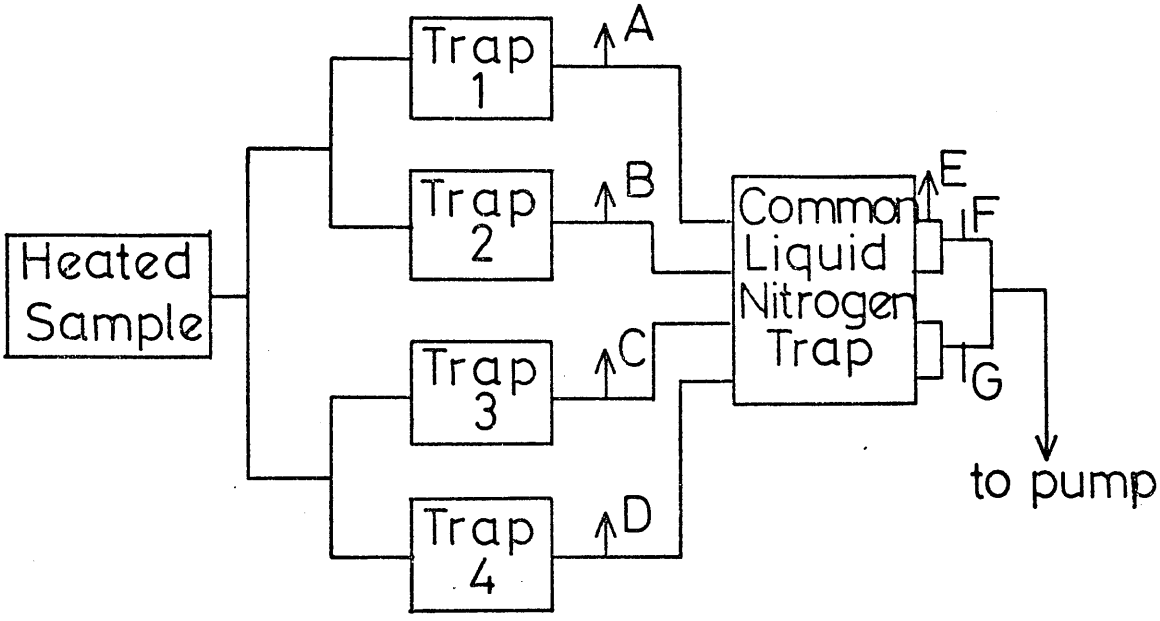

Normal Trap Temperatures(°C) 0,-45,-78,-100.
A,B,C,D,E are pirani gauge heads
F,G are receiving tubes eg. for gas i.r

Figure 3.7

Schematic Layout of T.V.A

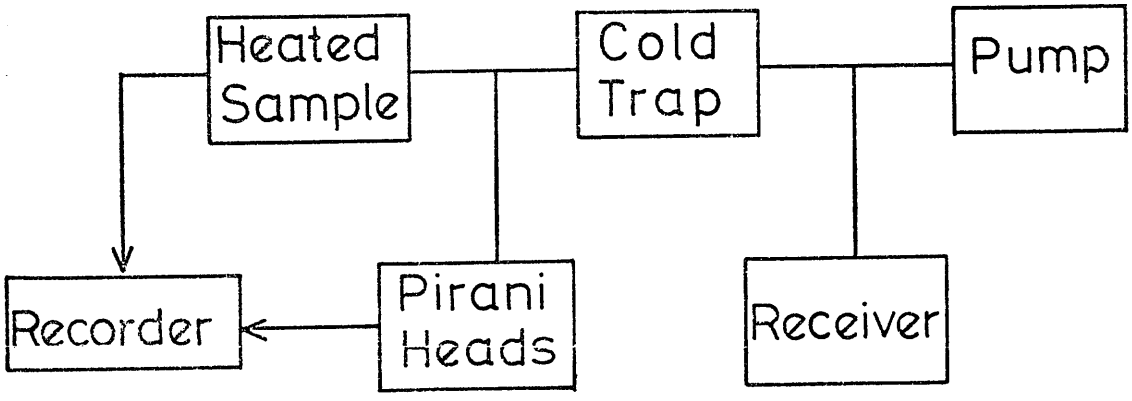

sample was ground to a fine powder and then mixed with a few drops of water. The resulting suspension was applied to a 2.3 mm specimen support copper grid covered with a carbon film. The sample was left to dry for 24 hours, after which it was in a suitable state for examination.

Catalyst samples were examined using a J.E.M. 100C Electron Microscope, operated at 100 kV. Magnification of x 50,000 and x 100,000 was achieved by the instrument itself, with a further magnification of x 10 being achieved by the enlarger in the photograph development process.

CHAPTER 4

TREATMENT OF RESULTS

4.1 Rates of Hydrogenation

A plot of pressure-fall against time is a measure of hydrogen uptake by the hydrocarbon in the course of the reaction. Thus the gradient of a tangent to any point on the pressure-time curve gives a measure of the change in reactant pressure with change in time at that particular point in the reaction, that is, a measure of the rate of hydrogenation. Therefore a tangent drawn to the pressure-time curve at time zero or alternatively at the end of the induction period gives a measure of the initial rate of hydrogenation (r_h).

4.2 Initial Rates of Isomerisation.

Initial rates of isomerisation could be calculated by means of a method first used by Twigg (8) and later developed by MacNab and Webb (13). From this method the following equation could be derived:

$$ri = \log_{10}(1-y_{eq.}) - \log_{10}(y - y_{eq}) \times 2.303\,(1-y_{eq})(p_B)_0/tex$$

where ri = initial rate of isomerisation

y = fraction of reactant butene remaining

y_{eq} = thermodynamic equilibrium fraction of reactant butene.

$(p_B)_0$ = initial pressure of reactant butene

tex = time from the start of reaction until sample was extracted from reaction vessel (extraction time).

4.3 Determination of Reaction Kinetics.

The determination of the dependence of the rates of hydrogenation and isomerisation upon the initial pressures of reactants was based on the assumption that the rates could be defined by the following expression.

$$r = k\, p_{H_2}^{x}\, p_{C_4H_8}^{y}$$

where r = rate of reaction

k = rate constant

p_{H_2} = initial pressure of hydrogen

$p_{C_4H_8}$ = initial pressure of butene

x, y = order of reaction with respect to hydrogen and butene respectively.

To determine the order with respect to one of the reactants, the initial pressure of that reactant was varied whilst the pressure of the other reactant remained constant in a series of reactions at a constant temperature. Orders of unity and zero could be recognised at once from plots of rate against initial pressure, whilst non-integral orders could be determined from a plot of $\log_{10}$ (rate) against $\log_{10}$ (initial pressure).

4.4 Determination of Activation Energy (Ea).

The relationship between the rate constant and temperature for a given reaction could be expressed in the form of the Arrhenius equation:

$$k = A\, e^{-Ea/RT}$$

By considering the more easily obtainable initial rates for the reaction and substituting those for the rate constants, the equation could be expressed in the related form:

$$r_i = A^1 e^{-Ea/RT}$$

where r_i = initial rate of reaction

Ea = activation energy

R = gas constant

T = temperature

A, A^1 = pre-exponential constants.

Initial rates were measured as a function of temperature in a series of reactions where the initial reactant pressures were constant and the variation of temperature was completely random. A plot of log (initial rates) against reciprocal absolute temperature resulted in a straight line of gradient $^{-Ea}/_{2.303R}$ from which a value for Ea could be obtained.

4.5 Interpretation of Chromatography traces.

As discussed in a previous chapter it was possible to relate the area under any given peak to a partial pressure of the product responsible for the peak. The sum of all the individual partial pressures of the products coming off the column agreed with the total pressure of products swept into the column as measured by the manometer in the sample inlet. Correspondingly, the percentage hydrogenation as measured from the trace in calculating butane as a fraction of total product mixture agreed with that measured directly from the change in pressure in the course of the reaction carried out in the static system.

The data obtained from the traces also supplied the necessary information for the calculation of initial rates of isomerisation as described earlier.

4.6 Product Analysis by Mass Spectrometry.

The hydrocarbon products of the reaction of deuterium with but-1-ene were analysed by mass spectrometry.

The sample was introduced to the mass spectrometer and subjected to an electron beam of energy 20eV. This voltage was sufficient to cause both ionisation and fragmentation.

The intensity of the parent ion in the hydrocarbon was by far the most abundant and was given the value of unity whilst the fragments $C_4H_7^+$ and $C_4H_6^+$ which were called f_1 and f_2 respectively were expressed as fractions of the intensity of the parent ion.

In calculating the distribution of deuterium in the deuterated products of reaction, it was required to have accurate values of f_1 and f_2 for each of the possible products of reaction. These values were unobtainable, but it was justifiable (132) to analyse a sample of light hydrocarbon for each possible product under the exact same operating conditions as for the deuterated products and use the values of f_1 and f_2 obtained from this.

The purpose of measuring f_1 and f_2 was that in examining the intensity of the observed ion current for each deuterated parent ion, a peak was being observed which consisted of two contributions:-

i) the parent ion of that particular $^m/_e$ ratio.

ii) the fragments of more deuterated hydrocarbon species.

In order to compensate for that contribution to each peak which rose as a result of fragmentation of species of higher mass, a series of simultaneous equations was set up, which enabled the true parent ion intensities to be calculated. These equations were dependent upon the assumption that the f_1 and f_2 values for the deuterated butenes were the same as those calculated for the light butenes. Apart from using f_1 and f_2 values in the determination of these equations, account also had to be taken of the statistical probability of whether hydrogen or deuterium atoms were lost in the process of fragmentation. The modifications made in the equations were based solely on the percentage of each atom in the butene, whilst the isotope effect on bond strength was not considered. The full series of equations used in the analysis of each hydrocarbon was calculated and is given in full in Appendix A.

Since naturally occurring carbon contains 1.1% of the ^{13}C, the observed parent ion intensities had to be modified to account for this isotopic abundance before correction for fragmentation is carried out. This was done by subtracting 4.4% of the ion current intensity for the d_0 species from that of the d_1 species. 4.4% intensity was then subtracted from the d_1 species, corrected for 13-carbon, to give the corrected d_2 species and so on.

The final deuterium distribution was determined by expressing each of the corrected ion current intensities as a percentage of the total intensity.

The deuterium number - the mean number of deuterium atoms per

molecule - could be calculated from the expression

$$D.N. = \sum_{i=1}^{n} i d_i$$

where d_i is the fractional abundance of the species containing i deuterium atoms.

RESULTS SECTION

CHAPTER 5

THE REACTIONS OF BUT-1-ENE WITH HYDROGEN ON SILICA SUPPORTED TRIOSMIUM DODECACARBONYL

5.1 Catalyst Characterisation

5.1.1 Initial Observations

The supported complex was a pale yellow colour at room temperature. On activation in vacuo this pale yellow colour initially intensified until at a temperature of about 170°C, the complex again turned a pale yellow colour. At 190 - 200°C the complex took on a light pink colouration, which at 250°C developed into a light grey colour. The colour persisted on heating to 320°C, while prolonged heating at this temperature resulted in the supported complex becoming darker grey.

5.1.2 Thermal Volatilisation Analysis (T.V.A.).

T.V.A. of a freshly prepared sample of the $Os_3(CO)_{12}/SiO_2$ showed that in broad terms, heating resulted in degradation occurring in three distinct stages (Figure 5.1). Stage 1 in the degradation began to occur at 125°C, reached a maximum at 158°C and terminated at 180°C. Between this temperature and 260°C there was minimal degradation. At 260°C, stage 2 in the degradation process commenced. This stage reached a maximum at about 340°C and evolution of decomposition products decreased above this temperature. Stage 3 in the degradation commenced at about 360°C and reached a maximum at 420°C before the evolution of gas levelled off. Stages 2 and 3 tended to overlap to a certain extent in that the products of

Figure 5.1 T.V.A. of 10% W/W $Os_3(CO)_{12}/SiO_2$

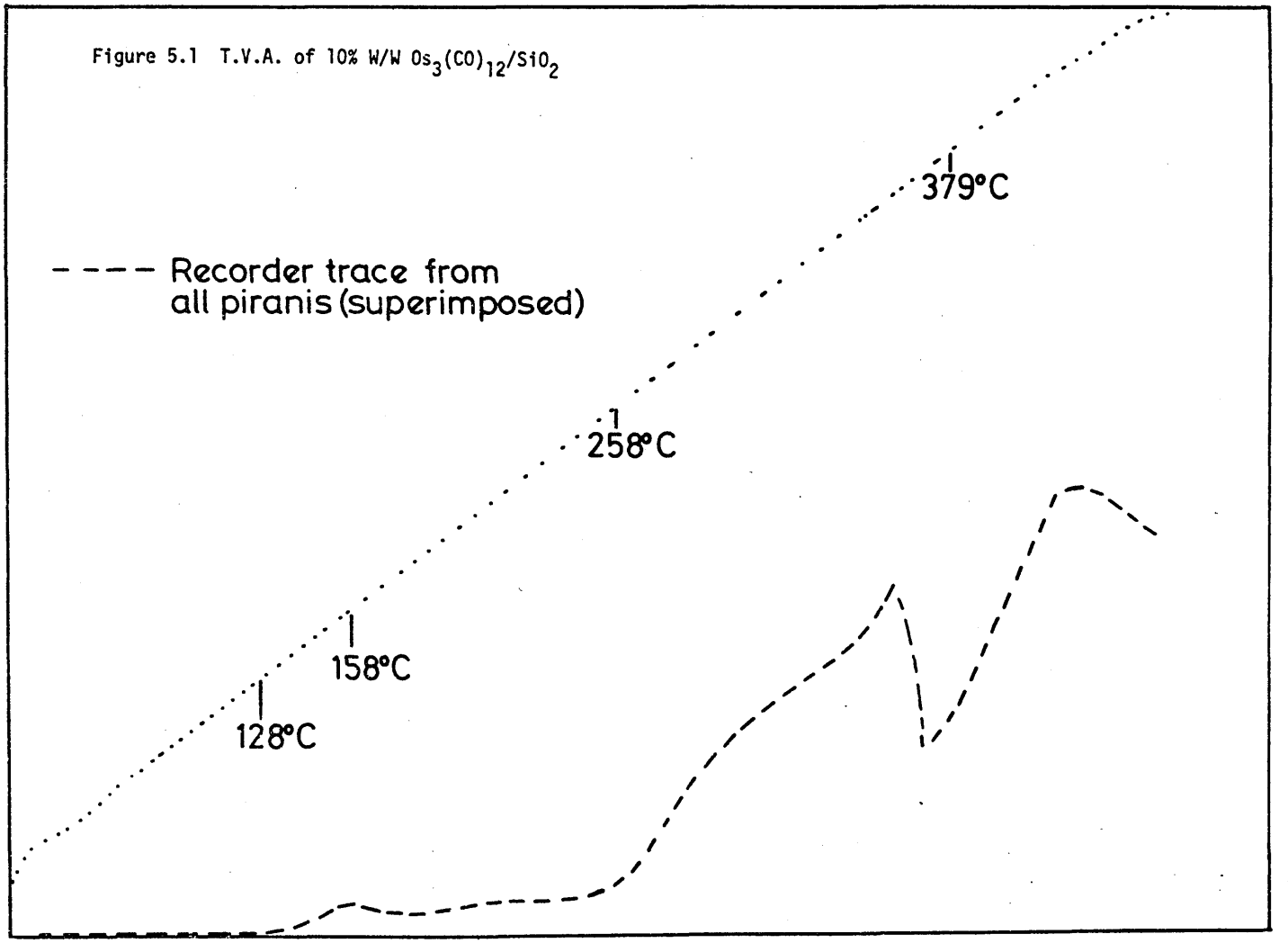

degradation from stage 2 were still being evolved as stage 3 began to occur.

All of the products of degradation were incondensable in that they passed through all of the cold traps between the sample source and the pirani gauges. It was concluded that the sole product of degradation was carbon monoxide.

5.1.3 Thermogravimetric Analysis (T.G.A.).

T.G.A. of the supported complex showed close agreement with the information obtained from T.V.A. in that degradation could be divided into three distinct steps commencing at 125°, 260° and 360°C respectively (Figure 5.2). In addition, it was shown that the total weight loss of 4% could be subdivided into these three steps, which involved 25, 33 and 42% loss respectively of the total weight loss.

5.1.4 Infra-Red Analysis.

Infra-red spectra were run of the supported complex at various stages of its activation. In addition, a comparison was made of the solution spectrum of $Os_3(CO)_{12}$ in methylene dichloride and that of the complex, having been supported on silica. The bands due solely to the silica support could be ignored, and the relevant bands appearing in the carbonyl stretching region are summarised in table 5.1.

The supported complex was extremely stable when exposed to air, irrespective of whether it was in its original "room temperature" state or whether it was in one of its "activated" states, as was concluded from i.r. analyses of all specimens on exposure to air. Similarly, the bands observed in each of the activated forms of the complex were independent of the length of activation time, except in

Figure 5.2 T.G.A. of 10% W/W $Os_3(CO)_{12}/SiO_2$

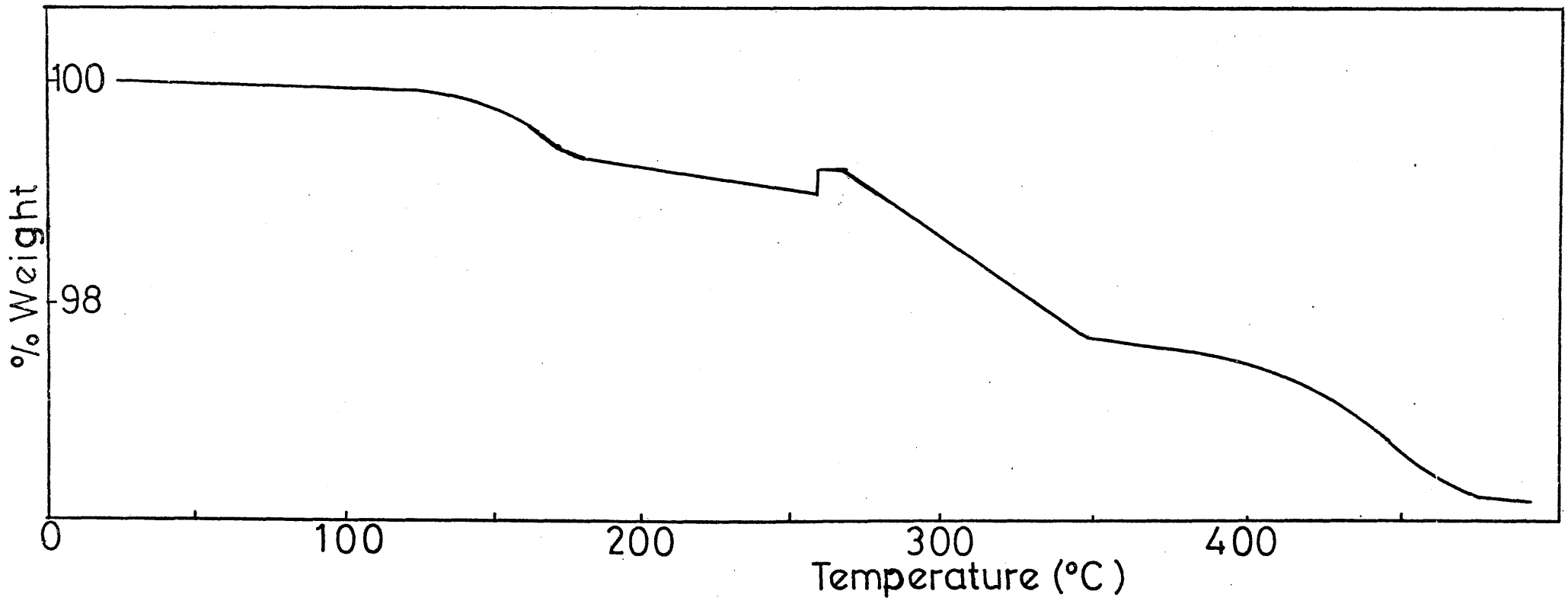

TABLE 5.1

Observed Carbonyl Bands of Various Forms of the Complex.

		(cm^{-1})
(i)	Solution of $Os_3(CO)_{12}$ in methylene chloride	2075(s), 2040(s), 2020(w), 2000(w)
(ii)	Supported complex at room temperature	2126(w), 2075(s), 2045(s), 2020(w), 2000(w)
(iii)	Supported complex activated to 150°C	2136(w), 2120(m), 2086(s), 2070(s), 2041(s), 2026(s), 2000(sh)
(iv)	Supported complex activated to 200°C	2136(m), 2120(m), 2086(s), 2070(s), 2036(s), 2000(sh)
(v)	Supported complex activated to 235°C	2136(s), 2056(s), 1965(s)
(vi)	Supported complex activated to 250°C	2136(s), 2056(s), 1965(s)
(vii)	Supported complex activated to 320°C overnight.	1986(m)

the case of the specimen activated to 320°C, where the number of bands were dependent on time of activation, decreasing in intensity with time.

5.1.5 Examination by Electron Microscopy.

The supported complex was examined in two forms:-

(i) after activation to 250°C *in vacuo*.

(ii) after activation to 320°C *in vacuo*

The electron micrograph of (i) showed a widespread distribution of metal particles on the support, averaging about 10Å in diameter. The particles in (ii) however were slightly larger, and aggregates of diameter 20Å were present on the support.

5.2 Reaction of But-1-ene with Hydrogen on 2% $Os_3(CO)_{12}/SiO_2$ Activated to 250°C.

5.2.1. Preliminary Investigation

The reaction of but-1-ene with hydrogen over 2% W/W $Os_3(CO)_{12}/SiO_2$ was studied in the temperature range 150 - 250°C, where the supported complex had been previously activated *in vacuo* at 250°C overnight. The supported complex was found to be a catalyst for the reaction in this temperature range.

For a series of reactions over one particular catalyst sample, the rate of hydrogenation was found to be reasonably consistent. A typical pressure-fall against time curve is in Figure 5.3, where the reaction was carried out at 220°C. Corresponding first and second order plots (Figure 5.4) suggest that the overall order of reaction is non-integral. Although the reaction rate appeared to be consistent

Figure 5.3 Pressure fall against time curve for hydrogenation of but-1-ene at 220°C ($2\%\ Os_3(CO)_{12}/SiO_2$)

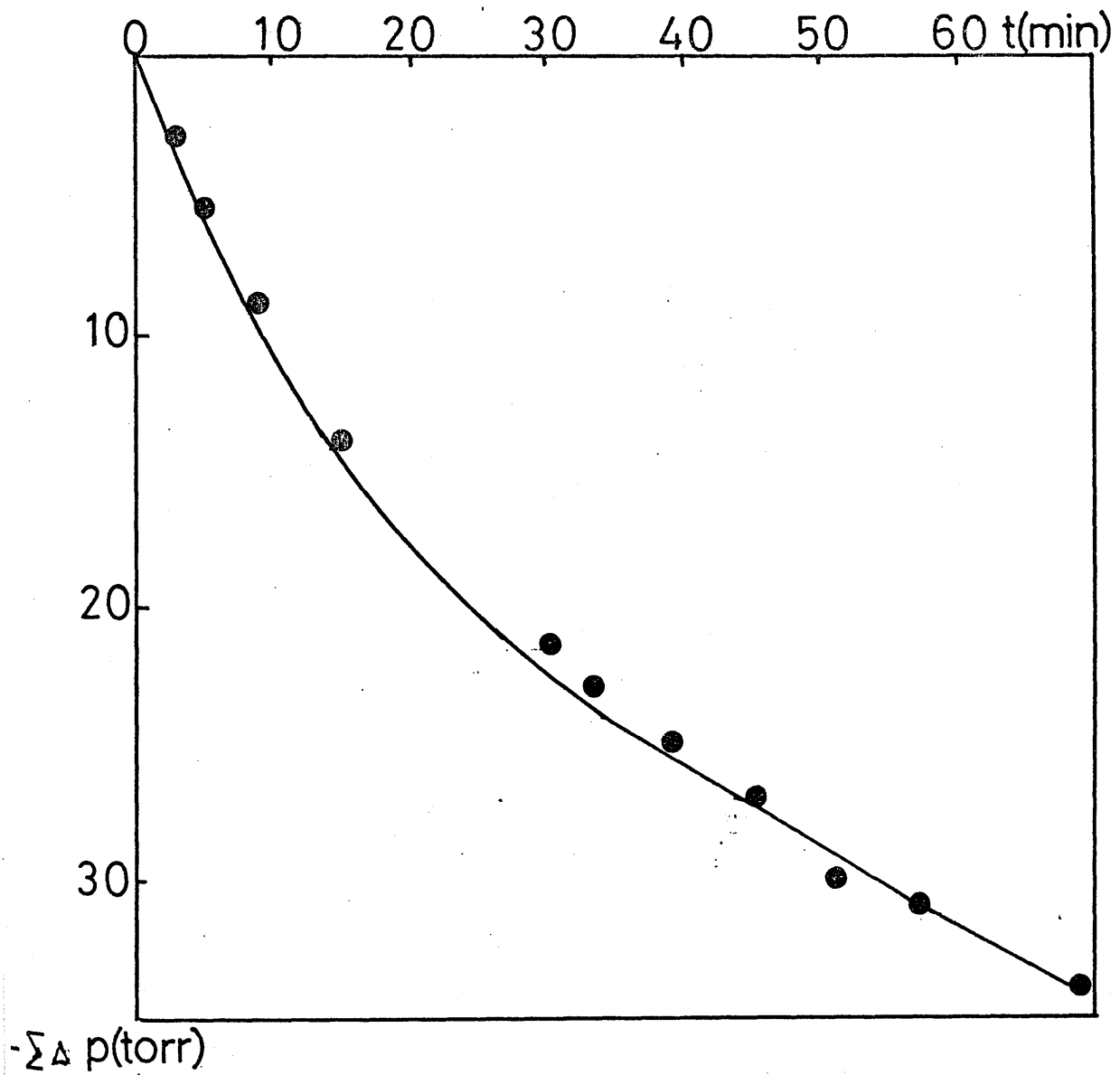

Figure 5.4 Corresponding first and second order plots for hydrogenation of but-1-ene at 220°C.

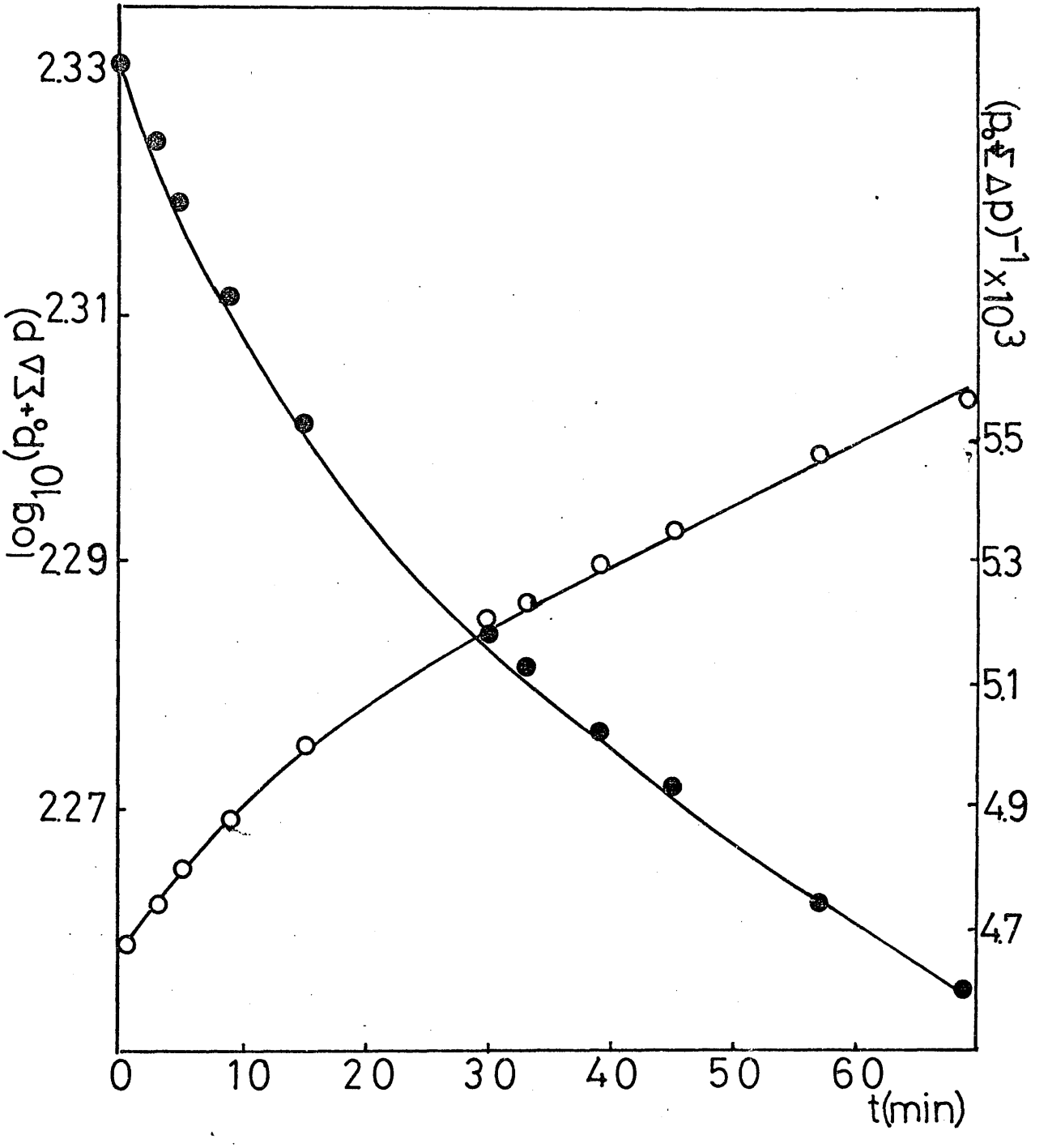

and independent of reaction number within one particular series, it was found that the reaction rate varied from one catalyst sample to the next.

The isomerisation of but-1-ene was studied in the temperature range 150 - 250°C by carrying out a series of reactions over varying periods of time up to 45 minutes at several temperatures within this range. The analysis figures for product composition, together with time (tex) at which the products were extracted for analysis are shown in table 5.2. The time of extraction in each series of reactions was varied randomly to account for any change in rate which may have occurred due to a "run number" effect. Similarly, any "temperature effect" was allowed for by carrying out each series of reactions in a random order with respect to temperature. The terms n-butane, but-1-ene, trans-but-2-ene and cis-but-2-ene are abbreviated to n-BUT, BUT-1, t-B-2, c-B-2 respectively in all tables.

The variation in butene composition with percentage conversion is shown in Figures 5.5 and 5.6 in which each butene is given as a percentage of total butene yield.

The possibility that the Aerosil silica itself may have catalysed the reaction was investigated. But-1-ene and hydrogen were introduced to the catalyst vessel, which contained 80 mg of support. The support had been subjected to the same treatment as was used in the preparation of the supported complex, namely, suspension in CH_2Cl_2, evaporation to dryness under N_2, followed by activation in vacuo to 250°C. It was found that silica itself was inactive for the hydrogenation or isomerisation of but-1-ene under the conditions of these experiments.

TABLE 5.2

Variation of Hydrocarbon Composition with Conversion over 2% $Os_3(CO)_{12}$/Aerosil Silica

Initial P_{H_2} = P_{BUT-1} = 100 ± 0.5 torr Catalyst weight = 0.08g

At 150°C	% hydrocarbon composition				
Reaction	n-BUT	BUT-1	t-B-2	c-B-2	tex (min)
C/3	0.8	88.6	6.0	4.6	5
C/4	1.5	67.9	17.5	13.1	7
C/1	2.3	59.0	21.9	16.8	15
C/5	4.3	15.9	49.3	30.5	30
C/2	5.3	13.4	48.6	32.7	45
At 170°C					
D/1	1.8	72.4	14.1	11.7	3
D/5	2.7	65.7	17.2	14.4	7
D/3	2.8	61.5	19.1	16.6	15
D/6	5.5	12.4	51.8	30.3	22.5
D/4	7.6	14.4	49.0	29.0	30
D/2	8.1	16.4	45.5	30.0	45
At 200°C					
B/4	2.0	59.2	21.2	17.6	3
B/2	4.1	23.6	41.5	30.8	7
B/1	10.6	14.8	47.3	27.3	15
B/5	18.8	11.6	40.5	29.1	30
B/3	20.3	11.8	41.2	26.7	45
At 220°C					
E/6	5.3	25.8	39.8	29.1	3
E/1	6.2	17.7	45.8	30.3	7
E/3	8.0	16.6	46.7	28.7	13
E/4	8.5	16.9	45.4	29.2	20
E/2	10.7	16.8	43.7	28.8	30
E/5	25.9	11.9	37.7	24.5	45

TABLE 5.2 (Continued)

Variation of Hydrocarbon Composition with Conversion over 2% $Os_3(CO)_{12}$/Aerosil Silica

Initial $^{p}H_2 = {}^{p}$BUT-1 = 100± 0.5 torr Catalyst weight = 0.08g

At 250°C % hydrocarbon composition

Reaction	n-BUT	BUT-1	t-B-2	c-B-2	tex (min)
A/2	6.1	19.2	43.1	31.6	3
A/5	16.3	18.7	38.2	26.8	7
A/1	29.8	13.7	33.5	23.0	15
A/4	34.7	11.8	31.9	21.6	20
A/3	56.5	9.0	21.1	13.4	45

Figure 5.5 Variation of butene composition with percentage hydrogenation at (a) 150°C (b) 170°C (c) 200°C (d) 220°C ($2\%\ Os_3(CO)_{12}/SiO_2$ ● = but-1-ene; o = trans-but-2-ene; ◐ = cis-but-2-ene).

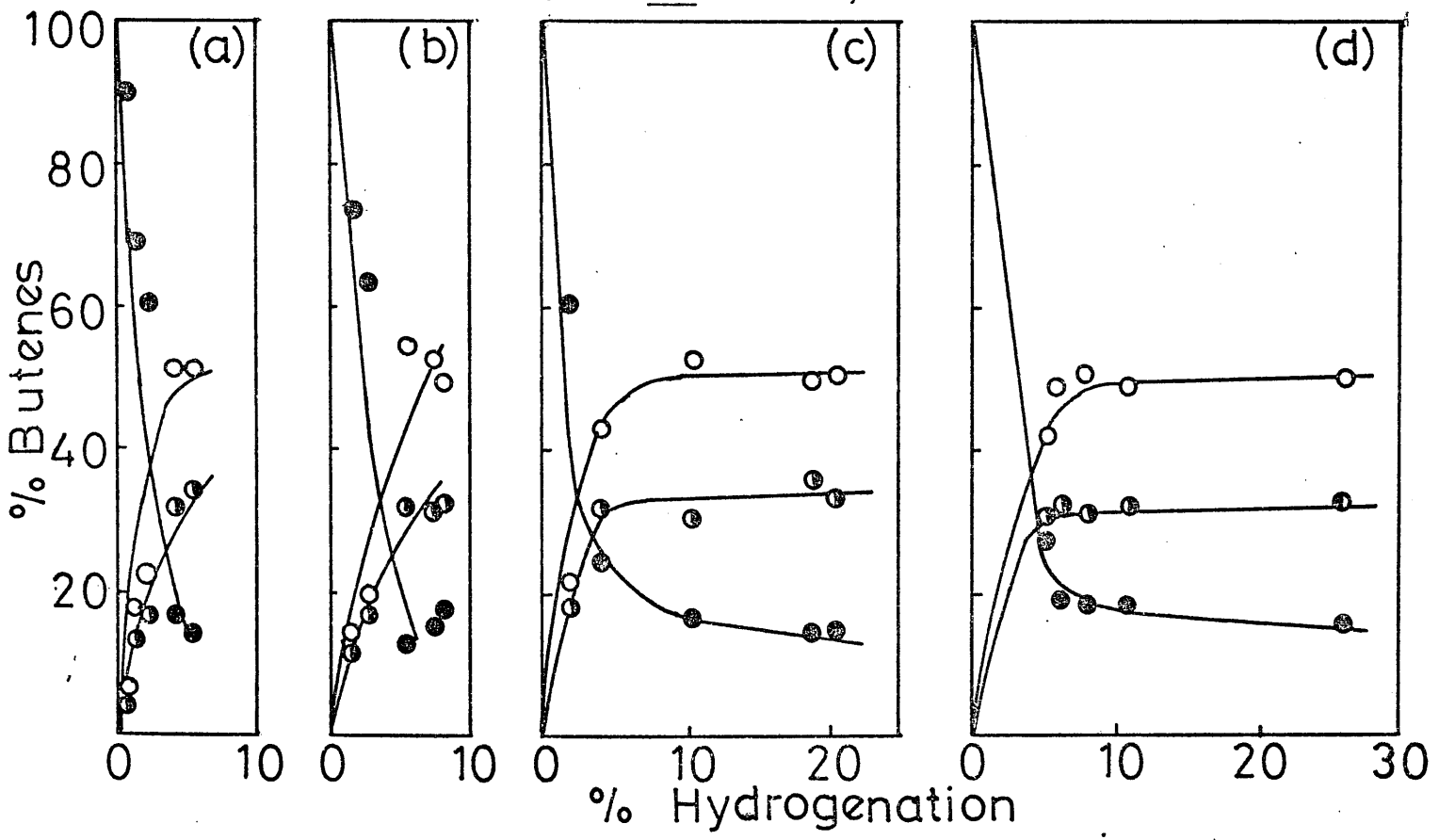

Figure 5.6 Variation of butene composition with percentage hydrogenation at 250°C ($2\%\ Os_3(CO)_{12}/SiO_2$ ● = but-1-ene; o = trans-but-2-ene; ◐ = cis-but-2-ene)

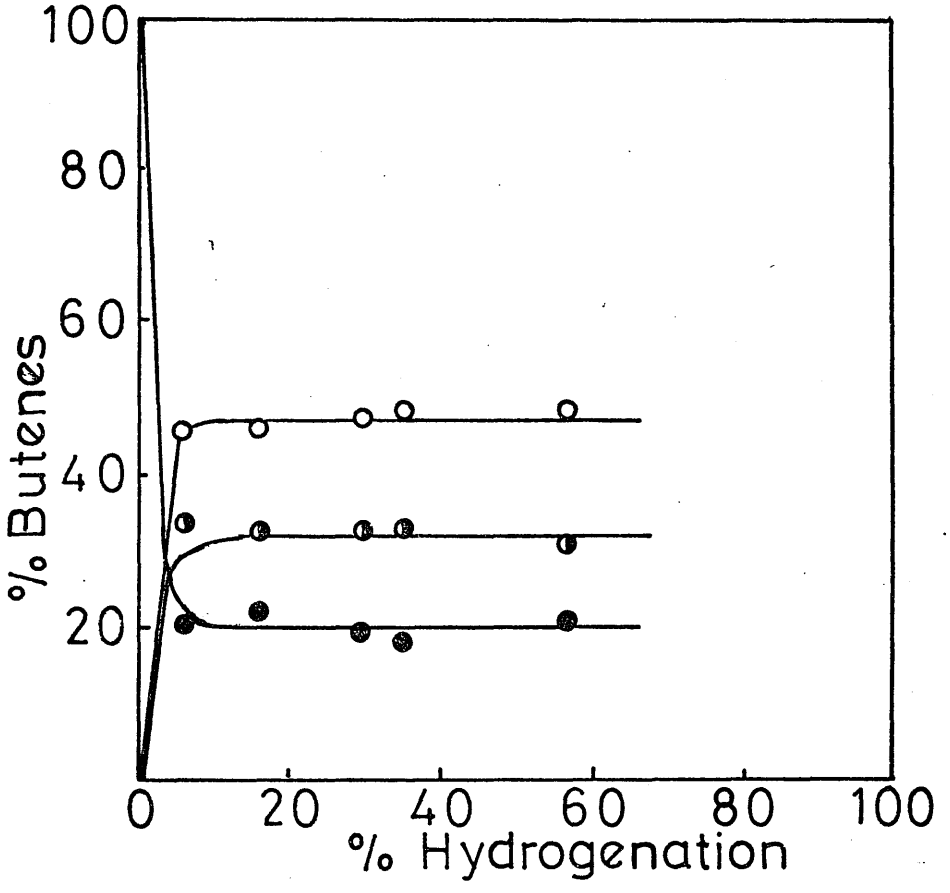

5.2.2 Kinetics of Reactions of But-1-ene and Hydrogen.

In the series of reactions to determine the dependencies of the initial rates upon initial hydrogen pressure, each reaction was carried out at 200°C for 20 minutes. Similar conditions were used in a second series of reactions to determine the dependencies of initial rates upon initial but-1-ene pressure.

The results of the series to determine the variation of rates of reaction with initial hydrogen pressure are shown in tables 5.3 and 5.4. Figure 5.7 illustrates that the rate of isomerisation is independent of the initial hydrogen pressure, whilst a plot of log r_h against log p_{H_2} in Figure 5.8 yields a good straight line of gradient 0.5, indicating that the rate of hydrogenation is 0.5 order with respect to initial hydrogen pressure.

Tables 5.5 and 5.6 show the dependence of the initial rates of reaction on the initial pressure of but-1-ene. Figure 5.9, in which r_i is plotted against p_{BUT-1} shows that the rate of isomerisation is virtually first order with respect to initial but-1-ene pressure up to 200 torr, but at above this pressure there is a poisoning effect by the butene. The plot of log r_h against log p_{BUT-1} in Figure 5.10 indicates an order of 0.85 for the hydrogenation reaction with respect to initial but-1-ene pressure.

These values are summarised below:-

Kinetics of Reaction of But-1-ene with Hydrogen

Reaction	Order of Reaction	
	Hydrogen	But-1-ene
Hydrogenation	0.5 ± 0.05	0.85 ± 0.1
Isomerisation	0 ± 0.1	1.0 ± 0.1

TABLE 5.3

Variation of Butene Distribution with Initial Hydrogen Pressure

Temperature = 200°C Initial p_{BUT-1} = 50 ± 0.5 torr

Samples extracted after 20 minutes

Reaction	p_{H_2} (torr)	% n-BUT	% butene composition BUT-1	t-B-2	c-B-2
F/A/6	25	3.7	22.3	46.4	31.3
F/A/3	50	12.9	19.5	48.6	31.9
F/A/1	100	16.7	21.0	49.0	30.0
F/A/5	125	18.2	25.7	41.3	33.0
F/A/4	200	25.2	18.3	50.7	31.0
F/A/2	300	32.1	21.5	48.4	30.1

TABLE 5.4

Variation of Initial Reaction Rates with Initial Hydrogen Pressure at 200°C

Reaction	p_{H_2} (torr)	ri (torr/min)	rh (torr/min)
F/A/6	25	5.03	0.18
F/A/3	50	5.91	0.32
F/A/1	100	5.39	0.41
F/A/5	125	4.23	0.45
F/A/4	200	6.44	0.63
F/A/2	300	5.24	0.80

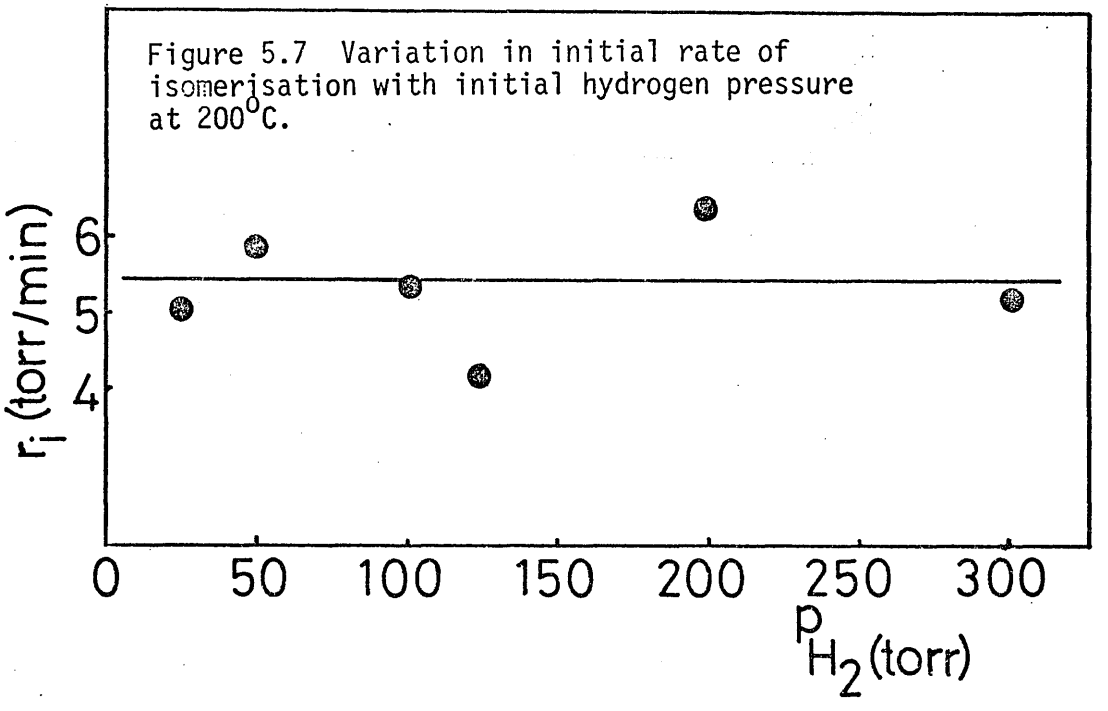

Figure 5.7 Variation in initial rate of isomerisation with initial hydrogen pressure at 200°C.

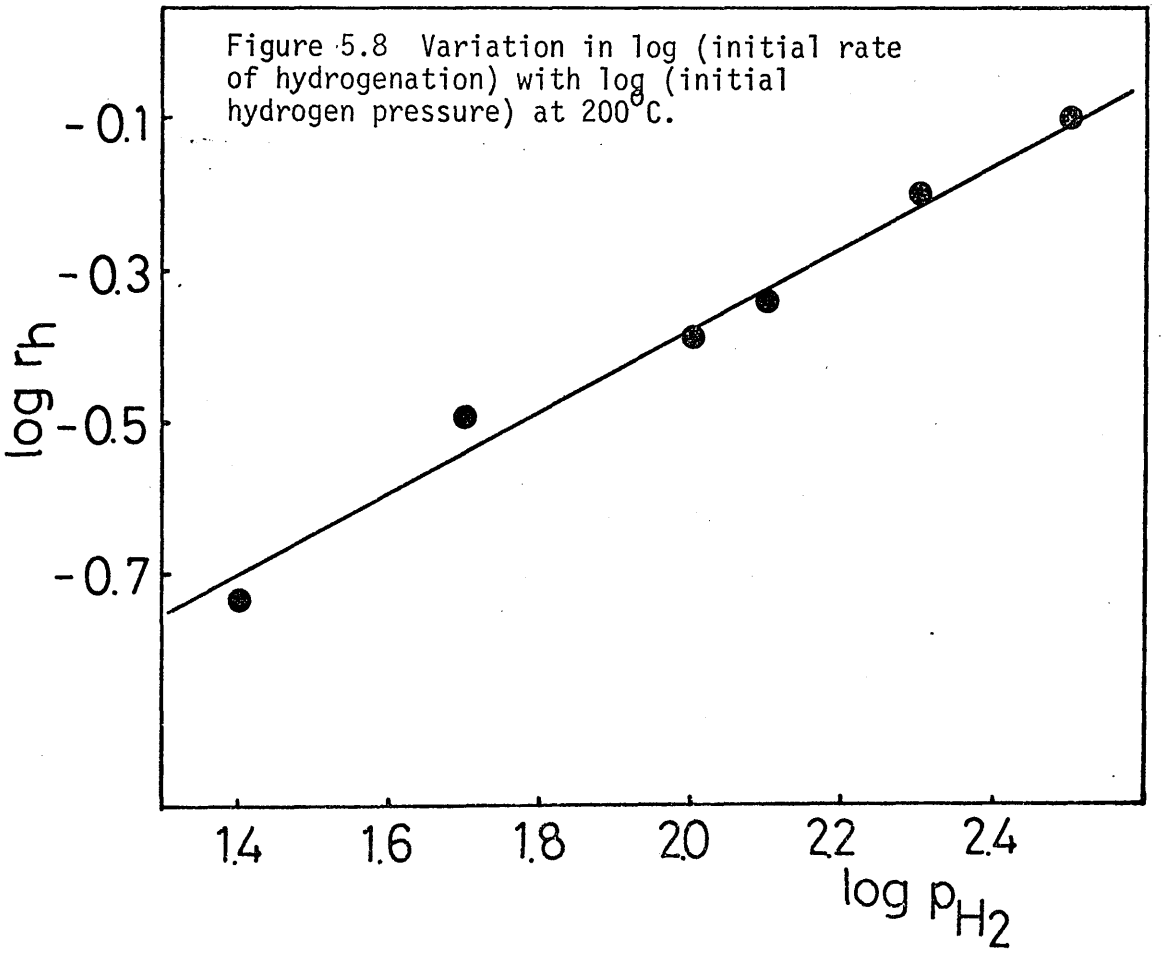

Figure 5.8 Variation in log (initial rate of hydrogenation) with log (initial hydrogen pressure) at 200°C.

TABLE 5.5

Variation of Butene Distribution with Initial But-1-ene Pressure

Temperature = 200°C Initial p_{H_2} = 50 ± 0.5 torr

Samples extracted after 20 minutes

			% butene distribution		
Reaction	p_{BUT-1} (torr)	% n-BUT	BUT-1	t-B-2	c-B-2
F/B/6	25	6.4	42.5	32.3	25.2
F/B/3	50	5.6	51.3	26.8	21.9
F/B/7	50	3.4	44.9	30.9	24.2
F/B/1	100	6.7	46.9	26.5	26.6
F/B/5	150	3.9	54.0	27.9	18.1
F/B/4	200	3.1	52.7	26.7	20.6
F/B/2	300	4.8	72.1	16.2	11.7

TABLE 5.6

Variation of Initial Reaction Rates with Initial But-1-ene Pressure at 200°C

Reaction	p_{BUT-1} (torr)	ri (torr/min)	rh (torr/min)
F/B/6	25	1.07	0.08
F/B/3	50	1.79	0.11
F/B/7	50	2.20	0.08
F/B/1	100	4.13	0.33
F/B/5	150	4.94	0.29
F/B/4	200	6.87	0.31
F/B/2	300	5.10	0.72

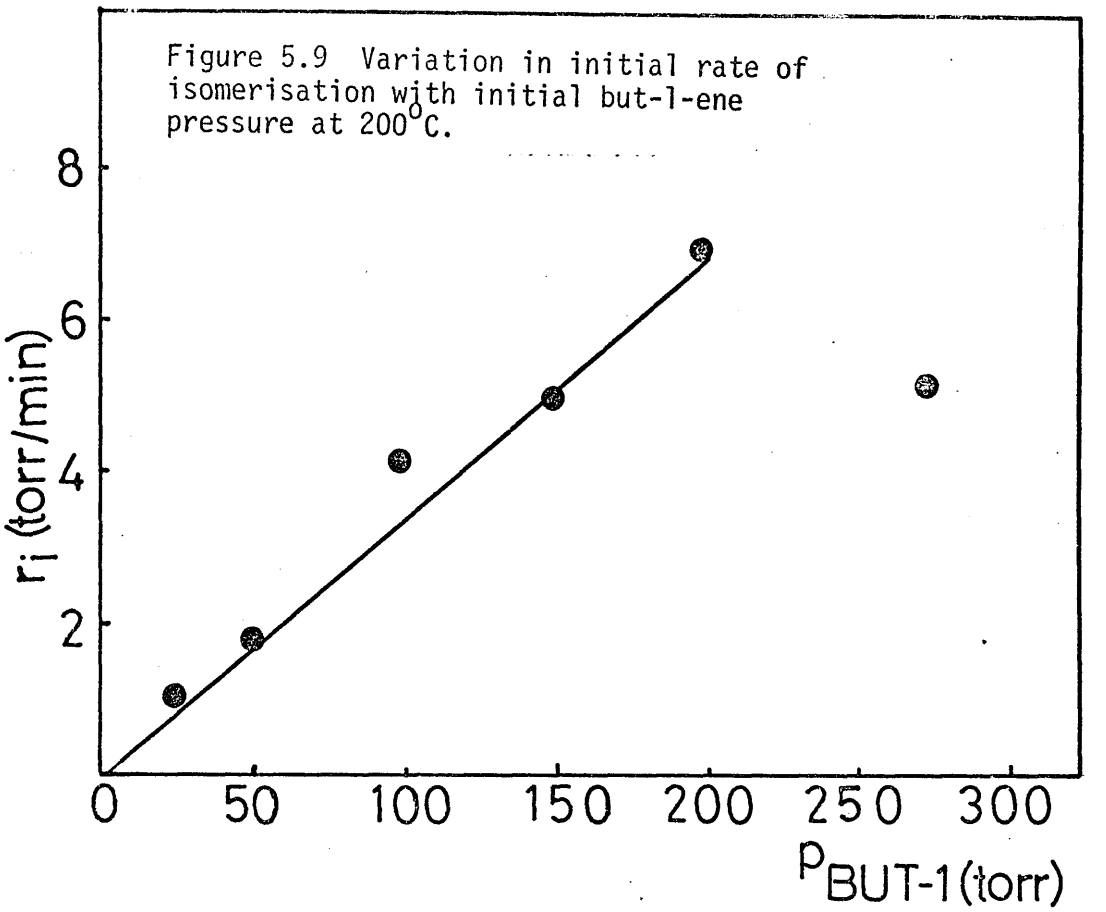

Figure 5.9 Variation in initial rate of isomerisation with initial but-1-ene pressure at 200°C.

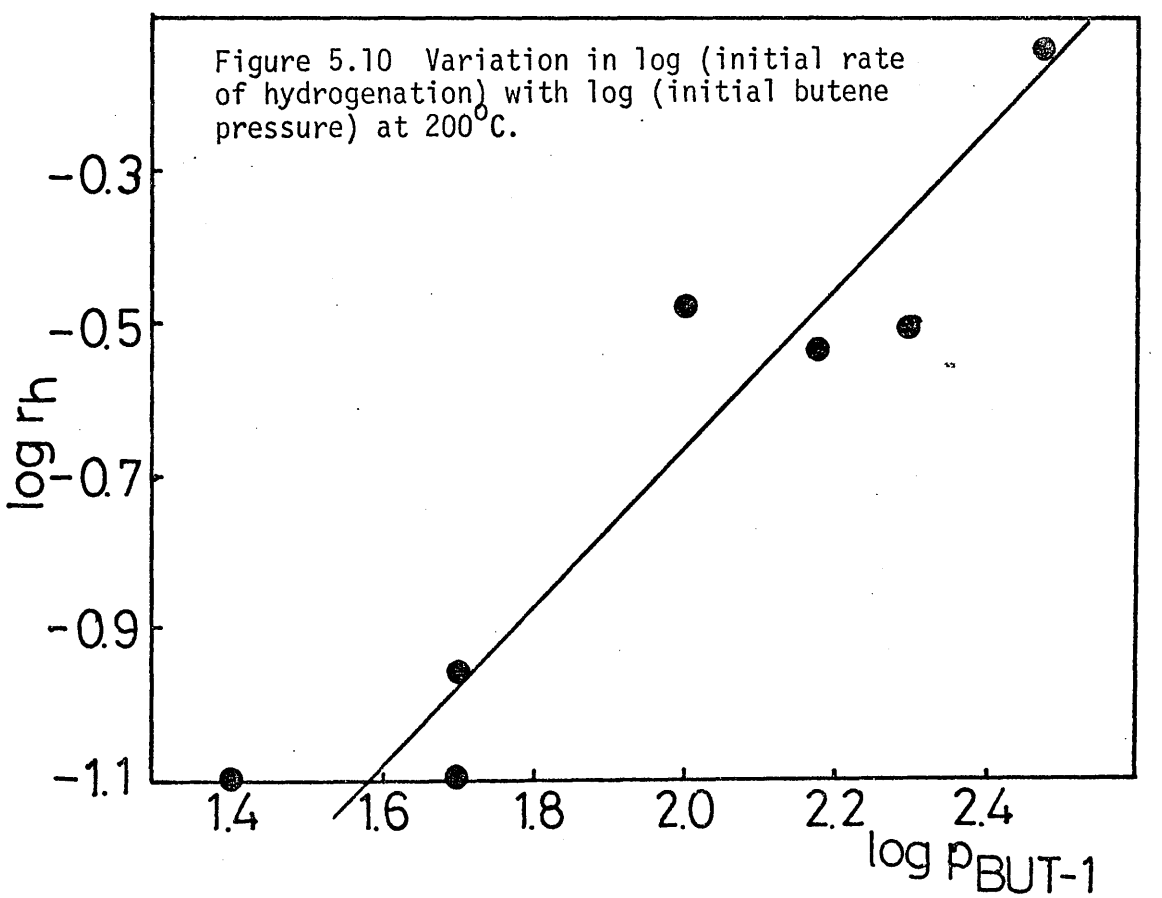

Figure 5.10 Variation in log (initial rate of hydrogenation) with log (initial butene pressure) at 200°C.

5.2.3 Determination of Activation Energies of Reactions of But-1-ene and Hydrogen.

The dependence of rates of reaction on temperature was studied in the temperature range 210 - 250°C. Reactions were carried out until a pressure fall of 5 torr was observed on the manometer, after which the products were extracted for analysis. Reactions were carried out with equal initial pressures of deuterium and but-1-ene of 100 ± 0.5 torr. This allowed the rate of olefin exchange to be calculated also.

The product distribution and initial rates of reaction are given in tables 5.7 and 5.8. Figure 5.11 shows the Arrhenius plots of log r against T^{-1}. There was an apparent loss of activity in the catalyst overnight, which meant that reactions J/4 and J/5 were considered separately from the other three reactions, since the former were carried out on the following day. There appeared to be an induction period for hydrogenation and olefin exchange in the first reaction of the series, indicating that these two processes occurred by a similar mechanism. Thus, in considering the best straight line to calculate Ea hyd and Ea oe, the r_h and r_{oe} values for reactions J/1 were ignored. From the slopes of the lines, the activation energies for hydrogenation, isomerisation and butene exchange were calculated as

$$38.0 \pm 5,\ 80.0 \pm 5,\ 48.7 \pm 5 \text{ kJ mole}^{-1} \text{ respectively.}$$

5.2.4 Deuterium Exchange Reactions of But-1-ene.

The reaction of but-1-ene with deuterium was carried out in exactly the same manner as those with hydrogen, using the same amount of catalyst (0.08g) and identical reaction proportions as before.

TABLE 5.7

Variation of Butene Distribution with Temperature

$P_{D_2} = P_{BUT-1} = 100 \pm 0.5$ Torr

			% butene distribution			
Reaction	Temp(K)	%n-BUT	BUT-1	t-B-2	c-B-2	tex(min)
J/1	523	4.6	34.4	40.8	24.8	24
J/2	483	5.1	68.1	17.3	14.6	31
J/3	503	5.9	51.5	25.5	23.0	23
J/4	515	3.6	62.9	19.1	18.0	28
J/5	495	3.2	79.8	10.3	9.9	34

TABLE 5.8

Variation of Initial Rates of Reaction with Temperature

	Reaction	Temp(K)	rh (torr/min)	ri (torr/min)	roe(torr/min)
	J/1	523	0.19	5.15	0.38
	J/2	483	0.16	1.28	0.38
	J/3	503	0.24	2.97	0.63
*	J/4	515	0.13	1.74	0.56
*	J/5	495	0.11	0.68	0.38

* carried out on separate day.

Figure 5.11 Arrhenius plots for isomerisation ⊖; hydrogenation ⊖ ; olefin exchange ● .
(2% $Os_3(CO)_{12}/SiO_2$)

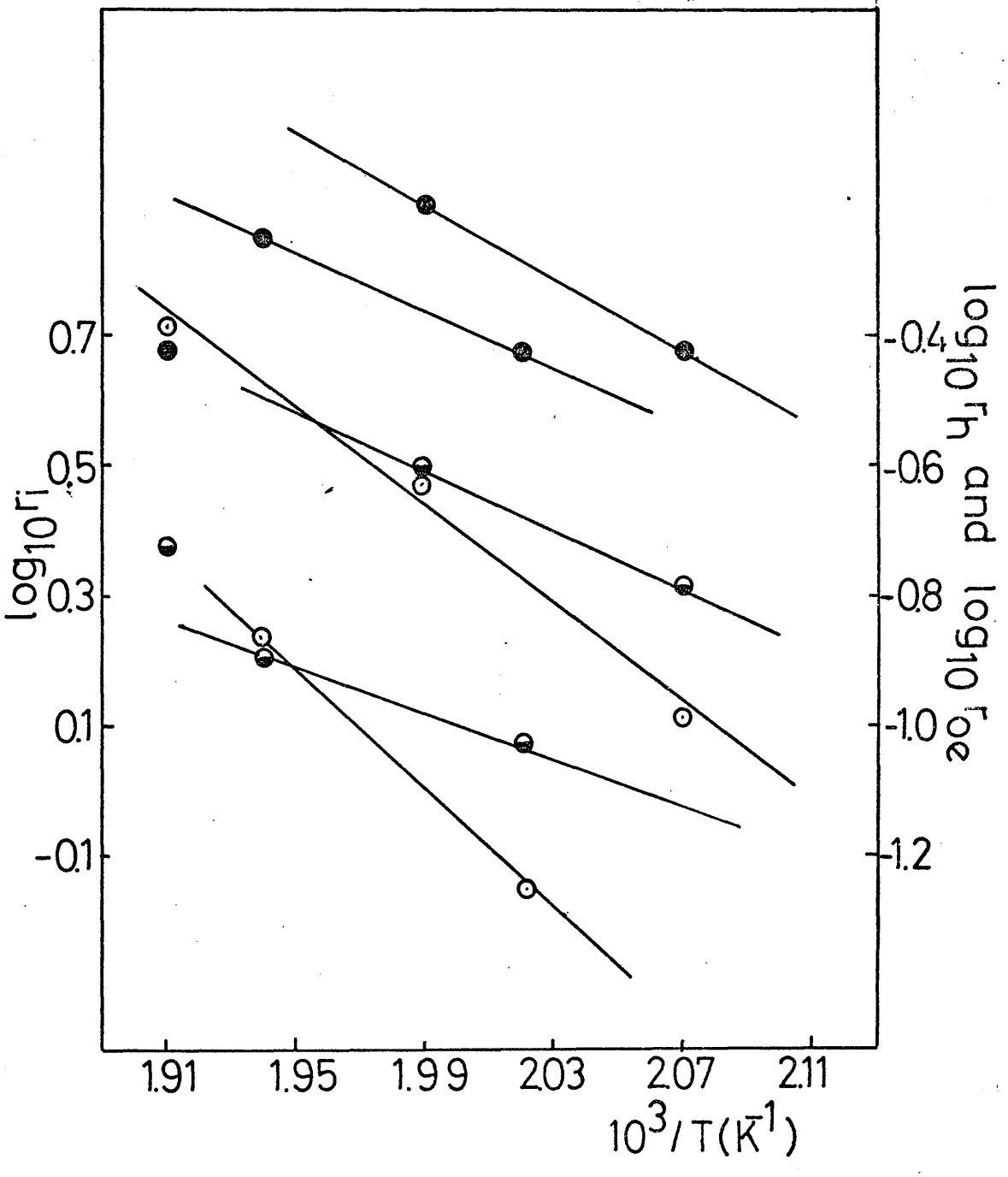

Mass spectrometric analysis of the products allowed the effect of two factors governing alkene exchange to be examined, namely, (a) the effect of temperature and (b) the effect of increasing conversion in the reaction. The effect of (a) was studied by carrying out a series of deuterations in the temperature range 150 - 250°C to 10% conversion, whilst the effect of (b) was examined by carrying out the deuteration at 250°C to varying conversions. The results are shown in tables 5.9 and 5.10 respectively, where the deuterated products are denoted by d_0, d_1 --- d_6, where the subscript indicates the number of deuterium atoms incorporated into each molecule. D.N. is the deuterium number for each product i.e. the mean number of deuterium atoms per hydrocarbon molecule.

5.2.5 Isomerisation of But-1-ene in the Absence of Hydrogen

A series of reactions were carried out over 2% W/W $Os_3(CO)_{12}/SiO_2$ (80 mg) to determine whether hydrogen was required for isomerisation of but-1-ene to occur. The supported complex was activated *in vacuo* at 250°C for 1 hour, after which the series of reactions was performed over varying periods of time. The variation of butene composition together with extraction times are shown in table 5.11

5.3 Reaction of But-1-ene with Hydrogen on 2% $Os_3(CO)_{12}/SiO_2$ Activated to 340°C.

5.3.1 Preliminary Investigation

The reaction of But-1-ene with hydrogen over 2% W/W $Os_3(CO)_{12}/SiO_2$ activated to this higher temperature was observed to differ markedly from the supported complex activated to 250°C.

Experiments were again carried out using an initial pressure

TABLE 5.9

Distribution of Deuterated Hydrocarbons over 2% $Os_3(CO)_{12}$/Silica (activated at 250°C) to 10 torr Conversion in Range of Temperatures

	d_o	d_1	d_2	d_3	d_4	d_5	d_6	D.N.
At 170°C								
n-butane	14.6	23.6	36.4	11.0	6.9	6.4	2.1	2.01
but-1-ene	76.9	17.6	3.7	1.3	0.3	0.1	0.1	0.31
t-but-2	78.9	15.2	3.7	1.3	0.4	0.3	0.2	0.31
c-but-2	76.5	17.1	3.8	1.5	0.6	0.3	0.2	0.34
At 185°C								
n-butane	9.7	26.2	39.0	12.1	6.1	5.4	1.5	2.01
but-1-ene	66.5	23.1	7.3	1.8	0.7	0.4	0.2	0.49
t-but-2	69.2	24.1	4.8	1.1	0.5	0.2	0.1	0.41
c-but-2	78.5	16.4	3.3	0.9	0.5	0.2	0.2	0.30
At 200°C								
n-butane	13.2	26.1	39.4	11.1	5.0	3.9	1.3	1.85
but-1-ene	63.7	26.4	6.9	1.9	0.7	0.3	0.1	0.51
t-but-2	61.0	26.2	8.7	2.6	0.9	0.4	0.2	0.58
c-but-2	60.2	25.3	9.2	3.4	1.1	0.5	0.3	0.62
At 220°C								
butane	11.9	21.9	34.3	13.9	8.2	6.7	3.1	2.17
but-1	58.8	27.2	9.6	2.9	0.9	0.4	0.2	0.62
t-but-2	64.4	23.6	7.6	2.7	1.0	0.4	0.3	0.54
c-but-2	63.3	24.1	8.1	2.6	1.1	0.5	0.3	0.57
At 220°C (to test reproducibility).								
butane	12.9	23.9	36.6	12.5	7.0	5.1	2.0	2.00
but-1-ene	54.2	31.8	9.7	2.8	0.9	0.4	0.2	0.66
t-but-2	66.1	23.4	6.8	2.2	0.8	0.4	0.3	0.51
c-but-2	62.9	24.9	7.8	2.4	1.1	0.6	0.3	0.57
At 250°C								
butane	18.3	22.5	29.6	15.2	7.7	4.6	2.1	1.94
but-1	41.4	25.3	16.4	10.4	4.0	1.7	0.8	1.19
t-but-2	61.6	25.1	8.6	3.0	1.0	0.4	0.3	0.59
c-but-2	56.1	28.2	10.2	3.7	1.1	0.5	0.3	0.68

TABLE 5.10

Distribution of Deuterated Hydrocarbons over 2% $Os_3(CO)_{12}/SiO_2$ at 250°C

(Activated at 250°C)

	d_0	d_1	d_2	d_3	d_4	d_5	d_6	D.N.
	Conversion 8.1%							
n-butane	15.1	17.4	38.2	10.3	7.7	7.9	3.4	2.10
but-1-ene	64.8	22.8	5.9	4.2	1.4	0.9	0	0.57
t-but-2	69.6	20.0	6.0	2.5	1.4	0.5	0	0.48
c-but-2	78.4	13.6	4.2	1.9	1.0	0.6	0.3	0.36
	Conversion 12.4%							
n-butane	13.0	21.2	33.8	11.9	8.3	6.4	2.3	2.10
but-1-ene	52.9	31.1	8.1	5.0	1.4	1.0	0.5	0.76
t-but-2	59.5	25.4	7.8	4.1	1.7	0.9	0.6	0.68
c-but-2	-	-	-	-	-	-	-	-
	Conversion 18.3%							
n-butane	15.3	16.9	36.4	15.3	9.3	6.8	-	2.10
but-1-ene	67.6	22.4	6.9	2.0	0.6	0.3	0.2	0.47
t-but-2	60.2	27.3	8.6	2.4	1.0	0.5	-	0.58
c-but-2	59.5	27.0	9.0	3.0	1.5	-	-	0.60
	Conversion 37.5%							
n-butane	10.4	20.9	29.3	21.2	12.6	3.9	1.7	2.20
but-1-ene	50.9	16.5	16.7	11.1	3.0	1.4	0.4	0.71
t-but-2	21.1	30.9	27.0	15.1	4.3	1.2	0.4	1.56
c-but-2	19.9	33.2	29.3	10.8	4.6	1.7	0.5	1.43
	Conversion 46.5%							
butane	18.5	23.6	28.9	15.3	8.4	3.8	1.5	1.89
but-1-ene	56.2	17.1	13.5	7.8	3.6	1.3	0.5	0.91
t-but-2	15.2	32.3	28.3	15.9	5.5	2.2	0.6	1.73
c-but-2	16.8	32.7	29.6	14.9	3.0	2.3	0.7	1.64

TABLE 5.11

Variation of Butene Composition with Time over 2% $Os_3(CO)_{12}/SiO_2$

$p_{BUT-1} = 200 \pm 0.5$ torr

Temperature = 250°C Catalyst Weight = 0.08g

		% butene distribution			
Reaction	% n-BUT	BUT-1	t-B-2	C-B-2	tex(min)
K/3	-	63.5	23.0	13.5	5
K/5	-	59.0	25.7	15.3	10
K/1	-	19.4	48.1	32.5	15
K/4	-	33.3	41.5	25.3	22
K/2	-	18.4	48.1	33.5	30

of a 1:1 mixture of hydrogen and but-1-ene. For a series of reactions over a given catalyst there was found to be a lack of consistency in the rates of hydrogenation.

A series of reactions were carried out at 240°C over a freshly prepared catalyst activated to 340°C overnight. These reactions were carried out over a period of days, with the catalyst being reactivated at selected times during the series. Pressure fall versus time curves are shown of these reactions in Figure 5.12, whilst Figure 5.13 indicates how the initial rate of hydrogenation varies depending on reaction number and treatment of catalyst between reactions. The products of each of these reactions were extracted for analysis. The variation in hydrocarbon composition, together with the time of extraction (tex) are listed in table 5.12, whilst Figure 5.14 shows that the butene distribution remains virtually constant with percentage conversion and independent of the time of reaction.

The isomerisation of but-1-ene was studied at 230°C over a freshly prepared 2% $Os_3(CO)_{12}/SiO_2$ catalyst activated to 340°C overnight, by carrying out a series of reactions over varying periods of time. To test for reproducibility, the series was repeated a second time, carrying out each reaction for the same period of time, over the same catalyst and in the same order as for the first series. The analysis figures for hydrocarbon composition, together with the time of extraction are shown in tables 5.13 and 5.14. Figures 5.15 and 5.16 show the variation of butene composition with percentage conversion for both series.

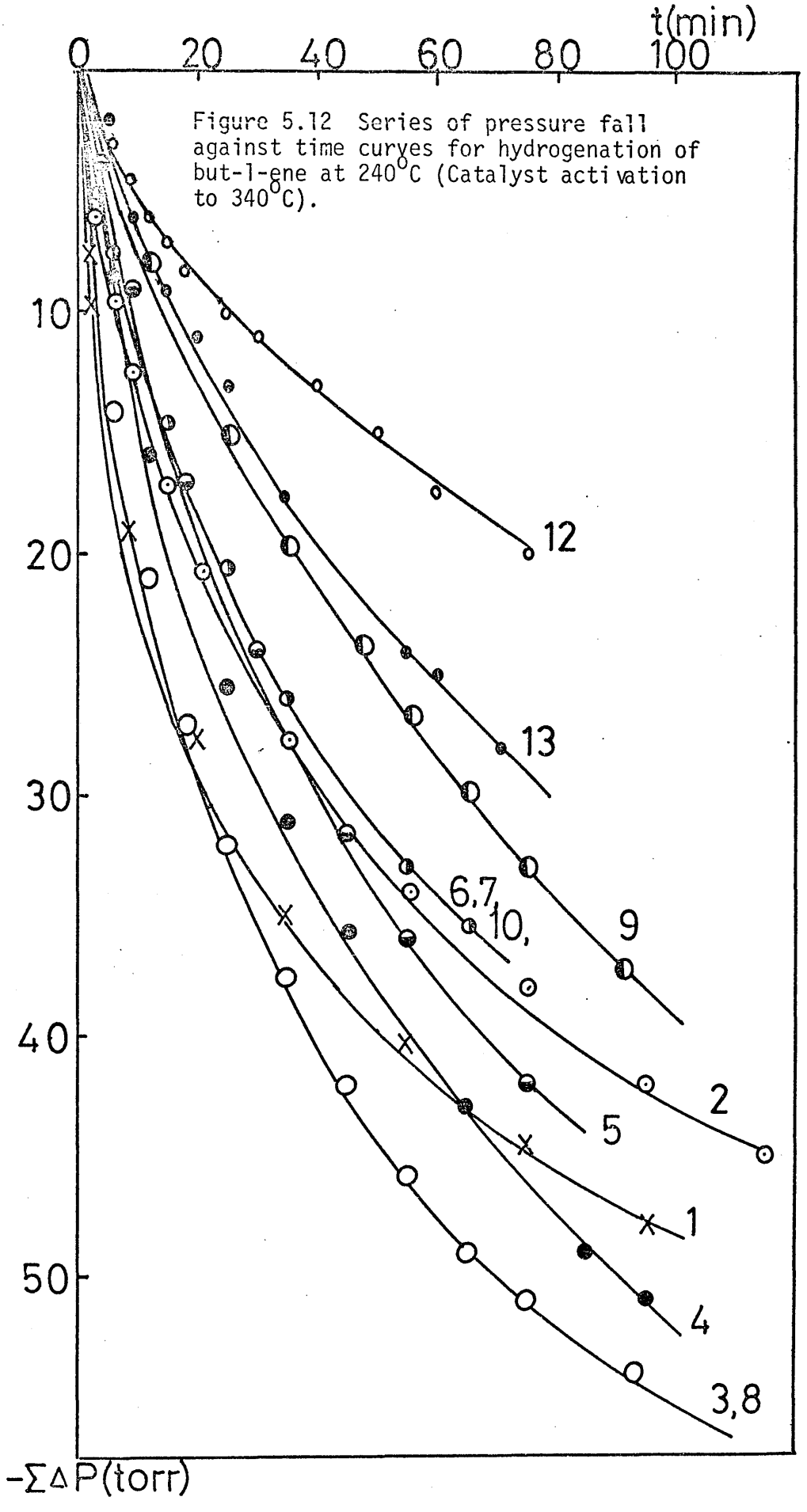

Figure 5.12 Series of pressure fall against time curves for hydrogenation of but-1-ene at 240°C (Catalyst activation to 340°C).

5.13 Variation of initial rate of hydrogenation with reaction number for previous series.

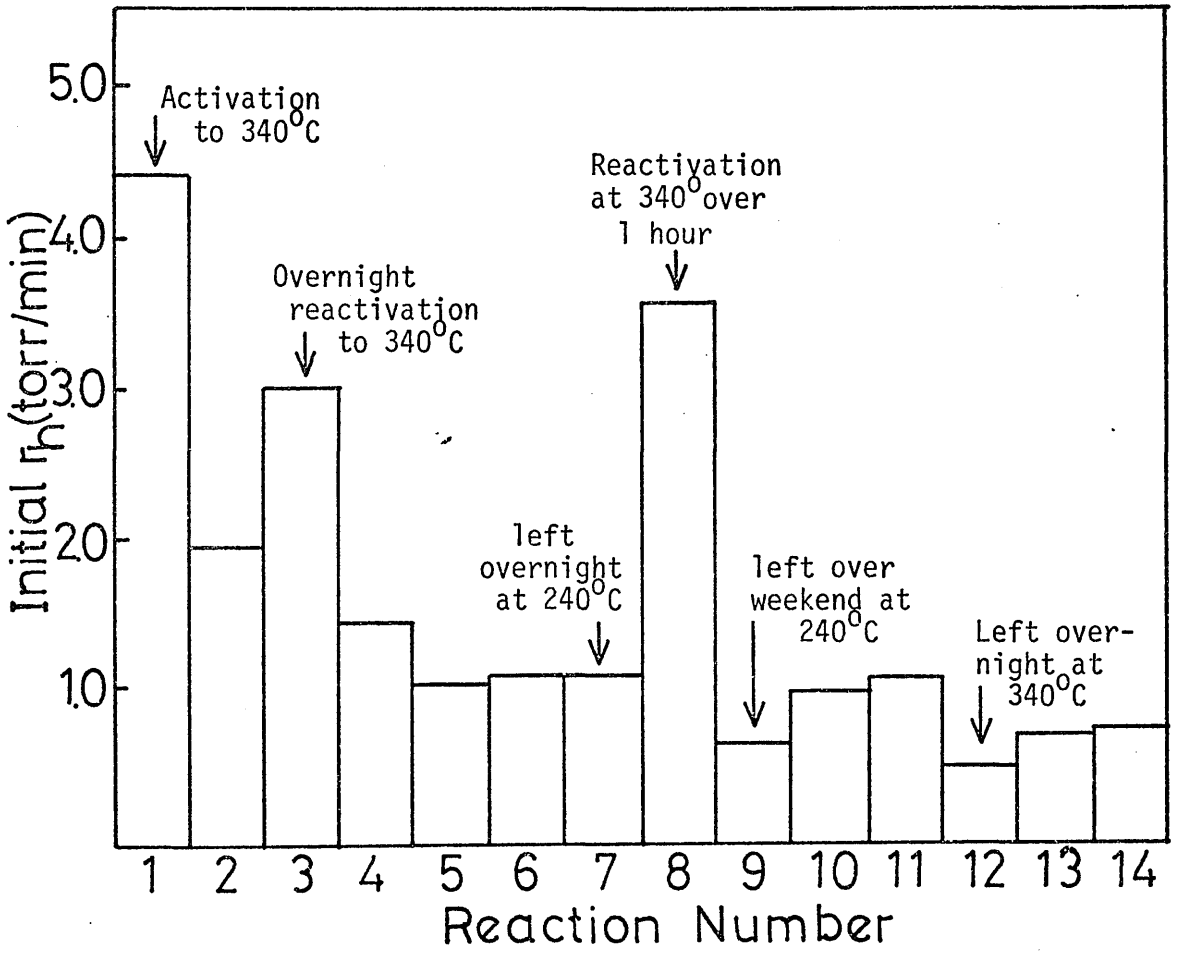

TABLE 5.12

Variation of Hydrocarbon Distribution with Reaction Number and Time over 2% $Os_3(CO)_{12}/SiO_2$

Initial $p_{H_2} = p_{BUT\text{-}1} = 100 \pm 0.5$ torr

Temperature = 240°C Catalyst weight = 0.08g

	% hydrocarbon composition				
Reaction	n-BUT	BUT-1	t-B-2	c-B-2	tex (min)
G/13	33.6	12.7	30.6	23.1	71
G/9	38.7	11.3	28.0	21.9	91
G/12	43.2	9.9	27.4	19.5	190
G/2	43.8	10.5	25.1	20.6	115
G/7	44.0	10.0	26.8	19.2	85
G/4	54.8	9.6	20.8	14.8	95
G/8	58.6	7.8	19.2	14.4	75
G/1	62.4	7.8	17.4	12.4	200
G/5	67.8	6.4	15.4	10.4	200
G/3	68.4	6.7	13.8	11.1	155

Figure 5.14 Variation of butene composition with percentage conversion for series of reactions in figure 5.12. (● = but-1-ene ; o = trans-but-2-ene ; ◐ = cis-but-2-ene).

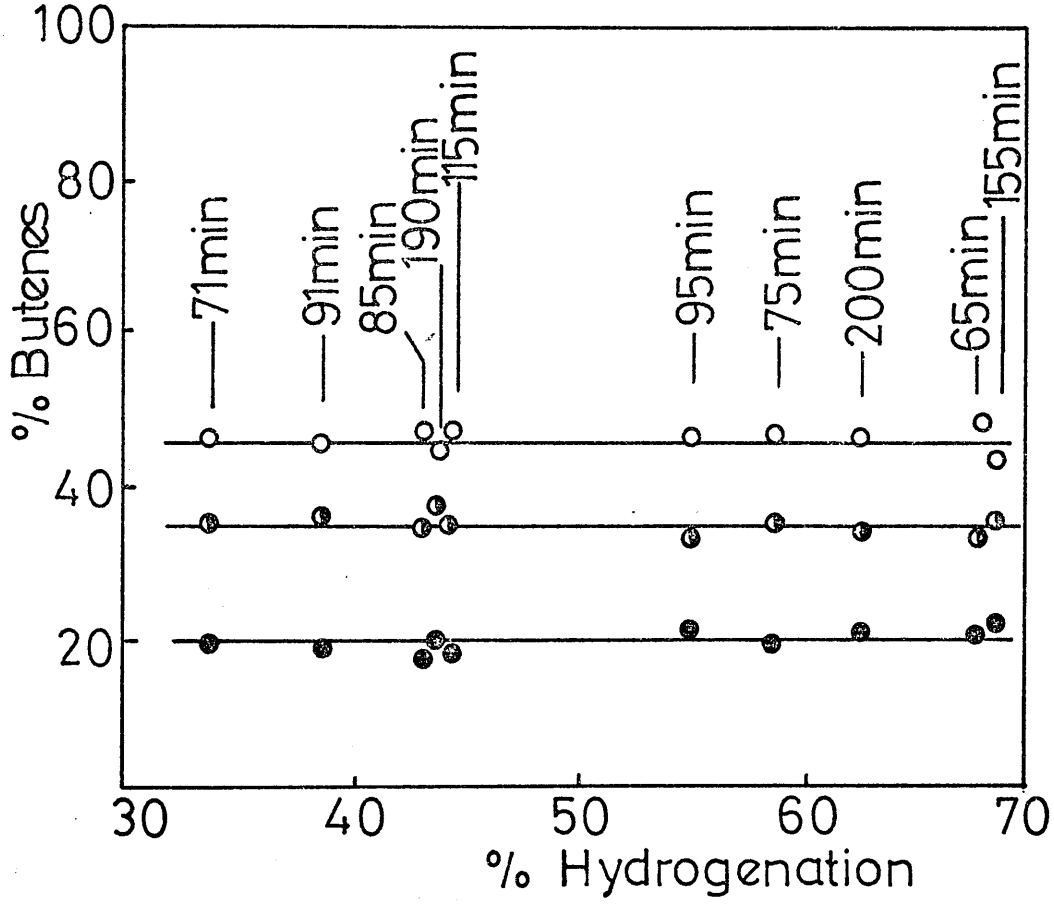

TABLE 5.13

Variation of Hydrocarbon Distribution with Conversion over 2% $Os_3(CO)_{12}/SiO_2$

Initial $p_{H_2} = p_{BUT-1}$ = 100 ± 0.5 torr

Temperature = 230°C Catalyst weight = 0.08g

	% hydrocarbon composition				
Reaction	n-BUT	BUT-1	t-B-2	c-B-2	tex(min)
L/5	3.1	82.4	8.1	6.4	2
L/2	5.9	56.6	19.9	17.7	5
L/1	12.7	22.4	35.5	29.4	10
L/4	17.7	16.4	37.1	28.8	22
L/3	31.7	12.8	31.3	24.2	42
L/6	52.4	10.2	21.8	15.6	135
L/7	85.3	5.0	5.7	4.0	1020

TABLE 5.14

	% hydrocarbon composition				
Reaction	n-BUT	BUT-1	t-B-2	c-B-2	tex(min)
M/5	3.1	78.0	9.5	9.4	2
M/2	4.1	63.8	16.9	15.2	5
M/1	3.8	67.7	14.2	14.3	10
M/4	18.9	17.8	35.5	27.7	22
M/3	20.8	14.3	36.6	28.3	42
M/6	45.1	11.1	25.4	18.4	135
M/7	81.5	5.7	7.3	5.5	1140

Figure 5.15 Variation of butene composition with percentage hydrogenation at 230°C. (2% $Os_3(CO)_{12}/SiO_2$ activated to 340°C. ● = but-1-ene ; o = trans-but-2-ene - ◐ = cis-but-2-ene).

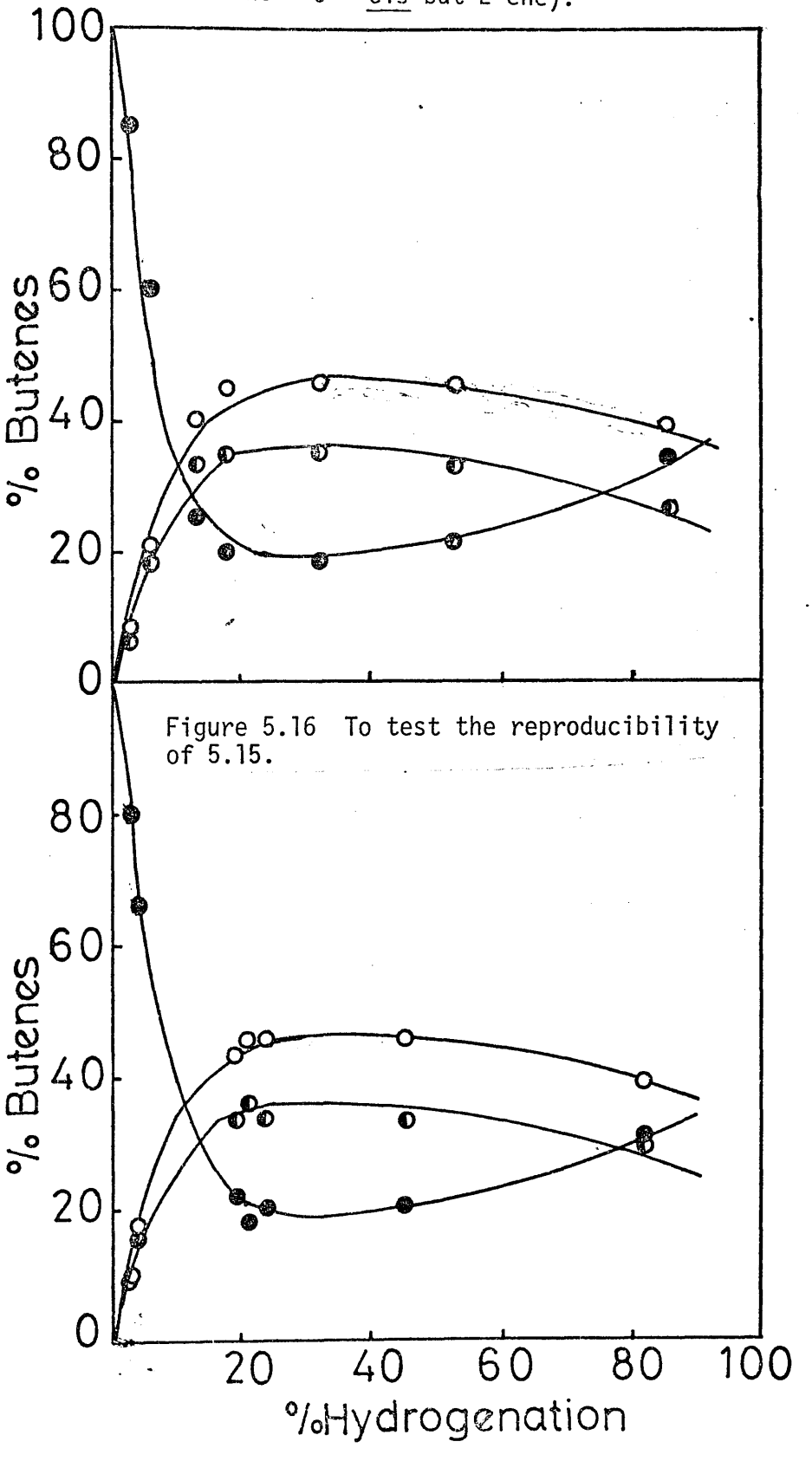

Figure 5.16 To test the reproducibility of 5.15.

5.3.2 Kinetics of Reaction of But-1-ene and Hydrogen.

The variations of the initial reaction rates and butene distribution with initial hydrogen and but-1-ene pressure were determined in exactly the same way as with the supported complex activated to 250°C. Each series of reactions was carried out at 230°C. As the catalyst activated at 340°C appeared to deactivate considerably from reaction to reaction, a "standard reaction" technique was used. The "standard reaction" was taken as that of 1:1 mixture of hydrogen and but-1-ene. By carrying out such reactions throughout the series, the change in catalyst activity towards the hydrogenation and isomerisation could be observed.

The variation of rates of reaction with initial hydrogen pressure is shown in tables 5.15 and 5.16. The plot of r_h against p_{H_2} shown in Figure 5.17 gives a good straight line through the origin, indicating an order of unity for the hydrogenation reaction with respect to initial hydrogen pressure. The plot of r_i against p_{H_2} (Figure 5.17) indicates that at low hydrogen pressures the rate is quite constant, whilst higher pressures of hydrogen act as a poison in isomerisation. Tables 5.17 and 5.18 show the variation of initial rates with initial but-1-ene pressure. Plots of log r_h and log r_i against log p_{BUT-1} as shown in Figure 5.18 indicate an order of 0.4 for the hydrogenation reaction and 0.5 for isomerisation.

The scattering of points observed in Figure 5.18 was probably due to the variability of initial rates which exists with this particular form of the supported complex. This would account particularly for the two points which are extremely far removed from the most suitable straight lines which could be drawn. These two

TABLE 5.15

Variation of Butene Distribution with Initial Hydrogen Pressure

Temperature = 230°C Initial p_{BUT-1} = 50 ± 0.5 torr

Samples extracted after 20 minutes

Reaction	p_{H_2}(torr)	%n-BUT	% butene distribution BUT-1	t-B-2	c-B-2
H/A/5	25	3.6	41.9	32.3	25.8
H/A/2	50	8.0	35.8	37.0	27.2
H/A/4	50	7.2	36.7	36.6	26.7
H/A/6	50	6.0	40.9	32.8	26.3
H/A/8	50	8.8	36.7	36.8	26.5
H/A/1	100	21.2	38.3	36.1	25.6
H/A/9	150	26.8	41.3	33.6	25.1
H/A/7	200	36.8	46.4	32.9	20.7
H/A/3	275	44.0	48.8	30.6	20.6

TABLE 5.16

Variation of Initial Reaction Rates with Initial Hydrogen Pressure at 230°C

Reaction	p_{H_2}(torr)	ri(torr/min)	rh(torr/min)
H/A/5	25	2.42	0.09
H/A/2	50	2.95	0.20
H/A/4	50	2.86	0.18
H/A/6	50	2.50	0.15
H/A/8	50	2.86	0.22
H/A/1	100	2.72	0.53
H/A/9	150	2.47	0.67
H/A/7	200	2.09	0.92
H/A/3	275	1.79	1.10

Figure 5.17 Variation in (a) initial rate of isomerisation (b) initial rate of hydrogenation, with initial hydrogen pressure at 230°C. (Catalyst activation to 340°C)

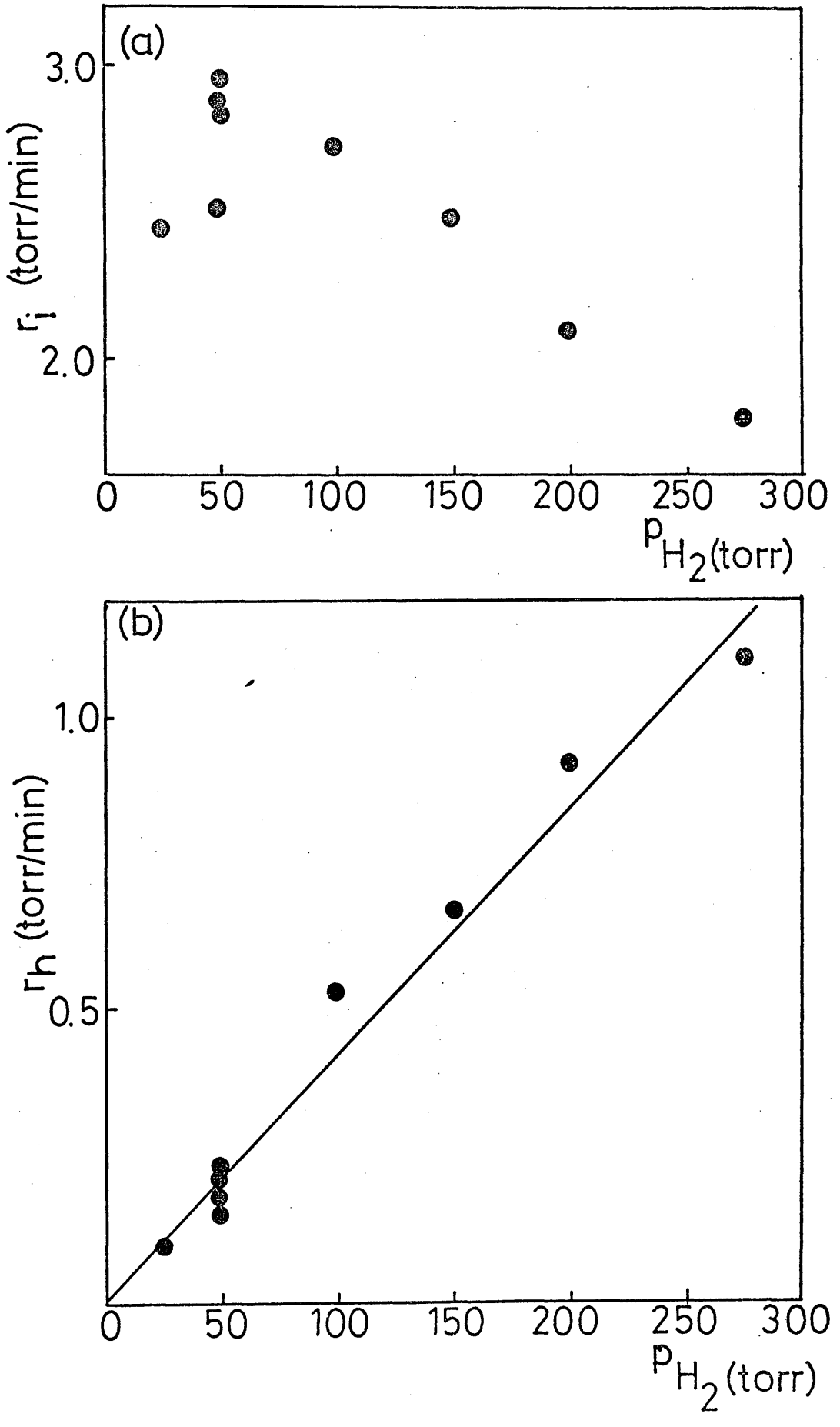

TABLE 5.17

Variation of Butene Distribution with Initial But-1-ene Pressure

Temperature = 230°C Initial p_{H_2} = 50 ± 0.5 torr

Samples extracted after 20 minutes

Reaction	p_{BUT-1}(torr)	%n-BUT	% butene distribution BUT-1	t-B-2	c-B-2
H/B/6	25	8.0	39.7	32.8	27.5
H/B/2	50	8.8	41.6	33.9	24.5
H/B/5	50	5.6	44.2	29.7	26.1
H/B/8	50	4.4	52.6	24.5	22.9
H/B/1	100	7.3	41.7	32.9	25.4
H/B/7	150	2.4	64.5	19.5	16.0
H/B/4	200	2.3	67.2	18.4	14.4
H/B/3	300	1.9	72.4	15.6	12.0

TABLE 5.18

Variation of Initial Reaction Rates with Initial But-1-ene Pressure at 230°C

Reaction	p_{BUT-1}	ri(torr/min)	rh(torr/min)
H/B/6	25	0.11	0.10
H/B/2	50	0.39	0.22
H/B/5	50	0.35	0.14
H/B/8	50	0.24	0.11
H/B/1	100	0.69	0.37
H/B/7	150	0.54	0.18
H/B/4	200	0.62	0.23
H/B/3	300	0.70	0.29

Figure 5.18 Variation in (a) log (initial rate of isomerisation) (b) log (initial rate of hydrogenation), with $\log_{10}$(initial but-1-ene pressure) at 230°C. (Catalyst activation to 340°C).

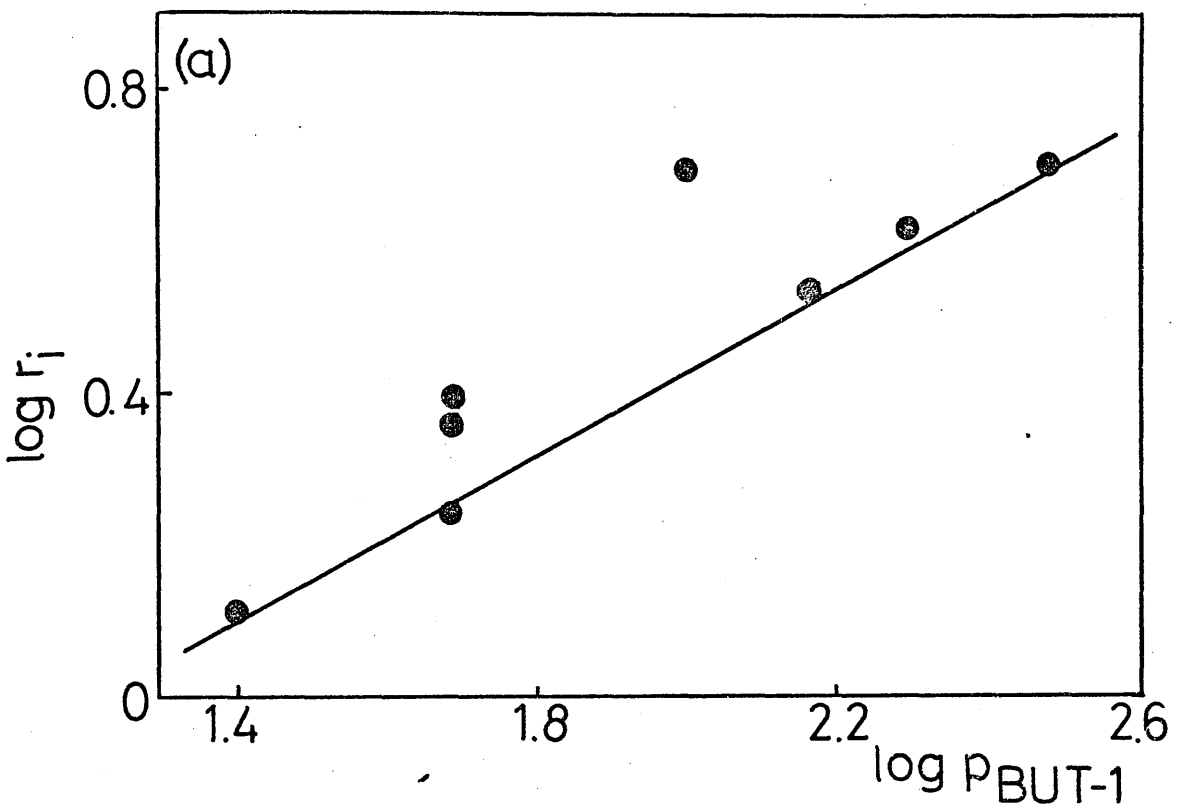

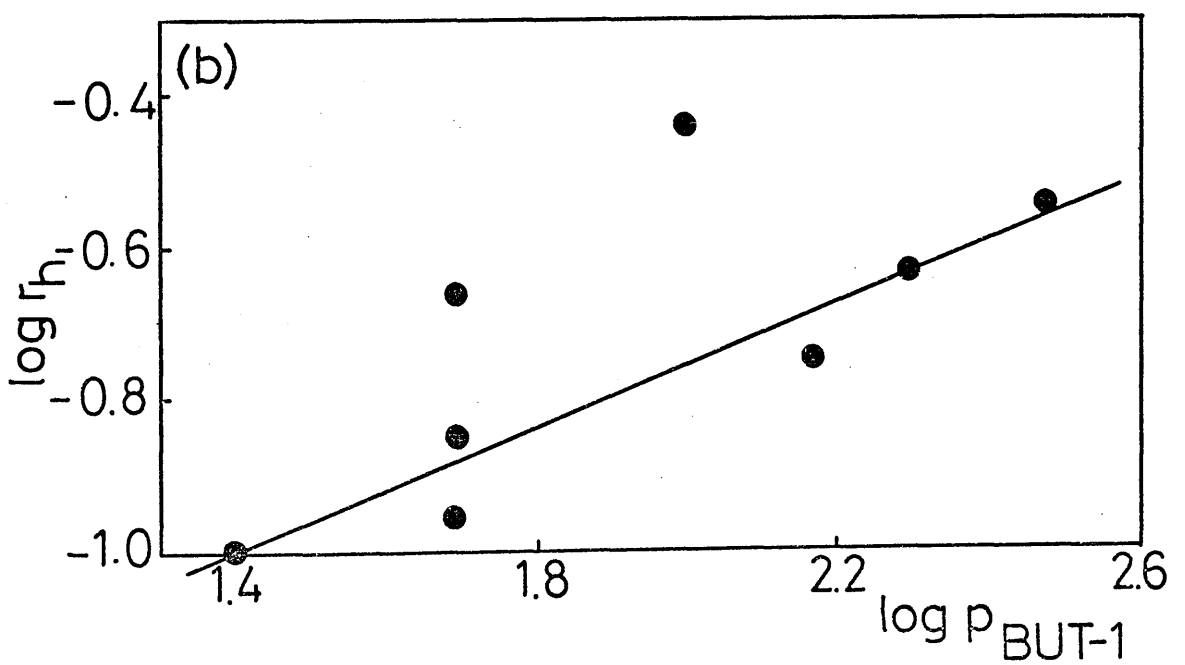

points represent the first two reactions performed in that particular series while the catalyst is at its most active.

The kinetics of the reaction are summarised below:-

Kinetics of Reaction of But-1-ene with Hydrogen

Reaction	Order of Reaction	
	Hydrogen	But-1-ene
Hydrogenation	1.0 ± 0.1	0.4 ± 0.1
Isomerisation	-	0.5 ± 0.1

5.3.3 Reactions of But-1-ene with Deutrium.

The reaction of but-1-ene with deutrium over $Os_3(CO)_{12}/SiO_2$ activated to 340°C were carried out in essentially the same manner as when hydrogen was used.

A series of reactions was carried out at 230°C over a freshly prepared $Os_3(CO)_{12}/SiO_2$ catalyst which had been activated overnight. By extracting the reaction products at varying reaction times and determining the butene distribution at each conversion, a graph could be plotted as illustrated in Figure 5.19. The corresponding hydrocarbon composition together with extraction times are shown in table 5.19. The distribution of deuterated products for each reaction product at the various conversions are shown in table 5.20.

Figure 5.19 Variation of butene composition with percentage deuteration at 230°C (Catalyst activation to 340°C.
● = but-1-ene ; o = trans-but-2-ene ;
◑ = cis-but-2-ene).

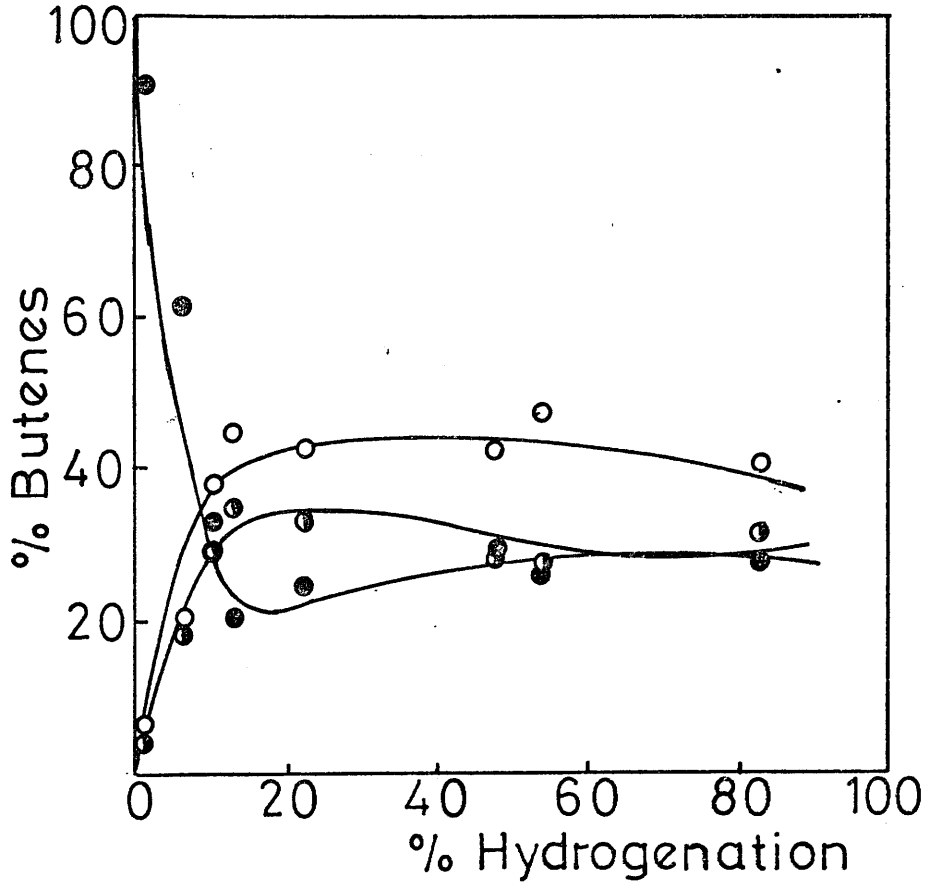

TABLE 5.19

Variation of Hydrocarbon Distribution with Conversion over 2% $Os_3(CO)_{12}/SiO_2$ for Reaction of But-1-ene with Deuterium

Initial $p_{D_2} = p_{BUT-1} = 100 \pm 0.5$ torr

Temperature = 230°C Catalyst weight = 0.08g

	% hydrocarbon composition				
Reaction	n-BUT	BUT-1	t-B-2	c-B-2	tex(min)
I/9	1.4	89.5	5.2	3.9	1
I/5	10.5	33.8	29.7	26.0	2
I/6	6.7	57.9	18.6	16.8	3
I/4	11.9	25.4	36.2	26.5	10
I/3	12.8	17.8	39.0	30.4	15
I/1	22.4	19.0	33.1	25.5	20
I/2	48.2	15.1	22.1	14.6	120
I/7	54.4	11.6	21.8	12.2	240
I/8	82.8	4.7	7.1	5.4	1080

TABLE 5.20

Distribution of Deuterated Hydrocarbons over 2% $Os_3(CO)_{12}/SiO_2$ (activated at 320°C) at 230°C

Reaction	d_o	d_1	d_2	d_3	d_4	d_5	d_6	D.N.
I/6	Conversion 6.7%			3 mins				
n-butane	20.0	12.3	52.3	9.2	3.5	2.7	0	1.72
but-1-ene	88.6	11.4	0	0	0	0	0	0.11
t-but-2	86.9	11.4	1.7	0	0	0	0	0.15
c-but-2	87.7	10.6	1.4	0.3	0	0	0	0.14
I/5	Conversion 10.5%			2 mins				
n-butane	20.3	21.0	34.1	13.0	5.8	4.4	1.4	1.77
but-1-ene	68.3	23.9	5.7	1.3	0.6	0.2	0	0.43
t-but-2	59.5	27.8	8.8	2.3	1.1	0.6	0	0.60
c-but-2	61.8	26.3	8.6	1.9	1.0	0.4	0	0.55
I/4	Conversion 11.9%			10 mins				
n-butane	10.0	18.6	50.2	13.6	4.0	2.6	1.0	1.95
but-1-ene	72.6	21.5	4.4	0.9	0.6	0	0	0.35
t-but-2	71.8	22.6	4.1	1.0	0.5	0	0	0.36
c-but-2	67.9	25.9	5.0	0.8	0.4	0	0	0.40
I/3	Conversion 12.8%			15 mins				

TABLE 5.20 (continued)

Distribution of Deuterated Hydrocarbons over 2% $Os_3(CO)_{12}/SiO_2$ (activated at 320°C) at 230°C

Reaction	d_o	d_1	d_2	d_3	d_4	d_5	d_6	D.N.
I/3	Conversion 12.8%			15 mins				
n-butane	11.3	24.0	39.5	15.4	6.7	3.1	0	1.91
but-1-ene	50.7	30.3	11.7	4.2	2.4	.7	0	0.79
t-but-2	43.5	40.1	12.4	3.0	.7	.3	0	0.78
c-but-2	49.6	35.3	11.1	2.9	.7	.4	0	0.71
I/1	Conversion 22.4%			60 mins				
butane	20.8	16.8	33.7	18.2	7.1	2.5	0.9	1.85
but-1-ene	42.5	28.8	19.9	6.6	1.9	0.3	0	0.97
t-but-2	27.1	35.1	26.7	8.7	2.2	0.2	0	1.20
c-but-2	26.4	40.0	22.7	8.7	1.8	0.4	0	1.20
1/2	Conversion 48.2%			120 min				
butane	16.1	22.0	29.0	18.5	9.1	3.9	1.4	2.00
but-1-ene	22.6	22.4	21.9	18.1	10.6	4.4	0	1.85
t-but-2	5.2	28.6	30.3	21.9	11.0	3.0	0	2.14
c-but-2	7.2	29.5	31.2	20.1	9.8	2.2	0	2.02

TABLE 5.20 (continued)

Distribution of Deuterated Hydrocarbons over 2% $Os_3(CO)_{12}SiO_2$(activated at 320°C) at 230°C

Reaction	d_o	d_1	d_2	d_3	d_4	d_5	d_6	D.N.
I/7	Conversion 54.4%			240 min				
butane	18.4	23.2	26.8	16.9	8.9	4.2	1.6	1.94
but-1-ene	31.7	18.3	22.3	14.3	8.9	3.5	1.0	1.65
t-but-2	7.9	23.2	32.9	21.7	10.6	3.2	0.5	2.15
c-but-2	9.6	26.3	31.4	19.6	9.7	2.9	0.5	2.04
I/8	Conversion 82.8%			1020 min				
butane	20.9	20.9	25.7	18.0	9.7	3.8	1.0	1.90
but-1-ene	37.6	11.7	16.8	14.1	10.6	6.5	2.7	1.80
t-but-2	5.4	21.7	26.7	26.5	13.3	5.0	1.4	2.40
c-but-2	7.8	22.6	24.7	25.9	12.7	4.8	1.4	2.40

5.4 Reaction of But-1-ene with Hydrogen on 2% W/W Os/SiO_2

The reaction of but-1-ene with hydrogen was examined over 2% Os/SiO_2(80mg) which had been reduced at 330°C for 2 hours. There was found to be virtually no difference in the initial rates of hydrogenation at the two temperatures at which the reaction was examined, namely 135°C and 230°C, although as the reaction proceeds to higher conversion the rate of hydrogenation at 230°C appears to slow down considerably compared with the lower temperature. Pressure fall against time curves for the reaction at both temperatures are shown in Figures 5.20 and 5.21, together with the corresponding first order plots. The hydrogenation reaction is first order at 135°C, but only first order initially at 230°C. It was observed that the catalyst was far more susceptible to poisoning when the reaction was carried out at 230°C.

Two series of reactions were carried out to examine the effect of temperature on the variation of product composition with percentage conversion. Series N was carried out to varying conversion at 230°C. The analysis figures, together with time of extraction are given in table 5.21, whilst Figure 5.22 illustrates the variation of butene distribution with percentage conversion. Series P was carried out over the same catalyst in a similar manner at 135°C. In reactions P/1 - P/5 the rates of reaction are rather slow due to the poisoning effect of the previous series, but reduction of the catalyst at 330°C regenerates the catalyst's activity. The product distribution, together with extraction times is given in table 5.22 whilst Figure 5.23 shows the variation of butene composition with percentage conversion.

Figure 5.20 Pressure fall against time curve for the hydrogenation of but-1-ene at 135°C. First order function plot is shown below (Osmium catalyst).

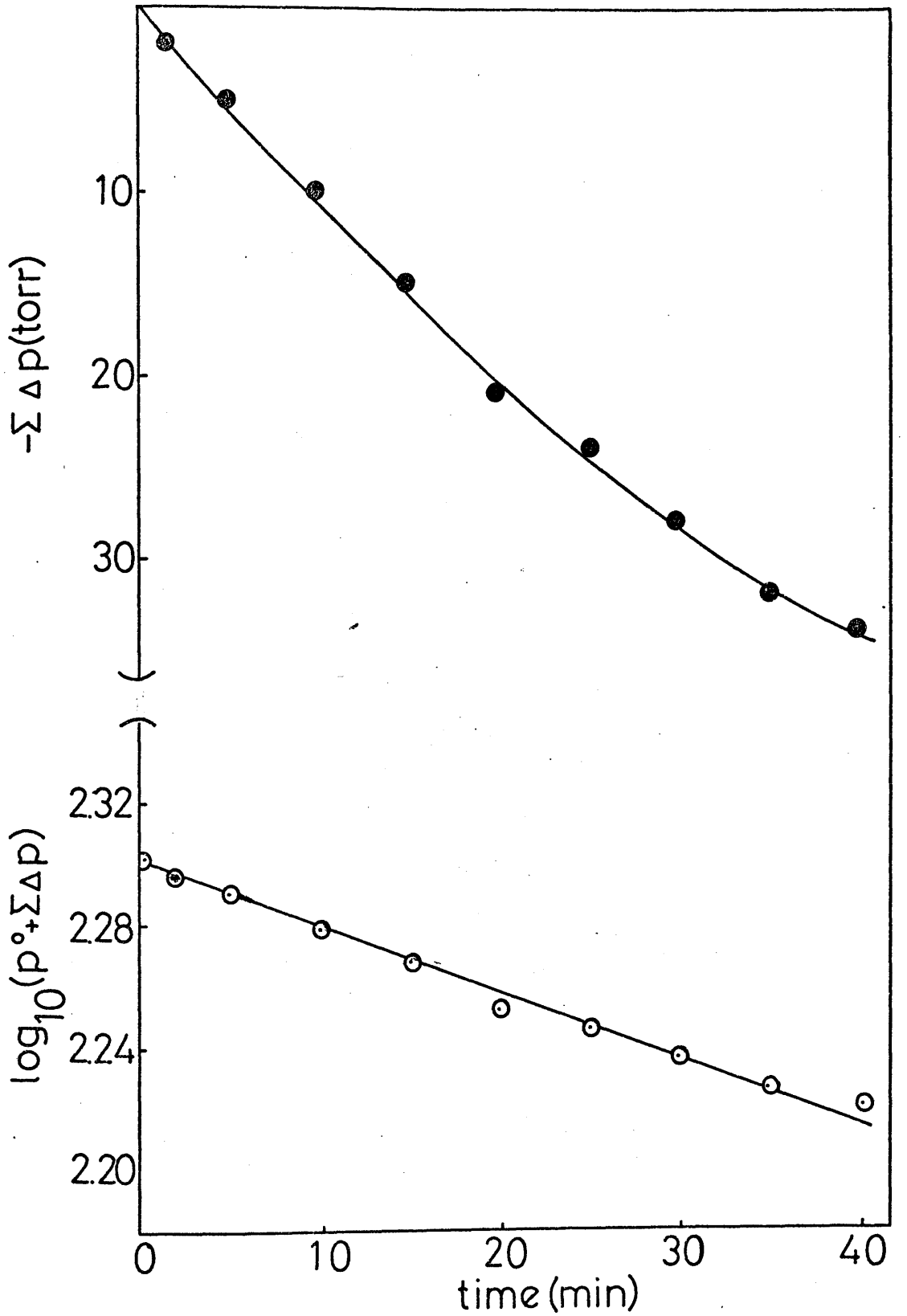

Figure 5.21 Pressure fall against time curve for the hydrogenation of but-1-ene at 230°C. First order function plot is shown below (Osmium catalyst).

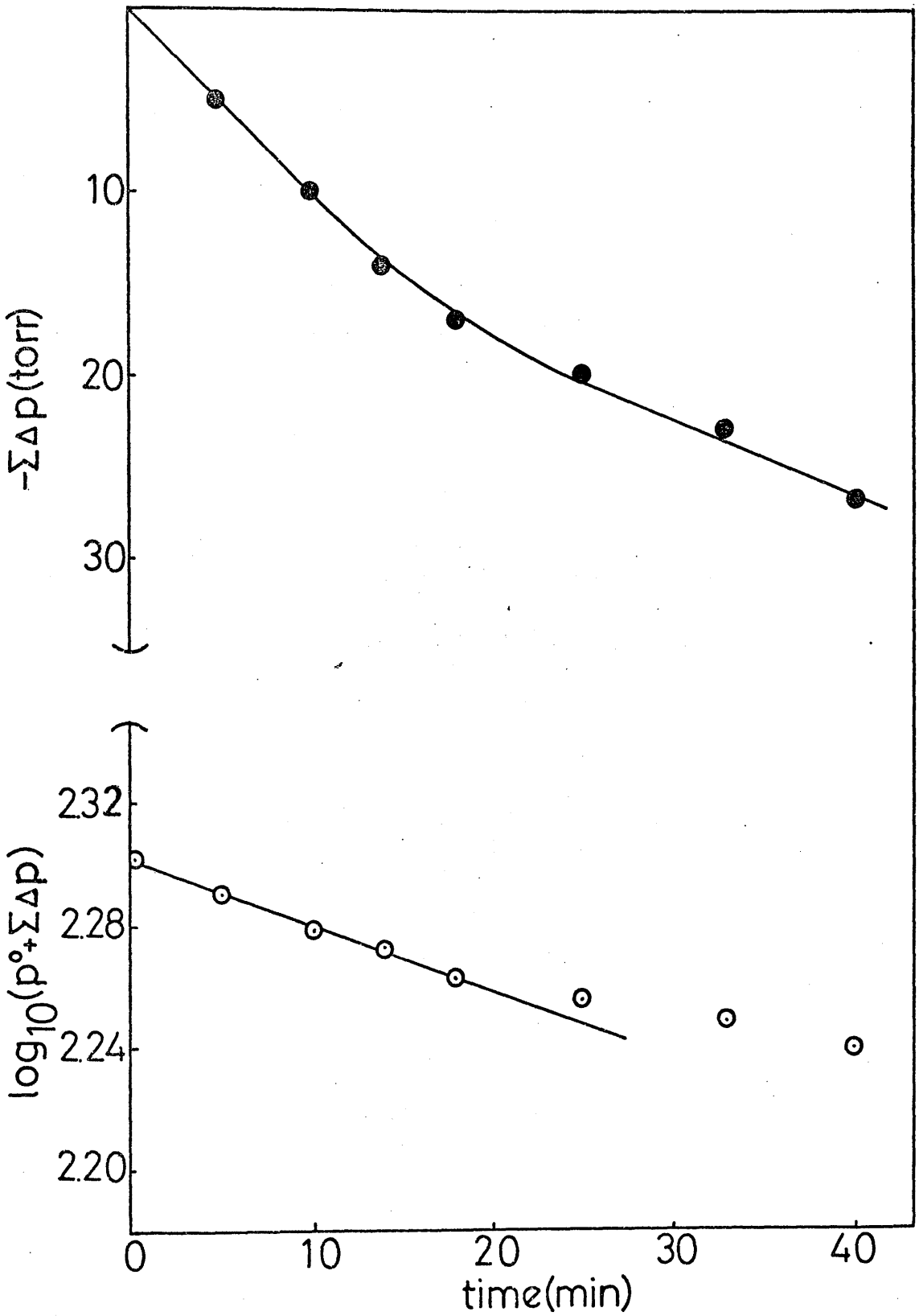

TABLE 5.21

Variation of Hydrocarbon Products with Conversion at 230°C over 2% Os/SiO_2

$p_{H_2} = p_{BUT-1} = 100 \pm 0.5$ torr

	% hydrocarbon composition				
Reaction	n-BUT	BUT-1	t-B-2	c-B-2	tex(min)
N/4	3.2	92.0	2.2	2.6	1
N/7	4.4	89.6	3.0	3.0	5
N/1	10.7	48.0	23.0	18.3	7.5
N/2	19.2	34.1	25.0	21.7	20
N/5	21.3	36.7	22.9	19.1	31
N/3	42.6	14.2	26.4	16.8	130
N/6	62.9	8.8	18.0	10.3	1020

TABLE 5.22

Variation of Hydrocarbon Products with Conversion at 135°C over 2% Os/SiO_2

$P_{H_2} = P_{BUT-1} = 100 \pm 0.5$ torr

% hydrocarbon composition

Reaction	n-BUT	BUT-1	t-b-2	c-B-2	tex(min)
P/4	2.8	92.4	1.8	3.0	7
P/5	6.9	82.8	4.2	6.1	26
P/2	21.8	43.8	16.1	18.3	40
P/7	27.6	33.7	19.0	19.6	30
P/3	32.1	20.9	24.6	22.4	80
P/9	39.4	17.6	23.3	19.7	35
P/8	40.3	18.8	22.2	18.7	20
P/1	49.2	9.1	27.8	13.9	195
P/10	52.6	9.1	25.7	12.6	80
P/11	56.7	8.0	23.4	11.9	140
P/6	68.1	8.2	16.5	7.2	100

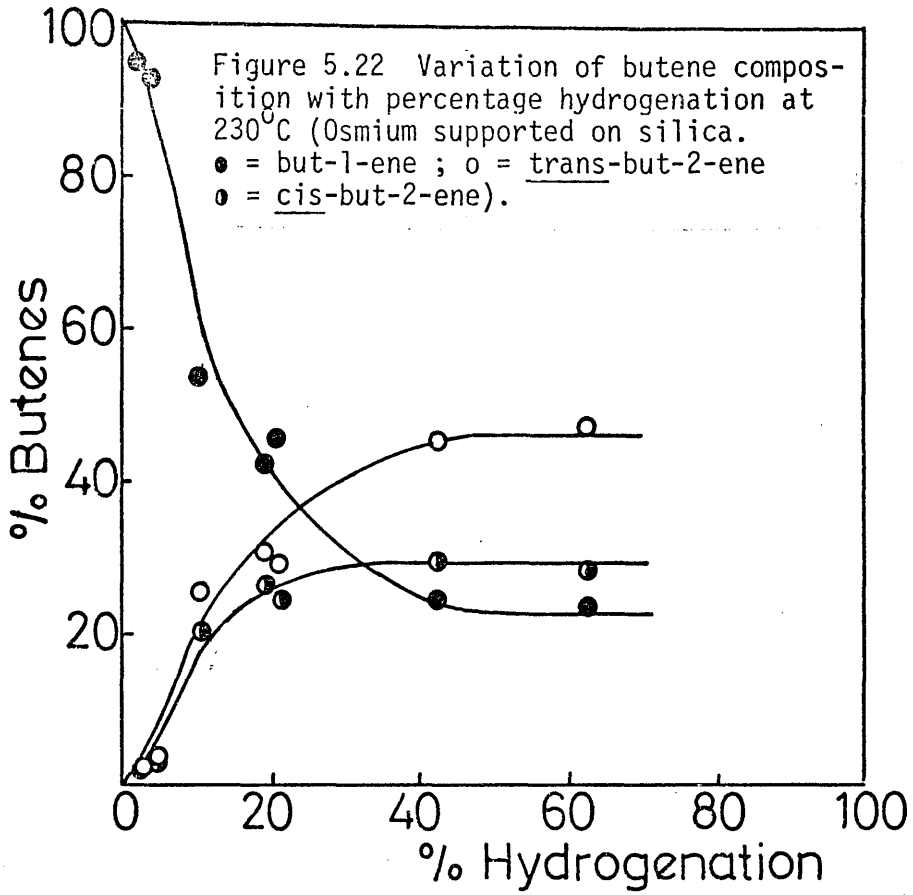

Figure 5.22 Variation of butene composition with percentage hydrogenation at 230°C (Osmium supported on silica. ● = but-1-ene ; o = trans-but-2-ene ◐ = cis-but-2-ene).

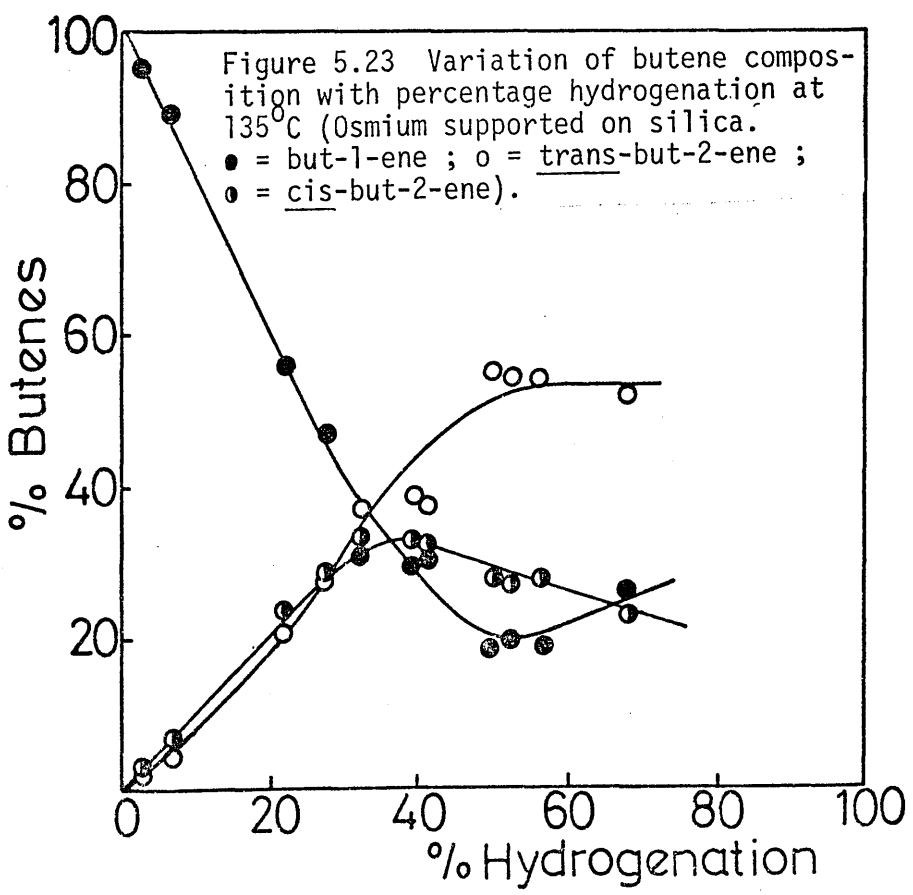

Figure 5.23 Variation of butene composition with percentage hydrogenation at 135°C (Osmium supported on silica. ● = but-1-ene ; o = trans-but-2-ene ; ◐ = cis-but-2-ene).

CHAPTER 6

REACTIONS OF n-BUTENES WITH HYDROGEN ON SILICA SUPPORTED DIRHENIUM DECACARBONYL

6.1 Catalyst Characterisation

6.1.1 Physical Appearance

The supported complex (2% w/w) was white at room temperature, but when activated in vacuo to 250°C over a period of a few hours it became a light grey colour. This colour persisted when the complex was activated to higher temperatures.

6.1.2 Examination of the Complex by Thermogravimetric Analysis (T.G.A.)

T.G.A. of a 10% $Re_2(CO)_{10}$/Aerosil silica sample showed that the complex began to degrade at about 70°C. Loss of weight occurred in the temperature range 70-170°C and was at a maximum at just over 100°C. Loss of weight was observed to be a one step process, with no further degradation taking place at over 170°C. As may be observed from Figure 6.1, there was a total weight loss of 4.2% which was equivalent to the loss of all ten carbonyls from the complex.

6.1.3 Examination of the complex by Infra-Red Spectroscopy.

A solution of infra-red spectrum of $Re_2(CO)_{10}$ in CH_2Cl_2 showed the presence of three bands in the $\bar{\nu}$co stretching region, which were observed at 2070(s), 2018(s) and 1975(s) cm^{-1}.

Figure 6.1 T.G.A. of 10% W/W $Re_2(CO_{10}/SiO_2$

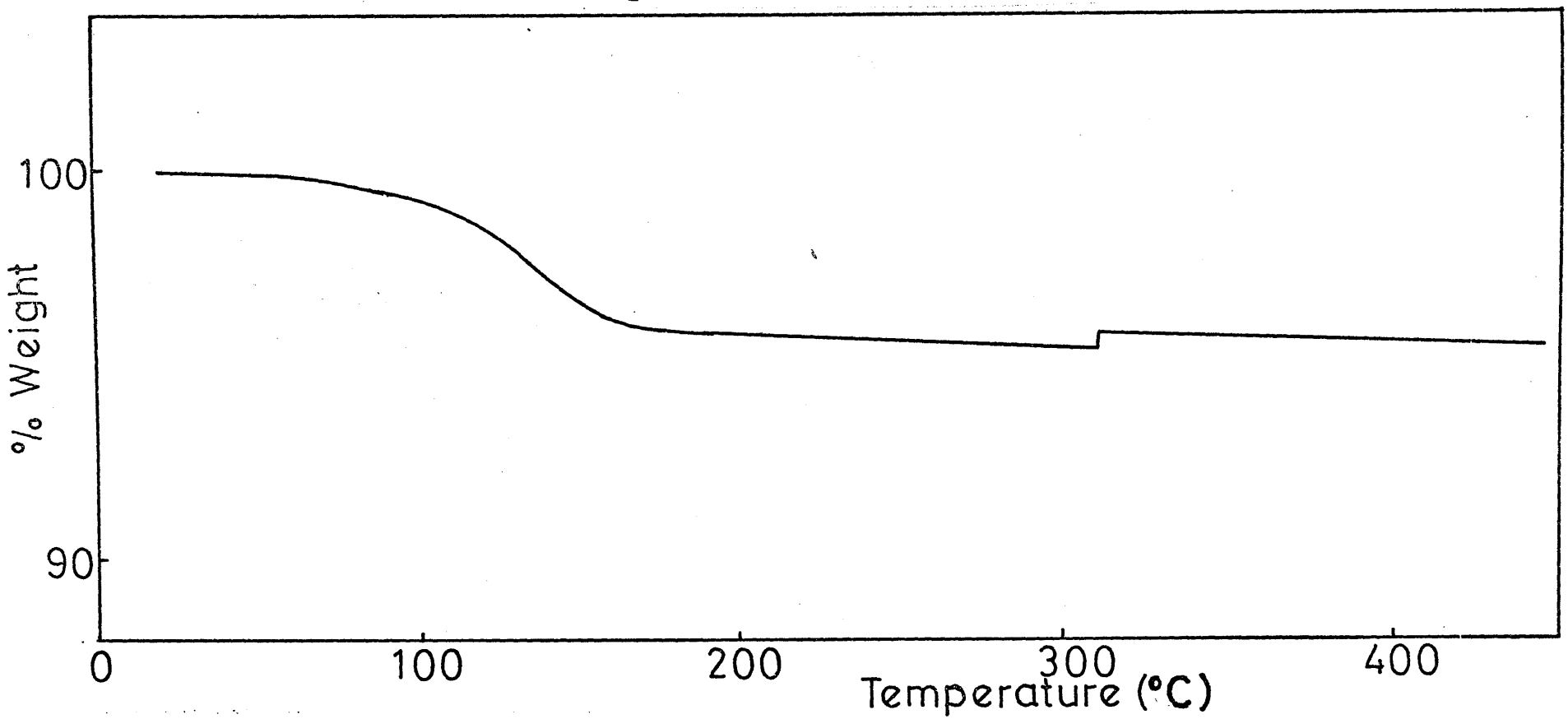

A disc infra-red spectrum of the complex when supported on silica indicated little change in the overall structure of the complex. Bands were observed at 2076(s), 2020(s) and 1976(m) cm^{-1}. In addition, a weak band was observed at 2061 cm^{-1}.

Activation of the supported complex in vacuo had little effect on the spectrum, although it seemed that the bands at 2076 and 1976 cm^{-1} diminished at a faster rate than the peak at 2020 cm^{-1}.

Examination of the complex after activation to 250°C indicated the loss of all carbonyl ligands from the complex.

The supported complex appeared to be particularly stable on prolonged exposure to air as this resulted in no change in the infra-red spectrum.

6.1.4 Examination of the complex by Electron Microscopy.

A sample of 2% w/w $Re_2(CO)_{10}$ on Aerosil silica was examined as follows:-

(a) after activation to 250°C in vacuo

(b) after activation to 320°C in vacuo

The electron micrograph of (a) showed the absence of any particles on the silica support, whilst in (b) aggregations were widespread on the silica support, ranging from 15-1000Å, with an average size of about 50Å.

6.2 Reactions of But-1-ene on $Re_2(CO)_{10}/SiO_2$ Activated to 250°C.

6.2.1 Preliminary Investigation

Preliminary experiments using $Re_2(CO)_{10}/SiO_2$ (2% w/w) were carried out using 86 mg of supported complex activated to 250°C for

2 hours. 200 torr of a 1:1 mixture of but-1-ene and hydrogen were introduced to the reaction vessel for a period of 85 minutes, at various temperatures. As can be seen from table 6.1, the rates of hydrogenation and isomerisation are extremely slow at 175°C, but there is a general increase with temperature as would be expected. The one anomalous result appears to be the first reaction carried out, where isomerisation and hydrogenation are not as favoured as would be expected at this temperature.

The possibility that Aerosil silica itself might catalyse the reaction of but-1-ene with hydrogen was investigated. The support alone was found to be inactive under these particular conditions.

6.2.2 The Isomerisation of But-1-ene over $Re_2(CO)_{10}/SiO_2$.

The isomerisation of but-1-ene was studied by carrying out a series of reactions over varying periods of time. This was done at 250°C and 230°C to ascertain whether or not temperature had any effect on the degree or mode of isomerisation. As the rate of hydrogenation was so slow at these temperatures, it was impossible to monitor the rate of conversion to n-butane using the mercury manometer. The products of reaction were merely removed for analysis after varying time intervals. The analysis figures for the variation in hydrocarbon products of reaction with the time of extraction (tex) are given in tables 6.2 and 6.3, whilst Figures 6.2 and 6.3 illustrate the variation of butene composition with percentage conversion.

6.2.3 Reaction of But-1-ene with Deuterium.

The reactions of but-1-ene with deuterium on $Re_2(CO)_{10}/SiO_2$

TABLE 6.1

Variation of Butene Distribution with Temperature on $Re_2(CO)_{10}/SiO_2$

Initial $p_{H_2} = p_{BUT-1} = 100 \pm 0.5$ torr catalyst weight = 0.08 g

			% butenes		
Reaction	Temp (K)	%n-BUT	BUT-1	t-B-2	c-B-2
A/4	448	1.2	93.2	4.1	2.7
A/3	483	3.2	58.7	23.0	18.3
A/1	506	2.0	61.3	20.9	17.8
A/2	523	4.8	25.8	42.2	32.0

TABLE 6.2

Variation of Hydrocarbon Distribution with Conversion at 250°C on $Re_2(CO)_{10}/SiO_2$

Initial $p_{H_2} = p_{BUT-1} = 100 \pm 0.5$ torr catalyst weight = 0.08 g

Reaction	% Hydrocarbon distribution. n-BUT	BUT-1	t-B-2	c-B-2	tex (min)
B/3	0.7	86.5	7.4	5.4	10
B/2	1.7	70.0	16.0	12.3	25
B/4	2.5	53.1	25.3	19.1	50
B/1	4.8	24.6	40.2	30.4	85
B/5	9.6	18.6	42.7	29.1	1020

TABLE 6.3

Variation of Hydrocarbon Distribution with Conversion at 230°C on $Re_2(CO)_{10}/SiO_2$

Initial $p_{H_2} = p_{BUT-1} = 100 \pm 0.5$ torr catalyst weight = 0.08 g

	% Hydrocarbon distribution.				
Reaction	n-BUT	BUT-1	t-B-2	c-B-2	tex (min)
C/3	0.3	97.0	1.6	1.1	3
C/4	1.0	84.0	8.7	6.3	15
C/11	1.2	78.2	10.5	10.1	120
C/1	2.9	46.4	29.2	21.5	35
C/8	3.3	48.2	27.8	20.7	165
C/2	3.4	38.7	33.9	24.0	85
C/6	3.7	37.2	24.8	24.3	150
C/9	4.5	29.9	37.2	28.4	360
C/7	9.0	25.7	37.4	27.9	1020
C/5	11.8	31.4	33.4	23.4	1080
C/10	16.5	19.4	38.8	25.3	3900

Figure 6.2 Variation of butene composition with percentage hydrogenation at 250°C (2% $Re_2(CO)_{10}/SiO_2$. ● = but-1-ene ; o = trans-but-2-ene ; ◑ = cis-but-2-ene).

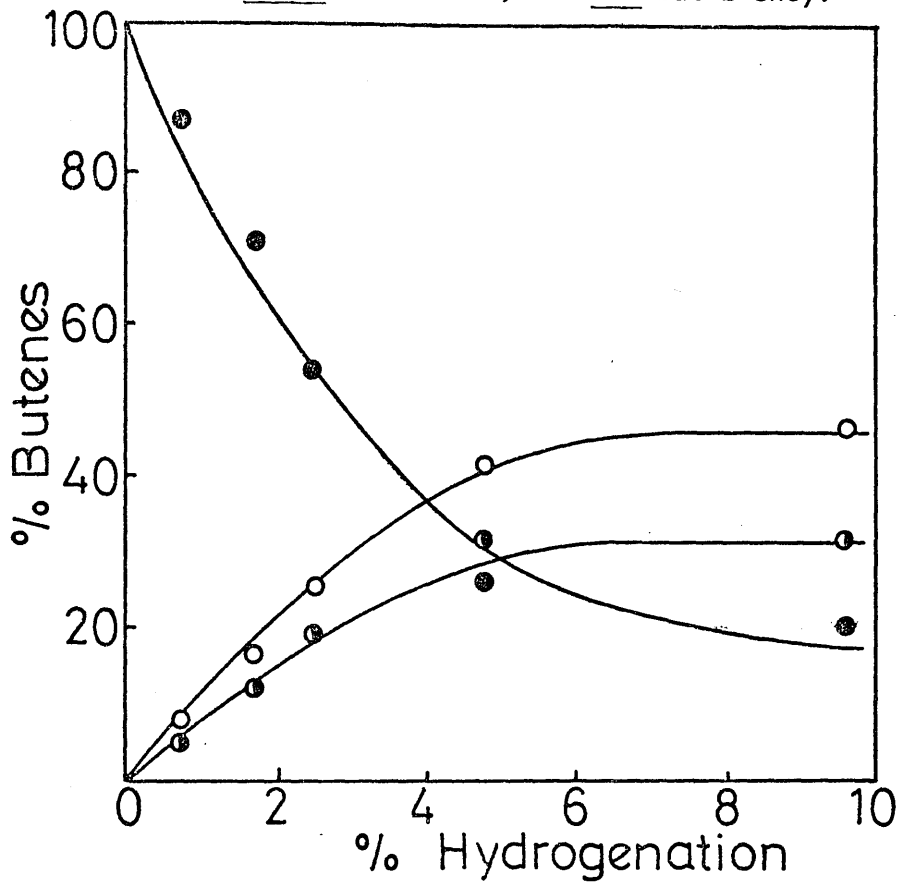

Figure 6.3 Variation of butene composition with percentage hydrogenation at 230°C (2% $Re_2(CO)_{10}/SiO_2$. ● = but-1-ene ; o = trans-but-2-ene ; ◑ = cis-but-2-ene).

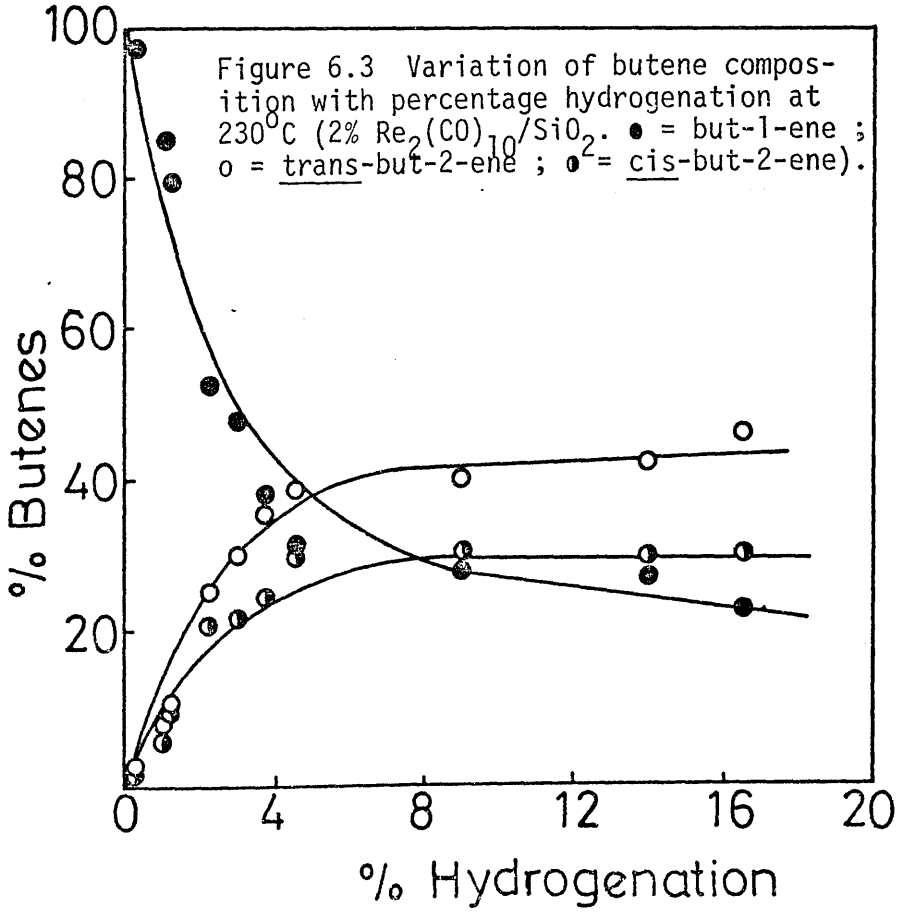

were carried out as in the reactions with hydrogen. The deuteration and isomerisation reactions were studied simultaneously using initial pressures of 100 torr of both deuterium and but-1-ene.

The isomerisation reaction was studied at 250°C. By extracting the reaction products at various reaction times and determining the butene distribution at each extraction time, the variation in butene distribution with percentage conversion was found. The analysis figures for the product composition are given in table 6.4, whilst the plot of percentage butene distribution against conversion is shown in Figure 6.4

For each of the above conversions, after analysis by gas chromatography, the separated products were collected and transferred to the mass spectrometer for analysis for deuterium content. The distributions of deutero-butane and the deutero-butenes at varying conversion to n-butane are shown in table 6.5. Analysis of deuterium content in n-butane proved to be impossible at low conversion due to the small amounts which were collected.

6.3 Reactions of n-Butenes on $Re_2(CO)_{10}/SiO_2$ Activated to 320°C.

6.3.1 Preliminary Investigation

In order to determine whether the rate of butene hydrogenation was enhanced any at higher temperatures, or if the activity of the catalyst could be increased by activation at a higher temperature, the supported complex was activated to 320°C in vacuo for 1 hour.

When a 200 torr (1:1) mixture of but-1-ene and hydrogen was introduced to a reaction vessel containing 80 mg of catalyst at 300°C,

TABLE 6.4

Variation of Hydrocarbon Distribution with Conversion in the Reaction of But-1-ene with Deuterium at 250°C

Initial $p_{D_2} = p_{BUT-1} = 100 \pm 0.5$ torr catalyst weight = 0.08 g

Reaction	% Hydrocarbon distribution. n-BUT	BUT-1	t-B-2	c-B-2	tex (min)
D/1	2.4	24.6	44.1	28.9	40
D/2	3.6	26.4	43.6	26.4	135
D/5	4.3	24.8	43.7	27.2	195
D/4	4.4	24.9	42.4	28.3	360
D/3	23.4	14.8	38.8	23.0	1080

Figure 6.4 Variation of butene composition with percentage deuteration at 250°C (2% $Re_2(CO)_{10}/SiO_2$. ● = but-1-ene ; o = trans-but-2-ene ; ◑ = cis-but-2-ene).

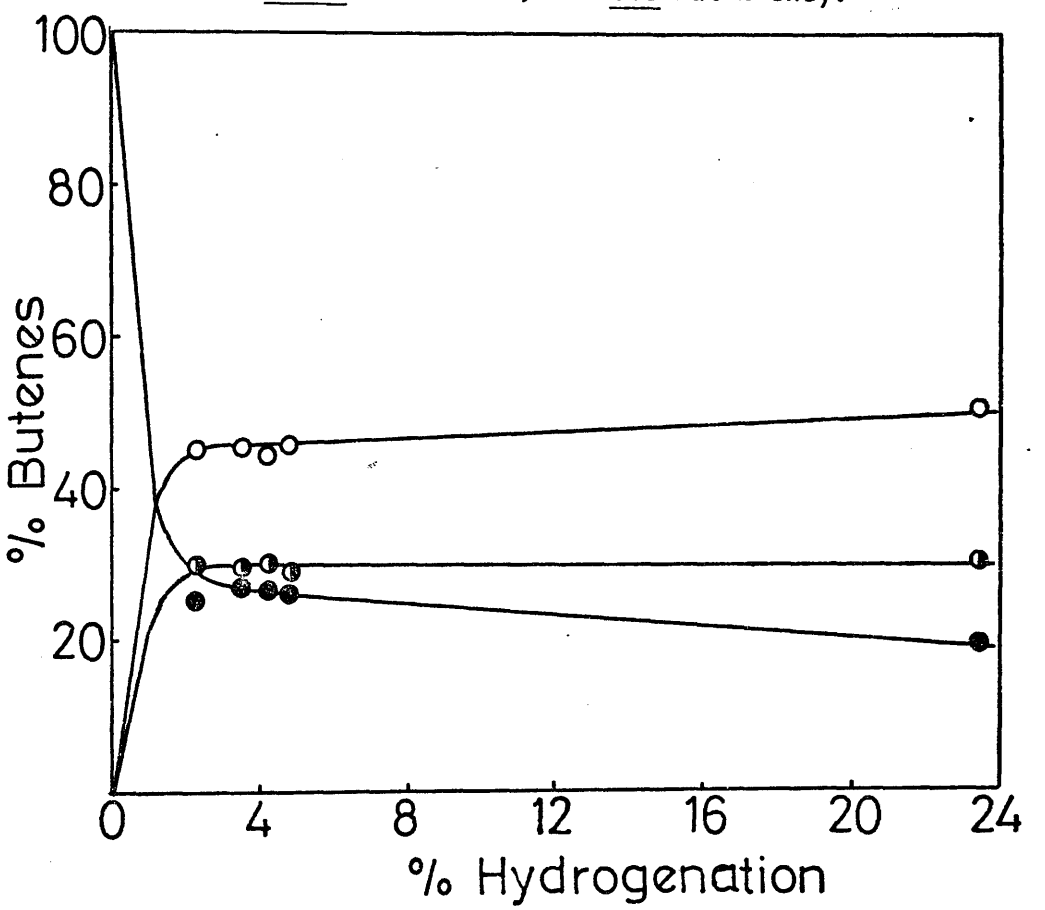

TABLE 6.5

Distribution of Deuterated Hydrocarbons with Conversion over 2% $Re_2(CO)_{10}$/silica at 250°C (Activation 250°C)

Reaction	d_0	d_1	d_2	d_3	d_4	d_5	d_6	D.N.
D/1	conversion = 2.4%			tex = 40 min.				
n-BUT	-	-	-	-	-	-	-	-
BUT-1	85.7	14.3	-	-	-	-	-	0.14
t-B-2	75.3	23.5	1.2	-	-	-	-	0.26
c-B-2	75.0	23.8	1.2	-	-	-	-	0.26
D/2	conversion = 3.6%			tex=135 min.				
n-BUT	-	-	-	-	-	-	-	-
BUT-1	74.0	21.3	4.7	-	-	-	-	0.31
t-B-2	68.3	29.3	2.4	-	-	-	-	0.34
c-B-2	67.0	30.9	2.1	-	-	-	-	0.35
D/5	conversion = 4.3%			tex = 195 min.				
n-BUT	36.4	20.9	32.4	8.8	1.5	-	-	1.20
BUT-1	68.6	23.1	7.0	1.3	-	-	-	0.41
t-B-2	61.6	30.1	7.5	0.7	-	-	-	0.47
c-B-2	59.8	30.4	8.4	1.4	-	-	-	0.51
D/4	conversion = 4.4%			tex=360 min.				
n-BUT	30.1	21.4	33.3	11.9	2.3	-	-	1.30
BUT-1	64.2	24.1	9.1	2.1	-	-	-	0.51
t-B-2	54.8	32.7	10.1	2.4	-	-	-	0.60
c-B-2	53.6	33.0	11.3	2.1	-	-	-	0.62
D/3	conversion = 23.4%			tex=1080 min.				
n-BUT	28.1	24.0	28.1	14.4	5.4	-	-	1.45
BUT-1	23.3	29.3	27.3	14.0	5.0	1.1	-	1.51
t-B-2	16.5	33.3	30.2	14.6	4.8	0.6	-	1.60
c-B-2	17.8	33.0	30.2	14.0	4.5	0.5	-	1.56

a pressure fall of only 6.5 torr was observed after 85 minutes.

A reaction mixture of (1:4) but-1-ene and hydrogen (200 torr) introduced to the same catalyst, resulted in a pressure-fall curve as shown in Figure 6.5. Also shown is the corresponding linear second order plot, showing that the overall order of the hydrogenation reaction was two.

6.3.2 Kinetics of Reactions of But-1-ene with Hydrogen.

In the series of reactions to determine the dependencies of the initial rates upon initial hydrogen pressure, each reaction was carried out at 275°C for 10 minutes. Similar conditions were used in a second series of reactions to determine the dependencies of initial rates upon initial but-1-ene pressure.

The results of the series to determine the variation of rates of reaction with initial hydrogen pressure are given in tables 6.6 and 6.7. The plot of log r_h against log p_{H_2} shown in Figure 6.6 gives a good straight line of gradient 1.2, which indicates that the order of the hydrogenation reaction is over unity with respect to the initial hydrogen pressure. The plot of log r_i against log p_{H_2} (Figure 6.6) gives a reasonably good straight line of gradient 0.35, hence the order of the isomerisation reaction is 0.35 with respect to the initial hydrogen pressure.

Tables 6.8 and 6.9 show the dependence of the initial rates of reaction on the initial pressure of but-1-ene. From figure 6.7, in which log r_h and log r_i are plotted against log p_{BUT-1}, the

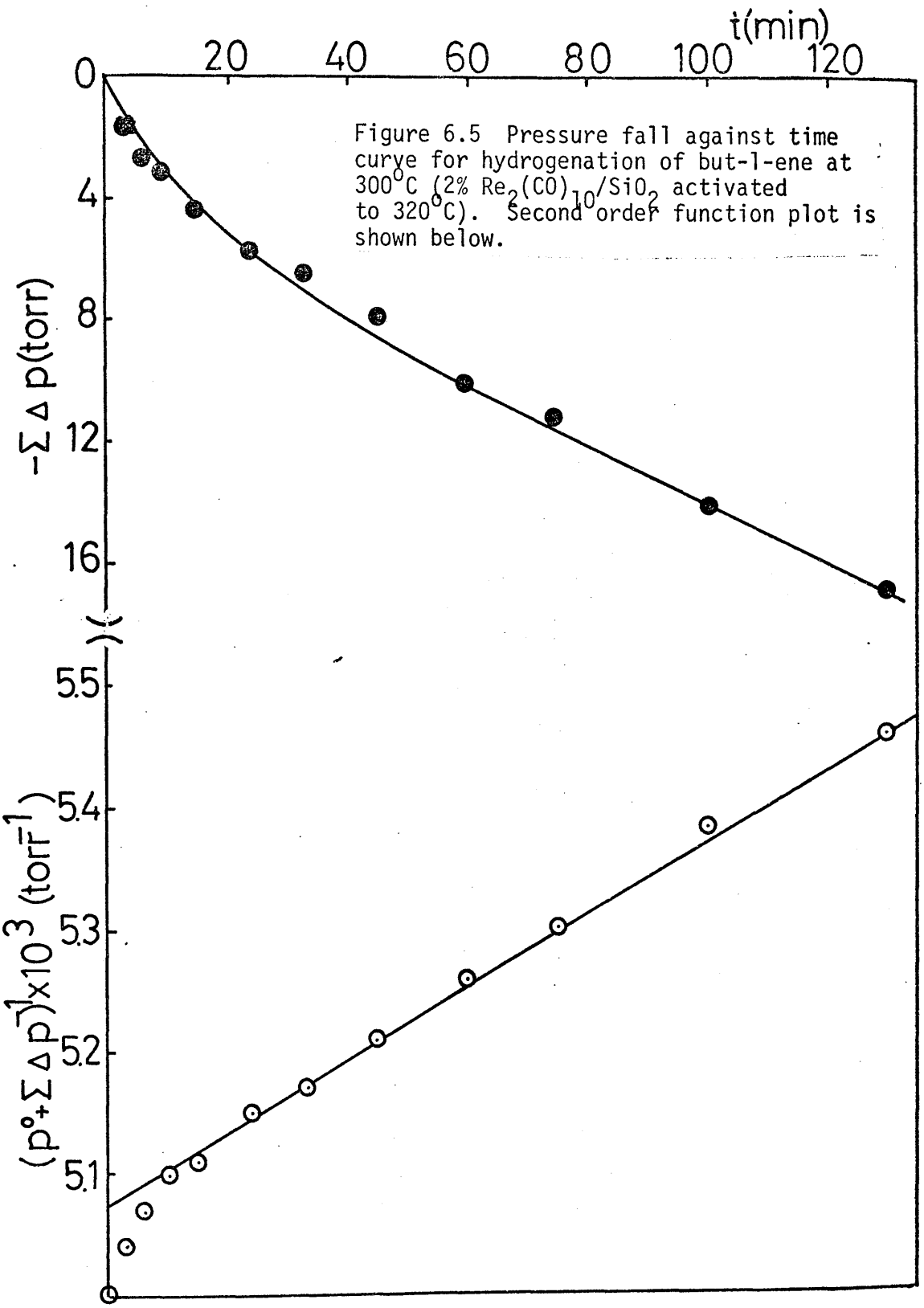

Figure 6.5 Pressure fall against time curve for hydrogenation of but-1-ene at 300°C (2% $Re_2(CO)_{10}/SiO_2$ activated to 320°C). Second order function plot is shown below.

TABLE 6.6

Variation of Butene Distribution with Initial Hydrogen Pressure

Temperature = 275°C Initial p_{BUT-1} = 50 ± 0.5 torr

Samples extracted at tex = 10 minutes

Reaction	p_{H_2} (torr)	%n-BUT	% butene distribution BUT-1	t-B-2	c-B-2
E/A4	25	0.4	71.1	16.4	12.5
E/A2	50	0.9	57.3	25.0	17.7
E/A3	100	1.7	56.8	22.3	19.2
E/A6	150	2.9	47.1	29.9	23.0
E/A1	200	4.5	43.2	33.0	23.8
E/A5	300	8.3	39.9	33.4	26.7

TABLE 6.7

Variation of Initial Reaction Rates with Initial Hydrogen Pressure at 275°C.

Reaction	p_{H_2} (torr)	rh (torr/min)	ri (torr/min)
E/A4	25	.02	1.76
E/A2	50	.05	2.95
E/A3	100	.09	3.00
E/A6	150	.15	4.10
E/A1	200	.22	4.64
E/A5	300	.41	5.16

Figure 6.6 Variation in (a) log (initial rate of isomerisation) (b) log (initial rate of hydrogenation), with log (initial hydrogen pressure) at 275°C. (2% $Re_2(CO)_{10}/SiO_2$ activated to 320°C).

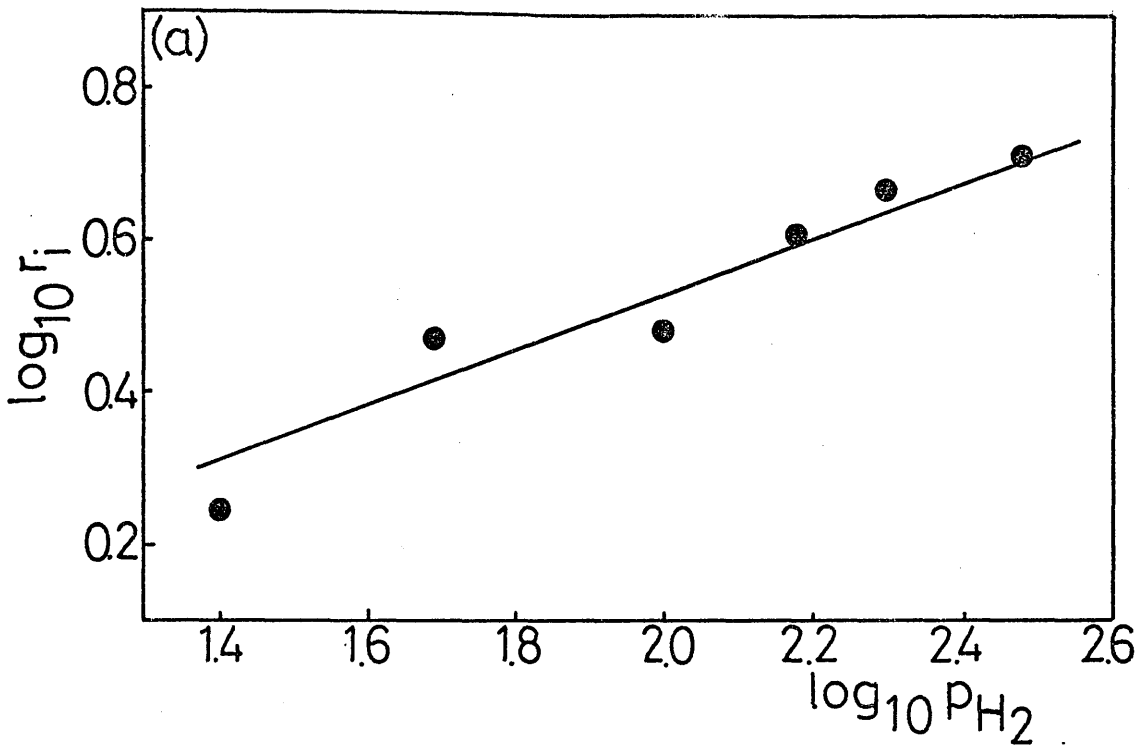

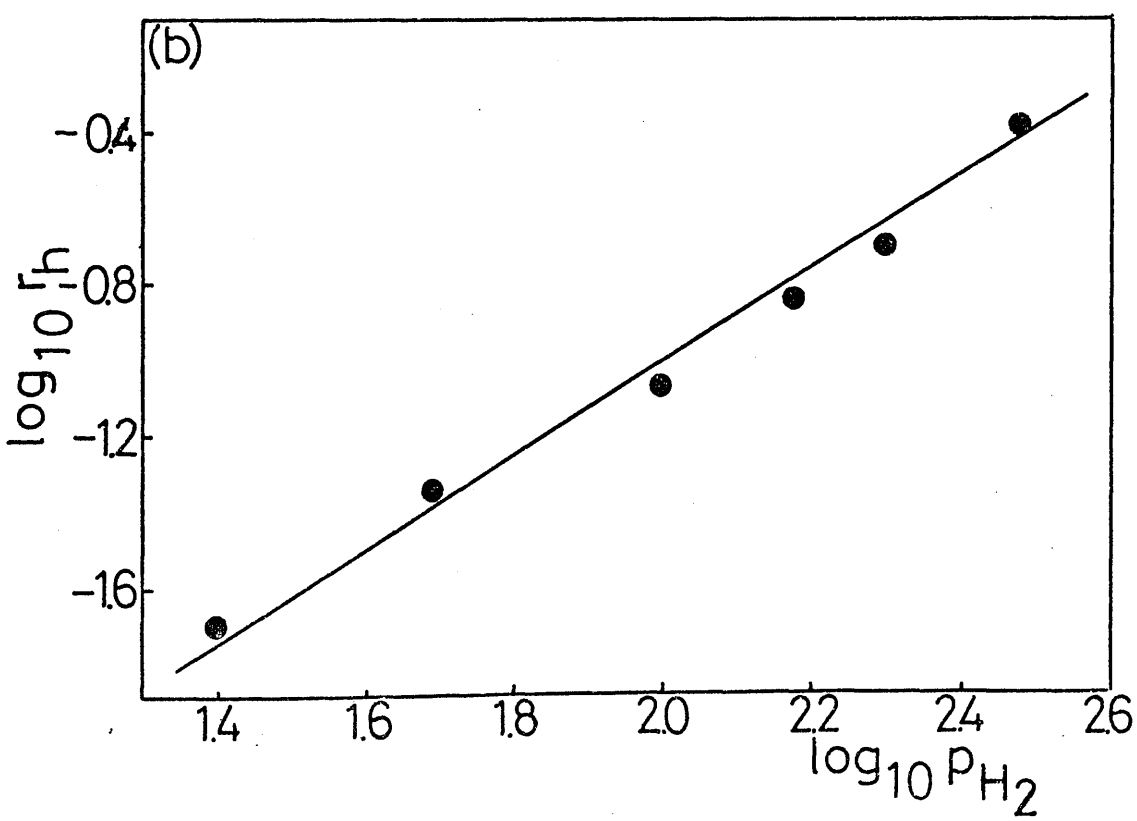

TABLE 6.8

Variation of Butene Distribution with Initial But-1-ene Pressure

Temperature = 275°C Initial p_{H_2} = 50 ± 0.5 torr

Samples extracted at tex = 10 minutes

Reaction	p_{BUT-1} (torr)	%n-BUT	% butene distribution BUT-1	t-B-2	c-B-2
E/B2	50	0.5	81.7	10.1	8.2
E/B3	100	0.3	85.1	8.7	6.2
E/B5	150	0.4	86.2	7.6	6.2
E/B1	200	0.3	85.6	8.4	6.0
E/B4	300	0.3	86.5	7.5	6.0

TABLE 6.9

Variation of Initial Reaction rates with Initial But-1-ene Pressure at 275°C

Reaction	p_{BUT-1} (torr)	rh (torr/min)	ri(torr/min)
E/B2	50	.02	1.03
E/B3	100	.03	1.64
E/B5	150	.06	2.26
E/B1	200	.06	3.15
E/B4	300	.09	4.40

Figure 6.7 Variation in (a) log (initial rate of isomerisation) (b) log (initial rate of hydrogenation), with log (initial but-1-ene pressure) at 275°C (2% $Re_2(CO)_{10}$/SiO_2 activated to 320°C).

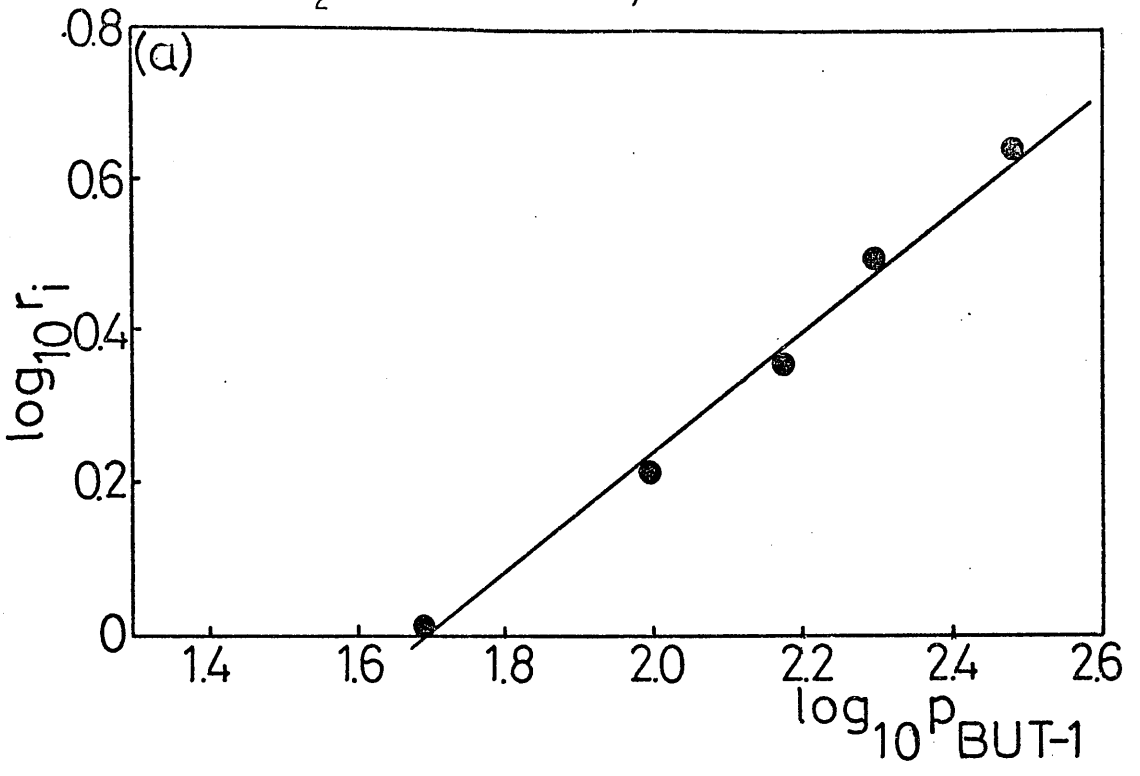

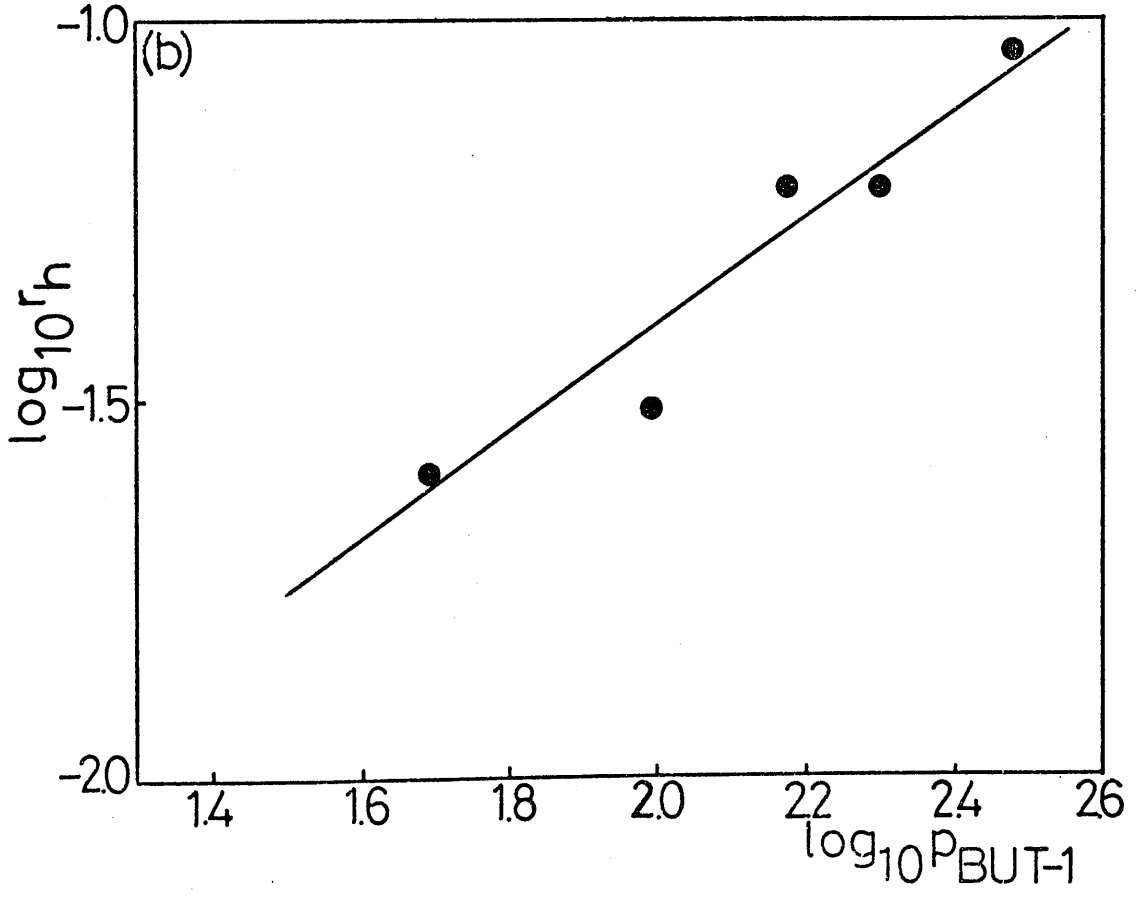

gradients of the straight lines shown therein suggest an order of about 0.7 with respect to initial but-1-ene pressure for the initial rate of hydrogenation, and an order of 0.8 with respect to initial but-1-ene pressure for the initial rate of isomerisation. The values obtained for the orders of reaction are listed below:-

Reaction	Order of Reaction	
	Hydrogen	But-1-ene
Hydrogenation	1.2 ± 0.05	0.7 ± 0.1
Isomerisation	0.35 ± 0.1	0.8 ± 0.05

6.3.3 Determination of Activation Energies of Reactions on $Re_2(CO)_{10}/SiO_2$

The dependence of rates of reaction and product distributions on the temperature of reaction was studied in the temperature range of 435 - 573^{o}K. Reactions were carried out with equal pressures (100 torr) of hydrogen and but-1-ene over 0.08 g of catalyst. The products were extracted after 30 minutes.

The butene distributions and initial rates of reaction are given in tables 6.11 and 6.12. Figure 6.8 illustrates the Arrhenius plots of log r_h and log r_i against $10^3T^{-1}(K^{-1})$. From the slopes of the lines, the activation energies for hydrogenation and isomerisation were calculated as 61.9 ± 2.0 kJ mole^{-1} and 106.6 ± 5.0 kJ mole^{-1} respectively.

6.3.4 The Effect of Oxygen on Activity of $Re_2(CO)_{10}/SiO_2$

The isomerisation of but-1-ene was studied by carrying out a series of reactions at varying conversions to n-butane at 250^{o}C.

TABLE 6.11

Variation of Butene Distribution with Temperature

$p_{H_2} = p_{BUT-1} = 100$ torr tex = 30 min

			% Butene distribution.		
Reaction	Temp (K)	%n-BUT	BUT-1	t-B-2	c-B-2
F/7	435	0.2	97.0	2.0	1.0
F/4	446	0.3	96.7	1.9	1.4
F/3	478	0.8	85.0	8.8	6.2
F/1	503	2.1	51.1	28.9	20.0
F/6	518	4.1	25.1	44.8	30.1
F/2	538	4.8	22.7	45.0	32.3
F/5	573	9.5	21.3	47.1	31.6

TABLE 6.12

Variation of Initial Rates of Reaction with Temperature

Reaction	Temp (K)	rh (torr/min)	ri (torr/min)
F/7	435	0.007	0.10
F/4	446	0.01	0.11
F/3	478	0.03	0.55
F/1	503	0.07	2.41
F/6	518	0.14	5.87
F/2	538	0.16	6.57
F/5	573	0.32	7.07

Figure 6.8 Arrhenius plots for (a) hydrogenation (b) isomerisation (2% $Re_2(CO)_{10}/SiO_2$ activated to 320°C).

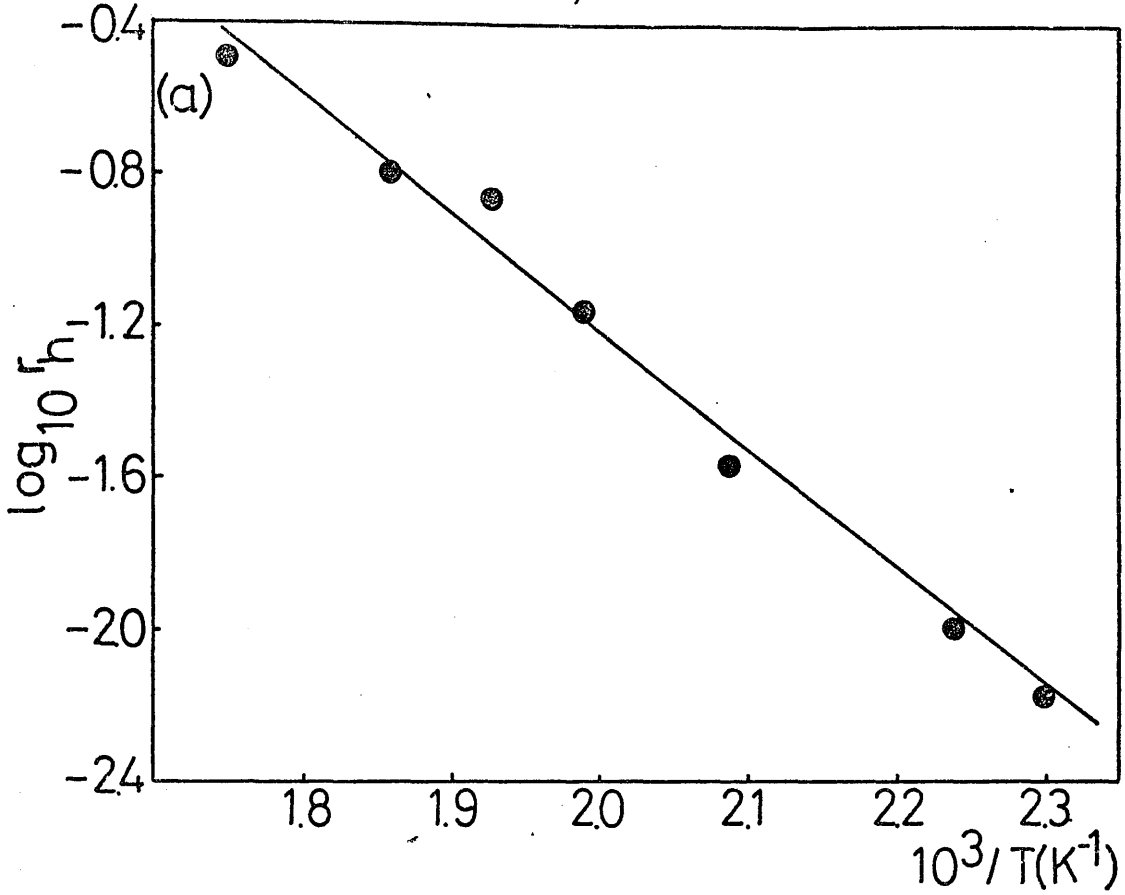

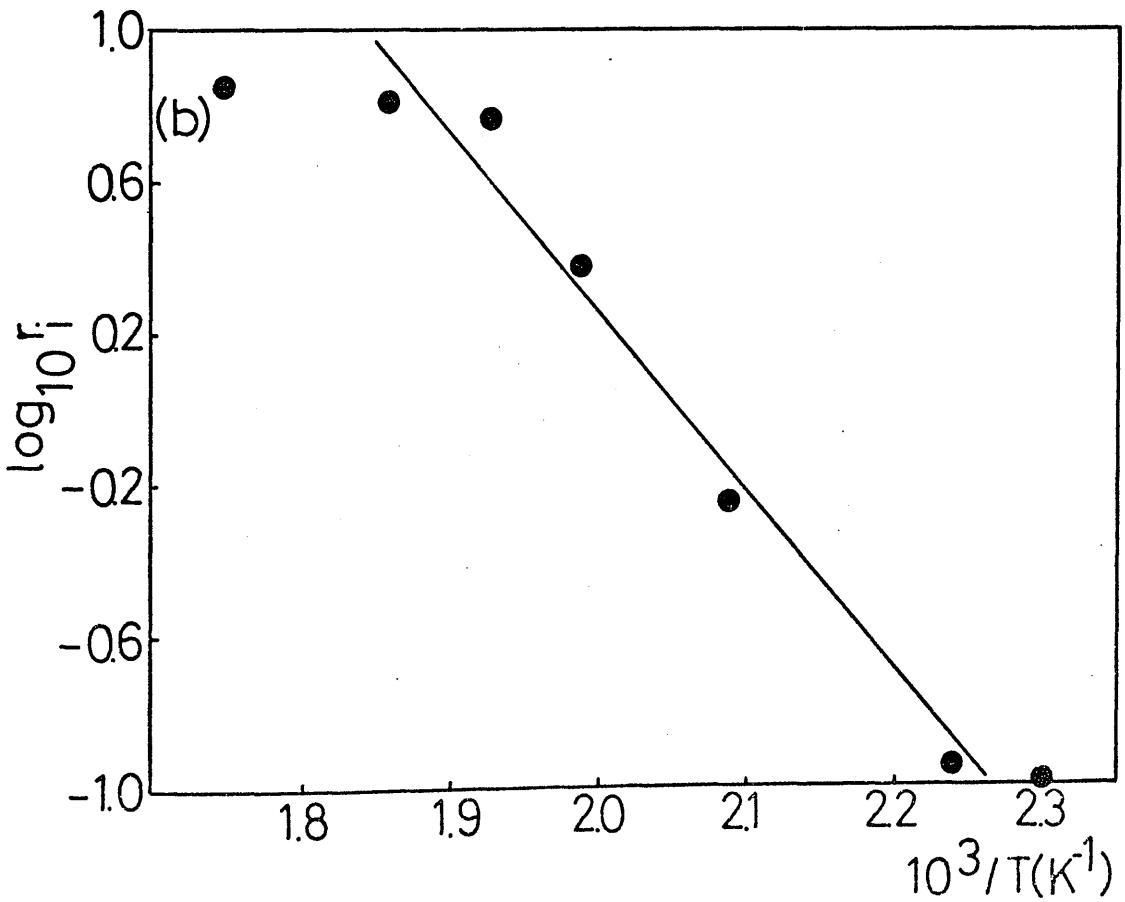

The variation in hydrocarbon composition with time of extraction is given in table 6.13, whilst Figure 6.9 illustrates the variation in butene composition as a function of percentage conversion.

When the catalyst sample was left under 200 torr of oxygen at 320°C for five days, it was found that it showed a distinct loss in activity for the same reaction, as may be seen from the analysis figures for a series of reactions carried out over the O_2 treated catalyst (table 6.14). The variation of butene composition with conversion for this series of reactions is illustrated in Figure 6.10.

The isomerisation reaction of trans-but-2-ene was studied in a similar manner to that of but-1-ene. A series of reactions was carried out at 250°C to varying conversions to n-butane. The product composition data obtained from these experiments are given in table 6.15, whilst the variation of butene as a function of conversion is shown graphically in Figure 6.11.

The effect of oxygen treatment over a shorter period of time was examined for the reaction of trans-but-2-ene with hydrogen. Treatment in this case was limited to 2 hours. An identical series of reactions was repeated over the catalyst. Table 6.16 gives the distribution of products along with the extraction times for this series of reactions, whilst the variation of butene composition with percentage conversion is depicted graphically in Figure 6.12.

The isomerisation reaction of cis-but-2-ene was examined over the same catalyst as above, which had been subsequently treated with hydrogen at 320°C overnight. The data obtained from the series of reactions carried out to various conversions are shown in table 6.17. Figure 6.13 illustrates the variation of butene composition with percentage conversion.

TABLE 6.13

Variation of Hydrocarbon Composition with Conversion at 250°C on $Re_2(CO)_{10}/SiO_2$

Initial $p_{H_2} = p_{BUT-1} = 100 \pm 0.5$ torr catalyst weight = 0.08 g

Reaction	% Hydrocarbon distribution n-BUT	BUT-1	t-B-2	c-B-2	tex (min)
G/1	1.9	57.9	22.1	18.1	12
G/2	4.2	20.9	46.6	28.3	45
G/3	4.2	21.8	48.1	25.9	70
G/4	4.5	22.1	46.5	26.9	105
G/5	17.5	15.5	41.5	25.5	1020

TABLE 6.14

Left Under O_2 at 320°C for 5 days

Reaction	% Hydrocarbon distribution n-BUT	BUT-1	t-B-2	c-B-2	tex (min)
H/1	0.4	94.7	2.9	2.0	20
H/2	1.2	74.2	14.2	10.4	60
H/3	3.3	39.1	34.6	23.0	240
H/4	7.0	21.3	44.3	27.4	1020
H/5	1.0	87.9	6.2	4.9	60
H/6	1.0	87.4	6.8	4.8	60

Figure 6.9 Variation of butene composition with percentage hydrogenation at 250°C ($2\%\ Re_2(CO)_{10}/SiO_2$ activated to 320°C. ● = but-1-ene ; o = trans-but-2-ene ; ◑ = cis-but-2-ene).

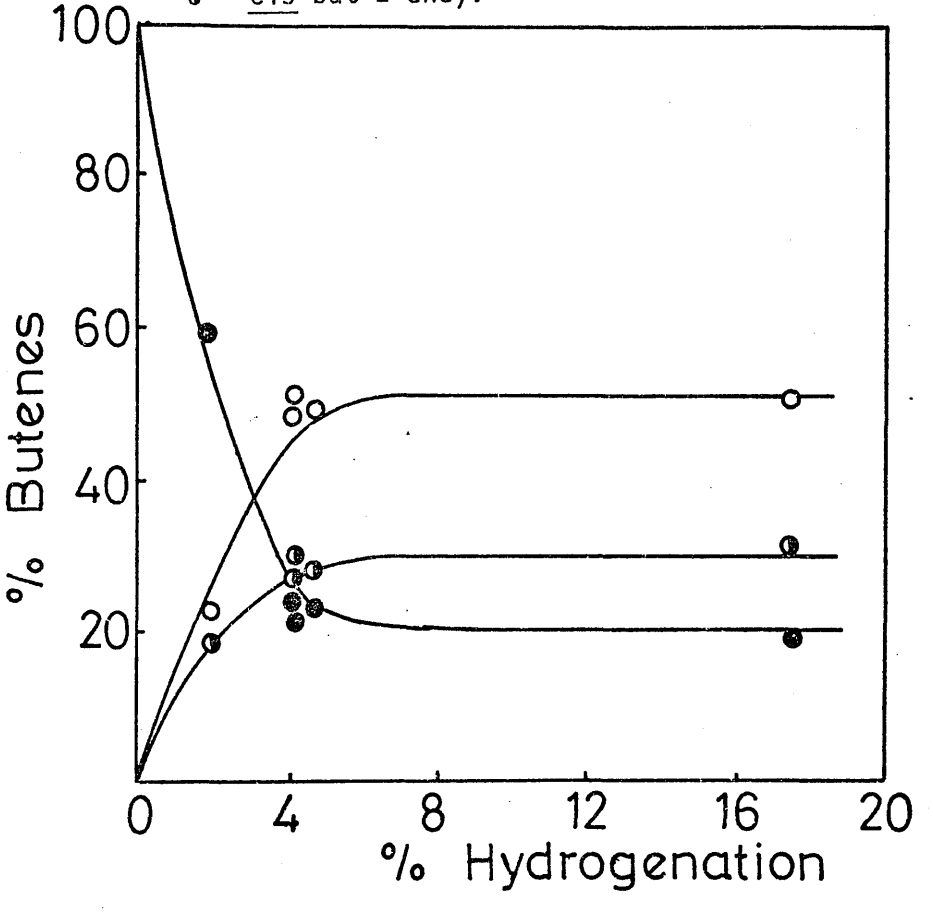

Figure 6.10 Effect of oxygen upon variation of butene composition with percentage hydrogenation at 250°C. (● = but-1-ene ; o = trans-but-2-ene ; ◑ = cis-but-2-ene).

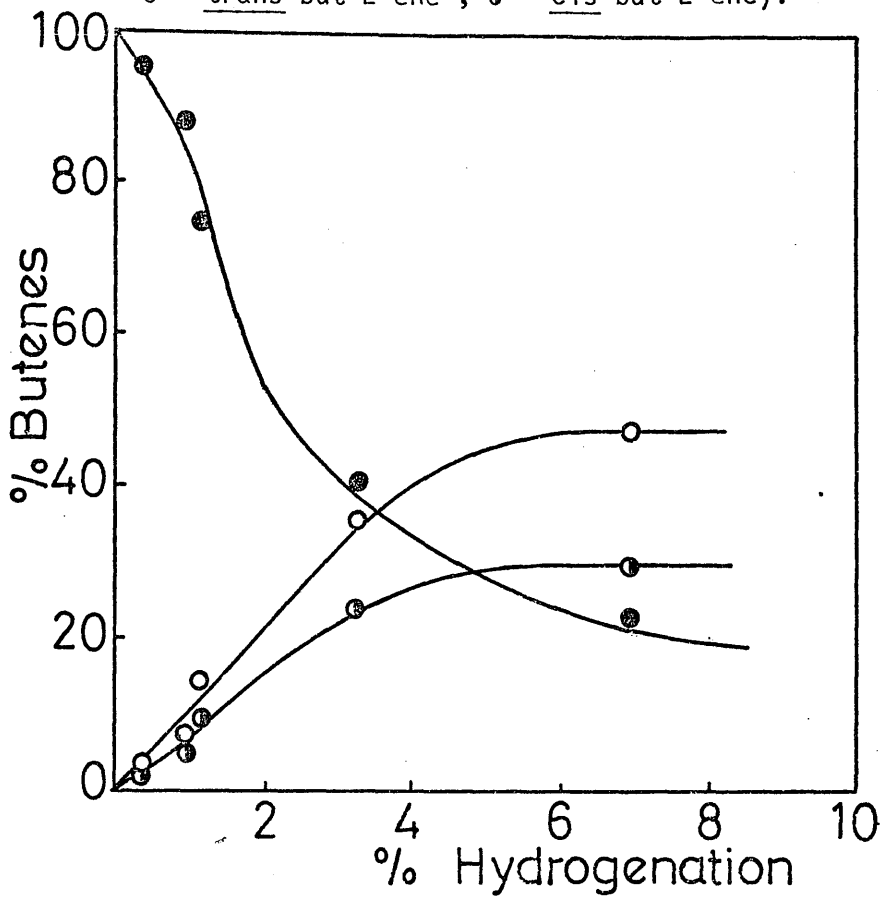

Figure 6.11 Variation of butene composition with percentage conversion for the hydrogenation of trans-but-2-ene at 250°C (● = but-1-ene ; o = trans-but-2-ene ; ◑ = cis-but-2-ene).

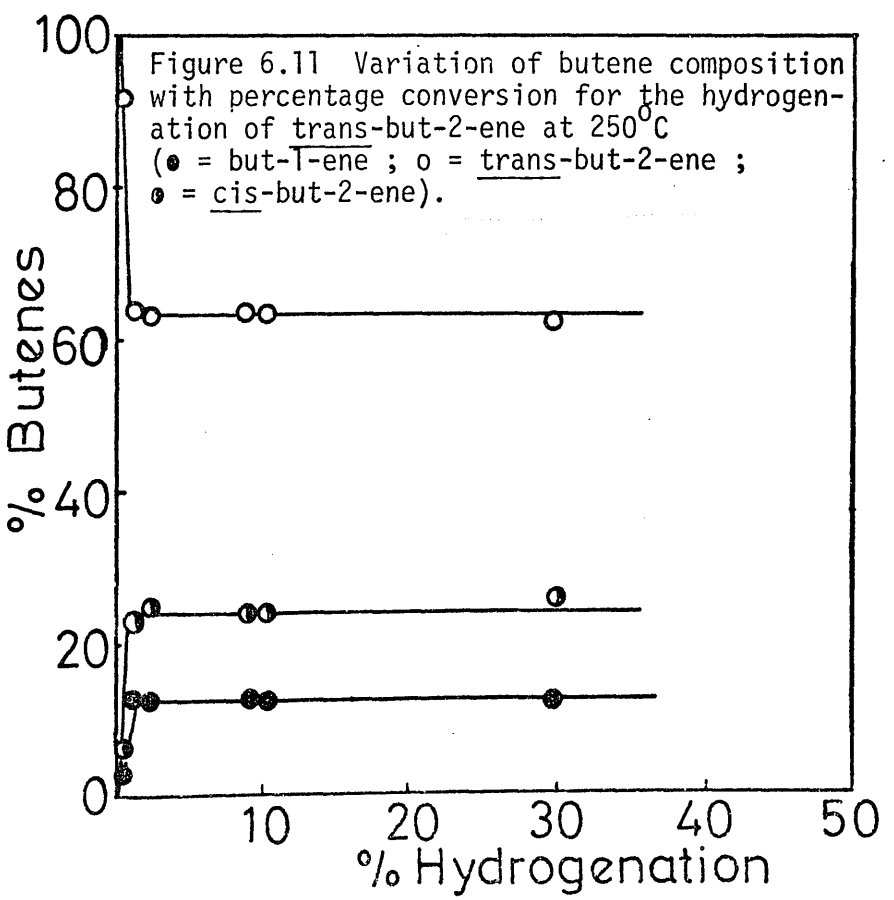

TABLE 6.15

Variation of Hydrocarbon Distribution with Conversion of trans-But-2-ene at 250°C on $Re_2(CO)_{10}/SiO_2$

Initial $p_{H_2} = p_{t\text{-}B\text{-}2} = 100 \pm 0.5$ torr

	% Hydrocarbon distribution				
Reaction	n-BUT	BUT-1	t-B-2	c-B-2	tex (min)
I/6	0.3	2.6	91.5	5.6	2
I/2	1.6	12.4	63.0	23.0	10
I/4	2.6	11.6	61.7	24.1	25
I/1	9.7	10.8	57.6	21.9	50
I/3	9.9	11.1	57.5	21.5	85
I/5	29.9	8.3	43.7	18.1	1020

TABLE 6.16

Left under 200 torr O_2 at 320°C for 2 hours

Reaction	n-BUT	BUT-1	t-B-2	c-B-2	tex (min)
J/5	0.3	0.6	98.0	1.1	2
J/1	0.6	3.6	87.3	8.5	10
J/2	2.0	10.2	67.6	20.2	25
J/3	9.3	10.2	55.9	24.6	50
J/4	53.1	7.0	29.5	10.4	1020

Figure 6.12 Effect of O_2 upon the variation of butene composition with percentage conversion for the hydrogenation of trans-but-2-ene at 250°C (◐ = but-1-ene ; o = trans-but-2-ene ; ● = cis-but-2-ene).

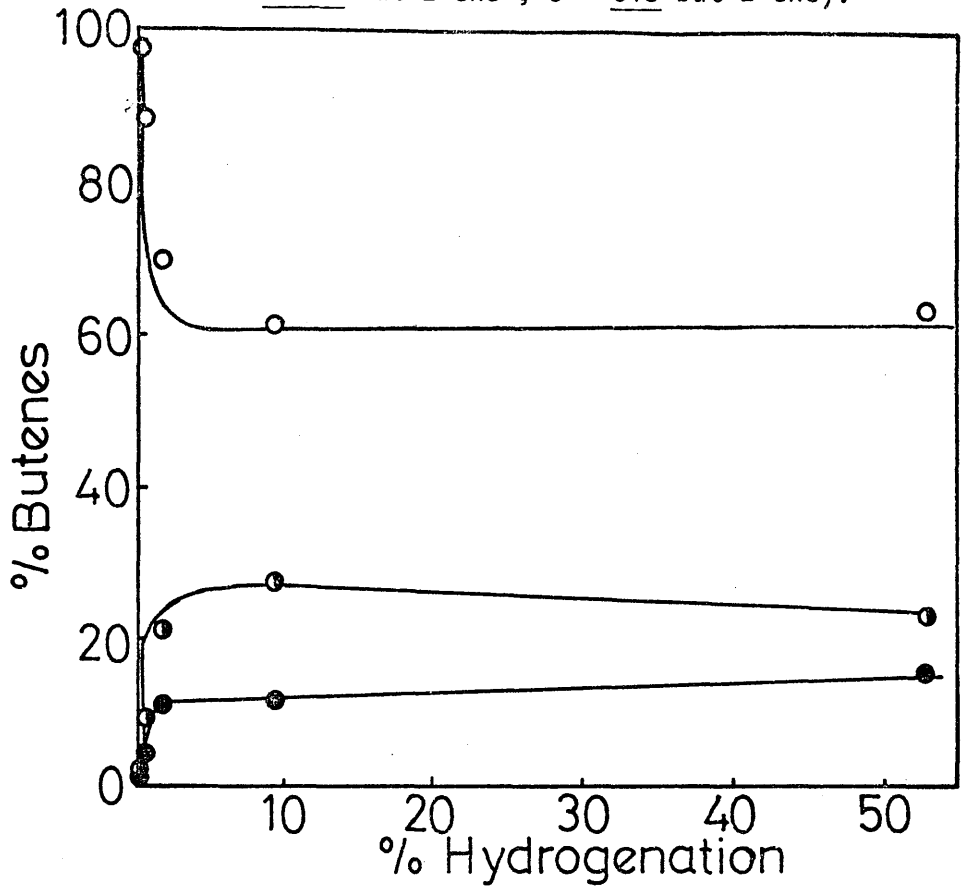

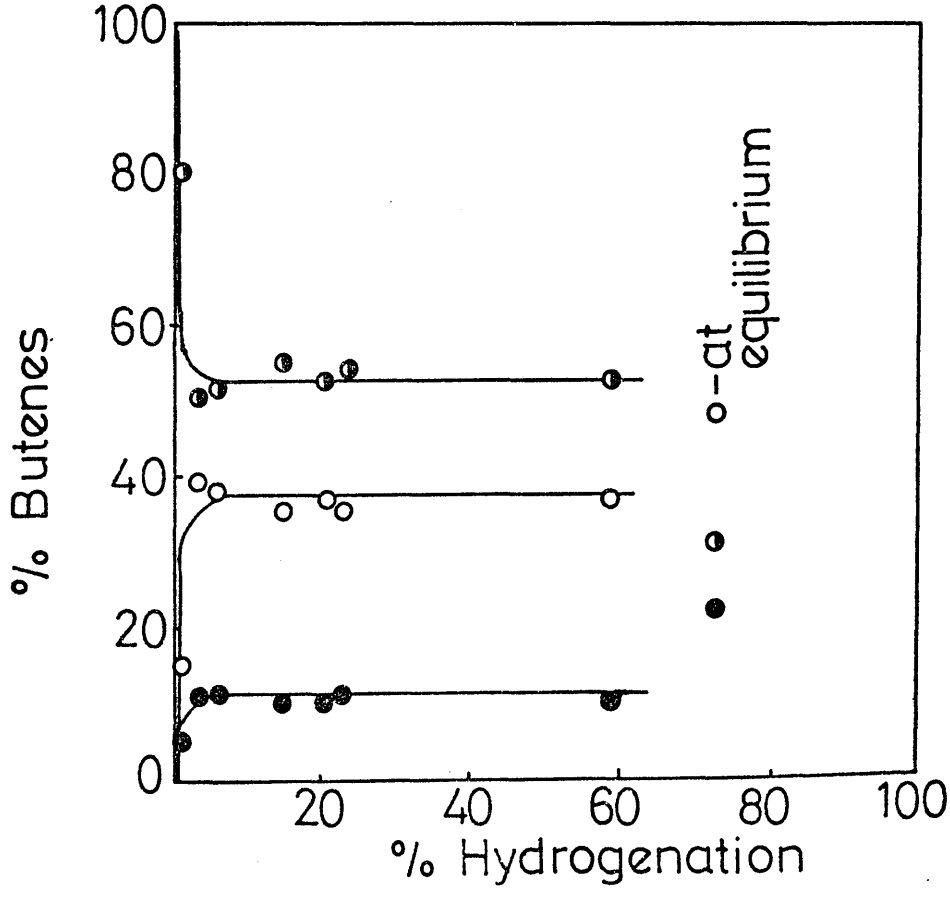

Figure 6.13 Variation of butene composition with percentage conversion for the hydrogenation of cis-but-2-ene at 250°C (◐ = but-1-ene ; o = trans-but-2-ene ; ● = cis-but-2-ene).

TABLE 6.17

Variation of Hydrocarbon Distribution with Conversion of cis-But-2-ene at 250°C on $Re_2(CO)_{10}/SiO_2$

	% Hydrocarbon distribution				
Reaction	n-BUT	BUT-1	t-B-2	c-B-2	tex (min)
J/2	1.0	5.0	14.5	79.5	3
J/1	6.3	10.8	35.3	47.6	10
J/5	4.1	10.5	37.1	48.3	25
J/3	15.0	8.5	29.7	46.8	50
J/4	22.9	8.3	27.0	41.8	105
J/7	20.6	8.0	27.7	43.7	270
J/8	59.3	4.2	15.0	21.5	1020
J/9	75.0	5.4	12.0	7.6	∞

6.3.5 Isomerisation of But-1-ene in the Absence of Hydrogen

The isomerisation of but-1-ene was examined by carrying out the reaction at various temperatures for a period of 60 minutes. From the results given in table 6.18, it seems that the threshhold temperature for isomerisation to occur within a reasonable time is at about 230^{o}C. Below this temperature, but-1-ene has to be left over a period of several days before isomerisation will occur to any noticeable extent. This compares with a threshhold temperature of about 165^{o}C for the isomerisation of but-1-ene in the presence of hydrogen.

TABLE 6.18

Variation of Butene Distribution with Temperature on $Re_2(CO)_{10}/SiO_2$

Initial p_{BUT-1} = 200 ± 0.5 torr

tex = 60 min

catalyst weight = 0.08 g

Reaction	Temp(°C)	% butene distribution BUT-1	t-B-2	c-B-2
K/1	310	35.9	37.2	26.9
K/2	258	45.6	31.4	23.0
K/3	238	91.3	5.1	3.6

CHAPTER 7

REACTIONS OF n-BUTENES WITH HYDROGEN ON SILICA SUPPORTED DICOBALTDIRHODIUM DODECACARBONYL

7.1 Catalyst Characterisation

7.1.1 Physical Appearance

The supported complex was of a light brown coloration when freshly prepared. This colour persisted when it was stored under dry nitrogen at room temperature. Heating in vacuo had no effect on the physical appearance or colour of the complex up to 200°C. Prolonged activation at 240°C resulted in it taking on a grey coloration.

7.1.2 Examination of the Complex by T.V.A.

T.V.A. of a 10% $Rh_2CO_2(CO)_{12}$/Aerosil silica sample showed that degradation commenced at 60°C; the products of degradation were incondensable in all of the cold traps in series (Figure 7.1). The trace reached a first maximum at 134°C where product evolution was at its greatest. Thereafter, there was a fall in product evolution to approximately zero, before a second stage in degradation took place, resulting in a maximum evolution at over 400°C.

A closed system gas infra-red spectroscopic examination of the products of degradation showed a small peak at just below 2000cm^{-1}.

The above data inferred that carbon monoxide was the sole product of degradation.

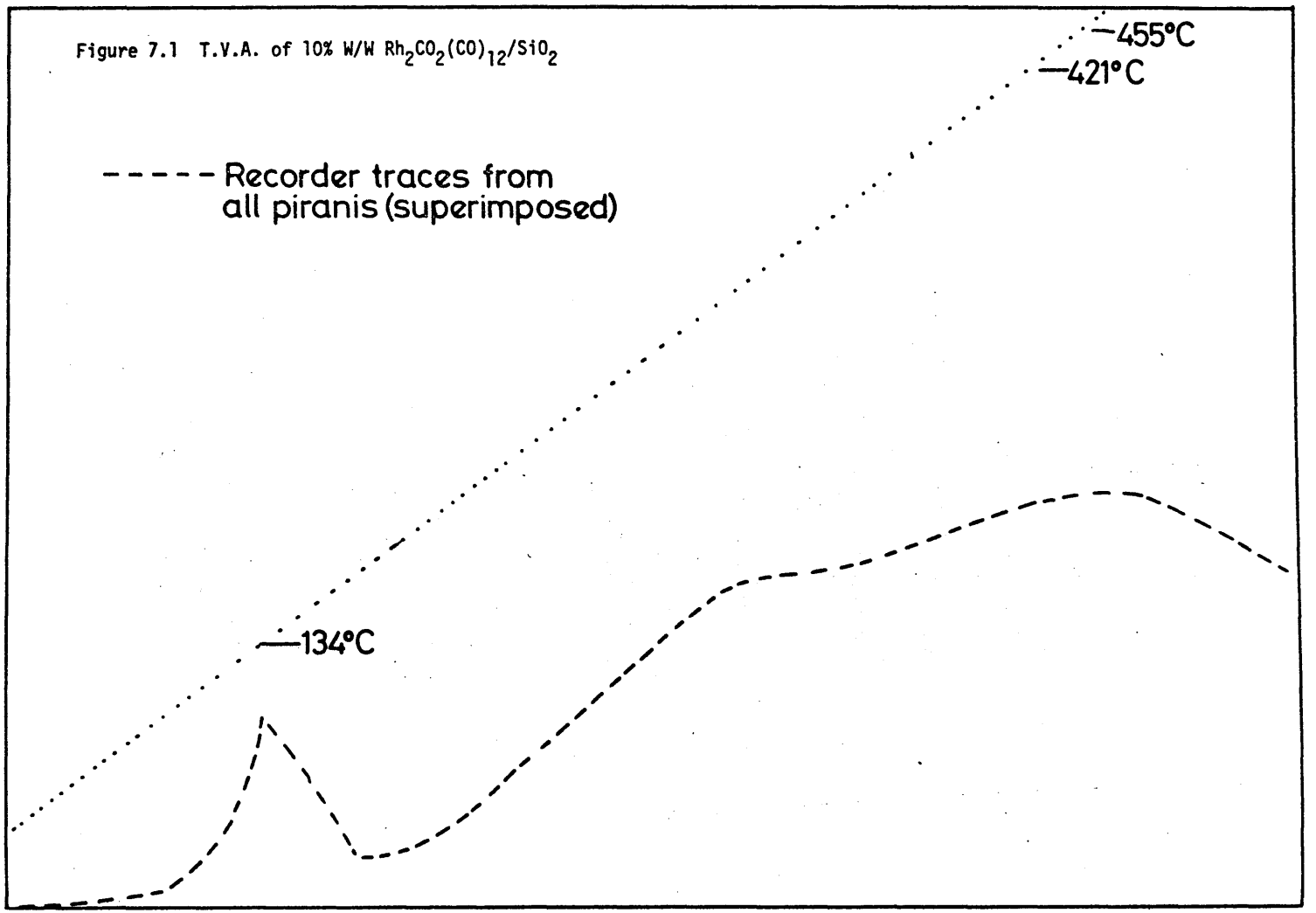
Figure 7.1 T.V.A. of 10% W/W $Rh_2CO_2(CO)_{12}/SiO_2$
455°C
421°C
Recorder traces from all piranis (superimposed)
134°C

7.1.3 Examination of the Complex by Infra-Red Spectroscopy

A disc infra-red examination of a freshly prepared 5.5% $Rh_2Co_2(CO)_{12}$/Aerosil silica catalyst sample showed the presence of the following bands in the 2000cm^{-1} region.

$\bar{\nu}$ = 2026(s), 2040(s), 2075(sh), 2080(sh), 2095(s) cm^{-1}

On leaving the disc sample in the instrument beam for a few hours, there was a noticeable decrease in the intensity of these bands, whilst long term exposure of the sample to air resulted in the complete disappearance of the bands.

There were no bands detectable in the 1800 - 1900 cm^{-1} region which would have been indicative of bridging carbonyls being retained on supporting the complex.

A disc infra-red examination of a freshly prepared sample of supported complex activated to 120^{o}C in vacuo overnight also indicated the facile removal of carbonyl ligands, as bands in the $\bar{\nu}_{CO}$ region were absent.

Storing the supported complex under nitrogen prevented its decomposition.

Preliminary reactions carried out over the supported complex (2% W/W) preheated in vacuo to various temperatures showed it to be a catalyst for the hydrogenation and isomerisation of n-butenes.

7.1.4 Examination of the Catalyst by Electron Microscopy

The catalyst was examined in three different forms:-

(1) having been activated to 100^{o}C in vacuo overnight and having

been instrumental in a few reactions.

(2) having been involved extensively in catalytic reactions, which involved activation to 240°C.

(3) having been exposed to air over a period of time, followed by extensive involvement in catalytic reactions, including activation to 130°C.

Examination by electron microscopy indicated that no particles were detectable on catalyst (1). In the case of catalyst (2) particles could be detected of size 9-45Å. These particles were widespread on the support. For catalyst (3), particles were again detectable, this time in the region of 9-18Å.

7.2 Reactions of n-Butenes with Hydrogen on 2% $Rh_2Co_2(CO)_{12}/SiO_2$

7.2.1 Preliminary Investigation

0.08g of $Rh_2Co_2(CO)_{12}/SiO_2$ was initially activated *in vacuo* at the arbitrary temperature of 100°C for 3 hours. All reactions over this catalyst were carried out using a 1:1 mixture of but-1-ene and hydrogen (200 torr).

The initial reaction, which was carried out at 100°C had an induction period of approximately 30 minutes, after which hydrogenation occurred at a rate of about 1 torr min^{-1}. In all subsequent reactions over this sample of catalyst, there was no induction period. A typical pressure fall against time curve is shown in Figure 7.2 along with the corresponding linear first order plot, showing that the overall order of the hydrogenation reaction

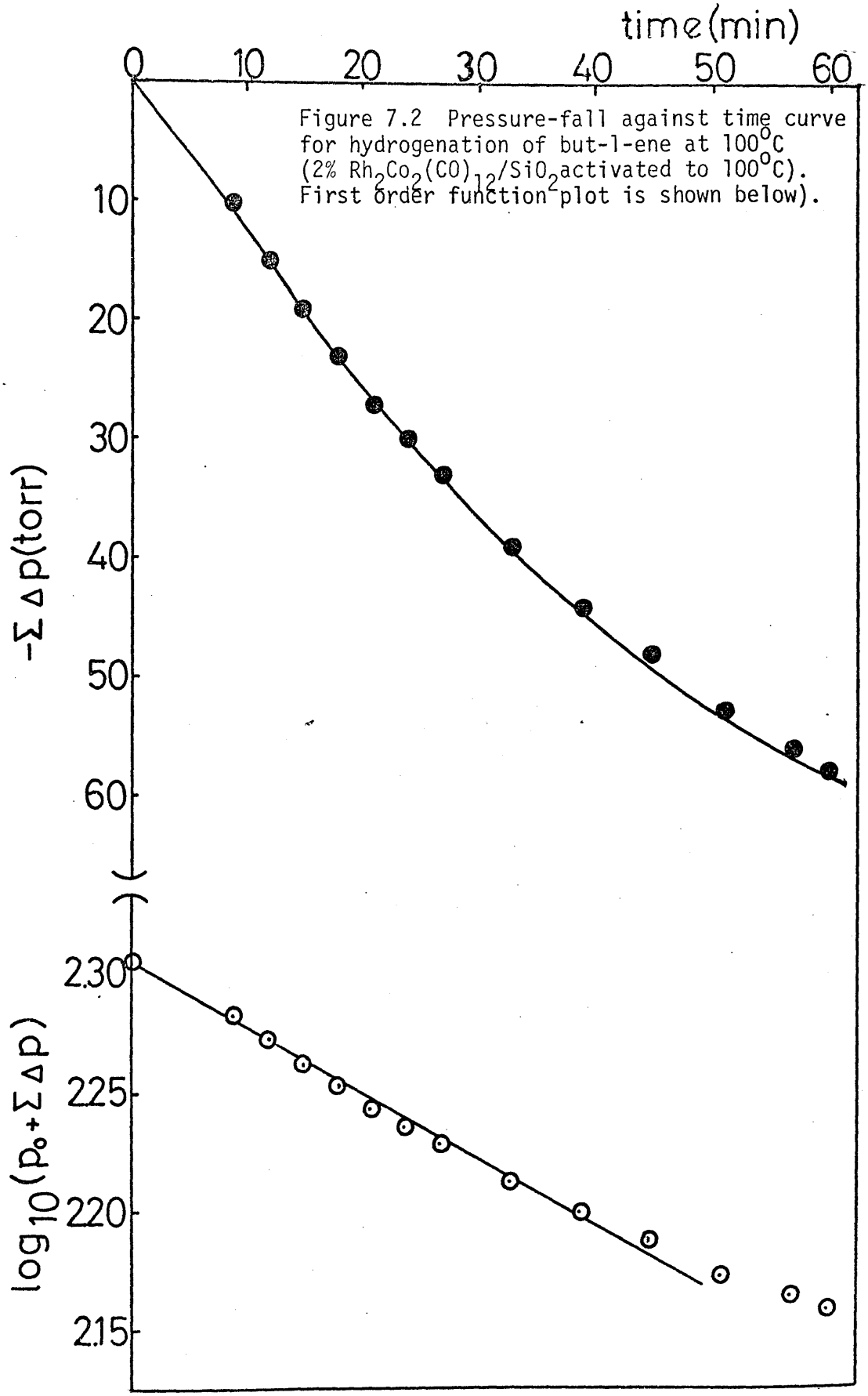

Figure 7.2 Pressure-fall against time curve for hydrogenation of but-1-ene at 100°C (2% $Rh_2Co_2(CO)_{12}/SiO_2$ activated to 100°C). First order function plot is shown below).

was unity. The rate of hydrogenation appeared to remain virtually constant from reaction to reaction at 100°C.

The isomerisation of but-1-ene was studied by carrying out a series of reactions at 100°C to varying conversions to n-butane. Table 7.1 shows the analysis figures for the variation in product distribution with conversion, whilst the percentage butene distribution is plotted as a function of hydrogenation in Figure 7.3.

7.2.2 Kinetics of the Hydrogenation and Isomerisation of But-1-ene

The dependencies of initial rates upon initial reactant pressures were determined as discussed earlier. A series of reactions were carried out for 20 minutes to ascertain the dependance of initial rate of hydrogenation upon initial hydrogen pressure. Since isomerisation to thermodynamic proportions occurred in most cases over this period, a second series of reactions were carried out for 5 minutes, which permitted a more accurate determination of the initial rates of isomerisation. A further series of reactions were carried out for 20 minutes in which the initial hydrogen pressure was kept constant whilst the but-1-ene pressure was varied between 25 and 300 torr.

The variation of butene distribution with initial hydrogen pressure is given in tables 7.2 and 7.3, along with the initial rates of isomerisation and hydrogenation in table 7.4. The plot of r_h against p_{H_2} shown in Figure 7.4 shows a good straight line through the origin, indicating an order of unity with respect to initial hydrogen pressure. A plot of log r_i against log p_{H_2} (Figure 7.5) indicates an order of 0.3 for the isomerisation reaction with respect to initial hydrogen pressure.

TABLE 7.1

Variation of Hydrocarbon Distribution with Conversion at 100°C on $Rh_2CO_2(CO)_{12}/SiO_2$.

Initial P_{H_2} = P_{BUT-1} = 100 ± 0.5 torr

Catalyst weight = 0.08g

% hydrocarbon distribution

Reaction	n-BUT	BUT-1	t-B-2	c-B-2	tex(min)
A/8	1.7	86.2	6.9	5.2	1
A/4	3.8	65.2	18.3	12.7	3
A/3	8.9	42.3	30.0	18.8	6
A/7	26.7	12.0	39.4	21.9	12
A/5	32.4	9.5	36.9	21.2	21
A/6	49.7	7.2	28.7	14.4	33
A/2	60.8	5.5	22.2	11.5	60
A/1	66.8	3.5	19.5	10.2	180

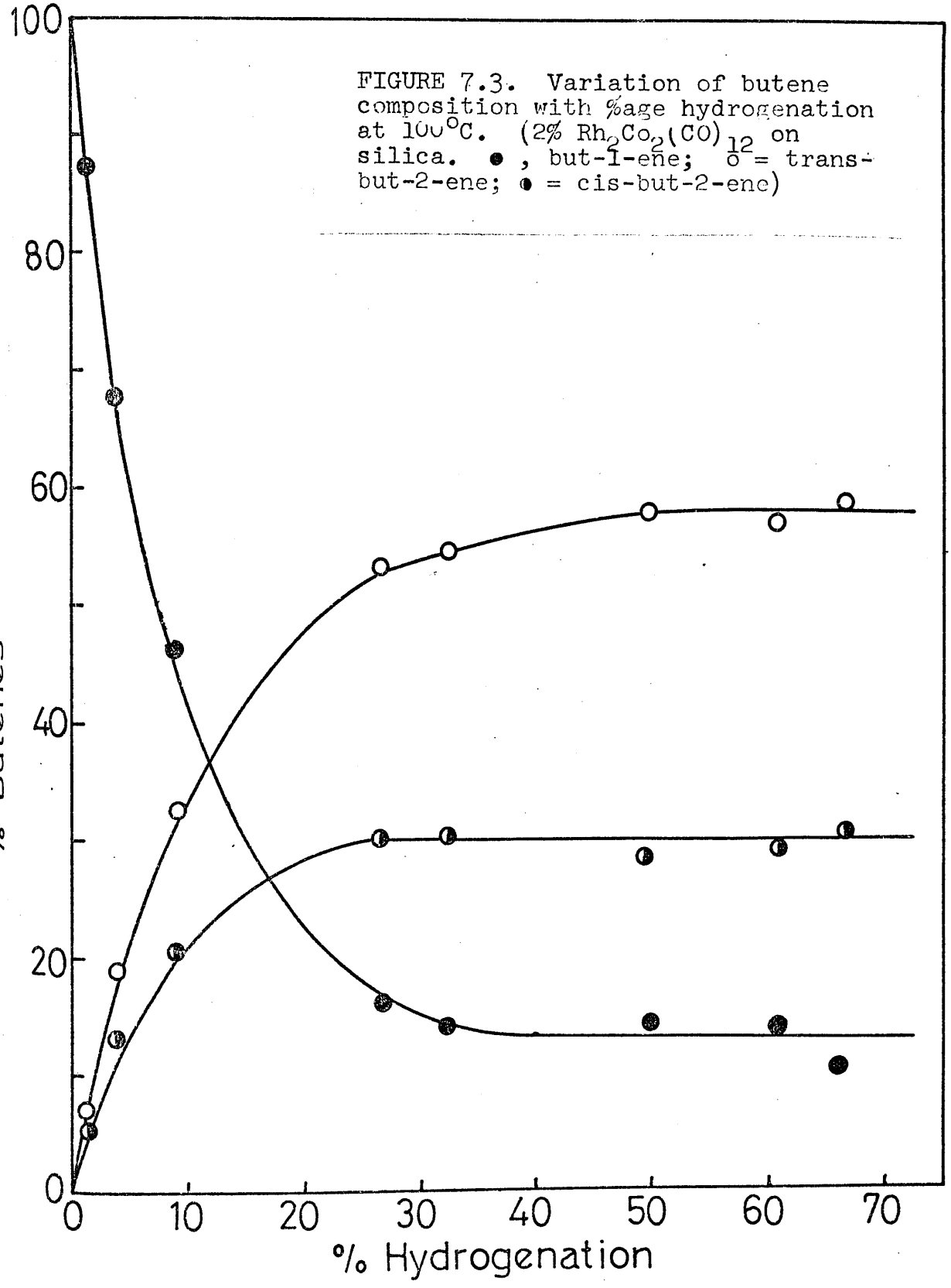

FIGURE 7.3. Variation of butene composition with %age hydrogenation at 100°C. (2% $Rh_2Co_2(CO)_{12}$ on silica. ● , but-1-ene; ○ = trans-but-2-ene; ◐ = cis-but-2-ene)

TABLE 7.2

Variation of Butene Distribution with Initial Hydrogen Pressure.

Temperature = 85°C Initial p_{BUT-1} = 50 ± 0.5 torr

Reaction	p_{H_2}(torr)	%n-BUT	% Butene distribution BUT-1	t-B-2	C-B-2	tex(min)
B/A5	25	2.3	47.5	29.8	22.7	20
B/A3	50	6.0	17.0	49.2	33.8	20
B/A1	100	10.4	13.0	56.0	31.0	20
B/A4	200	18.8	15.2	56.2	28.6	20
B/A2	300	33.2	11.7	58.5	29.8	20

TABLE 7.3

Variation of Butene Distribution with Initial Hydrogen Pressure

Reaction	p_{H_2}(torr)	% Butene distribution BUT-1	t-B-2	C-B-2	tex(min)
B/A5	25	47.5	29.8	22.7	20
B/B3	50	77.4	12.7	9.9	5
B/B1	100	75.0	14.1	10.9	5
B/B6	150	72.6	14.7	12.7	5
B/B4	200	71.4	16.3	12.3	5
B/B2	300	65.4	17.7	16.9	5

TABLE 7.4

Variation of Initial Rates with Initial Hydrogen pressure at 85°C

P_{H_2}(torr)	rh(torr/min)	ri(torr/min)
25	.06	1.92
50	.15	2.58
100	.26	2.90
150	-	3.24
200	.47	3.41
300	.83	4.31

Figure 7.4 Variation in initial rate of hydrogenation with initial hydrogen pressure at 85°C.

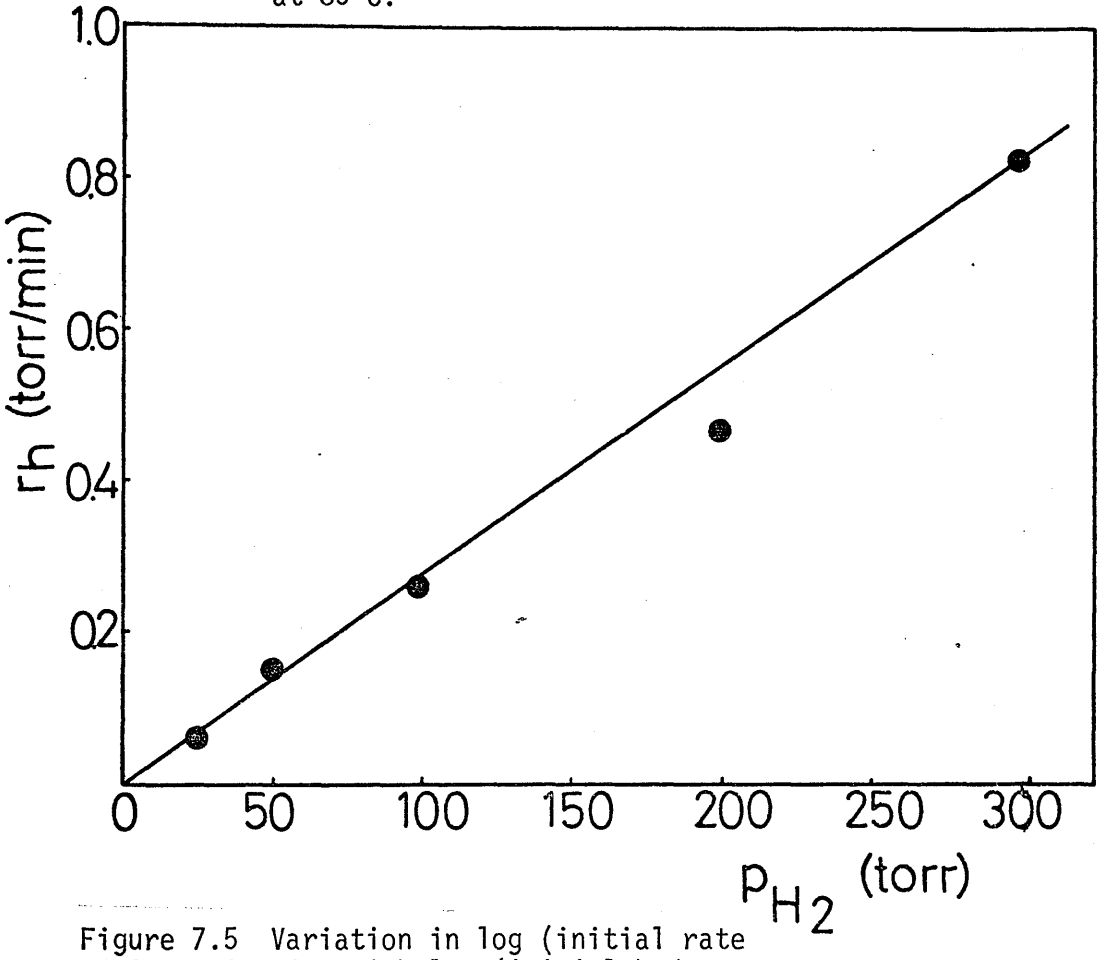

Figure 7.5 Variation in log (initial rate of isomerisation with log (initial hydrogen pressure) at 85°C.

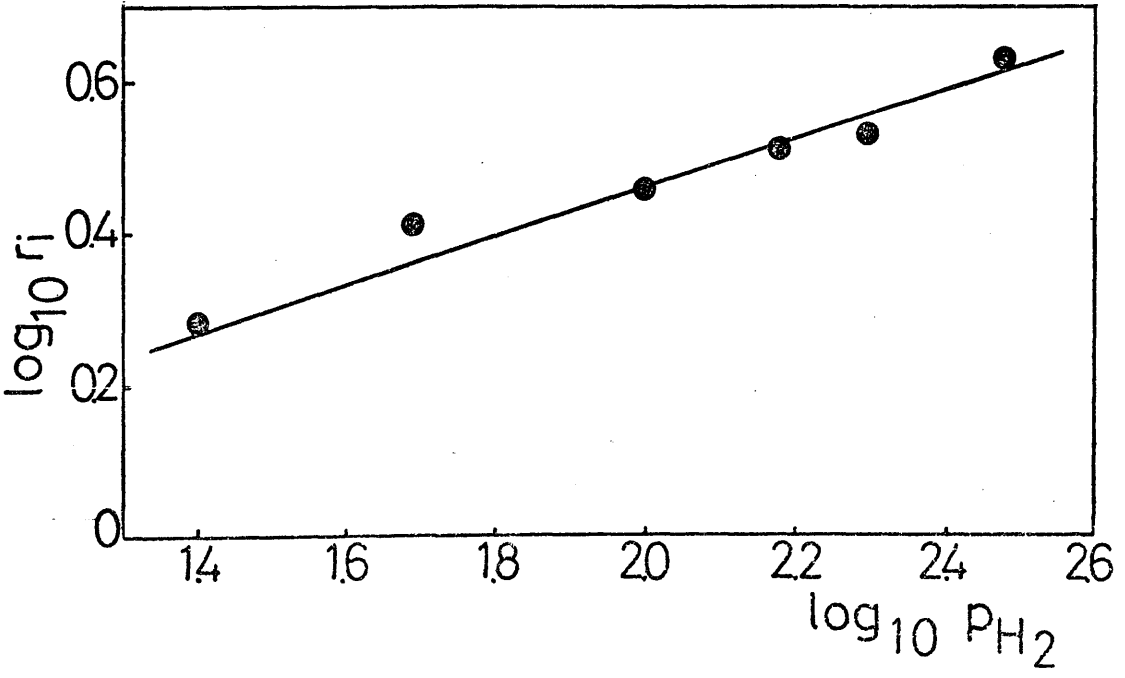

Similarly, the variation of butene composition with initial but-1-ene pressure is given in table 7.5, whilst the initial rates of isomerisation and hydrogenation are in table 7.6. Plots of r_i and r_h against P_{BUT-1} are illustated in Figure 7.6, and indicate that both the rate of hydrogenation and isomerisation are independent of the initial butene pressure. These results are summarised below.

Reaction	Order of Reaction	
	Hydrogen	But-1-ene
Hydrogenation	1.0 ± 0.05	0.0 ± 0.1
Isomerisation	0.3 ± 0.05	0.0 ± 0.1

7.2.3 The Change in Catalytic Activity of $Rh_2Co_2(CO)_{12}/SiO_2$

In order to examine the dependencies of the initial rates of reaction upon temperature, a fresh sample (0.08g) of complex was activated at 110°C overnight. On attempting to carry out the reaction of hydrogen with but-1-ene (200 torr of 1:1 mixture) at 95°C, hydrogenation was found to occur to completion in about 5-10 minutes. The hydrogenation of but-1-ene was observed to be exceedingly fast, even at room temperature.

To allow a more extensive study of the effects of activation temperature upon its catalytic activity and behaviour, a further fresh sample of the supported complex (13 mg) was activated *in vacuo* at gradually increasing temperatures for one hour. Reactions carried out at these temperatures of activation showed that in the temperature range 18-85°C, no reaction had taken place after one hour. Prolonged activation at 85°C resulted in the complex being an exceedingly good catalyst for hydrogenation and isomerisation at 80°C,

TABLE 7.5

Variation of Butene Distribution with Initial Pressure of But-1-ene

Temperature = 85°C Initial p_{H_2} = 50 ± 0.5 torr

Reaction	p_{BUT-1}	%n-BUT	% Butene Distribution BUT-1	t-B-2	C-B-2	tex(min)
B/C4	25	8.0	24.3	46.0	29.7	10
B/C2	50	6.0	17.0	49.2	33.8	20
B/C3	100	2.8	48.1	28.9	23.0	20
B/C5	200	1.5	73.8	14.4	11.8	20
B/C1	300	1.4	76.1	13.7	10.2	20

TABLE 7.6

Variation of Initial Reaction Rates with Initial Pressure of But-1-ene

Reaction	p_{BUT}(torr)	rh(torr/min)	ri(torr/min)
B/C4	25	.20	3.85
B/C2	50	.15	5.04
B/C3	100	.14	3.77
B/C5	200	.15	3.07
B/C1	300	.21	4.13

Figure 7.6 Variation in (a) initial rate of isomerisation (b) initial rate of hydrogenation; with initial but-1-ene pressure at 85°C.

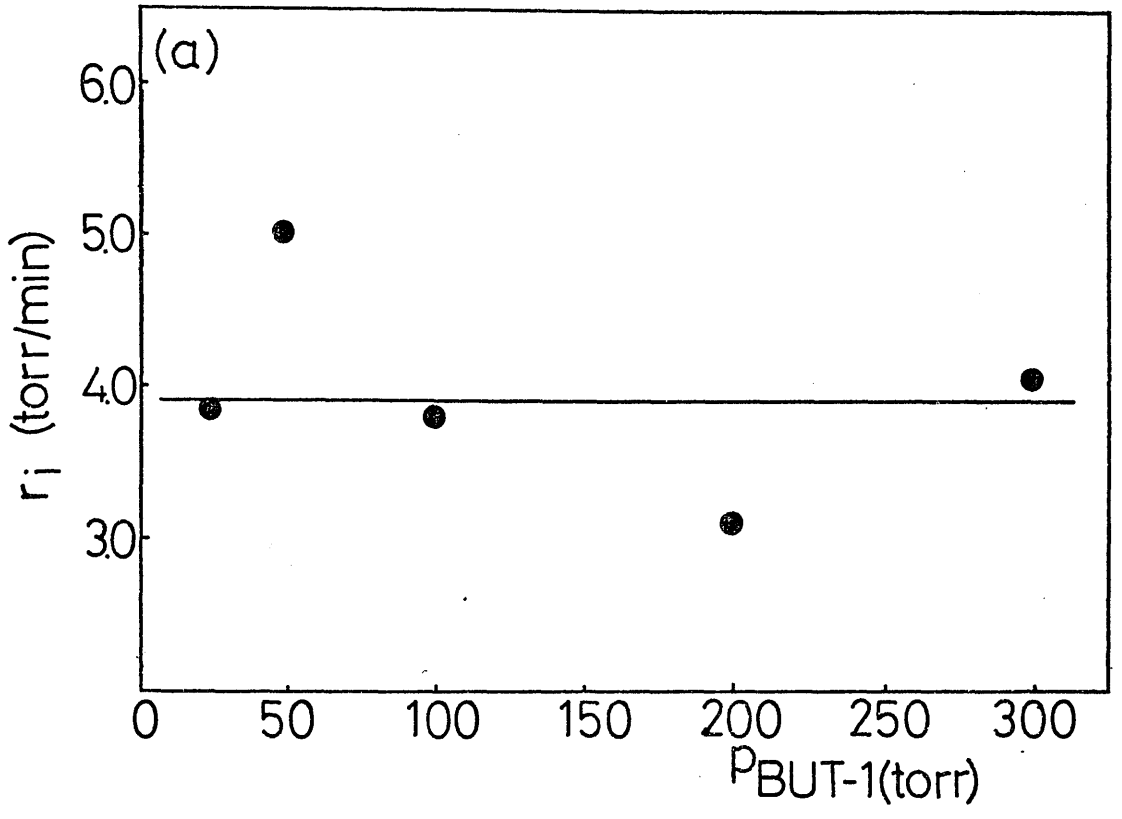

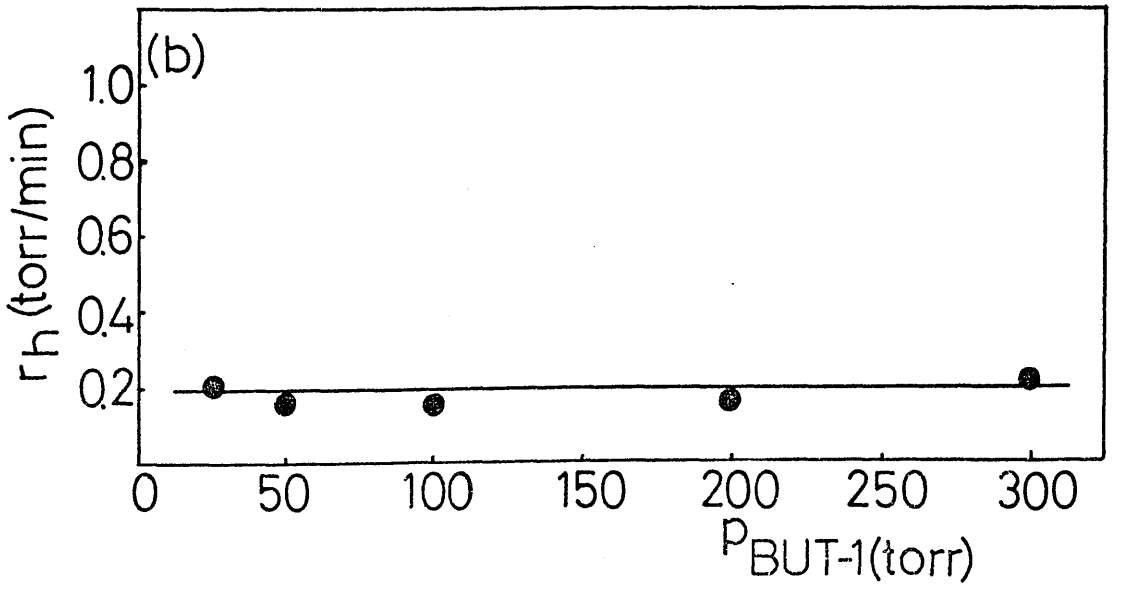

and also in the temperature range 18-80^{o}C.

A series of reactions were carried out at 48^{o}C to varying conversions over this sample of catalyst. The analysis figures for the variation of hydrocarbon composition are given in table 7.7 along with the extraction times(tex.). The variation of butene distribution is shown as a function of percentage conversion in Figure 7.7. A typical pressure-fall against time curve for the hydrogenation of but-1-ene in this series of reactions is plotted in Figure 7.8.

Whereas, in the case of the catalyst discussed in the previous section, the rate of hydrogenation was quite constant from reaction to reaction, the activity of the catalyst in this series of reactions was extremely variable and dependent on the pretreatment of the catalyst before each reaction was carried out.

A more detailed examination of how the intial rate of hydrogenation was affected by the variation of catalyst pretreatment was carried out using a further fresh sample of $Rh_2Co_2(CO)_{12}/SiO_2$ (20 mg). Initial activation at 93^{o}C for 2 hours resulted in the complex still being inactive. Prolonged activation at 115^{o}C rendered the supported complex active for hydrogenation and isomerisation. A series of reactions were carried out over this active species of the complex at 70^{o}C. As before, the reactions were carried out to varying conversions. The variation of hydrocarbon products, together with the extraction time is given in table 7.8. The variation of butene composition with percentage conversion is shown in Figure 7.9.

Figure 7.10 illustrates the considerable variation of the initial rate of hydrogenation, measured over the first 30 minutes, in this series

TABLE 7.7

Variation of Hydrocarbon Distribution with Conversion at 48°C on $Rh_2Co_2(CO)_{12}/SiO_2$

Initial $P_{H_2} = P_{But-1} = 100 \pm 0.5$ torr

Catalyst weight = 13mg

	% Hydrocarbon composition				
Reaction	n-BUT	BUT-1	t-B-2	C-B-2	tex(min)
C/5	4.0	80.4	8.3	7.3	20
C/10	5.1	62.8	17.2	14.8	90
C/8	12.0	49.1	22.2	16.7	50
C/3	17.4	40.6	23.2	18.7	50
C/9	31.2	22.6	29.6	16.5	80
C/2	42.1	27.9	18.6	11.4	30
C/7	59.2	16.8	16.8	7.2	80
C/1	65.0	14.9	13.0	7.1	50
C/11	80.0	13.7	3.9	2.4	235
* C/12	87.2	12.8	-	-	120
C/6	97.2	2.8	-	-	∞

* last reaction carried out after activation to 115°C

Figure 7.7 Variation of butene composition with percentage hydrogenation at 48°C (● = but-1-ene ; o = trans-but-2-ene ; ◐ = cis-but-2-ene).

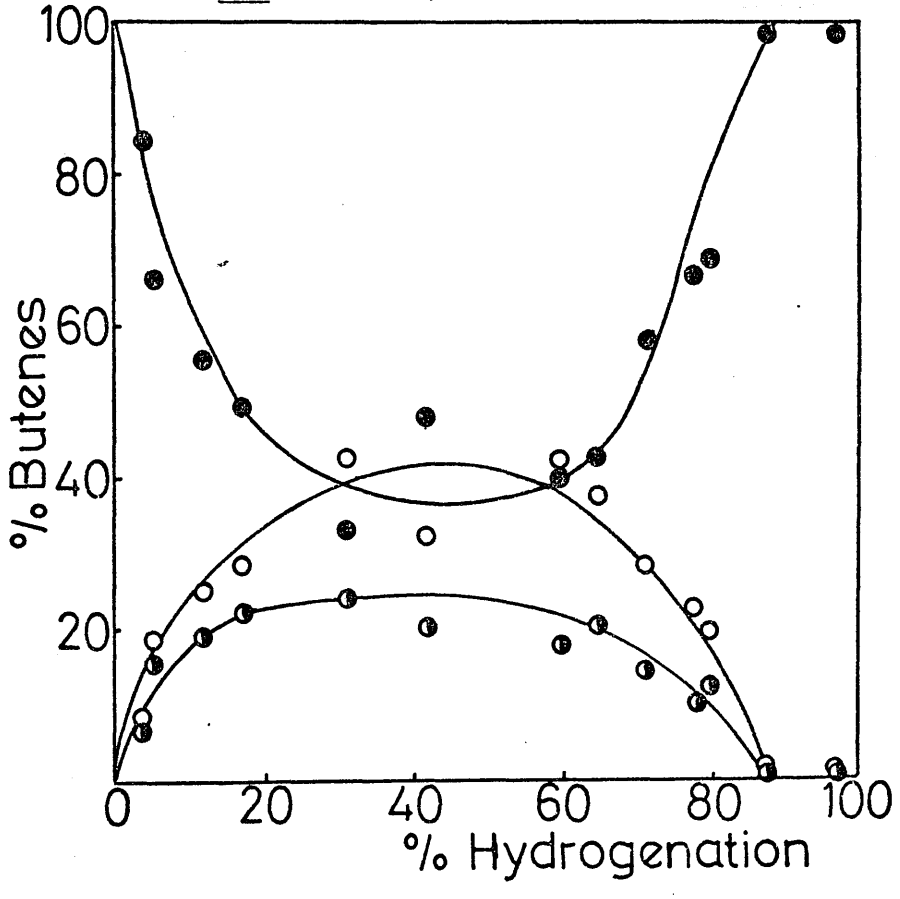

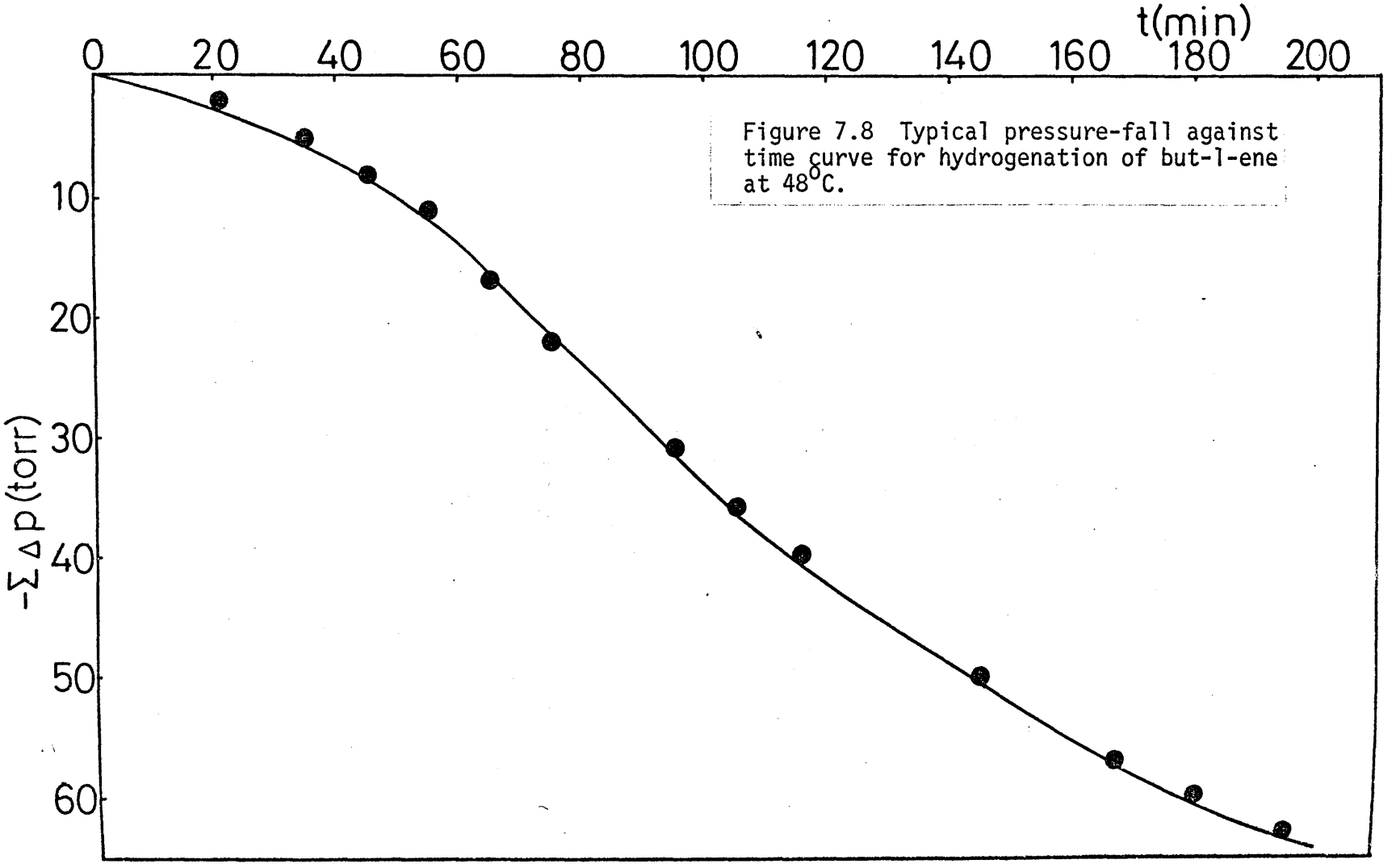

Figure 7.8 Typical pressure-fall against time curve for hydrogenation of but-1-ene at 48°C.

TABLE 7.8

Variation of Hydrocarbon Distribution with Conversion at 70°C on $Rh_2Co_2(CO)_{12}/SiO_2$ (activated initially at 115°C).

Initial $p_{H_2} = p_{BUT-1} = 100 \pm 0.5$ torr

Catalyst weight = 20mg

	% hydrocarbon composition				
Reaction	n-BUT	BUT-1	t-B-2	c-B-2	tex(min).
D/3	5.0	70.9	13.8	10.3	10
D/4	14.8	36.1	35.7	13.4	30
D/8	23.7	22.7	42.2	11.4	65
D/2	28.3	22.6	34.7	14.4	35
D/5	29.4	19.9	37.6	13.1	65
D/16	33.4	15.6	37.1	13.9	120
D/15	39.2	16.6	32.6	11.6	40
D/7	40.3	15.8	32.0	11.9	90
D/6	49.1	15.7	25.8	9.4	65
D/10	64.1	12.7	15.7	7.5	65
D/11	71.8	12.3	11.8	4.1	125
D/1	81.1	12.3	4.9	1.7	125

Figure 7.9 Variation of butene composition with percentage hydrogenation at 70°C (● = but-1-ene ; o = trans-but-2-ene ; ◑ = cis-but-2-ene).

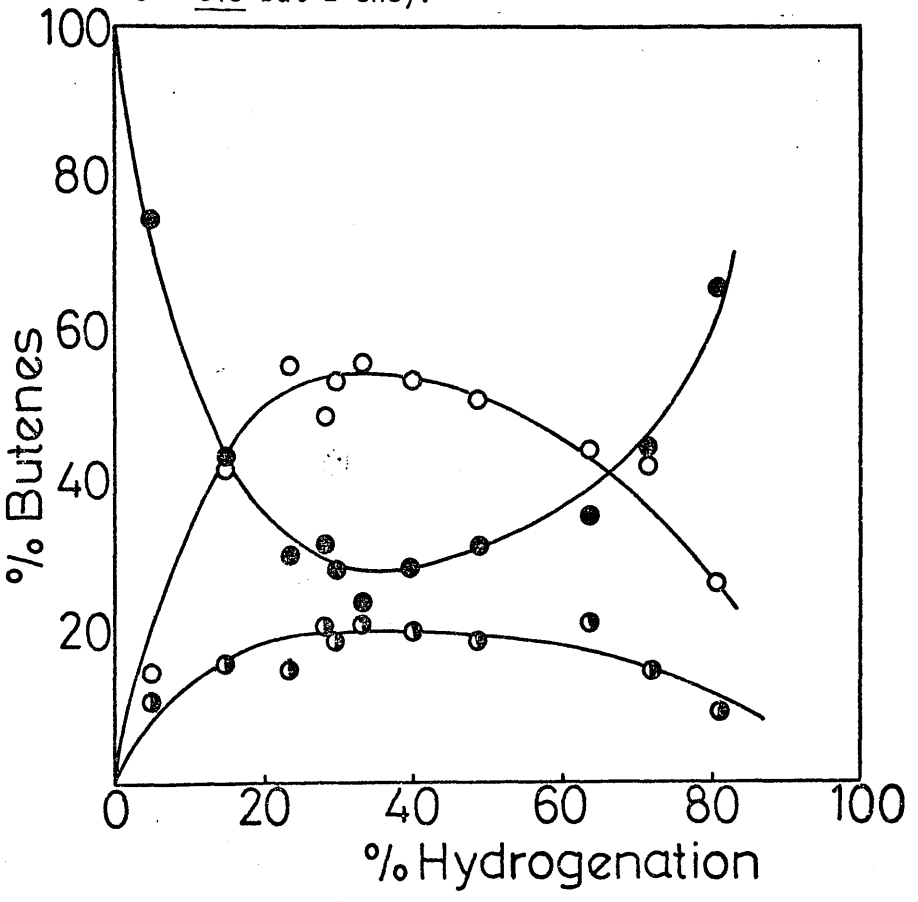

7.10 Variation of initial rate of hydrogenation with reaction number for series of reactions in Figure 7.9.

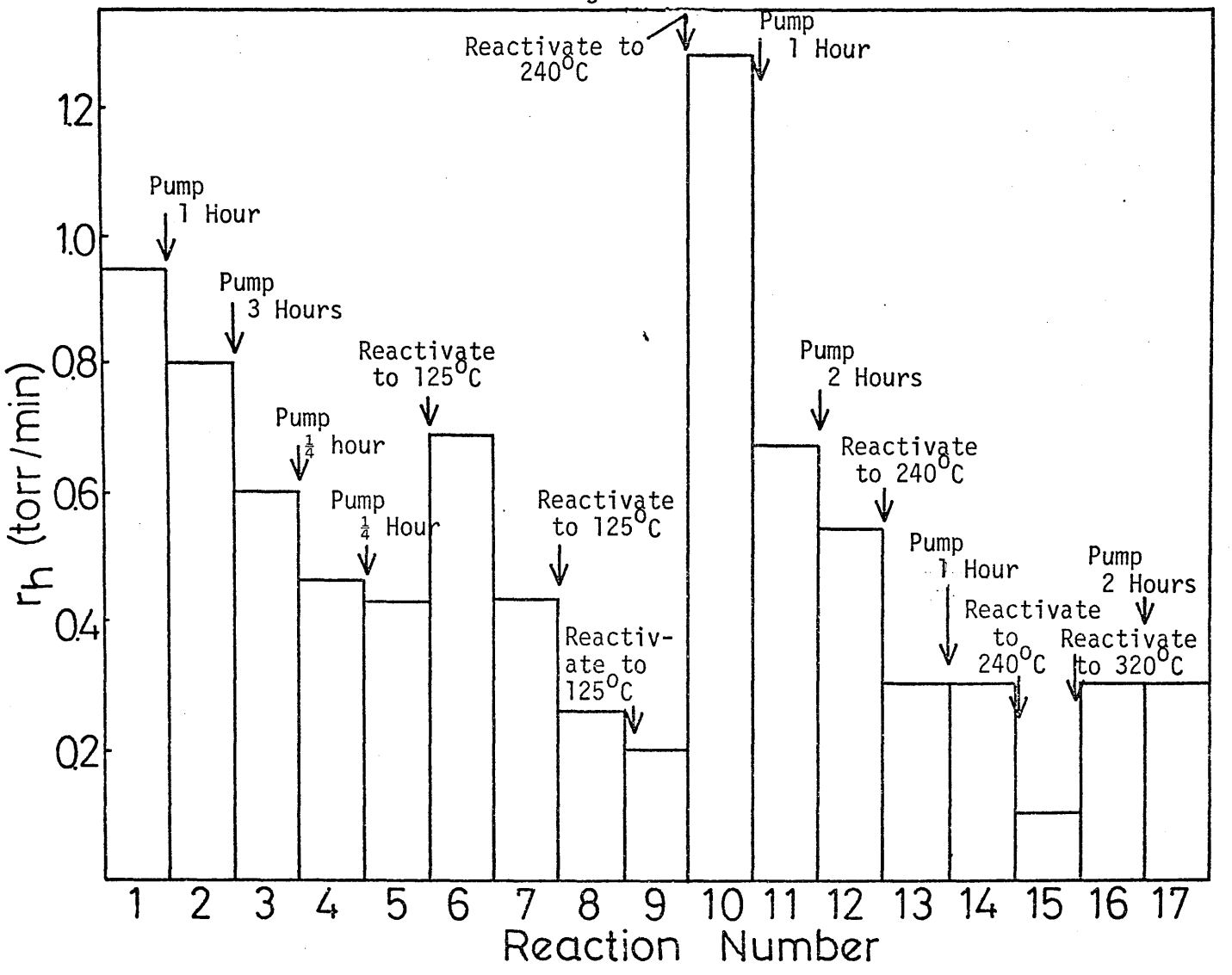

of reactions. The activity of the catalyst appears to be regenerated by reheating it to its former activation temperature, although the efficiency of this process decreases with time. Subsequent reactivation at a higher temperature results in the activity of the catalyst being increased accordingly. Pumping continuously on the catalyst between reactions appears to regenerate a certain amount of activity, although this is very inconsistent.

7.2.4 Reactions of But-1-ene with Deuterium

The reaction of but-1-ene with deuterium was examined over a sample of $Rh_2Co_2(CO)_{12}/SiO_2$ which had been activated *in vacuo* to 115°C for 24 hours. Preliminary reactions carried out over the catalyst showed that the rate was fairly constant from one reaction to the next at 115°C. The effect of percentage conversion upon deuterium incorporation in the products of reaction was examined at this temperature. The products of reaction were extracted at three different conversions, and separated for mass spectrometric analysis. The butene distribution together with percentage hydrogenation and extraction times are given in table 7.9.

A further two reactions, which were carried out to a similar conversion as reaction D/1, but at different temperatures, allowed the effect of temperature on butene exchange to be examined. The data on butene distribution obtained from these analyses are given in table 7.10.

The mass spectrometric analysis figures for the separated products of reaction are shown in tables 7.11 and 7.12.

TABLE 7.9

Variation of Butene Distribution with Conversion in the Reaction of But-1-ene with Deuterium

Initial p_{D_2} = p_{BUT-1} = 100 ± 0.5 torr

Temperature = 115°C Catalyst Weight = 20mg

		% butene distribution			
Reaction	%n-BUT	BUT-1	t-B-2	c-B-2	tex(min)
D/1	10.4	57.1	27.2	15.7	6
D/3	37.5	20.2	54.3	25.5	18
D/2	65.1	27.3	51.0	21.7	40

TABLE 7.10

Variation of Butene Distribution with temperature in the Reaction of But-1-ene with Deuterium

Initial p_{D_2} = p_{BUT-1} = 100 ± 0.5 torr

Catalyst Weight = 20 mg

Reaction	Temp(°C)	%n-BUT	BUT-1	t-B-2	c-B-2	tex(min)
E/2	50	9.9	64.2	20.7	15.1	300
E/1	70	10.0	55.8	29.5	14.7	43
D/1	115	10.4	57.1	27.2	15.7	6

TABLE 7.11

Distribution of Deuterated Hydrocarbons for the Reaction of But-1-ene and Deuterium over 2% $Rh_2Co_2(CO)_{12}$/Aerosil silica at 115°C (Activation 115°C).

Reaction D/1	10.4% conversion							
	d_0	d_1	d_2	d_3	d_4	d_5	d_6	D N.
butane	33.1	23.1	25.4	10.0	4.6	2.7	1.1	1.42
but-1-ene	86.5	11.0	2.5	-	-	-	-	0.16
t-but-2	58.9	23.7	11.1	3.9	1.9	0.5	-	0.68
c-but-2	62.6	22.5	9.8	3.4	1.4	0.3	-	0.60
Reaction D/3	**37.5% conversion**							
butane	26.4	26.4	23.8	13.2	7.1	3.1	-	1.57
but-1-ene	84.1	8.4	5.6	1.9	-	-	-	0.25
t-but-2	31.5	27.5	19.7	12.7	6.1	2.5	-	1.42
c-but-2	32.0	28.5	21.5	11.0	5.3	1.7	-	1.34

Continued..

TABLE 7.11 continued

Reaction

D/2 65.1% conversion

	d_o	d_1	d_2	d_3	d_4	d_5	d_6	D N.
butane	23.5	27.2	25.4	14.9	7.5	1.5	-	1.60
but-1-ene	79.0	7.3	7.3	4.6	1.8	-	-	0.42
t-but-2	17.3	28.3	28.3	18.6	6.3	1.2	-	1.77
c-but-2	18.7	24.3	27.4	18.1	8.3	2.8	.4	1.83

TABLE 7.12

Distribution of Deuterated Hydrocarbons for the Reaction of But-1-ene and Deuterium over 2% $Rh_2Co_2(CO)_{12}$/Aerosil silica (activation 115°C) at Various Temperatures to 10% Conversion

Reaction D/1 At 115°C	d_0	d_1	d_2	d_3	d_4	d_5	d_6	D N
butane	33.1	23.1	25.4	10.0	4.6	2.7	1.1	1.42
but-1-ene	86.5	11.0	2.5	-	-	-	-	0.16
t-but-2	58.9	23.7	11.1	3.9	1.9	0.5	-	0.68
c-but-2	62.6	22.5	9.8	3.4	1.4	0.3	-	0.60
Reaction E/1 At 70°C								
butane	32.1	25.0	28.1	8.5	3.6	2.7	-	1.35
but-1-ene	83.8	14.7	1.5	-	-	-	-	0.18
t-but-2	74.2	18.5	4.9	1.6	0.8	-	-	0.36
c-but-2	75.9	17.7	4.3	1.4	0.7	-	-	0.33

Continued..

TABLE 7.12 continued

Reaction E/2 At 50°C	d_o	d_1	d_2	d_3	d_4	d_5	d_6	D N
butane	31.4	20.8	34.0	7.5	3.8	2.5	-	1.39
but-1-ene	90.3	9.2	.5	-	-	-	-	0.10
t-but-2	86.3	11.6	2.1	-	-	-	-	0.16
c-but-2	87.2	10.8	2.0	-	-	-	-	0.15

7.2.5 The Reaction of Cis-But-2-ene with Hydrogen over 2% $Rh_2Co_2(CO)_{12}/SiO_2$

A series of reactions were carried out at 50°C to compare Cis-but-2-ene hydrogenation with but-1-ene hydrogenation over a fresh catalyst sample activated to 115°C. The reactions were stopped at varying conversions and extracted for analysis. The analysis figures for hydrocarbon composition and extraction times at various conversion are presented in table 7.13. Figure 7.11 illustrates the plot of variation of butene distribution with percentage conversion.

In a series of reactions to compare the rates of hydrogenation of but-1-ene, cis-but-2-ene and trans-but-2-ene, it was found that they were virtually the same.

The competitive hydrogenation of a mixture of but-1-ene and cis-but-2-ene was studied in a series of reactions carried out at 70°C. The hydrocarbon compositions, together with extraction times are presented in table 7.14, whilst Figure 7.12 shows graphically the variation of butene composition with hydrogenation.

7.2.6 The Effect of Hydrogen Treatment on a "Poisoned" Sample of 2% $Rh_2Co_2(CO)_{12}/SiO_2$.

The effect of hydrogen upon a sample of catalyst, which had become poisoned as a result of extensive use in the reaction of hydrogen and but-1-ene, was examined. Prolonged treatment with hydrogen (100 torr) at 115°C had the effect of cleaning the surface, since the rate of but-1-ene hydrogenation over the treated surface suggested that the activity of the catalyst compared with that of the

TABLE 7.13

Variation of Hydrocarbon Distribution with Conversion of Reaction of cis-But-2-ene with Hydrogen over $Rh_2Co_2(CO)_{12}/SiO_2$

Initial $p_{H_2} = p_{c\text{-}B\text{-}2} = 100 \pm 0.5$ torr

Catalyst weight = 20mg

	% hydrocarbon composition				
Reaction	n-BUT	BUT-1	t-B-2	c-B-2	tex(min)
F/5	3.3	2.5	18.7	75.5	5
F/1	10.5	2.6	34.7	52.2	10
F/3	18.0	2.7	41.5	37.8	22
F/2	37.9	1.5	30.8	29.8	40
F/6	45.9	1.2	28.8	24.1	65
F/4	71.9	0.8	9.5	17.8	100

TABLE 7.14

Variation of Hydrocarbon Distribution with Conversion of Reaction of 1:1 Mixture of Cis-But-2-ene and But-1-ene with Hydrogen.

Initial $p_{c\text{-}B\text{-}2} = p_{BUT\text{-}1} = 50 \pm 0.5$ torr; $p_{H_2} = 100 \pm 0.5$ torr

Catalyst weight = 20mg

% hydrocarbon composition

Reaction	n-BUT	BUT-1	t-B-2	c-B-2	tex(min)
G/3	1.3	47.7	4.0	47.0	2
G/5	5.8	30.5	18.3	45.4	10
G/1	11.4	20.6	29.2	38.8	15
G/7	26.4	11.1	37.7	24.8	42
G/6	38.2	11.3	31.7	18.8	60
G/2	53.3	9.3	20.8	16.6	85
G/4	64.0	9.1	14.8	12.1	120

7.11 Variation of butene composition with percentage hydrogenation of cis-but-2-ene at 50°C (● = but-1-ene ; o = trans-but-2-ene; ◐ = cis-but-2-ene).

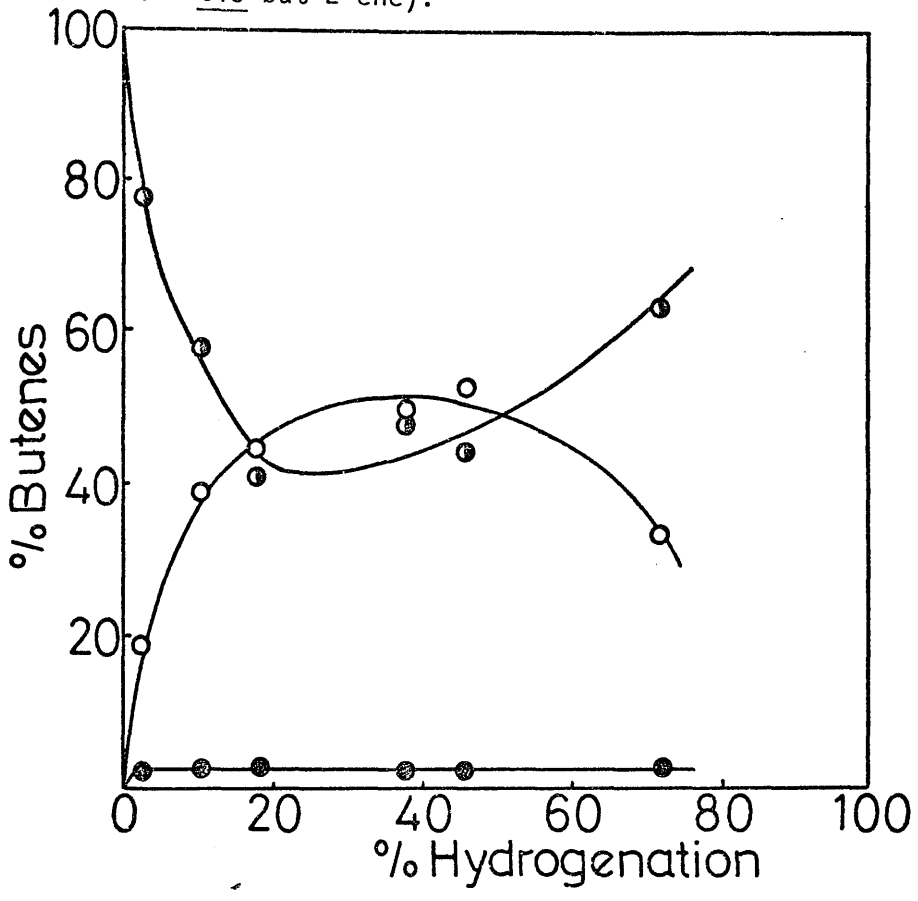

Figure 7.12 Variation of butene composition with percentage conversion for the competitive hydrogenation of but-1-ene and cis-but-2-ene. (● = but-1-ene ; o = trans-but-2-ene ; ◐ = cis-but-2-ene).

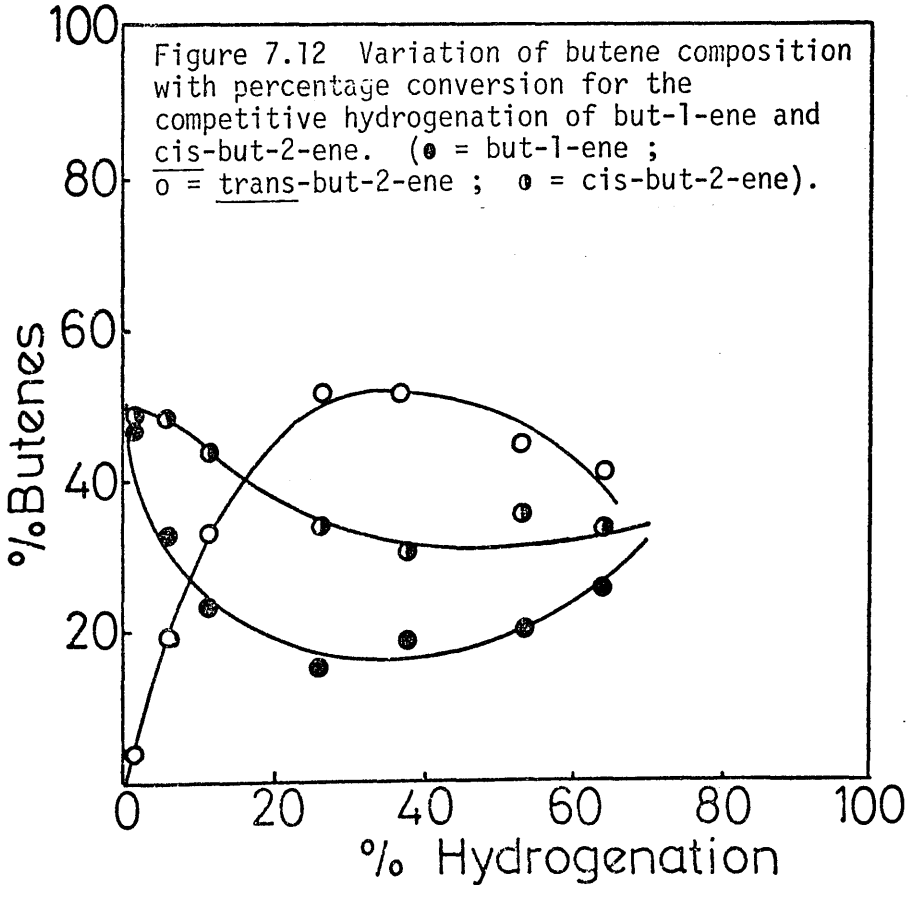

initially activated fresh catalyst.

A series of reactions were carried out at 50°C over the hydrogen treated catalyst to determine how the variation in product composition for but-1-ene hydrogenation compares with the reaction carried out over a fresh sample of catalyst. The results of this series are shown in table 7.15, whilst Figure 7.13 shows the variation of butene distribution with hydrogenation.

7.2.7 The Effect of Oxygen on the Catalyst

When the reaction of but-1-ene with hydrogen was carried out over the catalyst (activated to 120°C), after it had been exposed to air over a prolonged period, it was found that there was an induction period of 55 minutes in the first reaction, but thereafter no induction period existed. The catalyst was observed to be active in the temperature range 30 - 120°C. Subsequent re-exposure of the catalyst to air over a period of several days did not result in the induction period being re-introduced in the first reaction.

A second sample of catalyst, which had not been exposed to air did not have an initial induction period, whilst on exposure to air for several weeks after a few reactions, subsequent reactions appeared to be even faster than before exposure. Again, there was no observation of an induction period in the first reaction succeeding exposure to air.

TABLE 7.15

Variation of Product Composition with Conversion of Reaction of But-1-ene with Hydrogen over Regenerated Surface

Initial $p_{H_2} = p_{BUT-1} = 100 \pm 0.5$ torr

Temperature = 50°C Catalyst Weight = 20 mg

	% Hydrocarbon Composition				
Reaction	n-BUT	BUT-1	t-B-2	c-B-2	tex (min)
G/3	4.9	81.1	8.5	5.5	4
G/4	18.4	24.5	39.5	17.6	30
G/1	38.3	20.0	30.9	10.8	23
G/5	48.9	22.3	21.0	7.8	80
G/2	70.3	15.5	10.0	4.2	65

Figure 7.13 Variation of butene composition with percentage hydrogenation at 50°C over hydrogen treated catalyst.
(● = but-1-ene ; o = trans-but-2-ene ; ◑ = cis-but-2-ene).

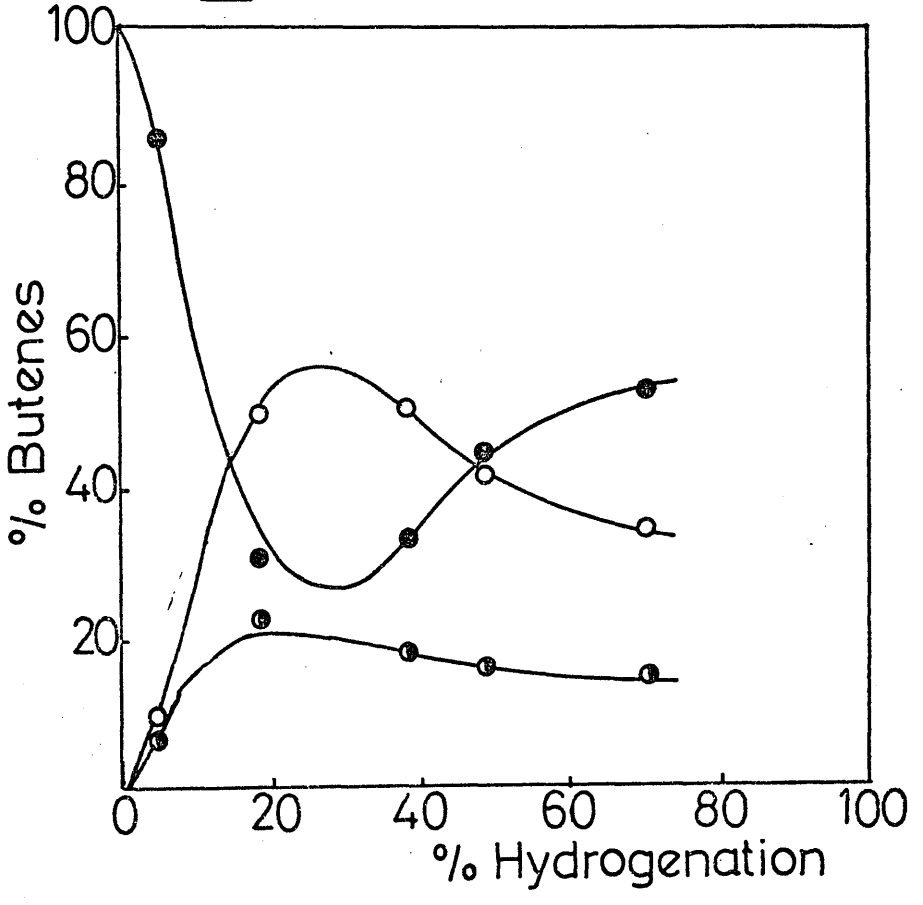

DISCUSSION SECTION

CHAPTER 8

REACTIONS OVER SILICA SUPPORTED TRIOSMIUM DODECACARBONYL

8.1 The Nature of the Supported Complex

8.1.1 Physical Properties

The structure of triosmium dodecacarbonyl is well established (109). As in the case of its ruthenium analogue, the complex consists of a metal triad, with each metal atom being bonded to four terminal carbonyl ligands. The corresponding iron complex has a similar structure, but with two bridging carbonyls between one pair of the iron atoms. Comparisons between the chemical stabilities of the three complexes have shown the iron complex to be extremely unstable, whilst the triruthenium complex is more resistant to metal-metal bond cleavage. The osmium complex is found to be the most stable cluster of the three.

A study of triosmium dodecacarbonyl by infra-red spectroscopy shows that when dissolved in methylene dichloride the complex gives rise to $\bar{\nu}$(CO) adsorptions at around 2075, 2040, 2020 and 2000 cm^{-1}. Supporting the complex on silica results in a similar spectrum in the carbonyl stretching region, with the exception of an additional weak band at 2126 cm^{-1}. This would seem to indicate that the complex undergoes little or no net change on contact with the support. Examination of the physical characteristics of the supported complex substantiates this conclusion, since the complex undergoes no colour

change when supported, but retains its pale yellow colour. Thus it appears that the silica has no chemical interaction with the complex. Similarly, exposure to air appears to have no effect upon infra-red or physical characteristics of the supported complex.

Activation of the supported complex in vacuo by heat treatment is accompanied by several colour changes, as well as variations in the infra-red spectrum, which indicate a change in the chemical structure of the complex. The initial increase in the number of carbonyl stretching bands suggests a decrease in the symmetry of the complex. The subsequent gradual decrease in the number and size of carbonyl stretching modes is evidence for the gradual loss of carbon monoxide.

There are a number of chemical changes which may occur, one or more of which may be responsible for the observed changes in colour and spectrum. These include:-

(1) The loss of one or more carbonyl ligand.

(2) The decomposition of the osmium triad.

(3) The oxidation of osmium.

(4) The substitution of the carbonyl ligands by other ligands.

Examination of a 10% W/W sample of supported complex by T.V.A. in conjunction with T.G.A. is further evidence for the loss of CO during activation. Both of these techniques are indicative of carbon monoxide being lost in a three-step process. Thus, sub-carbonyl forms of supported $Os_3(CO)_{12}$ are being formed of structure $Os_3(CO)_{12-x}$ when the complex is heated to a given temperature T^oC. T.G.A. suggests that the three steps involve the loss of 3, 4 and 5

carbonyl ligands respectively, and consequently the stable species formed on silica would be $Os_3(CO)_9$ and $Os_3(CO)_5$, in addition to an osmium network which would exist on the loss of all carbonyl groups. Whether this consists of separate osmium triads, that is osmium atomically dispersed, or as an aggregation of osmium atoms cannot be established from the present studies.

Electron microscopic examination of the supported complex after activation to 250°C showed the widespread distribution of particles in the region of 10Å although there is the possibility that smaller particles approaching molecular size, which would be undetected by this form of examination, do exist. A similar examination of the supported complex after the loss of all carbonyl ligands shows the appearance of slightly larger aggregates, which would suggest that activation to a higher temperature can induce a small degree of sintering. From this evidence it may be concluded that the catalyst particles used in the reactions are extremely small and approaching molecular size.

8.1.2 The Catalytically Active Forms of the Supported Complex.

(a) 2% $Os_3(CO)_{12}/SiO_2$ activated to 250°C.

Before attempting to deduce the structure of the supported complex formed following activation to 250°C, the relevance and relative importance of the following points must be considered:-

1) The supported complex in this state has lost three carbonyl groups.

2) Due to the stability of the metal-metal bonds in the complex, it is likely that on activation of the supported

complex to 250°C the osmium triad is retained. This conclusion is in agreement with the mass spectrometric analysis of $Os_3(CO)_{12}$, (137, 138) which shows that the fragmentation of the osmium triad is an unfavoured process compared with metal-carbonyl bond fragmentation.

3) Heat treatment must lead to the support having some kind of destabilising effect on the complex, since it has been reported (111) that heating the unsupported complex in inert conditions results in sublimation without degradation taking place. The destabilising effect probably takes the form of a direct chemical interaction between the complex and the silica, with possibly the support acting as a ligand through an -O-Si-group.

4) The observation of a band at 1965cm^{-1} for the supported complex in this state may indicate the presence of one or more hydride ligands, where the surface hydroxyl groups on the silica act as a source of hydrogen.

(b) 2% $Os_3(CO)_{12}/SiO_2$ activated to 340°C

The structure of the supported complex after activation to 340°C is uncertain. It is known that prolonged activation at this temperature results in the complete loss of carbon monoxide from the complex, but whether the osmium triad is retained at this point is unclear. Certainly electron microscopic examination indicates that the "particles" on the support are still extremely small, but the small increase in particle size which is observed at this temperature tends to suggest that a decomposition of the stable triad is beginning to occur, with a corresponding build up of osmium aggregates, which may or may not be chemically bound to the support.

8.2 Reactions of But-1-ene with Hydrogen over Silica Supported Triosmium Dodecacarbonyl (Activated to 250°C)

The generally accepted mechanism for the hydrogenation of but-1-ene over supported Group VIII metal catalysts involves the initial addition of a hydrogen atom to an adsorbed but-1-ene molecule to form a "half-hydrogenated" butyl radical which is adsorbed on the surface. This species may be formed by:-

(a) A Langmuir-Hinshelwood mechanism, which requires the adsorption of both hydrogen as dissociatively adsorbed hydrogen atoms and but-1-ene before reaction may occur.

(b) A Rideal-Eley mechanism, which involves the formation of the butyl radical from the reaction of an adsorbed butene molecule with molecular hydrogen.

In the present catalytic system the observed kinetics $r_h = kp_{H_2}^{0.5} p_{BUT-1}^{0.85}$ suggest the relatively weak adsorption of both hydrogen and but-1-ene, consistent with a Langmuir-Hinshelwood mechanism. The following type of reaction scheme may be envisaged:-

$$C_4H_8\ (g) \rightleftharpoons C_4H_8\ (a) \qquad (1, -1)$$

$$H_2\ (g) \rightleftharpoons 2H\ (a) \qquad (2, -2)$$

$$C_4H_8\ (a) + H\ (a) \rightleftharpoons C_4H_9\ (a) \qquad (3, -3)$$

$$C_4H_9\ (a) + H\ (a) \longrightarrow C_4H_{10}\ (g) \qquad (4)$$

Assuming competitive adsorption of but-1-ene and hydrogen, the surface coverage, Θ, of both the reactants may be approximated by the Langmuir adsorption isotherms to be:-

$$\Theta_{C_4 H_8} = \frac{b_B p_B}{(1 + b_B p_B + b_{H_2}^{0.5} p_{H_2}^{0.5})}$$

$$\Theta_H = \frac{b_{H_2}^{0.5} p_{H_2}^{0.5}}{(1 + b_B p_B + b_{H_2}^{0.5} p_{H_2}^{0.5})}$$

where B = C_4H_8, b = the adsorption coefficient k_a/k_d and p = the pressure of the given reactant gas in equilibrium with the surface. Assuming that $1 >> (b_B p_B + b_{H_2}^{0.5} p_{H_2}^{0.5})$, which is reasonable since both reactants are relatively weakly adsorbed, these equations may be simplified to:-

$$\Theta_{C_4 H_8} \propto b_B p_B \text{ and } \Theta_H \propto b_{H_2}^{0.5} p_{H_2}^{0.5}$$

If the addition of a dissociatively adsorbed hydrogen to an adsorbed butene molecule (step 3) is the rate determining step, the rate equation may be written as:-

$$\text{rate} = k_3 \Theta_{C_4 H_8} \Theta_H$$

which by substitution of the Langmuir approximations becomes:-

$$\text{rate} = k_3 b_B b_{H_2}^{0.5} p_B^{1.0} p_{H_2}^{0.5},$$

in close agreement with the observed kinetics.

Two possible reaction schemes must be considered in attempting to elucidate the mechanism whereby isomerisation of but-1-ene occurs:-

(a) An addition - abstraction mechanism involving the formation of a 2-butyl intermediate.

(a) continued

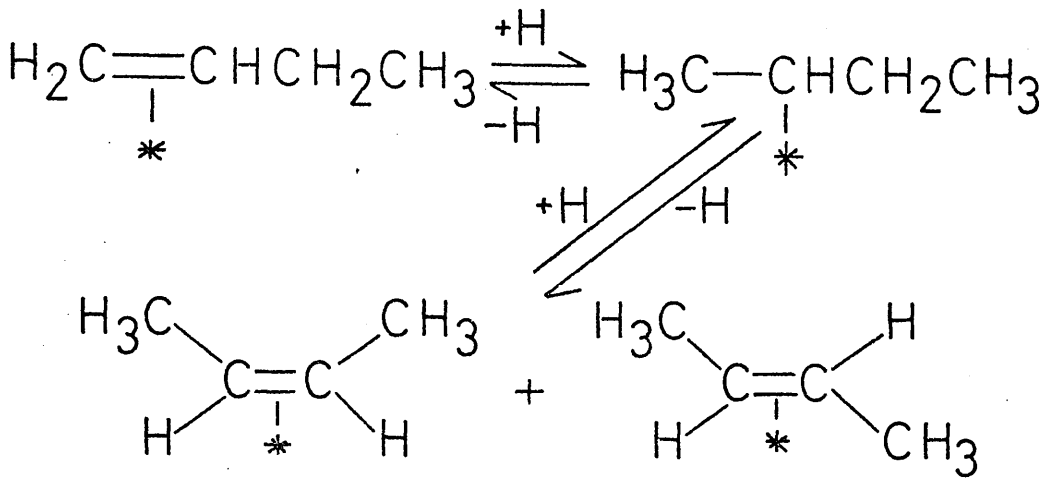

(b) An abstraction - addition mechanism, which requires the formation of a 1-methyl-Π-allyl intermediate and presents the possibility of either inter - or intra-molecular hydrogen transfer.

Since the mechanism proposed for the hydrogenation of but-1-ene requires the formation of a half-hydrogenated butyl intermediate, it is possible that alkyl reversal (step-3) may be responsible for double-bond migration. The observed kinetics for isomerisation show that the reaction has an order of unity with respect to but-1-ene pressure and zero with respect to hydrogen pressure. By inspection of the Langmuir isotherm for the adsorption of but-1-ene, it may be seen that in order to fulfil this requirement, the surface coverage of but-1-ene, Θ_{BUT-1}, must be very small, as $b_B\ p_B << 1$. A steady state treatment shows that

$$\Theta_{C_4\ H_9} = \frac{k_3\ \Theta_{C_4\ H_8}\ \Theta_H}{k_4\ \Theta_H + k_{-3}} \quad ,$$

therefore since the rate determining step for isomerisation is

independent of hydrogen pressure, it follows that for the alkyl reversal scheme to be valid, alkene desorption must be the rate-limiting step for isomerisation. Since from the hydrogenation mechanism, $\Theta_H \propto p_{H_2}^{0.5}$, any other rate-determining step would suggest an order of 0.5 or unity with respect to hydrogen pressure. It is possible that step-3 is limiting, but only on condition that $k_{-3} \ll k_4 \Theta_H$ which is extremely unlikely since a comparison of rates clearly shows that isomerisation is far faster then hydrogenation.

The observed kinetics would appear to be more compatible with an abstraction-addition reaction scheme, where double-bond migration could occur by:-

(1) Intermolecular hydrogen transfer, involving the formation of an adsorbed 1-methyl-Π-allyl intermediate (6, 18) in two conformations (I) and (II), which give rise, respectively to cis- and trans- but-2-ene.

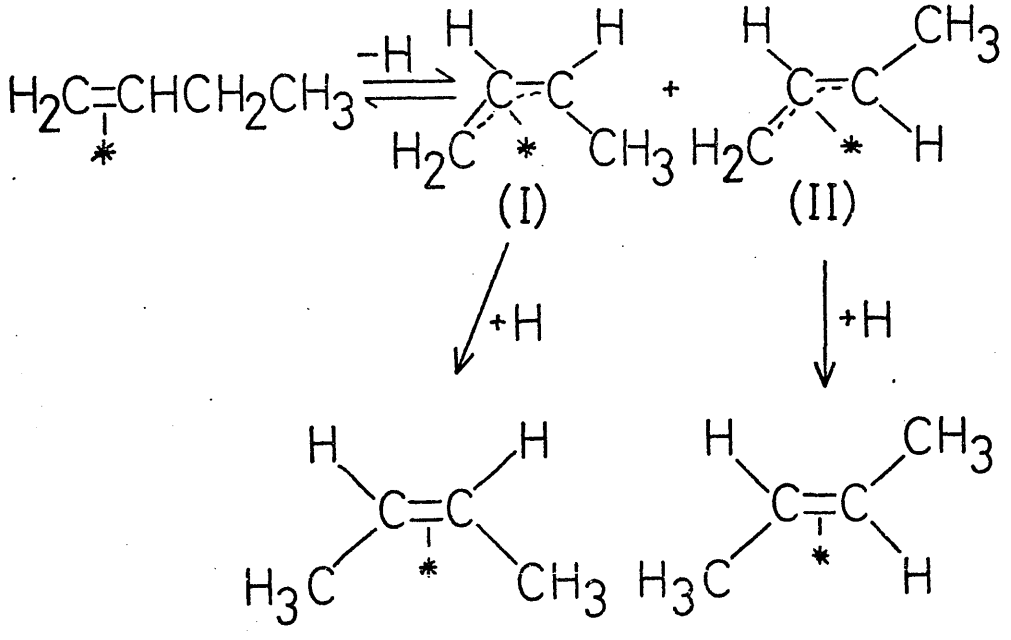

(2) Intramolecular hydrogen transfer, in which a symmetrical intermediate involving a bridged hydrogen between the α and γ-carbon atoms, is formed (22).

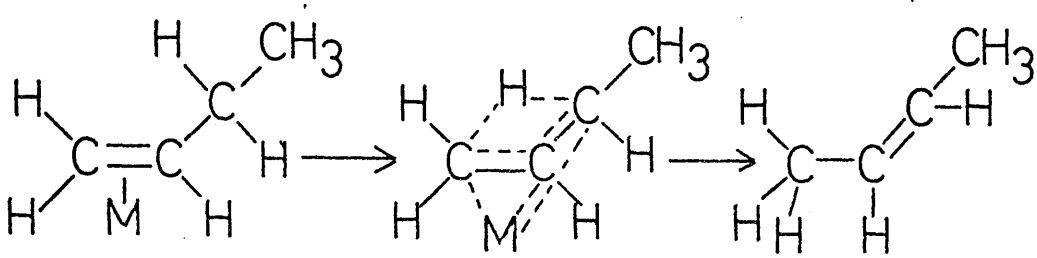

If the rate-determining step for such a mechanism is the rupture of a carbon-hydrogen bond to form C_4H_7, the rate expression can be written as

$$\text{rate} = k\Theta_{C_4H_8}$$

which is independent of hydrogen coverage and hence in agreement with the observed kinetics.

An important consequence of postulating different mechanisms for hydrogenation and isomerisation is that these reactions should take place completely independently of each other. This was verified by examining the butene distribution as a function of percentage conversion to butane. At all temperatures examined, isomerisation was found to occur to thermodynamic proportions before 10% hydrogenation had taken place. This is a significant point in favour of different mechanisms being operative for each reaction.

If an abstraction-addition mechanism, involving hydrogen transfer is operative in isomerisation, reaction should take place in the absence of molecular hydrogen, whereas the presence of hydrogen

atoms is essential for an alkyl reversal mechanism to be operative. In support of the abstraction-addition mechanism it was observed that isomerisation took place very readily in the absence of molecular hydrogen, although the rate of isomerisation appeared to decrease noticeably after three or four reactions. This poisoning effect could be due to the formation of carbonaceous residues on the catalyst surface (136) leading to a decrease in the number of sites available for the formation of the 1-methyl-II-allyl intermediate.

The deuterium tracer results also provide further evidence that isomerisation proceeds by a hydrogen transfer mechanism. The high percentage of but-2-ene-d_0 species which is initially observed indicates that whatever process is taking place on the surface does so in the absence of reactant deuterium. If isomerisation were to proceed via a 2-butyl intermediate, it would be expected that every but-2-ene molecule contained at least one deuterium atom. The high percentage of product but-2-ene-d_0 is evidence that interconversion does not occur via this intermediate.

Since tracer studies are firm evidence against double-bond migration via the formation of an adsorbed 2-butyl radical, it is extremely improbable that olefin exchange proceeds by this intermediate. Assuming that the exchange reaction occurs via an adsorbed alkyl intermediate, the reaction must proceed via a 1-butyl species, which would lead to deuterium incorporation at the 2-position. This would allow the exchange reaction to occur without the need for a corresponding isomerisation. Such a proposal allows us to rationalise the amount of deuterium incorporation - albeit very small -

into the initially formed but-2-enes. Subsequent isomerisation of exchanged but-1-ene-d_1 by an abstraction-addition mechanism initially forms a 1-methyl-Π-allyl - d_1 species which, on addition of a hydrogen atom, forms a but-2-ene-d_1 molecule. The degree of deuterium incorporation into the product butenes by this mechanism is dependent upon the comparative rates of but-1-ene exchange and isomerisation.

There exists the possibility that exchange proceeds via the formation of a 1-methyl-Π-allyl intermediate. The addition of a deuterium atom to such a species would lead to the formation of an exchanged but-1-ene or a deutero-but-2-ene. The higher deuterium content in but-1-ene than in the but-2-enes which is initially observed would not be consistent with an abstraction-addition reaction scheme for exchange. Such a mechanism would lead to a higher deuterium content for the but-2-enes than for but-1-ene, since the former will have been in contact with the surface at least once, whilst a large proportion of the latter has never been adsorbed.

A comparison of the activation energies E_i and E_{oe} is further evidence that the olefin-exchange mechanism is independent of isomerisation. The postulated rate - determining step for isomerisation is the cleavage of a C - H bond in the abstraction step, therefore the same limiting step would clearly be required for the exchange process. However, since the activation energies differ by 32 kJ $mole^{-1}$, clearly different reaction pathways are operative.

The possibility that exchange occurs via a 1-butyl intermediate satisfies the initially observed butene deuterium distributions.

A feature of this mechanism is that one would expect the but-2-ene deuterium content to initially reflect the change in that of but-1-ene but at a slower rate. As the reaction proceeds, however, the deuterium content of the butenes will depend upon the comparative ease with which but-1-ene and the but-2-enes undergo exchange.

A comparison of the activation energies $E_{\underline{h}}$ and $E_{\underline{oe}}$ shows that $(E_{\underline{oe}} - E_{\underline{h}}) = 10 kJ\ mole^{-1}$. Now, assuming that olefin exchange proceeds via an alkyl reversal pathway, hydrogenation and exchange must have a different rate-determining step. It has been concluded on kinetic evidence that the rate-limiting step for hydrogenation is the formation of the adsorbed alkyl (probably 1-butyl) intermediate. It seems logical to expect that for olefin exchange the rate-limiting step is the loss of a "hydrogen" atom from the half-hydrogenated intermediate to form the exchanged but-1-ene. The other possibility, namely that butene desorption is rate-determining, is incompatible with the observed $E_{\underline{oe}} > E_{\underline{h}}$, since the rate of attainment of equilibrium with the surface for butene is greater than the rate of formation of a 1-butyl species. It must be concluded that C-H bond cleavage is the limiting step for exchange.

There exists the alternative possibility that olefin exchange takes place on completely separate adsorption sites from those operative in hydrogenation. It is quite feasible that but-1-ene exchange occurs via a vinylic dissociative adsorption mechanism as reported by Gault and co-workers (23, 24) involving the preferential formation of an adsorbed but-2-enyl species:

$$H_2C{=}CHCH_2CH_3 \xrightarrow{-H} H_2C{=}\underset{*}{C}CH_2CH_3 \xrightarrow{+D} H_2C{=}CDCH_2CH_3$$

The slow rates of exchange and hydrogenation of but-1-ene as compared with isomerisation are a clear indication that the 1-butyl species formed in both of the former reactions is an extremely stable adsorbed species. The tracer studies indicate that, as hydrogenation proceeds, the but-2-enes become much more exchanged than the reactant butene. It is clear, therefore, that the rate of exchange of the but-2-enes is greater than that of but-1-ene. Assuming that but-2-ene exchange occurs via a 2-butyl intermediate, and this is a reasonable assumption, it is clear that the 2-butyl intermediate is less stable than the 1-butyl species and hence will lose a "hydrogen" atom more readily to form the exchanged but-2-ene. By this reasoning, it might be expected that the addition of a "hydrogen" atom to the 2-butyl species to form butane would be more favourable than the corresponding step for but-1-ene hydrogenation.

In conclusion it is evident that isomerisation proceeds by a different mechanism from hydrogenation and olefin exchange. It is considered that the principal mechanism for the isomerisation of but-1-ene is via a 1-methyl-Π-allyl intermediate by inter - or intra - molecular hydrogen transfer, whilst hydrogenation and olefin-exchange occur via a 1-butyl intermediate. Whereas in hydrogenation the slow step is the addition of an adsorbed hydrogen atom to an adsorbed but-1-ene molecule, in olefin exchange the rate-limiting step is the loss of a hydrogen atom from the adsorbed 1-butyl intermediate.

8.3 Reactions of But-1-ene with Hydrogen over Silica Supported Triosmium Dodecacarbonyl (Activated to 340°C)

Activation of the supported complex to 340°C results in a change

in the observed kinetics for hydrogenation from $r_{\underline{h}} = kp_{H_2}^{0.5} p_{BUT-1}^{0.85}$ to $r_{\underline{h}} = kp_{H_2}^{1.0} p_{BUT-1}^{0.4}$. The kinetics are still consistent with a Langmuir-Hinshelwood mechanism, with a change in the rate-determining step from step (3) to step (4). From a comparison of these two rate equations it may be seen that whilst hydrogen is the more strongly adsorbed of the two reactants after activation to 250°C, the opposite is the case after activation to 340°C.

The change in the rate expression from

$$r_{\underline{i}} = kp_{H_2}^{0} p_{BUT-1}^{1.0} \text{ to } r_{\underline{i}} = kp_{H_2}^{0 \rightarrow -ve} p_{BUT-1}^{0.5}$$

which is observed for the isomerisation reaction immediately suggests that butene is more strongly adsorbed on the complex activated at the higher temperature. Assuming that isomerisation continues to proceed independently of hydrogenation, for which there is evidence from the kinetic expressions alone, then if an inter - or intramolecular mechanism is still operative, the negative order with respect to hydrogen at higher pressure may be explained qualitatively by considering that the effect of increasing hydrogen pressure is to decrease the number of surface sites available to accept the ejected hydrogen atom.

An examination of the variation of initial rate of hydrogenation with reaction number (figure 5.13) indicates that in general the catalyst's activity decreases with reaction number. Reheating of the supported complex to 340°C between reactions, however, has the effect of regenerating the activity of the catalyst to almost its former efficiency. Reactivation by this method is found to be of only limited efficiency and the overall trend illustrates catalyst deactivation to a residual level, at which point reheating fails to

regenerate further activity. It may be concluded that the effect of heating the catalyst to 340°C is to promote the loss of carbon monoxide ligands from the complex. This results in the exposure of further potential active sites for adsorption and thus the corresponding increase in catalyst activity. This would also explain why the process of thermal reactivation is of only limited effectiveness, since there is a limit to the number of carbon monoxide ligands which may be lost.

An examination of rates for the supported complex activated to the elevated temperature indicates that hydrogenation becomes much more favoured in comparison to isomerisation. This observation manifests itself in other experimental results. For example, the variation in butene distribution with conversion to butane indicates that hydrogenation has occurred to over 20% completion before isomerisation has proceeded to thermodynamic proportions. Similarly the initial incorporation of deuterium into the exchanged butenes is less than is found with the supported complex activated to the lower temperature. This is evidence that the initial rate of hydrogenation has become faster with respect to olefin exchange.

Deuterium tracer studies indicate that the overall deuterium distributions observed for the deutero-butenes are very similar to those observed after activation to 250°C. The principal features which are similar for both forms of the catalyst are:-

(a) A slightly higher deuterium content initially for exchanged but-1-ene than for the product but-2-enes.

(b) A high percentage of butene-d_0 initially observed for all three butenes.

(c) The product but-2-enes, once formed, undergo exchange more readily than but-1-ene.

The broad similarities which exist for the deutero-butenes obtained over the two forms of the catalyst suggest that basically the same mechanisms exist in each case. However, the actual differences observed quantitatively for deuterium incorporation into the butenes, together with a change in the kinetic rate expressions are evidence that there has been a change in the comparative rates for hydrogenation, isomerisation and olefin exchange.

8.4 Reactions of But-1-ene with Hydrogen over "Conventional" Silica Supported Osmium Catalyst

Due to the limited study which was carried out over this catalyst, the discussion of a mechanism is severely restricted. However a number of interesting points emerge by comparing this catalyst and the catalysts derived from the 2% W/W $Os_3(CO)_{12}/SiO_2$ complex. An examination of the pressure-fall against time curves at the two temperatures studied (figures 5.20, 5.21) shows that the initial rates of hydrogenation are similar, which suggests a small energy of activation for hydrogenation in this temperature range. This contrasts sharply with the results obtained over the supported complex activated to 250°C, where an activation energy of 38kJ $mole^{-1}$ was obtained over this range. The pressure-fall against time curves also indicate that hydrogenation at the higher temperature becomes self-poisoned as conversion proceeds, whilst the reaction remains first-order throughout at the lower temperature. This may be explained by considering that dissociative adsorption occurs more readily at 230°C, hence

blocking potential adsorption sites for reaction as reaction time increases. The observed first-order kinetics for hydrogenation are in agreement with those obtained for the hydrogenation of but-1-ene over supported metal catalysts (10, 11, 13) and in contrast to the observed kinetics over the two forms of catalyst derived from the supported $Os_3(CO)_{12}$ complex.

A comparison of rates of hydrogenation over the three catalysts indicates that values of similar magnitude exist for the "conventional" osmium catalyst and the catalyst resulting from activation to 320^{o}C, whilst in the third case a catalyst of lesser activity for hydrogenation is operative. The reason for this could be that, as the activation temperature for the supported complex is increased there is a corresponding loss of further carbonyl groups and the possibility of triad fragmentation. Thus the complex may become increasingly similar in physical appearance and properties to the "conventional" osmium catalyst, hence also attaining similar catalytic properties. Comparison of the variation in butenes with hydrogenation obtained in both cases (figures 5.22, 5.15) at 230^{o}C is further evidence for the similarity in catalytic properties.

CHAPTER 9

REACTIONS OVER SILICA SUPPORTED DIRHENIUM DECACARBONYL

9.1 The Nature of the Supported Complex

9.1.1 Physical Properties

The structure of $Re_2(CO)_{10}$ is established as being similar to that of $Mn_2(CO)_{10}$, and is shown below.

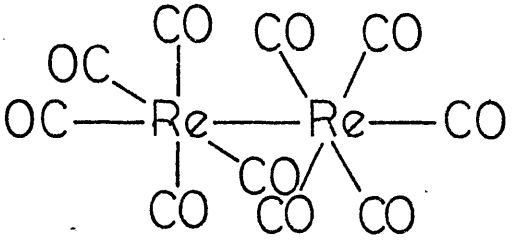

These dimers are held together by a metal-metal bond alone, without the presence of any bridging CO groups. As would be expected by direct comparison with the trends inherent in other transition metal groups, there is an increase in stability on going down the Group VII carbonyls and consequently whilst $Mn_2(CO)_{10}$ tends to oxidise slowly when exposed to air, $Re_2(CO)_{10}$ and $Te_2(CO)_{10}$ are extremely stable.

Mass spectrometric analysis of $Mn_2(CO)_{10}$ and $Re_2(CO)_{10}$ (142) shows that 96% of the ion fragments of $Re_2(CO)_{10}$ contain two metal atoms. This compares with 56% of the ion fragments containing two metal atoms in the case of $Mn_2(CO)_{10}$. It seems reasonable to

conclude that:-

(a) The M-M bond in the $Re_2(CO)_x^+$ cations is much stronger than in the corresponding manganese species.

(b) The M-M bond in $Re_2(CO)_{10}$ is stronger than the M-C bond.

Impregnation of $Re_2(CO)_{10}$ on a silica support appears to have little effect on the structure of the complex. A comparison of the infra-red spectra of $Re_2(CO)_{10}$ dissolved in methylene dichloride and a 2% $Re_2(CO)_{10}$/silica disc shows little difference in the bands observed in the carbonyl stretching region, which would seem to indicate that the complex undergoes little or no change on contact with the support. Examination of the physical characteristics of the supported complex shows that the complex remains colourless when supported, which is further evidence that the silica has no chemical interaction with the complex. In addition, the infra-red and physical characteristics of the supported complex are unaffected by exposure to air.

Activation of the supported complex in vacuo by heat treatment results in the carbonyl bands becoming diminished in intensity as the temperature rises, which indicates a gradual loss of carbon monoxide without a decrease in symmetry of the complex. The absence of any bands at around 2000cm^{-1} after activation to 250^oC is conclusive evidence that at this temperature there has been the loss of all carbonyl ligands from the complex.

Examination of a 10% W/W sample of $Re_2(CO)_{10}/SiO_2$ by T.G.A. gives results which support the above conclusions, since degradation indicates that carbonyl loss occurs in a one stage process in the

temperature range 70-170°C.

Electron microscopic examination of the supported complex after activation to 250°C indicates that the rhenium "particles" must be approaching atomic size, since they are undetected by this form of examination. Activation to 320°C brings about widespread aggregation on the surface and particles up to 1000Å may be observed.

9.1.2 The Catalytically Active Form of the Supported Complex

Although it is suspected that the loss of all carbonyl ligands from the supported complex results in the formation of a highly dispersed zero-valent rhenium catalyst, there exists the possibility that this is not the case. The loss of carbonyl groups from the complex may be accompanied by a corresponding substitution reaction with possibly the support acting as a ligand through an -O-Si- group. This could have the effect of changing the oxidation state of rhenium to anything between +1 and +7. However, the exact oxidation state cannot be established from present studies, although the application of e.p.r. spectroscopy and titration studies would be useful in this respect.

The effect of oxygen treatment upon the behaviour of the catalyst may be used as a sensitive probe to obtain evidence of the existence or otherwise of highly dispersed rhenium particles in various oxidation states. The evidence available suggests that a long-term oxygen treatment at 320°C causes the catalyst to be much less active for but-1-ene hydrogenation, although the butene distribution as a function of percentage hydrogenation (figure 6.10) remains similar

to figure 6.9. Exposure to oxygen over a shorter length of time indicates that for the hydrogenation of trans-but-2-ene the initial rates remain virtually the same (Tables 6.15 and 6.16). However, conversion carried out over the oxygen treated catalyst proceeds to a greater extent.

It may be concluded that the loss of catalytic activity after prolonged oxygen exposure is due to the formation of rhenium in a thermodynamically more stable high oxidation state. Limited oxidising conditions in the second case have little effect on the catalytic activity of the catalyst, but the oxidation state attained is such that it prevents the formation of dissociatively adsorbed reactants or other species which would limit the extent of reaction. In the first instance, oxidation may have led to the formation of Re^{7+}, whilst in the following system an intermediate oxidation state may have been in evidence.

The degree of dispersion observed for the complex activated at 320°C is far less than after activation at the lower temperature, as may be adjudged from electron microscopic data. However, a comparison of the rates of hydrogenation over both forms of the catalyst, together with an examination of the butene distributions obtained (figures 6.2 and 6.9) suggests that similar active sites are available, and that the reaction is structure insensitive. The main difference between the complex activated to 250°C and to 320°C is that hydrogenation proceeds to a greater extent before self-poisoning when activated at the higher temperature. Self-poisoning is also more pronounced when hydrogenation is carried out at higher

temperatures as is indicated by a comparison of reaction carried out at 230°C and 250°C (figures 6.2 and 6.3). The reason for this is unclear, but it is probable that a conglomeration of dissociatively adsorbed hydrocarbon species on the surface sites prevents further reaction. This process would be favoured at the higher temperature. Another cause may well be the polymerisation of but-1-ene on the catalyst surface, effectively blocking off sites of adsorption. This would explain why cis- and trans-but-2-ene hydrogenation proceed to a greater conversion as polymerisation would not be possible.

9.2 Reactions of n-Butenes with Hydrogen over Silica Supported Dirhenium Decacarbonyl

The rate expressions which are obtained to describe the kinetics of hydrogenation and isomerisation are of only limited value in that they give no information as to whether hydrogenation proceeds via a Langmuir-Hinshelwood or Rideal-Eley mechanism, or what the slow steps in the reactions are.

The rate equations may be expressed as follows:-

$$r_{\underline{h}} = kp_{H_2}^{1.2} \, p_{BUT\text{-}1}^{0.7}$$

$$r_{\underline{i}} = kp_{H_2}^{0.35} \, p_{BUT\text{-}1}^{0.8}$$

Certain deductions may be made about the degree of adsorption of the reactants. A comparison of the two expressions leads us to

expect that a different mechanism is operative for each reaction. An examination of the reaction orders with respect to each reactant suggests the relatively weak adsorption of both reactants. It may be further deduced that hydrogen is the more strongly adsorbed reactant in the isomerisation reaction, but the more weakly adsorbed species for hydrogenation. These observations are inconsistent with the same species being an intermediate in both the hydrogenation and isomerisation reactions. From kinetic evidence alone therefore, it would appear that these reactions occur via different intermediates and that they do not occur on the same surface site.

Verification that hydrogenation and isomerisation take place completely independently of each other is obtained by examination of the butene variation as a function of percentage hydrogenation. Under all conditions studied, isomerisation was found to be by far the more favoured reaction, thermodynamic equilibrium proportions being attained before hydrogenation has occurred to more than 5%. This is a significant point in agreement with the observed kinetics that each reaction proceeds by a different mechanism.

Evidence obtained from an examination of butene hydrogenation and isomerisation in the absence of hydrogen, shows that whilst hydrogen is essential for butene hydrogenation its presence is not required for isomerisation to take place. It is found, however, that in the presence of hydrogen, isomerisation proceeds significantly faster, leading us to believe that two mechanisms are responsible for the isomerisation of but-1-ene. In one mechanism the presence of hydrogen is a prerequisite for isomerisation, whilst in the other its

presence is not required and indeed may poison reaction by that mechanism.

For the double-bond migration of but-1-ene it is quite feasible that addition-abstraction and abstraction-addition mechanisms do occur concomitantly. In the process of cis-trans isomerisation, however, the alkyl reversal scheme via the formation of a 2-butyl intermediate must be the major pathway since isomerisation via a 1-methyl-Π-allyl intermediate would require the intermediate formation of but-1-ene. The observed results for cis-but-2-ene hydrogenation (Figure 6.13) indicate that the cis/trans ratio remains constant over a wide range of conversions to n-butane and that there is only a tendency towards thermodynamic proportions at about 70% conversion. This indicates that the adsorbed 2-butyl species undergoes the relatively rapid hydrogenation to n-butane, whilst the loss of hydrogen occurs less readily. Therefore, since the hydrogenation of the butenes has been shown to be considerably slower than isomerisation, the addition of hydrogen to the butyl intermediate is obviously not rate-limiting.

Deuterium tracer studies do not disprove the theory that isomerisation involves two separate mechanisms. The initially observed high percentage of the but-2-ene-d_0 species indicates that isomerisation occurs without the incorporation of deuterium into the product butenes. Thus it would be expected that initially isomerisation is proceeding via an inter- or intramolecular hydrogen transfer. The fairly substantial amount of but-2-ene-d_1 which is observed may be accounted for either by the subsequent isomerisation of exchanged

but-1-ene-d_1 via inter- or intramolecular hydrogen transfer, or by the possibility that an alkyl reversal process is occurring concomitantly with the former mechanism. From the available evidence it is impossible to differentiate between the two. Tracer studies indicate that the deuterium incorporation in the three butenes is similar at high conversions, which would lead one to expect similar exchange rates for each butene. However a comparison of the rates of hydrogenation of the butenes shows that they increase in the order

$$\text{but-1-ene} < \underline{\text{trans}}\text{-but-2-ene} \simeq \underline{\text{cis}}\text{-but-2-ene}$$

From these results it may be deduced that the rate-determining step which is operative in hydrogenation has a different value for but-1-ene as compared with but-2-ene. On the other hand, a comparison of the rates for exchange suggests that the slow step for this process proceeds at the same rate for all three butenes. Assuming that both of these reactions proceed via the formation of a butyl radical, it is very doubtful whether one may justifiably rationalise the difference in rates of hydrogenation for but-1-ene and but-2-ene in terms of the relative adsorption strengths of the butenes or of their intermediate butyl radicals without applying the same argument to explain the relative rates of olefin exchange. It is possible that exchange proceeds according to the proposal of Gault (24) by the dissociative adsorption of a vinylic species of the type

$$\overset{*}{\underset{|}{CH}}=CHCH_2CH_3 \quad \text{or} \quad CH_2=\overset{*}{\underset{|}{C}}CH_2CH_3$$

Thus hydrogenation and olefin exchange may satisfactorily proceed by independent reaction pathways.

A comparison of the activation energy values (E_h = 61.9 kJ mole^{-1} and E_i = 106.6 kJ mole^{-1}) for hydrogenation and isomerisation is further evidence that these two reactions do not proceed via the same reaction mechanism, and since it has been proposed that hydrogenation and exchange occur independently, it is probable that a separate mechanism explains each of the three processes.

Thus it may be concluded that:-

1) Hydrogenation occurs either by a Langmuir-Hinshelwood or Rideal-Eley mechanism.

2) Isomerisation may occur concomitant with hydrogenation, but from tracer studies, product distribution examination and the comparison of activation energies, an independent reaction involving inter- or intramolecular hydrogen transfer is more favoured.

3) Olefin exchange proceeds independently of both hydrogenation and isomerisation via a dissociatively adsorbed vinylic species.

CHAPTER 10

REACTIONS OVER SILICA SUPPORTED DICOBALT DIRHODIUM DODECACARBONYL

10.1 The Nature of the Supported Complex.

10.1.1 Physical Properties.

Infra-red and crystallographic data have established (130) that the mixed tetranuclear carbonyl $Co_2Rh_2(CO)_{12}$ has the following structure:-

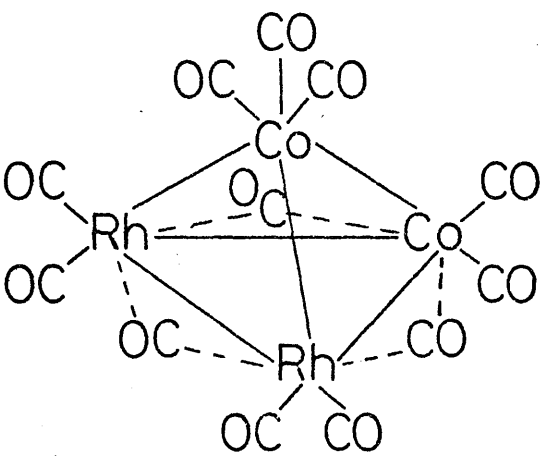

This compound, in common with the other known mixed tetranuclear carbonyls composed of cobalt and rhodium, is unstable in air and decomposes with the evolution of carbon monoxide at 120°C. It is particularly difficult to elucidate decomposition temperatures in connection with metal clusters since in many cases there are a number of different processes including, evolution of carbon monoxide with the corresponding decomposition to the metal, redistribution processes, formation of hexanuclear species, which are known to occur. For example, a thermogravimetric analysis of $Rh_4(CO)_{12}$, in a

nitrogen atmosphere, shows that the carbonyl begins to decompose at about 90°C, carbon monoxide evolution becoming faster at 115°C. After this point carbon monoxide evolution ceases, until the temperature of 160°C is reached when the $Rh_6(CO)_{16}$ formed in the first stage begins to decompose until finally at about 200°C only the metal remains.

As with the other mixed metal carbonyls of Group VIIIB mass spectrometric analysis of $Co_2Rh_2(CO)_{12}$ has shown the appearance of tetranuclear ions containing metal ratios different from those present in the original carbonyl complex. These ions arise from complicated redistribution phenomena such as, for example,

$$2\ Co_2Rh_2(CO)_{12} \rightarrow Co_3Rh(CO)_{12} + CoRh_3(CO)_{12}$$

which probably occur when the sample is introduced into the hot source. Such processes make it much more difficult to compare the relative ease of bond-breaking within the original tetranuclear complex upon changing the atomic weight of metals present in the cluster, as has been reported in the literature for the trinuclear $M_3(CO)_{12}$ carbonyls (139).

Other "decomposition" reactions which are known to occur with $Rh_2Co_2(CO)_{12}$ include:

$$Co_2Rh_2(CO)_{12} \xrightarrow[60^{\circ}C]{\text{n-heptane}} Co_2Rh_4(CO)_{16} + Co_3Rh(CO)_{12}$$

and the associated reaction

$$Co_3Rh(CO)_{12} \xrightarrow[60^{\circ}C \text{ or more}]{\text{n-heptane}} \text{hexanuclear species} + Co_4(CO)_{12}$$

A study of dicobaltdirhodium dodecacarbonyl by infra-red spectroscopy shows that when dissolved in n-hexane the complex gives rise to $\bar{\nu}$(CO) adsorptions at 2073, 2064, 2059, 2040, 2030, 1920, 1910, 1885, 1870 and 1855 cm^{-1}. Supporting the complex on silica shows the presence of bands at 2095, 2080, 2075, 2040 and 2026 cm^{-1}. The shift in stretching frequencies for the terminal carbonyls is accompanied by a disappearance of all bands in the bridging carbonyl region at around 1900 cm^{-1}, although it may be that these peaks are being masked by the band at 1830 cm^{-1} arising from the silica support. These observations would seem to indicate that a change in structure is undergone by the complex on contact with the support, although examination of the physical characteristics of the supported complex shows that the brown colour of the original carbonyl is retained. Exposure of the supported complex to air results in a disappearance of all bands in the carbonyl region after a few days, although there is a retention of the original brown colour. Infra-red analysis also shows that the facile removal of all carbonyl groups is achieved by heating the supported complex to 120°C in vacuo overnight.

Examination of a 10% W/W sample of supported complex by T.V.A. provides further evidence for the loss of carbon monoxide during activation. This technique shows that the carbon monoxide is evolved in essentially two stages, the first stage occurring between 60-140°C, whilst the second stage in degradation proceeds at 150°C. However, the carbon monoxide evolved in the second stage must be removable by prolonged heating at a lower temperature as indicated by the infra-red data.

Electron microscopic examination of the supported complex indicates that it remains highly dispersed on the silica after activation in vacuo to 100°C, consisting of particles of diameter < 10Å. Particles in the region of 10-18Å become detectable as a result of extensive use in catalytic reactions, whilst particles ranging between 10-45Å are observed after activation to 240°C.

10.1.2 The Catalytically Active Forms of the Supported Complex.

A basic prerequisite for catalytic activity in the supported complex is that it be heated in vacuo at a temperature not less than about 85°C for 1-3 hours, after which it is found to be active for the hydrogenation and isomerisation of the n-butenes at ambient temperature. This particular pretreatment could have a number of effects on the supported complex, one or more of which could be responsible for the origins of the catalytic activity. These include:-

1) A loss of carbonyl ligands from the complex which may produce vacant sites for the adsorption of reactants to occur.

2) A redistribution of the complex similar to that which may be observed for the unsupported species. This could possibly occur before the loss of carbonyl ligands, resulting ultimately in the appearance on the silica of Rh_3Co and $RhCo_3$ clusters, either of which may be a more effective catalyst for hydrogenation and isomerisation than the Rh_2Co_2 cluster. In addition there is the possibility that clusters of the type Rh_4Co_2, Co_4 or Rh_4 are being formed.

3) The cleavage of the M - M bonds in the cluster, with the formation of discrete Rh and Co atoms on the surface.

The suggestion that there are potentially several types of adsorption sites on the catalyst surface can perhaps help to explain why the observed butene distribution (figure 7.3) for the first catalyst sample examined reaches thermodynamic proportions after about 40% conversion, whilst with all succeeding catalyst samples the initial stages of hydrogenation indicate a similar process, although preferential hydrogenation of the but-2-enes as the reaction proceeds results in the appearance of mostly but-1-ene in the butene mixture in the later stages. The anomalous results observed with the first sample may have been due to the presence of a certain type of adsorption site, which was inherent only within that sample.

Activation of the complex is seen (figure 7.10) to be a reproducible process, but reactivation to the same temperature fails to regenerate the catalyst to its former activity and a limiting rate is reached. Reactivation to the elevated temperature of $240^{o}C$ regenerates the catalyst to its most active form. Electron microscopy shows that there is certainly an aggregation of "particles" on the support at this temperature. It is possible that each "particle" may consist exclusively of either rhodium or cobalt atoms but it is statistically more probable that a coprecipitation of both atoms occurs in each aggregate.

The effect of hydrogen treatment at $100^{o}C$ on a "poisoned" catalyst surface is to effectively replenish surface sites and

regenerate the catalyst to its former activity. This can be explained if it is accepted that the "poisoning" is due to the formation of dissociatively adsorbed hydrogen deficient species, which block potential sites of adsorption of the catalytically active species. Hydrogen treatment must cause the removal of a proportion of these species into the gaseous phase and thus regenerate the sites of adsorption. However, since the hydrogen treatment declines in efficiency as the process is repeated, a certain percentage of the species must be irreversibly adsorbed. Similar effects have been observed with other supported metal complexes (133, 135, 136). Examination of the butene distribution (figure 7.13) carried out over a hydrogen "treated" catalyst indicates that similar mechanisms and thus similar surface adsorption sites to those present on the original catalyst are involved.

The possibility has also to be considered that one or other of the component metals has undergone oxidation in the presence of surrounding - O-Si groups. The effect of oxygen on the supported complex by long-term exposure to air results in the complex exhibiting normal activity for the hydrogenation and isomerisation of the butenes. The first reaction succeeding exposure, however, showed an induction period of nearly one hour. If oxidation has occurred due to exposure to air, it is probable that this is the cause of the initial inactivity. It is clear, however, that only extremely mild conditions (55 minutes at 120^{o}C) were required to reduce the metals to their original form. Ease of reduction is probably due to the very high dispersion of metal on the surface.

A similar induction period is not observed when a catalyst, which has been used for a series of butene-hydrogen reactions, is exposed to air and then used for further reactions. The reason for this is unclear, although it suggests that the oxidation of the original supported complex must be more favoured than when it has been activated in vacuo and exists as metal clusters on the surface.

10.2 Reactions of the n-Butenes with Hydrogen over Silica Supported Dicobaltdirhodium Dodecacarbonyl.

The observed kinetics of unity in hydrogen and zero in butene are consistent with either a Langmuir-Hinshelwood or a Rideal-Eley mechanism. For the former the following reactions must be considered.

$$C_4H_8\,(g) \rightleftharpoons C_4H_8\,(a) \qquad (1, -1)$$

$$H_2\,(g) \rightleftharpoons 2H\,(a) \qquad (2, -2)$$

$$C_4H_8\,(a) + H\,(a) \rightleftharpoons C_4H_9\,(a) \qquad (3, -3)$$

$$C_4H_9\,(a) + H\,(a) \longrightarrow C_4H_{10}\,(g) \qquad (4)$$

Assuming competitive adsorption, the surface coverages, Θ, of but-1-ene and hydrogen are given by the adsorption isotherms:

$$\Theta_{BUT\text{-}1} = \frac{b_B p_B}{(1 + b_B p_B + b_{H_2}^{0.5} p_{H_2}^{0.5})}$$

$$\Theta_H = \frac{b_{H_2}^{0.5} p_{H_2}^{0.5}}{(1 + b_B p_B + b_{H_2}^{0.5} p_{H_2}^{0.5})}$$

Under conditions where the alkene is adsorbed much more strongly than hydrogen, these equations simplify to:

$$\Theta_{BUT\text{-}1} \rightarrow 1 \text{ and } \Theta_H \propto b_{H_2}^{0.5} \, p_{H_2}^{0.5}$$

If the addition of an adsorbed hydrogen atom to the butyl species (step 4) is rate limiting, the rate equation may be written as:-

$$\text{rate} = k_4 \, \Theta_{C_4H_9} \, \Theta_H$$

A steady state analysis shows that

$$\Theta_{C_4H_9} = \frac{k_3 \, \Theta_{C_4H_8} \Theta_H}{k_4 \, \Theta_H + k_{-3}} \, ,$$

Substitution into the rate expression yields

$$\text{rate} = \frac{k_3 \, k_4 \, \Theta_{C_4H_8} \, \Theta_H^2}{k_4 \, \Theta_H + k_{-3}}$$

which by substitution of the Langmuir approximations becomes:-

$$\text{rate} = \frac{k_3 \, k_4 \, b_{H_2} \, p_{H_2}}{k_4 \, b_{H_2}^{0.5} \, p_{H_2}^{0.5} + k_{-3}}$$

Thus if Θ_H and k_4 are small compared with k_{-3} such that $k_{-3} >> k_4\Theta_H$, the rate expression agrees with the observed kinetics.

The Rideal-Eley mechanism, however, involves the formation of the butyl radical from the reaction of an adsorbed butene molecule with molecular hydrogen:-

$$C_4H_8\ (g) \rightleftharpoons C_4H_8\ (a) \qquad (1, -1)$$

$$C_4H_8\ (a) + H_2\ (g) \rightleftharpoons C_4H_9\ (a) + H\ (a) \qquad (2, -2)$$

$$C_4H_8\ (a) + H\ (a) \rightleftharpoons C_4H_9\ (a) \qquad (3, -3)$$

$$C_4H_9\ (a) + H\ (a) \longrightarrow C_4H_{10}\ (g) \qquad (4)$$

A steady state analysis to determine the surface coverages of the intermediate species shows that

$$\Theta_{C_4H_9} = \left[\frac{k_2\, k_3\, p_{H_2}}{k_{-3}\,(k_{-2} + k_4)}\right]^{0.5}$$

and

$$\Theta_H = \left[\frac{k_2\, k_{-3}\, p_{H_2}}{k_3\,(k_{-2} + k_4)}\right]^{0.5}$$

Thus if step 4 is rate limiting, the order of the reaction with respect to hydrogen is unity. Similar kinetics may be obtained, if step 2 is rate limiting. The observed kinetics for hydrogenation are, therefore, compatible with both the Langmuir-Hinshelwood and Rideal-Eley mechanisms and it is impossible to distinguish between them on kinetic evidence alone.

For the isomerisation reaction the order with respect to but-1-ene is zero. By inspection of the Langmuir isotherm for but-1-ene adsorption, it may be seen that in order to fulfil this requirement, the surface coverage of but-1-ene, Θ_B, must approach unity, as $b_B p_B >> 1$. Under the conditions where hydrogen is adsorbed much

less strongly than the but-1-ene, the Langmuir approximation for hydrogen surface coverage simplifies to:-

$$\theta_H \propto p_{H_2}^{0.5}$$

Therefore, the observed kinetics for isomerisation $r_i = k\, p_{H_2}^{0.3}\, p_{BUT\text{-}1}^{0}$ are compatible with a reaction scheme for isomerisation whereby double-bond migration occurs via reversal of the adsorbed butyl step. Such a mechanism allows either the formation of the butyl radical or the alkyl reversal step to be rate-limiting in isomerisation.

Deuterium tracer studies alone are insufficient to differentiate between an alkyl reversal scheme and an abstraction-addition mechanism for isomerisation. As was discussed in Chapter 8, isomerisation which proceeded via a 2-butyl radical would result in the product butenes having a greater deuterium content than but-1-ene and furthermore each but-2-ene molecule formed should contain initially one deuterium atom. Results (table 7.11) show that initially the but-2-enes have a greater deuterium content than but-1-ene, but this in itself is insufficient evidence for the existence of a 2-butyl intermediate, since many of the but-1-ene molecules have never been in contact with the catalyst surface. The high but-2-ene-d_0 yields might suggest the occurrence of an abstraction-addition mechanism with either inter- or intra-molecular hydrogen transfer. However such a mechanism does not readily permit an understanding of the observations that both hydrogenation and isomerisation are occurring on similar surface sites.

An examination of the butene distributions as a function of percentage hydrogenation indicates that, unlike the previous two systems where isomerisation occurred extremely rapidly relative to the hydrogenation process, the variation in the composition of the butenes is consistent with a mechanism whereby isomerisation is proceeding concomitant with hydrogenation. Furthermore, it has been shown that as the catalyst becomes poisoned due to sintering, the formation of carbonaceous residues on the surface, or some associated effect, both hydrogenation and isomerisation are affected in a similar manner indicating that similar reaction sites and intermediates are operative in each case.

An examination of the relative rates of hydrogenation of but-1-ene and the but-2-enes indicates a similar rate in each case. However, consideration of the variation of the butene distribution with extent of hydrogenation in figures 7.7, 7.9, 7.11 and 7.12 indicates that in a competitive situation the rates of hydrogenation increase in the order but-1-ene < cis-but-2-ene < trans-but-2-ene. Assuming that the addition of a hydrogen atom to the butyl intermediate is the slow step these reaction rates may be rationalised in terms of the relative strengths of adsorption of the 1-butyl and 2-butyl intermediates. If, however, the addition of molecular hydrogen to the adsorbed butene is rate determining, the relative strengths of but-1-ene, cis-but-2-ene and trans-but-2-ene adsorption will determine comparative rates of hydrogenation. The former suggestion does not explain why the rates of cis- and trans-but-2-ene hydrogenation should differ as a similar intermediate exists in each case. The latter suggestion, on the other hand, seems more probable since it is known that, due to a combination

of a steric effect and an electronic effect, the strength of butene co-ordination with various transition metals (140, 141) decreases in the order

but-1-ene > cis-but-2-ene > trans-but-2-ene

which is consistent with the relative rates of hydrogenation.

Although the activation energies for hydrogenation, isomerisation and olefin exchange are unavailable, it is reasonable to expect that olefin exchange also proceeds via an alkyl reversal pathway. If it were assumed that the addition of a deuterium atom to the adsorbed butene was rate-limiting for exchange, it would be expected that the rate of exchange would be dependent upon the adsorption strengths of each. By this reasoning, trans-but-2-ene would be expected to undergo exchange more rapidly than cis-but-2-ene. However, since the rates of exchange for the but-2-enes are similar it is clear that this step is not rate-determining. The proposal that alkyl reversal is the slowest step would require that the relative rates of exchange be dependent upon the relative stabilities of the 1-butyl and 2-butyl radicals. The observed deuterium distributions indicate that but-1-ene exchange is far slower than for the but-2-enes, which have similar rates. Thus it is clear that the alkyl reversal as the slowest step is more compatible with the observed results.

It may be concluded that hydrogenation occurs by a Rideal-Eley mechanism and that activation of hydrogen proceeds by the reaction of physically adsorbed molecular hydrogen with an adsorbed butene molecule. It is further concluded that isomerisation proceeds on similar surface sites to those involved in the hydrogenation reactions,

via an addition-abstraction mechanism involving the reversible formation of a 2-butyl intermediate. Finally, it is concluded that olefin-exchange also proceeds via an alkyl reversal pathway, the slow step being the loss of a "hydrogen" atom from the half-hydrogenated butyl radical.

APPENDIX A

Equations for the calculation of parent ion concentration in mass spectrometric analyses

The need to correct the measured intensity of each peak in the mass spectrum for the fragmentation of species of higher mass has been discussed in Chapter 4. The full equations are listed below.

x = measured positive ion current.
(x = a, b, c, ---- etc.)

X' = measured positive ion current after correction for ^{13}C.
(X' = A', B', C' --- etc.)

X = parent ion concentration
(X = A, B, C ---- etc.)

f_1 and f_2 are the fractions of the first and second fragments respectively.

(a) n-Butane

Correction for ^{13}C

m/e			
58	L'	=	l
59	K'	=	k - 0.044L'
60	J'	=	j - 0.044K'
61	I'	=	i - 0.044J'
			etc.

Parent ion concentrations

m/e

68 $A = A'$

67 $B = B'$

66 $C = C' - f_1 (A + 0.10B)$

65 $D = D' - f_1 (0.90B + 0.20C)$

64 $E = E' - f_1 (0.80C + 0.30D) - f_2(A + 0.20B + 0.022C)$

63 $G = G' - f_1 (0.70D + 0.40E) - f_2(0.80B + 0.356C + 0.67D)$

62 $H = H' - f_1(0.60E + 0.50G) - f_2(0.623C + 0.467D + 0.133E)$

61 $I = I' - f_1(0.50G + 0.60H) - f_2(0.467D + 0.534E + 0.222G)$

60 $J = J' - f_1(0.40H + 0.70I) - f_2(0.333E + 0.556G + 0.333H)$

59 $K = K' - f_1(0.30I + 0.80J) - f_2(0.222G + 0.534H + 0.467I)$

58 $L = L' - f_1(0.20J + 0.90K) - f_2(0.133H + 0.467I + 0.623J)$

57 $M = M' - f_1(0.10K + L) - f_2(0.067I + 0.356J + 0.800K)$

56 $N = N' - f_2(0.022J + 0.20\ K + L)$

(b) n-Butenes

Correction for ^{13}C

m/e

56 $J' = j$

57 $I' = i - 0.044J'$

58 $H' = h - 0.044I'$

59 $G' = g - 0.044H'$

etc.

Parent ion concentrations

m/e

64 $A = A'$

63 $B = B'$

62 $C = C' - f_1(A + 0.125B)$

61 $D = D' - f_1(0.875B + 0.25C)$

60 $E = E' - f_1(0.375D + 0.750C) - f_2(0.250B + 0.036C + A)$

59 $G = G' - f_1(0.500E + 0.625D) - f_2(0.107D + 0.429C + 0.750B)$

58 $H = H' - f_1(0.625G + 0.500E) - f_2(0.214E + 0.536D + 0.536C)$

57 $I = I' - f_1(0.750H + 0.375G) - f_2(0.357G + 0.572E + 0.357D)$

56 $J = J' - f_1(0.875I + 0.250H) - f_2(0.536H + 0.536G + 0.214E)$

55 $K = K' - f_1(J + 0.125I) - f_2(0.750I + 0.429H + 0.107G)$

54 $L = L' - f_2(J + 0.250I + 0.036H)$

REFERENCES

1. J. E. Douglas and B. S. Rabinovitch, J. Am. Chem. Soc., 74, 2486 (1952).
2. G. C. Bond and J. Turkevich, Trans. Faraday Soc., 49, 281 (1953)
3. G. H. Twigg, Disc. Faraday Soc., 8, 152 (1950).
4. J. Horiuti, G. Ogden, M. Polanyi, Trans. Faraday Soc., 30, 663 (1934).
5. J. Horiuti and M. Polanyi, Trans. Faraday Soc., 30, 1164 (1934).
6. J. J. Rooney and G. Webb, J. Catalysis, 3, 488 (1964).
7. J. I. McNab and G. Webb, J. Catalysis, 26, 226 (1972).
8. G. H. Twigg, Proc. R. Soc., A178, 106 (1941)
9. T. I. Taylor and V. H. Diebler, J. Phys. and Colloid Chem., 55, 1036 (1951).
10. G. C. Bond, J. J. Phillipson, P. B. Wells and J. M. Winterbottom, Trans. Faraday Soc., 60, 1847 (1964).
11. G. C. Bond, G. Webb and P. B. Wells, Trans. Faraday Soc., 64, 3077 (1968).
12. G. C. Bond and J. M. Winterbottom, Trans. Faraday Soc., 65, 2779 (1969).
13. J. I. McNab and G. Webb, J. Catalysis, 10, 19 (1968).
14. S. D. Mellor and P. B. Wells, Trans. Faraday Soc., 65, 1883 (1969).
15. W. M. Hamilton and R. L. Burwell, Proc. 2nd Intern. Congress on Catalysis (Editions Technip, Paris 1961), 1, 989.
16. J. E. Kilpatrick, E. J. Prosen, K. S. Pitzer and F. D. Rossini, J. Res. Bur. Stand., 36, 590 (1946).
17. S. D. Mellor and P. B. Wells, Trans Faraday Soc., 65, 1873 (1969).
18. J. J. Phillipson and P. B. Wells, Proc. Chem. Soc., 222 (1964).
19. P. B. Wells and G. R. Wilson, J. Catalysis, 9, 70 (1967).
20. S. Carra and V. Ragaini, J. Catalysis, 10, 230 (1968).
21. V. Ragaini, J. Catalysis, 34, 1 (1974).

22. G. V. Smith and J. R. Swoap, J. Org. Chem., 31, 3904 (1966).

23. R. Touroude and J. G. Gault, J. Catalysis, 32, 288; 294 (1974).

24. J. G. Gault, M. Ledoux, J. J. Masini and G. Roussy, Proc. 6th Intern. Cong. Catalysis, paper A37 (1976).

25. G. C. A. Shuit and L. L. Van Reijan, Adv. Catalysis, 10, 298 (1958).

26. M. Boudart, A. W. Aldag, J. E. Benson, N. A. Dougharty and C. H. Girvin, J. Catalysis, 6, 92 (1966).

27. G. I. Jenkins and E. K. Rideal, J. Chem. Soc., 2590 ; 2496 (1955).

28. B. A. Morrow and N. Sheppard, J. Phys. Chem., 70, 2406 (1966).

29. L. Whalley, B. J. Davis and R. L. Moss, Trans. Faraday Soc., 66, 3143 (1970).

30. B. A. Morrow and N. Sheppard, Proc. R. Soc., A311,391 (1969).

31. S. J. Thomson and G. Webb, J. Chem. Soc. Chem. Comm., 526 (1976).

32. F. J. McQuillan, Chem. Ind., 941 (1976).

33. S. Carra and R. Ugo, Inorg. Chim. Act. Rev., 1, 49 (1967).

34. J. Halpern, Adv. Chem. Series, 70, 1 (1968).

35. B. R. James, Inorg. Chim. Act. Rev., 4, 73 (1970).

36. G. Dolcetti and N. W. Hoffman, Inorg. Chim. Act. Rev., 9, 269 (1974).

37. J. Chatt and J. Halpern, Catal. Prog. Res. Proc. NATO Sci. Comm. Conf. 107 (1972).

38. J. A. Osborn, F. H. Jardine, J. F. Young and G. Wilkinson, J. Chem. Soc., 1711 (1966).

39. J. Halpern, J. F. Harrod and B. R. James, J. Am. Chem. Soc., 88, 5150 (1966).

40. J. Kwiatek, I. L. Mador and J. K. Seyler, Adv. Chem. Series 37, 201 (1963).

41. J. C. Bailar Jr. and H. Italani, J. Am. Chem. Soc., 89, 1592 (1967)

42. R. D. Cramer, E. L. Jenner, R. V. Lindsey Jr. and U. G. Stolberg, J. Am. Chem. Soc., 85, 1691 (1963).

43. H. A. Tayim and J. C. Bailar Jr., J. Am. Chem. Soc., 89, 3420 (1967).

44. R. Cramer, J. Am. Chem. Soc., 88, 2272 (1966).

45. J. F. Harrod and A. J. Chalk, J. Am. Chem. Soc., 88, 3491 (1966).

46. J. F. Harrod and A. J. Chalk, J. Am. Chem. Soc., 86, 1776 (1964).

47. L. Roos and M. Orchin, J. Am. Chem. Soc., 87, 5502 (1965).

48. G. C. Bond and M. Hellier, J. Catalysis, 7, 217 (1967).

49. R. Cramer, J. Am. Chem. Soc., 87, 4717 (1965).

50. A. J. Canale, W. A. Hewett, T. M. Shryne and E. A. Youngman, Chem. Ind., 1054 (1962).

51. J. Halpern, B. R. James and A. L. W. Kemp, J. Am. Chem. Soc., 83, 4097 (1961).

52. P. M. Henry, Adv. Chem. Series, 70, 126 (1966).

53. J. Halpern, Ann. Rev. Phys. Chem., 16, 103 (1965).

54. G. Wilke, Angew. Chem., Intern. Ed., 2, 105 (1963).

55. L. Vaska and J. W. DiLuzio, J. Am. Chem. Soc., 84, 670 (1962).

56. J. Halpern and B. R. James, Can. J. Chem., 44, 671 (1966).

57. G. C. Bond and P. B. Wells, Adv. Catalysis, 15, 92 (1964).

58. R. S. Nyholm, Proc. 3rd Intern. Cong. Catalysis, (Amsterdam 1965).

59. M. G. Burnett, P. J. Connolly and C. Kemball, J. Chem. Soc. A, 800 (1967).

60. G. C. Bond, Adv. Chem. Series, 70, 25 (1968).

61. J. L. Garnett, Catalysis Rev., 5, 229 (1972).

62. O. Johnson, Catalysis Proc. Int. Symp. on Relations between Heterogeneous and Homogeneous Catalyses 497 (Brussels 1974).

63. D. G. H. Baillard, Ibid. 521.

64. J. Chatt and L. A. Duncanson, J. Chem. Soc., 2939 (1953).

65. J. C. Bailar, Jr., Catalysis Rev., 10, 17 (1974).

66. J. C. Bailar, Jr., S. Carra, M. Graziani, K. Mosbach, R. C. Pitkethly, E. K. Pye, J. J. Rooney, Catal. Prog Res. Proc. NATO Sci. Comm. Conf. 177 (1972)

67. G. J. K. Acres, G. C. Bond, B. J. Cooper and J. A. Dawson, J. Catalysis 6, 139 (1966).

68. K. E. Hayes, Nature, 210, 412 (1966).

69. M. Misono, Y. Saito and Y. Yoneda, J. Catalysis, 10, 200 (1968).

70. J. Robertson and G. Webb, Proc. R. Soc. Lond., A341, 383 (1974).

71. E. S. Davie, D. A. Whan and C. Kemball, J. Catalysis, 24 272 (1972).

72. R. F. Howe, D. E. Davidson and D. A. Whan, J. Chem. Soc., Faraday Trans. 1, 68, 2266 (1972).

73. G. M. Schwab, Discuss. Faraday Soc., 8, 166 (1950)

74. D. A. Dowden, J. Chem. Soc., 242 (1950).

75. L. Pauling, Proc. R. Soc., A196, 343 (1949).

76. M. F. Mott and H. Jones "Theories of the Properties of Metals and Alloys" Oxford University Press, London 1936

77. D. A. Dowden and P. W. Reynolds, Disc. Faraday Soc., 8, 184 (1950).

78. A. Couper and D. D. Eley, Disc. Faraday Soc., 8, 689 (1950).

79. D. D. Eley and P. Luetic, Trans. Faraday Soc., 53, 1483 (1957).

80. A. G. Daglish and D. D. Eley, Proc. 2nd Intern. Cong. Catalysis (Editions Technip. Paris 1960) 1615

81. G. C. Bond and R. S. Mann, J. Chem. Soc., 3566 (1959).

82. R. J. Best and W. W. Russell, J. Am. Chem. Soc., 76, 838 (1954).

83. H. G. Rushford and D. A. Whan, Trans. Faraday Soc., 67, 3577 (1971)

84. J. H. Sinfelt, Plat. Met. Rev., 20, 114 (1976).

85. J. H. Sinfelt, Science, 195, (4279), 641 (1977).

86. J. L. Carter, D. J. C. Yates, J. H. Sinfelt, J. Catalysis, 24, 283 (1972).

87. J. H. Sinfelt, J. Catalysis, 29, 308 (1973).

88. A. E. Barnett, J. A. Cusumano, Y. L. Lam and J. H. Sinfelt, J. Catalysis, 42, 227 (1976).

89. V. Ponec and W. M. H. Sachtler, J. Catalysis, 24, 250 (1972).

90. J. M. Beelen, V. Ponec and W. M. H. Sachtler, J. Catalysis, 28, 376 (1973).

91. A. A. Balandin, Adv. Catalysis, 10, 96 (1958).

92. D. A. Dowden, Proc. 5th Intern. Cong. Catal., 621 (1972).

93. Y. Soma-Noto and W. M. H. Sachtler, J. Catalysis, 32, 315 (1974).

94. M.F.L. Johnson and V. M. Leroy, J. Catalysis, 35, 434 (1974).

95. A. N. Webb, J. Catalysis, 39, 485 (1975).

96. M. F. L. Johnson, J. Catalysis, 39, 487 (1975).

97. D. J. C. Yates and J. H. Sinfelt, J. Catalysis, 14, 182 (1969).

98. M. Shelef and H. C. Yao, J. Catalysis, 44, 392 (1976).

99. A. A. Olsthoorn and C. Boelhouwer, J. Catalysis, 44, 207 (1976).

100. J. A. Dumesic, R. A. Fridman, M. Y. Kushnerev, Y. V. Maksimov, A. E. Nechitailo, J. Catalysis, 45, 114 (1976).

101. C. J. Lin, A. W. Aldag, A. Clark, J. Catalysis, 45, 287 (1976).

102. R. Edreva-Kardjieva, A. Andriev, React. Kinet. Catal. Lett., 5, 465 (1976).

103. C. J. Lin, A. W. Aldag and A. Clark, J. Catalysis, 34, 494 (1974).

104. J. Grant, R. B. Moyes and P. B. Wells, J. Chem. Soc., Faraday Trans. 1, 69, 1779 (1973).

105. C. H. Bamford and S. U. Mullik, Polymer, 17, 94 (1976).

106. C. Bolivar, H. Charcosset, R. Frety et al., J. Catalysis, 39, 249 (1975).

107. C. Bolivar, H. Charcosset, R. Frety et al., J. Catalysis, 45, 163 ; 179 (1976).

108. E. L.Muetterties, Bull. Soc. Chim. Belg., 84, 959 (1975).

109. E. R. Corey and L. F. Dahl, Inorg. Chem., 1, 521 (1962).

110. B. F. G. Johnson, P. A. Kilty and J. Lewis, J. Chem. Soc., A, 2859 (1968).

111. P. Banditelli, A. Cuccuri and F. Sodi, Thermochim. Acta, 16, 89 (1976).

112. A. J. Deeming, S. Hasso. M. Underhill, A. J. Canty, B. F. G. Johnson, W. Jackson, J. Lewis and T. W. Matheson, J. Chem. Soc., Chem. Comm., 807 (1974).

113. A. J. Deeming and M. Underhill, J. Organo. Chem., 42, C60 (1972).

114. A. J. Deeming and M. Underhill, J. Chem. Soc., Chem. Comm., 277 (1973).

115. A. J. Canty, B. F. G. Johnson, J. Lewis, J. Organo. Chem., 43, C35 (1972).

116. W. G. Jackson, B. F. G. Johnson and J. Lewis, J. Organo Chem., 90, C13 (1975).

117. See e.g. R. P. Eischens and W. A. Pliskin, Adv. Catalysis, 10, 1 (1958).

118. J. P. Yesinowski, D. Bailey, J. Organo. Chem., 65, C27 (1974).

119. A. J. Deeming, S. Hasso and M. Underhill, J. Chem. Soc., Dalton, 1614 (1975).

120. A. J. Deeming and S. Hasso, J. Organo Chem., 114, 313 (1976).

121. M. Tachikawa, J. R. Shapley and C. G. Pierpont, J. Am. Chem. Soc., 97, 7172 (1975).

122. J. B. Keistner and J. R. Shapley, J. Am. Chem. Soc., 98, 1056, (1976).

123. M. Tachikawa, J. R. Shapley, R. C. Haltiwanger and C. G. Pierpont, J. Am. Chem. Soc., 98, 4651 (1976).

124. W. G. Jackson, B. F. G. Johnson, J. W. Kellard, J. Lewis and K. T. Shorpp. J. Organo. Chem., 87, C27 (1975).

125. V. W. Day, R. O. Day, J. S. Kristoff, F. J. Hirsekorn and E. L. Muetterties, J. Am. Chem. Soc., 97, 2571 (1975).

126. G. C. Demitras, E. L. Muetterties, J. Am. Chem. Soc., 99, 2796 (1977).

127. M. G. Thomas, B. F. Beier and E. L. Muetterties, J. Am. Chem. Soc., 98, 1296 (1975).

128. A. J. Deeming and M. Underhill, J. Chem. Soc., Dalton, 1415 (1974).

129. J. A. McCleverty and G. Wilkinson, Inorg. Synth., 8, 211 (1966).

130. S. Martinengo, P. Chini, V. G. Albano, F. Cariati and T. Salvatori, J. Organo. Chem., 59, 379 1973).

131. J. Knight and M. J. Mays, Chem. Ind., 1159 (1968).

132. F. H. Field and J. R. Franklin, "Electron Impact Phenomena" Academic Press, New York (1957)

133. D. Cormack, S. J. Thomson and G. Webb, J. Catalysis, 5, 224 (1966).

134. G. F. Taylor, S. J. Thomson and G. Webb, J. Catalysis, 12, 150 (1968).

135. J. Altham and G. Webb, J. Catalysis, 18, 133 (1970).

136. A. S. Al-Ammar, S. J. Thomson and G. Webb, J. Chem. Soc., Chem. Comm., 323 (1977).

137 B. F. G. Johnson, J. Lewis, I. G. Williams and J. M. Wilson, J. Chem. Soc. A, 341 (1967).

138. B. F. G. Johnson and J. Lewis, Acc. Chem. Res., 1, 245 (1968).

139. M. I. Bruce, Adv. Organometal. Chem., 6, 273 (1968).

140. F. R. Hepner, K. N. Trueblood and H. J. Lucas, J. Am. Chem. Soc., 74, 1333 (1952).

141. H. B. Jonassen and W. B. Kirsch, J. Am. Chem. Soc., 79, 1279 (1957).

142. J. Lewis, A. R. Manning, J. R. Miller and J. M. Wilson, J. Chem. Soc., (A), 1663 (1966).